



HANS MEINHARDT

THE
ALGORITHMIC
BEAUTY
OF SEA SHELLS

FOURTH EDITION

The Virtual Laboratory

Hans Meinhardt

The Algorithmic Beauty of Sea Shells

Fourth Edition

With Contributions and Images
by Przemyslaw Prusinkiewicz
and Deborah R. Fowler

With 148 Illustrations, 134 in Color,
and CD-ROM



Hans Meinhardt
Max-Planck-Institute for Developmental Biology
Spemannstr. 35
72076 Tübingen
Germany
hans.meinhardt@tuebingen.mpg.de

Series Editor
Przemyslaw Prusinkiewicz

ISSN 1431-939X
ISBN 978-3-540-92141-7 e-ISBN 978-3-540-92142-4
DOI 10.1007/978-3-540-92142-4
Springer Dordrecht Heidelberg London New York

Library of Congress Control Number: 2009926970

© Springer-Verlag Berlin Heidelberg 1995, 1998, 2003, 2009

This work is subject to copyright. All rights are reserved, whether the whole or part of the material is concerned, specifically the rights of translation, reprinting, reuse of illustrations, recitation, broadcasting, reproduction on microfilm or in any other way, and storage in data banks. Duplication of this publication or parts thereof is permitted only under the provisions of the German Copyright Law of September 9, 1965, in its current version, and permission for use must always be obtained from Springer. Violations are liable to prosecution under the German Copyright Law.

The use of general descriptive names, registered names, trademarks, etc. in this publication does not imply, even in the absence of a specific statement, that such names are exempt from the relevant protective laws and regulations and therefore free for general use.

Springer-Verlag or the author make no warranty of representation, either express or implied with respect to this CD-ROM or book, including their quality, merchantability, or fitness for a particular purpose. In no event will Springer-Verlag or the author be liable for direct, indirect, special, incidental, or consequential damages arising out of the use or inability to use the CD-ROM or book, even if Springer-Verlag or the author have been advised of the possibility of such damages.

Cover design: deblik, Berlin

Printed on acid-free paper

Springer is part of Springer+Business Media (www.springer.com)

It has turned out to be impossible . . . to get at the meaning of these marks . . . They refuse themselves to our understanding, and will, painfully enough, continue to do so. But when I say refuse, that is merely the negative of reveal - and that Nature painted these ciphers, to which we lack the key, merely for ornament on the shell of her creature, nobody can persuade me. Ornament and meaning always run alongside each other; the old writings too served for both ornament and communication. Nobody can tell me that there is nothing to communicate here. That it is an inaccessible communication, to plunge into this contradiction, is also a pleasure.

Thomas Mann, Doctor Faustus, III. Chapter: Jonathan Leverkühn contemplating a pattern on a New Caledonien sea shell. After the translation from the German by H. T. Lowe-Porter, Penguin Books.

Preface

The pigment patterns on tropical shells are of great beauty and diversity. Their mixture of regularity and irregularity is fascinating. A particular pattern seems to follow particular rules but these rules allow variations. No two shells are identical. The motionless patterns appear to be static, and, indeed, they consist of calcified material. However, as will be shown in this book, the underlying mechanism that generates this beauty is eminently dynamic. It has much in common with other dynamic systems that generate patterns, such as a wind-sand system that forms large dunes, or rain and erosion that form complex ramified river systems. On other shells the underlying mechanism has much in common with waves such as those commonly observed in the spread of an epidemic.

A mollusk can only enlarge its shell at the shell margin. In most cases, only at this margin are new elements of the pigmentation pattern added. Therefore, the shell pattern preserves the record of a process that took place over time in a narrow zone at the growing edge. A certain point on the shell represents a certain moment in its history. Like a time machine one can go into the past or the future just by turning the shell back and forth. Having this complete historical record opens the possibility of decoding the generic principles behind this beauty.

My interest in these patterns began at a dinner in an Italian restaurant. During the meal I found a shell with a pattern consisting of red lines arranged like nested W's. Since I had been working on the problem of biological pattern formation for a long time, this pattern caught my interest, more out of curiosity. To my surprise it seemed that the mathematical models we had developed to describe elementary steps in the development of higher organisms were also able to account for the red lines on my shell. Thus, the shell patterning appeared to be yet another realization of a general pattern-forming principle. But this observation did not remain unchallenged for long. Soon thereafter I saw the complexity and beauty of tropical shells and realized that these patterns cannot be explained by the elementary mechanisms in a straightforward manner.

We do not know what these patterns are good for. Presumably there is no strong selective pressure on the shell pattern. Variations are possible without severely influencing the viability of the animals. Since, as will be described in this book,

the patterns result from the superposition of several pattern-forming reactions, their diversity provides a natural picture book to study complex nonlinear pattern formation.

Finding models for these complex patterns turned out to be much more difficult than I thought. Of course, before making a simulation I was convinced that I had found the correct model. Using the simulation I learned frequently where mistakes in my thinking were and to what patterns my hypothesis really would lead. This led to new insights and new models. I am far from having a satisfactory model for every shell. However, I hope that this book invites you to search for alternative and new solutions.

The book is accompanied by computer programs for performing the simulations on a PC. Most simulations shown can be reproduced. Seeing these patterns emerge on the screen provides a much more intuitive feel for the dynamics of the system. Since minor fluctuation can play a decisive role, even the repetition of the same simulation can produce a somewhat different pattern. This corresponds to the fact that the patterns on any two shells are never identical. The programs allow you to change parameters such as the half-life of a substance or its spread by diffusion. The consequences of these changes can be seen immediately as an alteration of the pattern. The programs are provided with full source code (FreeBasic for Windows/Linux; Microsoft QBX or QB, and PowerBasic for DOS). Therefore, new model interactions can be easily inserted.

What has been added in the new editions

As mentioned already in the first edition, the models describing shell patterning are only special applications of mechanisms developed to account for biological pattern formation in general. To illustrate these close connections, in the second edition a new chapter was added in which models are discussed that describe, for instance, how an embryo can obtain its primary axes, how legs and wings obtain their own coordinate system at the correct positions, and how gene activation can proceed under the influence of graded signals in a position-dependent manner. We started our modeling with the freshwater polyp hydra. Meanwhile it turned out that these primitive organisms can be regarded, as far as the body plan is concerned, as living fossils that provide information of how the formation of body axes of higher organisms evolved. As explained now in Chapter 12, pattern formation in such simple organisms provides a key to understanding how the body axes are established in higher organisms.

Models originally developed to describe some sea shell patterns turned out to provide a key to understanding other developmental systems, it turned out. Overtly the arrangement of leaves on a growing shoot, the patterning of bird feathers, the localization of the plane of cell division in a bacterium, blood coagulation, and the chemotactic orientation of cells seem to have little in common with patterns on a

sea shell. Now, in the fourth edition, a new chapter shows that these systems have a common logical basis. They depend on signals that become quenched shortly after they are generated. This leads to highly dynamic pattern-forming systems that never reach a stable state; avoiding to enter into a state in which the system is irreversibly trapped. Such flexibility then accounts for biological systems that require a permanent adaptation to changing situations.

To provide easier access to the highly dynamic behavior of the interactions on which shell patterning is based, animated simulations were added to the accompanying CD-ROM in the third editions. These can be inspected like conventional websites with any browser in any system. For most of these reactions only a single click is required to see the equations and parameters. The animated simulations are given as separate files that can be integrated, e.g., into a PowerPoint presentation if desired. Also included are animated simulations of models that describe general steps in the development of higher organisms, for instance, regeneration and transplantation experiments with hydra. In the fourth edition PowerPoint presentations were added for the major topics. They also contain many animated simulations.

The best way to become familiar with these reactions is to run these programs enclosed. They are written in the easy-to-use language BASIC. New on the CD of the fourth edition are versions that run under WINDOWS® and LINUX. The corresponding compilers are freely available on the Web and working versions are supplied. Since the source code is enclosed, too, new interactions can be easily added and their behavior can be investigated by running simulations, changing parameters, and performing ‘experimental’ manipulations. Moreover, it is now straightforward to save simulation results in a form that allows printing or integration into other applications.

Acknowledgements

This book could not have been completed without encouragement from many quarters, foremost from my wife Edeltraud Putz-Meinhardt. I would like to express my thanks to those who contributed to the book. The basic ideas grew out of a theory I developed with Alfred Gierer. His concept of local autocatalysis and long-ranging inhibition has formed the basis of most of my work on biological pattern formation. In his diploma thesis Martin Klingler described many interactions capable of reproducing shell patterns in fine detail. Discussions with Andre Koch and Kai Kumpf have been stimulating for me. I thank Drs. Ellen Baake, Jon Campbell, Christa McReynolds, Arthur Roll, Adolf Seilacher, and Ruthild Winkler-Oswatitsch for shells and photographs. Christa Hug helped to prepare the manuscript and Karl Heinz Nill made several of the drawings. I am very grateful to Deborah Fowler and Przemyslaw Prusinkiewicz from the University of Calgary, Canada, for contributing their chapter on shell shapes (Chapter 10). Lynn Mercer and Sherryl Sundell provided very careful corrections of the manuscript.

To prepare the later editions, I am most grateful to Hans Bode, Piet de Boer, Ute Grieshammer, Matthew Harris, Bert Hobmayer, Thomas Holstein, Lydia Lemaire, Richard Prum, Florian Siegert, Ulrich Technau, and Cornelius Weijer for supplying figures for the new chapters describing their experimental results. During the preparation of a German edition, Isolde Tegtmeier found several minor errors in the first edition that are now corrected. Jens Hemmen provided some corrections in the nomenclature of shells. My son Christoph Meinhardt supported me with the LINUX - and C-implementation of the program. I thank Alfred Gierer, Thurston Lacalli, Sanjeev Kumar, and Afonso Guerra Assunção for a critical reading and comments. Very encouraging was the continuous support of Hermann Engesser and Dorothea Glaunsinger from the Springer Company.

Last but not least, I am most grateful for the excellent working conditions provided by the Max-Planck-Institut für Entwicklungsbiologie in Tübingen over many years.

Contents

1	Shell patterns - a natural picture book to study dynamic systems and biological pattern formation	1
1.1	Dynamic systems everywhere	1
1.2	Pattern formation	2
1.3	Dynamic systems are difficult to predict	3
1.4	Pattern formation in biology	4
1.5	Most shell patterns preserve a faithful time record	5
1.6	Elementary patterns: Lines perpendicular, parallel and oblique to the direction of growth	6
1.7	Oblique lines	8
1.8	Relief-like patterns follow the same rules	9
1.9	Many open questions and some hints	10
1.10	The hard problem: complex patterns	15
1.11	Earlier attempts to understand shell patterns	17
2	Pattern formation by local self-enhancement and long range inhibition	19
2.1	The activator – inhibitor scheme	19
2.2	Stable patterns require a rapid antagonistic reaction	20
2.3	Periodic patterns in space	21
2.4	The width of stripes and the role of saturation	25
2.5	Early fixation of a pattern	27
2.6	The activator - depleted substrate scheme	29
2.7	The influence of growth	30
2.8	Inhibition via destruction of the activator	32
2.9	Autocatalysis by an inhibition of an inhibition	33
2.10	Formation of graded concentration profiles	35
2.11	Pattern formation in two dimensions	38
3	Oscillations and traveling waves	41
3.1	The coupling between the oscillators by diffusion	44
3.2	The width of bands and interbands	47

3.3	Oblique lines: traveling waves in an excitable medium	47
3.4	Traveling waves require a pace-maker region	49
4	Superposition of stable and periodic patterns	53
4.1	The formation of undulating lines and the partial synchronization of cells by activator diffusion	54
4.2	Reducing wave termination with a longer activation period	58
4.3	Interconnecting wavy lines and the formation of arches	58
4.4	Hidden waves	60
4.5	Pattern on the shell of <i>Nautilus pompilius</i>	61
4.6	Stabilizing an otherwise oscillating pattern by diffusion	62
4.7	Combinations of oscillating and nonoscillating patterns	63
4.8	Rows of patches parallel to the direction of growth	63
4.9	The possible role of a central oscillator	66
4.10	Conclusion	68
5	Crossings, meshwork of oblique lines and staggered dots: the combined action of two antagonists	71
5.1	Displacement of stable maxima or enforced de-synchronization by a second antagonist	71
5.2	Pattern variability	73
5.3	Global pattern rearrangements	74
5.4	Traces of the additional inhibition: oblique lines initiated or terminated out of phase	76
5.5	Crossings and branching	79
5.6	Changing the wave speed before and during collisions	82
5.7	Parallel and oblique rows of staggered dots	84
5.8	Conclusion	89
6	Branch initiation by global control	91
6.1	Branch formation: the trigger of backwards waves	91
6.2	Simultaneous pattern change in distant regions	93
6.3	No <i>Oliva</i> shell is like another	98
6.4	The influence of parameters	99
6.5	Alternative mechanisms	100
6.6	A very different pattern generated by the same interaction	101
7	The big problem: two or more time-dependent patterns that interfere with each other	105
7.1	Inherent similarities in complex patterns	105
7.2	White nonpigmented drop-like pattern on a pigmented background	108
7.3	Evidence of a sudden extinguishing reaction	110
7.4	Resolving an old problem with the separate extinguishing reaction	111
7.5	The next step in complexity: an additional stabilizing pattern	112

7.6	Branch formation by a temporary stabilization	116
7.7	Intimate coupling of an enhancing and an extinguishing reaction	119
7.8	Extinguishing that results from a depletion of resources due to an enhancing reaction	121
7.9	Related patterns reveal unsolved problems	123
7.10	Apparently different patterns can be simulated by closely related models	126
7.11	Conclusion	128
8	Triangles	131
8.1	The crossing solution through the backdoor	132
8.2	Triangle <i>versus</i> branch formation	135
8.3	The involvement of three inhibitory reactions	139
8.4	Breakdown as a failure of the enhancing reaction	143
8.5	Conclusion	145
9	Parallel lines with tongues	147
9.1	Survival using a precondition pattern	147
9.2	Tongue formation: refresh comes too late	150
9.3	Variations on a common theme	157
9.4	<i>Conus textile</i> : tongues and branches on the same shell	159
9.5	Missing elements, missing links	162
10	Shell models in three dimensions	167
10.1	Mathematical descriptions of shell shape: a brief history	167
10.2	Elements of shell shape	168
10.3	The helico-spiral	169
10.4	The generating curve	171
10.5	Incorporating the generating curve into the model	171
10.6	Modeling the sculpture on shell surfaces	174
10.7	Shells with patterns	179
11	The computer programs	187
11.1	Introductory remarks	187
11.2	Using the program	187
11.3	GUIDED TOURS	190
11.4	Implementation of the interactions	190
11.5	Numerical instabilities that may cause errors	192
11.6	Compilers and versions	193
11.7	Parameters used in the program	194
12	Pattern formation in the development of higher organisms	205
12.1	Hydra, a versatile model system	208
12.2	Tissue polarity and graded competence	211
12.3	How to avoid periodic structures during growth	212
12.4	How to generate structures at a distance: head and foot of hydra	214

12.5	Induction of adjacent structures	215
12.6	The evolution of the main body axes	216
12.7	Gene activation under the control of a morphogen gradient	219
12.8	Position-dependent activation of several genes	221
12.9	A problem that the mollusks don't have: the initiation of legs and wings	224
12.10	Conclusion	228
13	Pattern formation in development in which shell-related mechanisms are implicated	231
13.1	Arrangement of leaves and staggered dots on shells - two similar patterns	231
13.2	Veins and nerves: the formation of net-like structures	235
13.3	Chemotactic orientation of cell polarity	239
13.4	Highly dynamic effects in preparing cell division in budding yeast	242
13.5	Out-of-phase oscillations in <i>E.coli</i> bacteria for center-finding to determine the plane of cell division	244
13.6	<i>Dictyostelium</i> : traveling waves at the border to multicellular organisms	245
13.7	Feather patterns	247
13.8	Color patterns of feathers	248
13.9	Barbs of flight feathers are separated by traveling waves of local signals	250
13.10	Nerve conduction as a traveling wave phenomenon	251
13.11	Activation and extinguishing waves in blood coagulation	252
References	255
Index	265

Shell patterns - a natural picture book to study dynamic systems and biological pattern formation

1.1 Dynamic systems everywhere

Everyday we are confronted with systems that have an inherent tendency to change. The weather, the stock market, or the economic situation are examples. Dramatic changes can be initiated by relatively small perturbations. In the stock market, for instance, even a rumour may be sufficient to trigger sales, lowering quotations and causing panic reactions in other shareholders.

An essential element of dynamic systems is a positive feedback that self-enhances the initial deviation from the mean. The avalanche is proverbial. Cities grow since they attract more people, bacteria or viruses can replicate and the progeny start replicating too. In the universe a local accumulation of matter may attract more dust, eventually leading to the birth of a star.

Earlier or later self-enhancing processes evoke antagonistic reactions. A proliferating virus may trigger an immune response that neutralizes the virus. A collapsing stock market stimulates the purchase of shares at a low price, thereby stabilizing the market. The increasing noise, dirt, crime and traffic jams may discourage people from moving into a big city.

In addition to the balance between self-reinforcing and antagonistic tendencies, several other elements play a decisive role in the fate of dynamic systems. For instance, if the antagonistic reaction follows with some delay, the self-enhancing reaction can cause an overshoot or even an explosion. The explosion of dynamite is a good example. After ignition of a small portion the resulting heat and the shock wave ignite more of the explosives in the neighborhood. The reaction is so vehement because the oxygen required for burning is part of the chemical and is available immediately. Thus, no antagonistic effect slows down the reaction until the explosive is used up. Of course, afterwards a further ignition is impossible.

But let us consider a fire. Fire is also a self-enhancing process since more heat releases more burnable gases from the fuel. But the depletion of oxygen may represent an antagonistic reaction that keeps the fire down to the point that only smouldering is possible. In such a case, the rapid antagonistic reaction, the oxygen

depletion, hinders the development of a big fire. The burning process can go on for a much longer period although at a lower level. Thus the ratio of reaction times between the self-enhancing and the antagonistic processes plays a decisive role.

Another example should illustrate the same fact. As a rule, it takes about two days to fully develop an influenza but it takes about a week to get rid of it. Thus, it appears that our immune system responds too slowly when compared with the growth rate of the virus. Initially the virus proliferates in an avalanche-like manner and we become sick. But what appears at first as a misconstruction turns out to be an advantageous strategy. The slower responding immune system accumulates more and more specific antibodies until the entire virus can be trapped. The body can completely rid itself of the virus. If the immune system responded much faster, a balance between the proliferating virus and the immune system would be established at a lower level. The body would have to fight for the rest of its life against the ever proliferating virus since partial removal of the virus would lead to a corresponding down-regulation of the immune response, providing a new chance for the virus. With the system as it is, we are sick for a week, but after this week we are healthy again and free of the virus.

1.2 Pattern formation

Another decisive parameter in a dynamic system is the spread of its components. In the example mentioned above, the virus may be transmitted to another person who will also become sick after some delay. The infection spreads like a traveling wave. This spread is possible only since the self-enhancing agent, the virus, but not the antagonistic reaction, the immune response, can be transmitted to another individual.

In other systems, it is the antagonistic reaction that spreads more rapidly, and this can lead to stable patterns. Let us regard the formation of sand dunes in the desert (Figure 1.1). Dunes are formed despite the fact that the wind very quickly redistributes the sand. Dune formation may be initiated by a stone in the desert that provides a wind shelter. Sand accumulates behind the wind shelter, and a dune begins to grow. But the sand, once settled in the dune, cannot participate in dune formation somewhere else. The growth of a dune lowers the sand content in the air. The antagonistic reaction results from this removal of sand particles being moved by the wind, and has a long range effect. In this way, the probability of initiating new dunes and the growth of existing dunes in the surrounding area is reduced. In contrast, the increased accumulation of sand behind the wind shelter has a range comparable with the size of the dune. Thus, the basic elements for the formation of stable patterns are a short range self-enhancing reaction and a long range antagonistic reaction.

A similar argument can be made for the formation of valleys and rivers by erosion. The pattern of a ramified river system is certainly not preceded by a

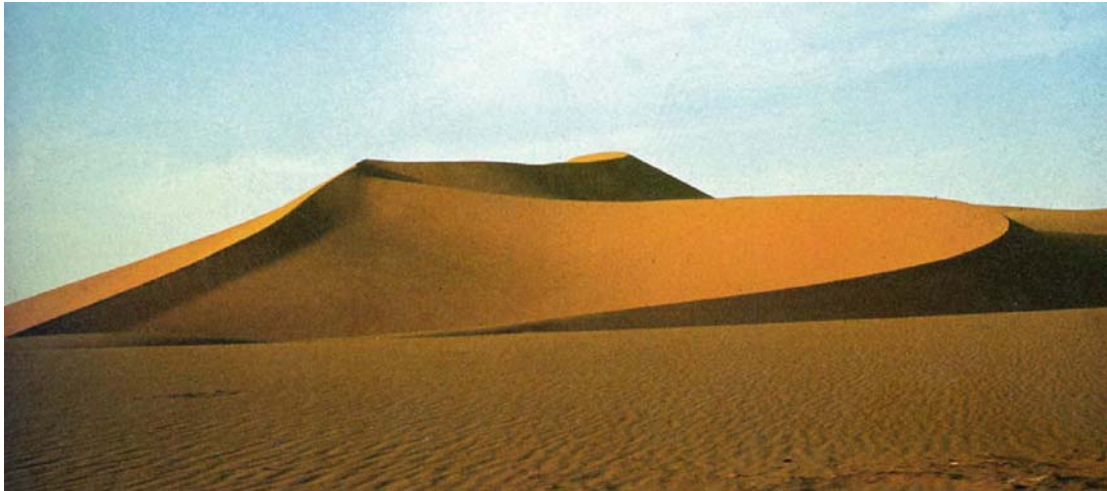


Figure 1.1. The sand dune paradox. Naively, one would expect that the wind in the desert causes a structureless distribution of the sand. However, wind, sand and surface structure together represent an unstable system. Sand deposits more rapidly behind a wind shelter. This increases the wind shelter which, in turn, accelerates the deposition of more sand - a self-enhancing process.

corresponding pattern of rain fall, but results from a self-organizing process. The deepening of a valley proceeds essentially by the erosion of a meandering river. A larger valley collects water from a more extended portion of the surface. Thus, a larger valley has a better chance of becoming even deeper.

The antagonistic reaction can result from a depletion of material trapped by the self-enhancing process, such as in the sand dune example mentioned above. Alternatively, a direct inhibitory effect may spread out from such a self-enhancing center. In the formation of stars both effects play a role. A local increase of matter attracts more cosmic material - the self-enhancing process. One of the antagonistic reactions results from the depletion of cosmic dust in the surroundings. In addition, there is an active antagonistic effect produced by the developing star: the emitted light exerts a so-called light pressure that repels dust particles.

1.3 Dynamic systems are difficult to predict

Investigations of so-called chaotic systems have emphasized the fact that processes exist that are inherently unpredictable on the long term although each step is unequivocally determined by the preceding situation. The weather is an example. Calculation of future developments would require the knowledge of a given situation with an arbitrary precision - a knowledge that is impossible to obtain.

The situation is similar in the systems discussed above where strong positive feedback couplings are involved. Minute differences in the initial conditions can cause a completely different outcome if the situation is just on the border at which a

self-enhancing process becomes dominant. If self-enhancement is triggered in such a “revolutionary” situation, it will obtain a dynamic fairly independent of the mode of ignition.

If small differences are responsible for the selection of different pathways, our intuition of such systems is unreliable. Many attempts have been made to obtain a better understanding using mathematical modeling. For complex systems this is possible only using approximations since one can never be sure that all critical parameters have been considered. The problem becomes even more severe if the feelings and thinking of human beings have a strong influence on the fate of a system, as it is the case in politics or economy. The difficulty in making a prediction is obvious if even a rumour can induce a panic that is not justified by the real situation.

There are two main reasons for modeling dynamic systems: to provide a check on whether a system is fully understood, and to make predictions, at least for the near future.

To obtain the laws that govern a system, a comparison with its development in the past is an important check on whether a system is correctly understood, at least in retrospect. This requires good historical data.

Due to the importance of dynamic systems, on the one hand, and the difficulty of understanding them, on the other, it seems advisable to study relatively simple model systems. A very particular model will be discussed in the present book - the patterns on the shells of mollusks. These motionless calcified patterns are more reminiscent of artistic decorations on china than dynamic systems. However, a closer inspection of many shells reveals dramatic events in their history.

1.4 Pattern formation in biology

The generation of patterns on the shells of mollusks is, of course, only a very special case of the general problem of how an organism obtains its complex structure during development. The life cycle of a higher organism starts, as a rule, with a single fertilized cell. At the end of embryonic development a very sophisticated arrangement of highly specialized cells is generated. The similarity of identical twins is an indication of how stringent this process is under genetic control. But reference to genes does not provide an explanation of this process *per se* since, as a rule, with each cell division both daughter cells obtain the same genetic information.

It appears to be a hopeless enterprise to find a mathematical description (and thus an unequivocal understanding) of a process as complex as the formation of a higher organism. However, it turns out that this process can be separated into many steps that can be regarded, as a first approximation, to be independent of each other. For instance, a very important process for a developing embryo is the formation of the primary embryonic axes. Some signals must be present to determine where to form a head, tail and so on in the initially more or less uniform (usually hollow) sphere of cells. It turns out that for the fruit fly *Drosophila*, for instance,

the anteroposterior axis (head to tail) is under the control of a completely different set of genes than the dorsoventral (back to belly) axis (Nüsslein-Volhard, 1991). Another example of the independence of a structure from the surrounding tissue is the formation of legs. After its initiation, an amphibian leg develops fairly normally even after transplantation to an ectopic position. Its development proceeds under the control of a local coordinate system. Because of this partial independence one can make models of the individual elementary steps. Of course, the steps must be linked together in order to position the individual structures in correct relation to each other. For instance, in a developing organism it is essential that the head-to-tail and the back-to-belly axes are arranged perpendicular to one another, but this is already a refinement. These issues will be discussed in detail in chapter 12.

We have proposed several models of biological pattern formation for specific developmental situations (Gierer and Meinhardt, 1972, Gierer, 1981, Meinhardt, 1982). It came as a surprise to me that the patterns on the shells of mollusks could be described with basically the same equations that were initially derived to describe elementary steps in biological pattern formation, such as the formation of embryonic axes, the head formation of the freshwater polyp *Hydra*, or the initiation of periodic structures such as leaf formation at the tip of a growing shoot. Thus, the shell patterns will be used as a natural picture book to become more familiar with a general mechanism that is the basis for a very important process, biological pattern formation.

1.5 Most shell patterns preserve a faithful time record

In normal development, a strong evolutionary pressure exists to reproduce a given structure faithfully. Moreover, a structure, once formed, usually remains stable at least for a certain time interval. In contrast, the functional significance of the pigment patterns on shells is not clear. Many mollusks live buried in the ground; some are covered with an opaque layer, the periostracum that disappears only after the death of the animal. One hypothesis is that mollusks dispose waste products into their shells (Comfort, 1951). In this view, it would be unimportant whether pigment depositions occur in certain time intervals, permanently at regular distances or in waves that move periodically over the shell-producing mantle gland. Thus, presumably there is no strong selective pressure on a particular shell pattern. The diversity indicates that it is possible to modify the pattern drastically without endangering a species. Nature is allowed to play.

Shells consist of calcified material. The animals can increase the size of their shells only by accretion of new material at the margin, the growing edge. In Figure 1.12 later in this chapter the edge of a shell is clearly to be seen. Most decorations of shells result from the incorporation of pigments during this growth process. Once made, as the rule, the patterns remain unchanged. The patterns are therefore



Figure 1.2. Different modes of pattern formation on shells of *Cypraea diluculum*. The banding pattern results during the growth of the shell by the sequential addition of new material. The pattern is a time record of a linear pattern forming process taking place at the growing edge. The dot-pattern around the opening results from a two-dimensional pattern forming process at later stages. The snail engulfs its shell by an ectodermal protrusion in which the corresponding pattern is generated. Pigment produced in this layer becomes deposited on the shell.

historical records of what happens at the growing edge, i.e., they are a time record of a pattern forming process in a more or less linearly arranged array of cells.

Some shells, however, produce their pattern in a totally different way. Ectodermal protrusions engulf the shells and pattern forming processes within these sheets are copied onto the shell. Thus, in these cases pattern formation results from a two-dimensional process. The pattern represents a snapshot of a particular moment, not a time record. Some snails change from one mode to the other after reaching adulthood. On the shell of *Cypraea diluculum* (Figure 1.2) one can see both types of patterns on the same shell. While the juvenile pattern consists of oblique lines, the later pattern formed around the shell opening consists of isolated dots. Although the patterns look so different, we will see that they can be explained by basically similar mechanisms.

For the purpose of the book, the first type of patterns, those that are generated over the course of time, are most interesting since they bear the historical record of their formation. They provide therein a key for deciphering the underlying pattern forming process. I will deal mostly with this type of pattern.

1.6 Elementary patterns: Lines perpendicular, parallel and oblique to the direction of growth

Shells show an enormous diversity of patterns whereby related species can show very different patterns while nonrelated species can show very similar patterns. The shells shown in Figure 1.3 provide an example: one shell belongs to a snail, the

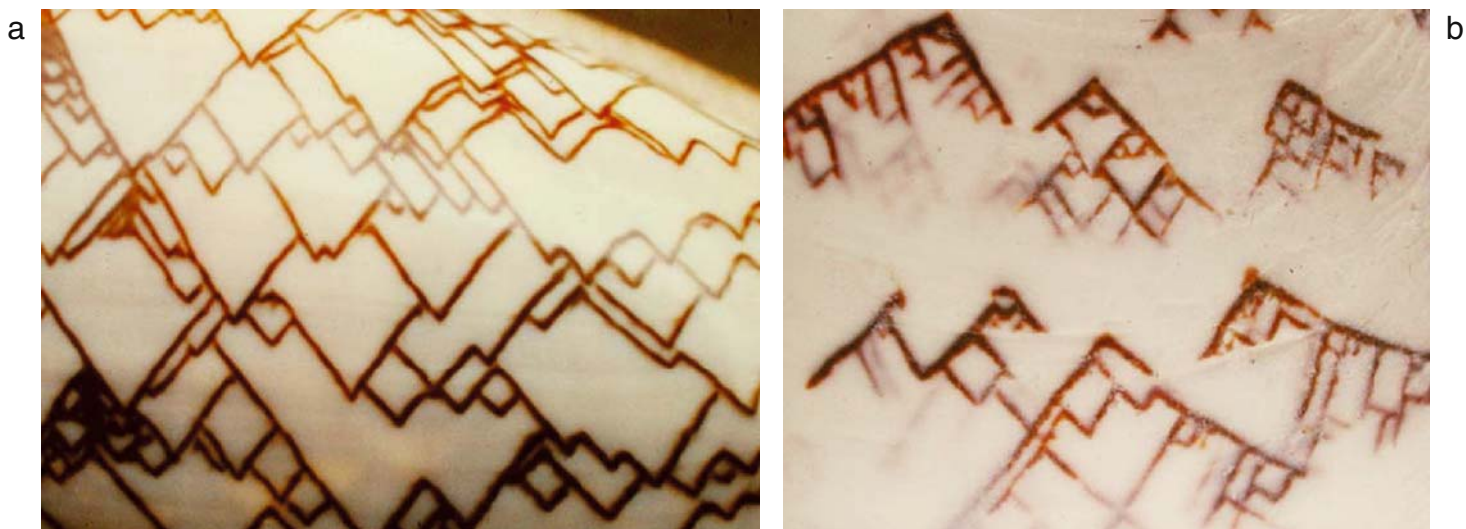


Figure 1.3. Similar pattern on nonrelated mollusks. Details of the shell patterns of *Oliva porphyria* (left) and the bivalved mussel *Lioconcha hieroglyphica*. Both patterns consist of branching oblique lines. The branching occurs frequently at the same level on distant lines indicating that control of branch initiation is a nonlocal process (see Figure 6.1)

other to a bivalved mussel. Both shells show oblique lines that branch. They share a very characteristic element. The initiation of several branches occurs frequently at the same horizontal level, i.e., it can take place simultaneously at distant positions, a feature that will be discussed later in detail. The similarity in nonrelated species indicates that the different patterns are generated by a common mechanism and that the diversity is generated by minor modifications.

To find an inroad into the logic behind these patterns, it is advisable to start with more elementary patterns. Figure 1.4 shows shells with lines parallel and perpendicular to the direction of growth. Keeping in mind the space-time character of the shell pattern, lines parallel to the direction of growth indicate the formation of a spatial periodic pattern of pigment production along the edge that is stable in time. At more or less regular distances, groups of cells in the mantle gland produce permanent pigment while cells in between never do so. This is the usual situation in morphogenesis where particular structures such as leaves, hairs or feathers become initiated at regularly spaced positions.

Other patterns indicate that pigment deposition oscillates. A particular cell produces pigment only during a certain time interval and then enters into an inactive (refractory) period until the next pigment producing phase occurs. A synchronous oscillation in pigment production leads to stripes parallel to the axis. In the example given in Figure 1.4 it can be clearly seen that the oscillations are almost but not completely synchronous. Some regions of the edge are white, others are pigmented. Thus, the synchronization cannot be a result of external influences, like daily or seasonal fluctuations, in contrast to the situation, for instance, in tree rings.



Figure 1.4. Elementary pattern: stripes parallel and perpendicular to the direction of growth. In the upper shell pigmentation has occurred at regular time intervals more or less synchronous. Axial stripes (i.e., stripes perpendicular to the direction of growth) result. In the lower shell pigmentation occurred permanently at regularly spaced positions leading to stripes parallel to the direction of growth.

The mechanisms that lead either to synchronous oscillations or to a stable pattern in space cannot be very different from each other. The specimen at the bottom of Figure 1.4 has on its cone a pattern resulting from oscillations while the main pattern was generated by a stable system. As shown below, a change of the ionic strength in the water can be sufficient to cause a corresponding pattern alternation (see Figure 1.11).

1.7 Oblique lines

Oblique lines originate from traveling waves of pigment production. Such waves arise if pigment-producing cells trigger their neighboring cells so that - after a certain delay - these cells also start to produce pigment and so on, analogous to the formation of the influenza wave mentioned earlier.

Pure elementary patterns - stripes parallel, perpendicular or oblique to the growing edge - are more the exception than the rule. For instance, the perpendicular lines in the lower shell of Figure 1.4 show small gaps at regular intervals suggesting that

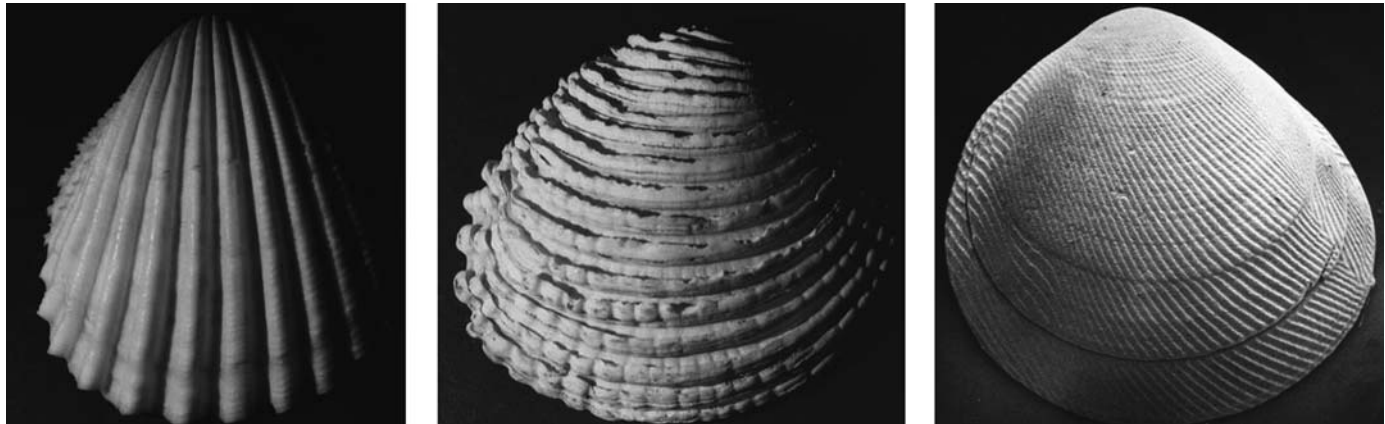


Figure 1.5. Bulges instead of pigmentation: elementary patterns of the relief type showing ripples parallel, perpendicular and oblique to the direction of growth. These ripples have a biological function; they increase the friction of the shell in the sand or mud.

an oscillating pattern was superimposed. The branching of the oblique lines shown in Figure 1.3 indicates that the traveling waves involved in shell patterning can have unusual properties. At a certain moment, a wave can split producing a wave that moves backwards - a process that never occurs, for instance, in a nerve pulse that travels along a nerve fibre.

1.8 Relief-like patterns follow the same rules

Pigmentation is not the only possible decoration on shells. Relief-like structures are also very frequent. The same elementary patterns as listed above occur. Figure 1.5 shows corresponding examples.

As a rule, relief-like patterns are less complex and more reproducible from specimen to specimen. Relief-like patterns also have biological functions. For bivalved mussels, the rough surface increases the friction with the sand during the opening and closing of the two shells and facilitates in this way burrowing into the sand or mud. As shown by paleontological work (Seilacher, 1972), species that originally appear different can develop towards similar shapes and surface structures if they populate the same habitat and are forced to behave in a similar way. Therefore, in contrast to pigmentation patterns, relief-like patterns seem to be shaped by strong selective pressure.

1.9 Many open questions and some hints

Very little is known about the mechanisms that lead to shell patterning. The models worked out in this book can only describe which type of interaction could in principle account for such patterns. No information can be obtained about the chemical nature of the substances involved. Sometimes two different models can reproduce the natural counterpart with reasonable agreement. Usually, however, related species with similar patterns are available that can be described much better by one or the other mechanism. Therefore, the model's handling of natural variability provides one of the criteria for its quality.

Some shells show very particular features that are helpful in getting ideas about the underlying mechanism. Some examples will follow.

Occasionally shells show an obvious perturbation of the normal pattern. A traumatic event must have happened in the animal's history such as temporary dryness, lack of food or injury by a predator. After such a perturbation, the pattern may be very different for a long period. There is strong support for a model that is able to account not only for the normal pattern but also for the pattern regulation after such a perturbation. Several examples will be given later on.

Since the shell grows in several rounds around the axis, parts of the progressing shell formation are in direct contact with parts formed in a previous round. On some shells oblique lines extend from an older (inner) region to a newer (outer) winding without major discontinuity (Figure 1.6). This indicates that an existing pigmented region, if touched by a growing mantle gland, can initiate a traveling wave of pigment production on the newly formed portion of the shell. The result is that both stripes appear in register. These snails can "taste" the old stripe. Such tasting has been proposed by Ermentrout *et al.* (1986) for other reasons, namely to account for the sometimes very long periods in the oscillation of pigment depositions.

A very interesting phenomenon can be seen on the right shell of Figure 1.6. There, only every second oblique line is in register with an old line. Obviously, the spontaneous oscillation frequency was too high during the last round of growth. Only every second initiation of pigment production could be triggered by the old pattern while in between a spontaneous trigger took place.

Similarly, on bivalved mollusks, a synchronization can take place between shells such that the two shells become mirror-symmetric to each other. Figure 1.7 shows two pairs. Obviously, some cross-talk took place between the two shell-producing mantle glands. If one produces pigment, the other produces pigment too. This, however, takes place only if relatively coarse patterns are generated. If more detailed patterns are formed, both patterns may have common features but the details may be different. Figures 5.1 and 5.8 show two complementary and more complex shells.

Sometimes it is difficult to decide what is pattern and what is background. The two shells in Figure 1.8 show dots. One shell carries pigmented dots on



Figure 1.6. An existing pigment pattern can trigger the formation of a new one. Oblique lines are frequently in register on parts of the shell that have been formed during the preceding round of shell growth. The arrows mark some instances. This can only be interpreted by the assumption that in the pigment-forming mantle gland the previously deposited pigmentation is detected, which activates, in turn, the new pigmentation. In these cases, traveling waves are initiated. In the right shell only every second line continues (arrows).

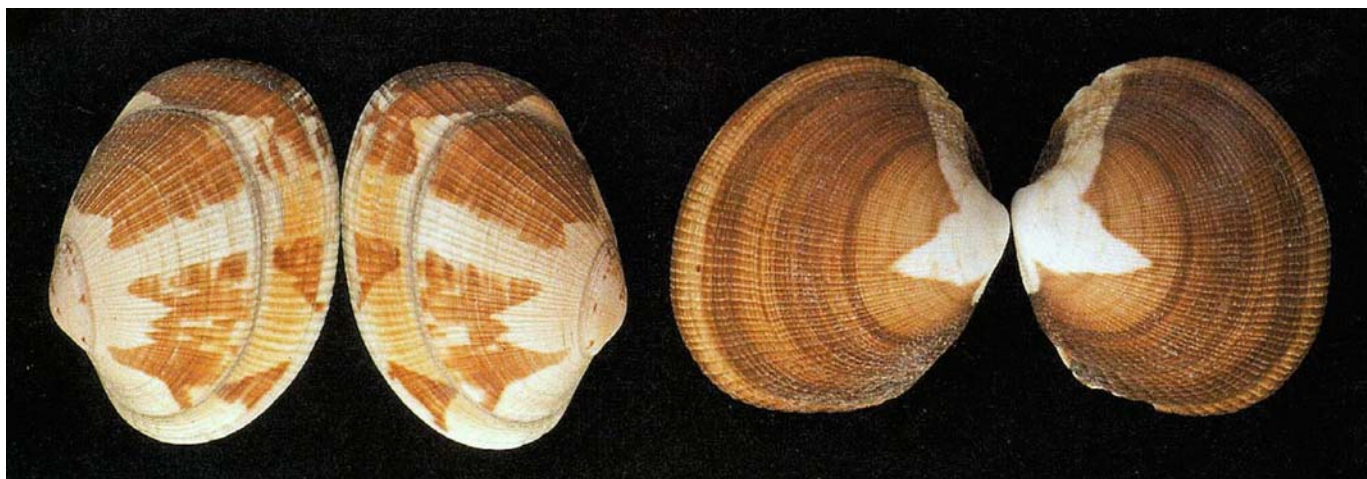


Figure 1.7. Mirror-symmetry in bivalved shells of mollusks. Some cross-talk must take place between the two shell-producing glands such that pigment formation on one shell triggers pigment formation on the other. Finer patterns have common features but are different in the details.



Figure 1.8. Figure and ground: Staggered dots in reverse pigmentation on *Babylonia papillaris* and *Neritina natalensis*. Finer details, for instance, the dark border at the lower edge of the white patches (insert) indicate that the two patterns depend on different mechanisms.

less-pigmented background; on the other shell the situation is the reverse. The similarity could indicate that a common mechanism generates a signal, but the two mollusks make different use of that signal. In one case the signal promotes, and in the other case the signal inhibits pigmentation.

However, a detailed inspection reveals more differences. The unpigmented patches on the right shell show narrow, very dark borders at their lower edge and the pigmented background has a fine structure of densely packed narrow lines. It is an extreme form of a general pattern that will be treated in detail further on (see Figure 9.7). The common feature is the offset of a particular pattern element along the space and time coordinates. But this feature can be achieved by several mechanisms that differ in their degree of complexity.

Other shell patterns indicate that two interacting systems are involved. For instance, on the shell of *Conus zeylanicus* (Figure 1.9) rows of dark, crescent-like patches are visible. The patches within a row are at very irregular distances from each other. A closer inspection reveals that the irregularity results from a random alternation of the pigmented patches with patches that are significantly less pigmented than the light gray background. Thus, two signals seem to be produced, one that causes pigmentation and another one that suppresses pigmentation. The irregularity excludes the idea that the dark and white patches result from a single oscillating system at different stages of the cycle. However, some coupling between the two systems must exist since the dark and the white spots always keep a certain distance from each other.

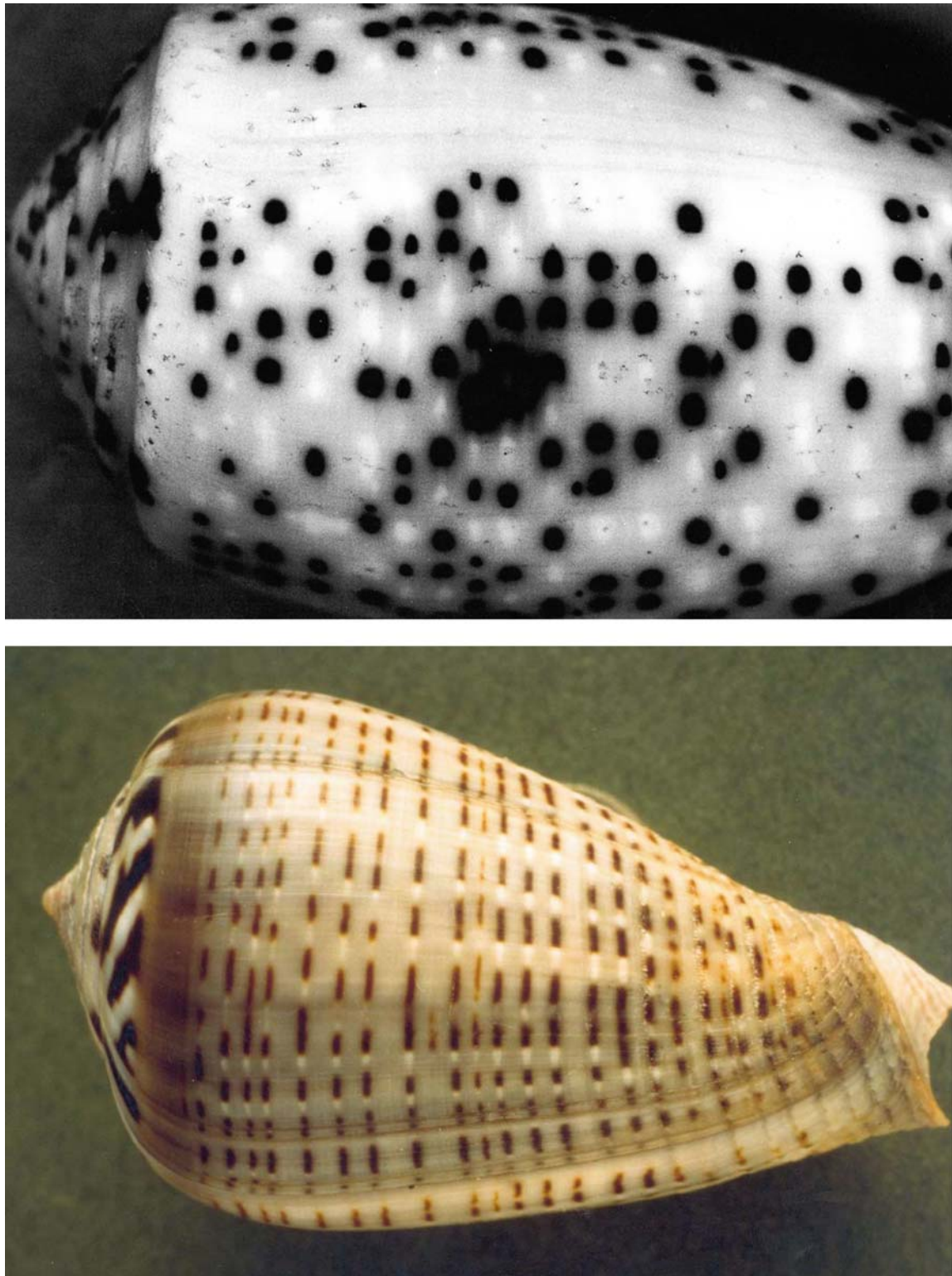


Figure 1.9. Alternation of dark and white regions. The alternating pattern is restricted to particular stripes. On the upper shell, *Conus zeylanicus*, dark pigmentation and pigmentation lighter than the grey background alternate in a more irregular fashion. On the bottom shell this alternation is more regular, although some brown stripes are not followed by a white stripe. These patterns indicate the involvement of two different signal systems, one that enhances and another that suppresses pigmentation.



Figure 1.10. Global oscillations and pigmentation pattern. The modulation of the background in the left shell indicates a global oscillation that controls or synchronizes the dark pigmentation, causing the ladder pattern. In the right shell some pigmentation lines are occasionally shifted against each other. This indicates the absence of global control. Also no background modulation is visible. Thus, even in related species the pattern forming mechanism can be different. The synchronizing influence of a global oscillation on pigment deposition is responsible for several other phenomena (see Figure 4.14).

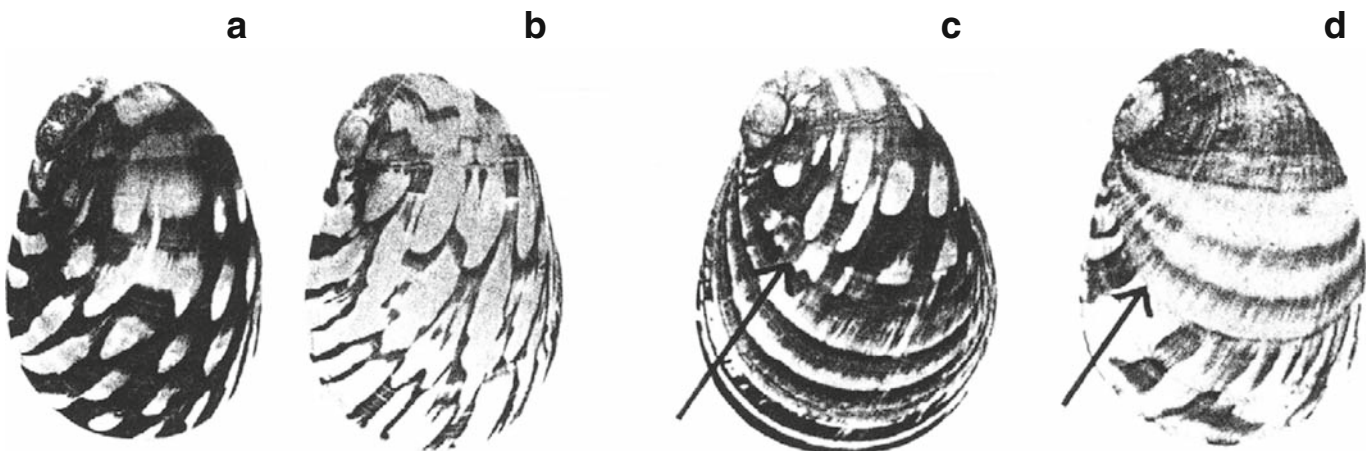


Figure 1.11. Modification of shell patterns by changes in the ionic strengths. (a, b) Variants of a fresh water snail with dense and sparse shell pigmentation, kept at low ionic strengths. (c, d) Dramatic pattern modifications after changes in the salt concentration in the aquarium, either from low (freshwater) to high salt concentrations (0.37%) or (d) from high to low salt concentrations. Arrows indicate the time of change. (Photographs kindly supplied by D. Neumann, see Neumann, 1959b)

Another example where a faint pigmentation provides some hints of the mechanism is given in Figure 1.10. Parallel lines are framed by oblique lines, providing an overall impression of connected triangles. A closer inspection of the yellowish background reveals that there is a modulation in the same phase as the dark horizontal lines. Obviously, a global oscillation exists that acts either as a precondition or it modulates the oscillation that causes the darker pigmentation. As a note of precaution, the second shell of Figure 1.10 is a related species with a similar pattern. In this shell, however, the horizontal lines are partially out of phase. No synchronization by a global oscillation and no modulated background can be seen. Therefore, even in related species it is dangerous to generalize too much.

Little experimentation has been reported with shell patterns. The pattern of the freshwater snail *Theodoxus fluviatilis* depends on the salt concentration (Neumann, 1959a-c). In Germany, waste water with high salt concentrations from potassium mining is introduced into the river Werra. He found pattern changes downstream from the waste water dispersal. These pattern changes can be reproduced in the laboratory. Figure 1.11 shows the pattern after a shift from high to low salt concentrations and *vice versa*. Obviously, there is no strong regulatory system in the animal to maintain its typical pattern. To the contrary, all the examples mentioned above indicate that the pigment-producing system is very sensitive. A change in the external conditions, an influence from pigmentation laid down earlier or from the shell counterpart can modify pigment production.

1.10 The hard problem: complex patterns

Many shells show highly complex patterns. The shell of *Conus textile*, Figure 1.12, provides an example. The complexity is not without rules. Some regions show a light brown, others a white background. Darker oblique lines are visible whose general characters depend on the background, more faint in the white but thicker in the light brown region. Moreover, there is a strong tendency to change from parallel lines (synchronous oscillation) in the brown region to oblique lines (traveling waves) that branch in the white region. Keeping the space-time character in mind, it is clear that the transition from white to brown is preceded by a dark brown line, while the brown-white transition is not. The faint oblique lines in the white region frequently have their origin in a thick dark line in the brown region. The brown-white transition occurs usually simultaneously in an extended region, causing a light brown white border parallel to the edge.

This complexity cannot result from a single pattern-forming reaction. Two or more reactions must be superimposed that influence each other. Usually only one pattern, the pigmentation, is visible. A second pattern that modifies the pigmentation pattern may be invisible but must be deduced from the unusual behaviour of the pigmentation pattern. In the case of *Conus textile* the light brown pattern is presumably an exception in that a visible trace of the second pattern



Figure 1.12. An example of a complex pattern: *Conus textile*. Two pigmentation systems appear to be superimposed. Light brown pigmentation occurs preferentially in two bands that cover large regions. In addition oblique lines with a much darker pigmentation exist. The dark pigmentation system is influenced by the light one. In the light brown region the dark brown pigmentation lines are much thicker and are preferentially oriented parallel to the growing edge. In regions with nonpigmented background the dark lines are much narrower.

system exists. The different behaviour of the pigment system - synchronous oscillations *versus* traveling waves depending on whether the light brown pattern is in the ON or OFF state - suggests general modifications of one system by the other. The problem in understanding complex patterns lies in the enormous number of combinatorial possibilities between two or more systems. Each component of one system can activate or suppress another; the influence may involve changes in the production or destruction rates; and so on. The simulation of the complex patterns provided in this book should be regarded only as an attempt to decipher the complex interaction and as an invitation to search for other possibilities.

1.11 Earlier attempts to understand shell patterns

Several attempts to model patterns on mollusk shells have been made. Formal models have been proposed by Waddington and Cowe (1969) for the tent-like patterns of *Oliva* shells and by Lindsday (1982) for bivalved mollusks. Cellular automata models have been discussed by Herman and Liu (1973), by Wolfram (1984) and by Plath and Schwietering (1992). Wanscher (1971) tried to explain shell patterning by a shielding mechanism between the pigment-producing mantle gland and the periostracum, the side of pigment deposition. The white drop-like nonpigmented regions in *Conus textile* (Figure 1.12) or in *Conus marmoreus* (Figure 7.3) have been discussed as an example. The idea of using reaction-diffusion mechanisms to model shell patterns dates back to 1984 (Meinhardt, 1984). A model based on similar interactions but emphasizing the role of the nervous system was proposed by Ermentrout, Campbell and Oster (1986; see also Murray, 1989). Many of the ideas outlined in this book were first published by Meinhardt and Klingler (1987).

In the next two chapters, a general theory of biological pattern formation will be outlined and applied to shell patterning. The elementary patterns result from a straightforward application of this basic theory. In subsequent chapters extensions of the elementary mechanisms will be discussed that account for the many unusual features of these beautiful pattern forming systems.



Figure 2.1. Patterns stable in time and their traces on shells. Stripes perpendicular to the growing edge, i.e., parallel to the direction of growth, result from stable pigment production at a particular position and its suppression at locations in between. In the lower shell, different sets of stripes are formed on the inner and the outer surface of the shell. On the outer pattern, the stripes are formed in pairs. An explanation for this phenomenon will be given in Figure 2.4f. (*Conus loroisi*, top, and *Neptunea lyrata*)

Pattern formation by local self-enhancement and long range inhibition

Like other biological processes pattern formation is based on the interaction of molecules. In order to find a mathematical description for a particular process the concentrations of the substances involved must be described as a function of space and time. This is possible by using equations that describe the *changes* in concentration over a short time interval as a function of other substances. Adding these concentration changes to given initial concentrations provides us with the concentration at a somewhat later time. Repetition of such a calculation provides the total over the course of time. Three factors are expected to play a major role in the concentration change: the rate of production, the rate of removal (or decay), and the loss or gain due to an exchange with neighboring cells, for instance by diffusion.

As mentioned earlier, we have proposed that pattern formation starting from initially more or less homogeneous conditions requires local self-enhancement coupled with a long range antagonistic effect (Gierer and Meinhardt, 1972, Gierer, 1981, Meinhardt, 1982). Patterns are formed because small deviations from a homogeneous distribution create a strong positive feedback which causes the deviations to grow even more. A long-range antagonistic effect restricts the self-enhancing reaction and causes a localization.

2.1 The activator – inhibitor scheme

The scheme of a biochemically feasible realization of this general principle is shown in Figure 2.2. A short-range substance, the activator, promotes its own production (autocatalysis) as well as that of its rapidly diffusing antagonist, the inhibitor. The concentrations of both substances can be in a steady-state. A general increase in the activator is compensated by an increase in the inhibitor concentration. However, such an equilibrium is locally unstable. Any *local* increase of the activator will increase further due to autocatalysis despite the fact that a surplus of inhibitor is also produced by this local increase. It diffuses rapidly into the surroundings and slows down the autocatalysis while the local activator elevation increases further (Figure 2.2). A set of partial differential equations is given in Equation 2.1

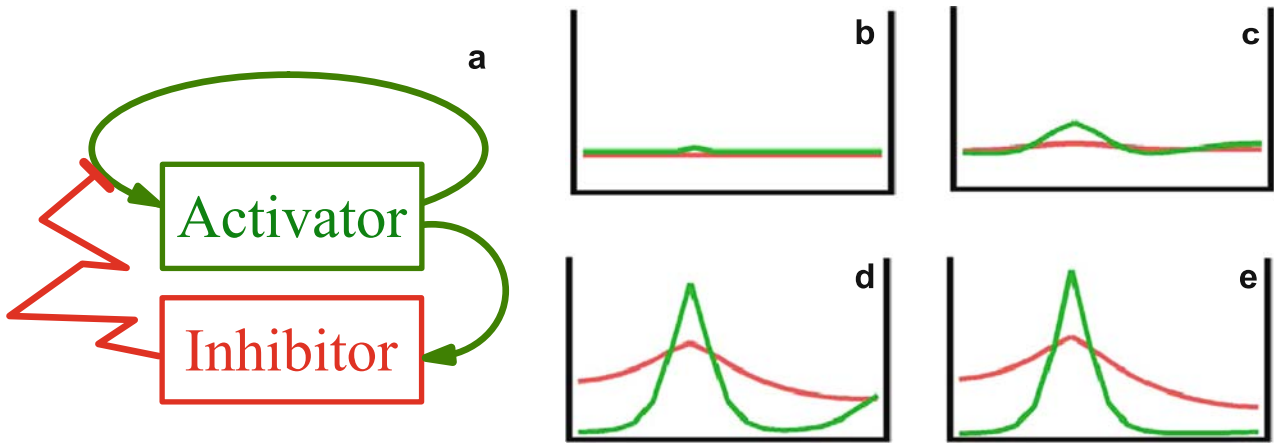


Figure 2.2. Pattern formation by autocatalysis and long-range inhibition. (a) Reaction scheme. An activator catalyses its own production and that of its highly diffusing antagonist, the inhibitor. (b-e) Stages in pattern formation after a local perturbation. Computer simulation in a linear array of cells. A homogeneous distribution of both substances is unstable. A minute local increase of the activator (green) grows further until a steady-state is reached in which self-activation and the surrounding cloud of inhibitor (red) are balanced [S22, GT29].

(see box on page 23)¹. In terms of these equations the crucial condition for pattern formation is that the diffusion of the inhibitor is much higher than that of the activator, i.e., the condition $D_b \gg D_a$ must be fulfilled. As shown by Granero *et al.* (1977) the inhibitor must diffuse at least seven times faster. A simple calculation is given in Equations 2.2 (page 24) that should provide some intuition into why this interaction can generate stable patterns starting from nearly homogeneous initial conditions.

2.2 Stable patterns require a rapid antagonistic reaction

Patterns that are stable in time for a certain period are most common in biological pattern formation. They are required, for instance, in the early development of an embryo when the anteroposterior (head to tail) and the dorsoventral (back to belly) axes are determined. These signals may disappear once their purpose is fulfilled, but they should not reappear in a periodic manner in different positions. On shells, stable patterns lead to permanent pigment production in some positions and its suppression in between. This leads to an elementary pattern of stripes parallel to the direction of growth. Examples are given in Figure 2.1 In normal biological pattern formation a strong selective pressure exists to maintain a decision once it is made, for instance to form a head at a particular position. No such preference for stable

¹ The names of parameters are partially changed from our previous publications in order to use identical names in the equations and the computer program (see chapter 11).

patterns exists on shells. Therefore these stripes are only one pattern among many others.

In order for a pattern to become stable over time the antagonist must react very quickly to changes in activator concentration. Otherwise oscillations will occur, a mode that is also of special significance for shell patterning (see chapter 3). A rapid adaptation of the antagonist regulates any deviation from a steady-state concentration. In the activator - inhibitor scheme this means that the inhibitor must have a higher turn-over rate than the activator in order for a rapid adaptation of the inhibitor concentration to be possible. In terms of Equation 2.1, the rate of decay or removal of the inhibitor r_b must be larger than that of the activator, *i.e.* the condition $r_b > r_a$ must be satisfied for stable patterns.

In the following section, the properties of reactions under these conditions will be discussed. At the end of the chapter, other molecular feasible realizations using the same principle will be given.

The best way to intuitively understand these mechanisms is to experiment with some of the computer simulations, changing parameters and conditions and observing the outcome. The program accompanying this book provides the tools required for this. For most of the simulations shown, prerecorded parameter files are available. The commands for starting the computer simulations are given in the figure captions. For instance, the command S23a and S23b will produce the simulations shown in Figure 2.3 (for details of the computer simulations see chapter 11).

2.3 Periodic patterns in space

If the range of the antagonist, *i.e.*, the mean distance between the birth of a molecule and its decay, is smaller than the total field, several activator maxima will be formed at more or less regular distances. If we assume that the activator controls pigment production, stripes perpendicular to the growing edge will result, as seen on many shells. A simulation based on the activator - inhibitor scheme is shown in Figure 2.3. The inhibitor maxima are centered around the activator maxima, but have a more shallow distribution. Also, a possible reason for the irregularity in the spacing is clearly visible. Initially, some maxima develop too close together and don't survive the competition with the long-range inhibitor, leaving irregular-sized gaps in between. Since each maximum is surrounded by a cloud of inhibition, the maxima will not be shifted in order to form a more regular pattern.

Patterns in which particular structures are formed at more or less regular distances are common in many morphogenetic situations. The regular initiation of leaves on a growing shoot, the spacing of bristles, feathers and hairs may serve as examples. One case of a periodic pattern in a one-dimensional array of cells is the formation of heterocyst in the blue-green algae *Anabaena* (Wilcox *et al.*, 1973).

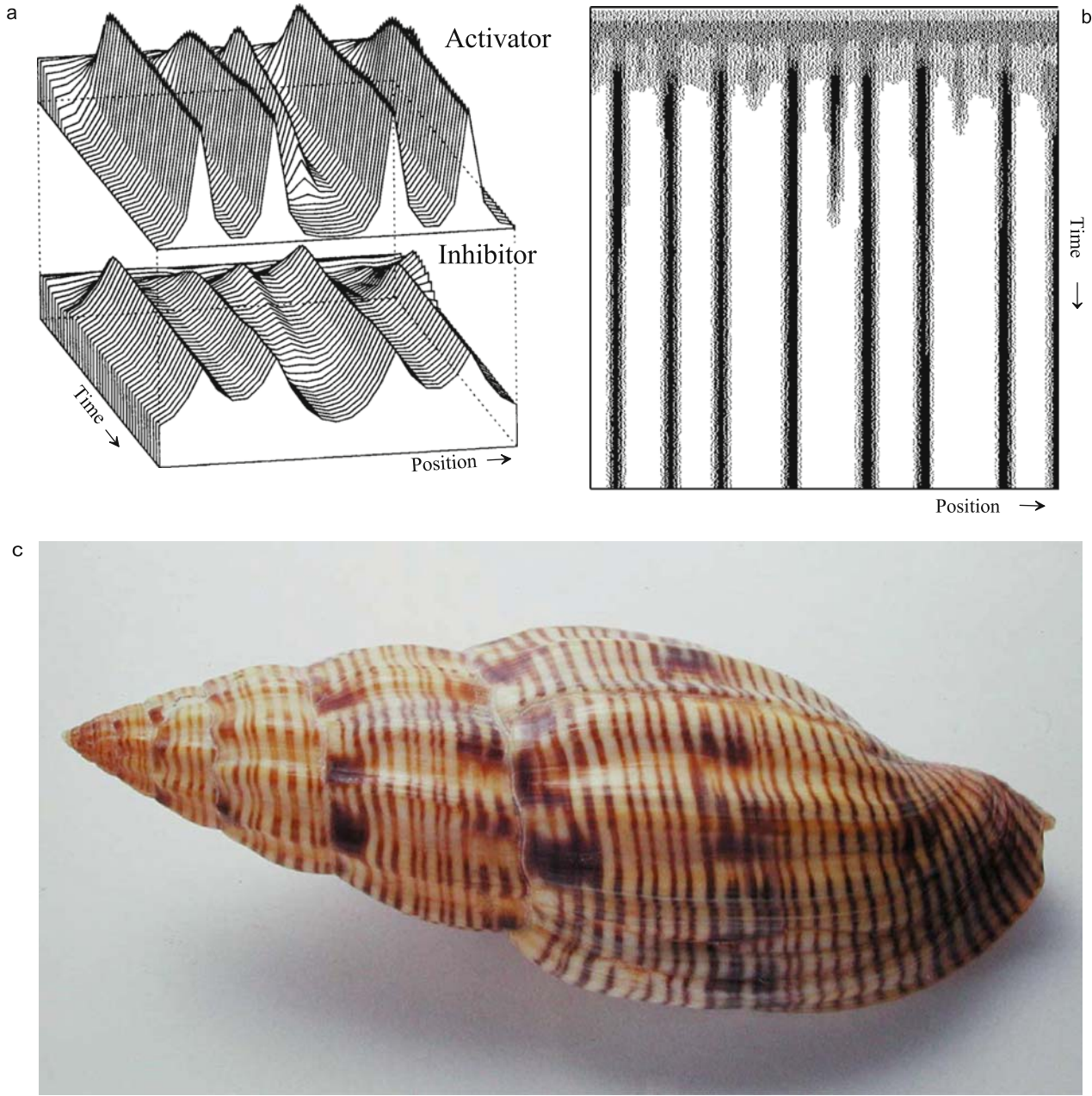


Figure 2.3. Stable periodic patterns in space. (a) Computer simulation in a linear array of cells. Concentrations of the activator (top) and the inhibitor (bottom) are plotted as functions of time. Since the size of the field is assumed to be much larger than the range of the inhibitor several maxima are formed. Due to the initiation by random fluctuations the spacing is somewhat irregular. Maxima can appear too close together and some of them will not survive the mutual inhibition. However, a maximum and minimum distance is maintained. The pattern is more regular if pattern formation is already at work during growth (see Figure 2.7). (b) A similar simulation with a space-time plot analogous to that on shells. (c) Shell of *Lyria planicostata taiwanica* [S23a, S23b].

Equation 2.1: the activator - inhibitor system

The following partial differential equations describe a possible interaction between the autocatalytic activator $a(x)$ and its antagonist, the inhibitor $b(x)$. They relate the concentration change per time unit of both substances as a function of the concentration present.

$$\frac{\partial a}{\partial t} = s \left(\frac{a^2}{b} + b_a \right) - r_a a + D_a \frac{\partial^2 a}{\partial x^2} \quad (2.1.a)$$

$$\frac{\partial b}{\partial t} = sa^2 - r_b b + D_b \frac{\partial^2 b}{\partial x^2} + b_b \quad (2.1.b)$$

where t is time, x is the spatial coordinate, D_a and D_b are the diffusion coefficients, and r_a and r_b the decay rates of a and b . A more detailed list of the individual terms will facilitate the reading of the equations.

sa^2/b The production rate. The activator a has a nonlinear autocatalytic influence. For instance, two activator molecules must form a complex in order to satisfy the required nonlinearity. The production is slowed down by the inhibitor b . The source density s describes the ability of the cells to perform the autocatalysis.

$-r_a a$ The rate of removal. The rate at which molecules disappear is, as a rule, proportional to the number of molecules present (like the number of individuals dying per year in a city is proportional to the number of inhabitants).

$D_a \partial^2 a / \partial x^2$ The exchange by diffusion. The exchange is proportional to the second derivative for the following reason. The net exchange of molecules by diffusion is, of course, zero if all cells have the same concentration. But the net exchange is also zero if a constant concentration difference exists between neighboring cells, i.e. in the case of a linear concentration gradient. In this case each cell obtains the same amount of substance from its higher neighbor as it loses to its lower neighbor. In other words, it is not the change of concentrations but the change of concentration changes in space that is decisive in loss or gain by diffusion.

b_a Basic activator production. A small activator-independent activator production can initiate the system at low activator concentrations. It is required for pattern regeneration, for the insertion of new maxima during growth, or for sustained oscillations.

b_b Basic inhibitor production. A small activator - independent inhibitor production can cause a second homogeneous stable state at low activator concentrations. The system can be asleep until an external trigger occurs, for instance an influx of activator from a neighboring activated cell. This term will play a role in the simulation of travelling waves (chapter 3).

Equation 2.2: local instability and global stabilization - a simple calculation

A simple calculation should provide some intuition into why the interaction given in (2.1) can lead to stable patterns. For simplicity, we assume all constants are equal to 1, disregard diffusion and assume that even the inhibitor concentration is constant and equals 1. Equation 2.1.a would be simplified to

$$\frac{\partial a}{\partial t} = a^2 - a \quad (2.2.a)$$

In this simplified version, the activator a has a steady-state ($\partial a / \partial t = 0$) at $a = 1$. However, this steady-state is unstable since for any concentration of a larger than 1, $a^2 - a$ will be positive and the concentration of a will further increase and *vice versa*. The reason for this instability lies in the over-exponential autocatalytic production in conjunction with a normal exponential decay. Now let us include the action of the inhibitor. Disregarding again any constants and diffusion, Equation 2.1.b simplifies to

$$\frac{\partial b}{\partial t} = a^2 - b \quad (2.2.b)$$

which has a steady-state at $b = a^2$. If we assume that the inhibitor reaches equilibrium relatively rapidly after a change in activator concentration, this change can be expressed as function of the activator concentration alone:

$$\frac{\partial a}{\partial t} = \frac{a^2}{b} - a \approx \frac{a^2}{a^2} - a = 1 - a \quad (2.2.c)$$

Therefore, if we include the action of the inhibitor, we obtain a steady state at $a = 1$ but this is stable since if a is larger than 1, $1 - a$ is negative and the concentration will return to the steady-state of $a = 1$. To see why an interaction according to (2.1.a,b) can generate a pattern we must take into consideration the fact that the inhibitor is assumed to diffuse much faster than the activator. Let us assume an array of cells in which all cells are at the steady-state concentrations of a and b , except one cell that has a slightly increased activator concentration. It will also produce more of the inhibitor. However, after a small local perturbation the inhibitor concentration remains nearly constant since it diffuses rapidly (Figure 2.2). Thus, it is the average activator concentration that is decisive in inhibitor production. As mentioned, if the inhibitor remains constant, any deviation from the activator steady-state will continue to grow since the steady-state is unstable. However, after a substantial increase of the activator maximum, the inhibitor concentration can no longer be regarded as constant. As shown above, the action of the inhibitor leads to the stabilization of the autocatalysis. A new stable, steady-state pattern will be reached. Thus, the formation of a stable pattern depends on local instability and global stabilization.

Equation 2.3: saturation of autocatalysis

Saturation of activator production can be included in Equation 2.1.a in the following way:

$$\frac{\partial a}{\partial t} = s \left(\frac{a^2}{b(1 + s_a a^2)} + b_a \right) - \dots \quad (2.3)$$

At low a -concentrations, $s_a a^2$ is negligible compared to 1 and the autocatalysis works as outlined above. With an increase in a , the term $s_a a^2$ becomes more dominant. Autocatalysis does not increase further since self-enhancement and slowing down due to saturation both become proportional to a^2 .

When cell division causes the distance between two heterocyst cells to become more than about 7 cells, a new heterocyst is formed in between, corresponding to the insertion of a newly activated region during growth, as shown in Figure 2.7a.

2.4 The width of stripes and the role of saturation

Several factors determine the width of stripes, their distance apart, and the regularity of the distances. The range, i.e. the average distance that a molecule can travel in the time interval between its production and its disappearance depends on its diffusion rate as well as its half life. An increase in the diffusion rate of the activator leads to a broadening of the stripes, while an increase in the range of the inhibitor creates a larger region over which activated cells can suppress other cells from becoming activated. Thus a short range activator and a long range inhibitor would cause very narrow stripes at large distances. An example is given in Figure 2.4.

So far, the only limitations of autocatalysis that have been considered result from the action of the antagonist. It is conceivable, however, that other factors limit the maximum rate of autocatalysis too. For instance, an enzyme required for autocatalysis may be available only in limited amounts. At high activator concentrations the reaction would slow down since all available enzyme molecules would already be occupied. The consequence is a saturation of the autocatalysis since the maximum activator concentration reaches its upper bound (see Equation 2.3). Such saturation has severe influences on the outcome pattern and a comparison between actual and simulated patterns indicates that saturation is frequently involved.

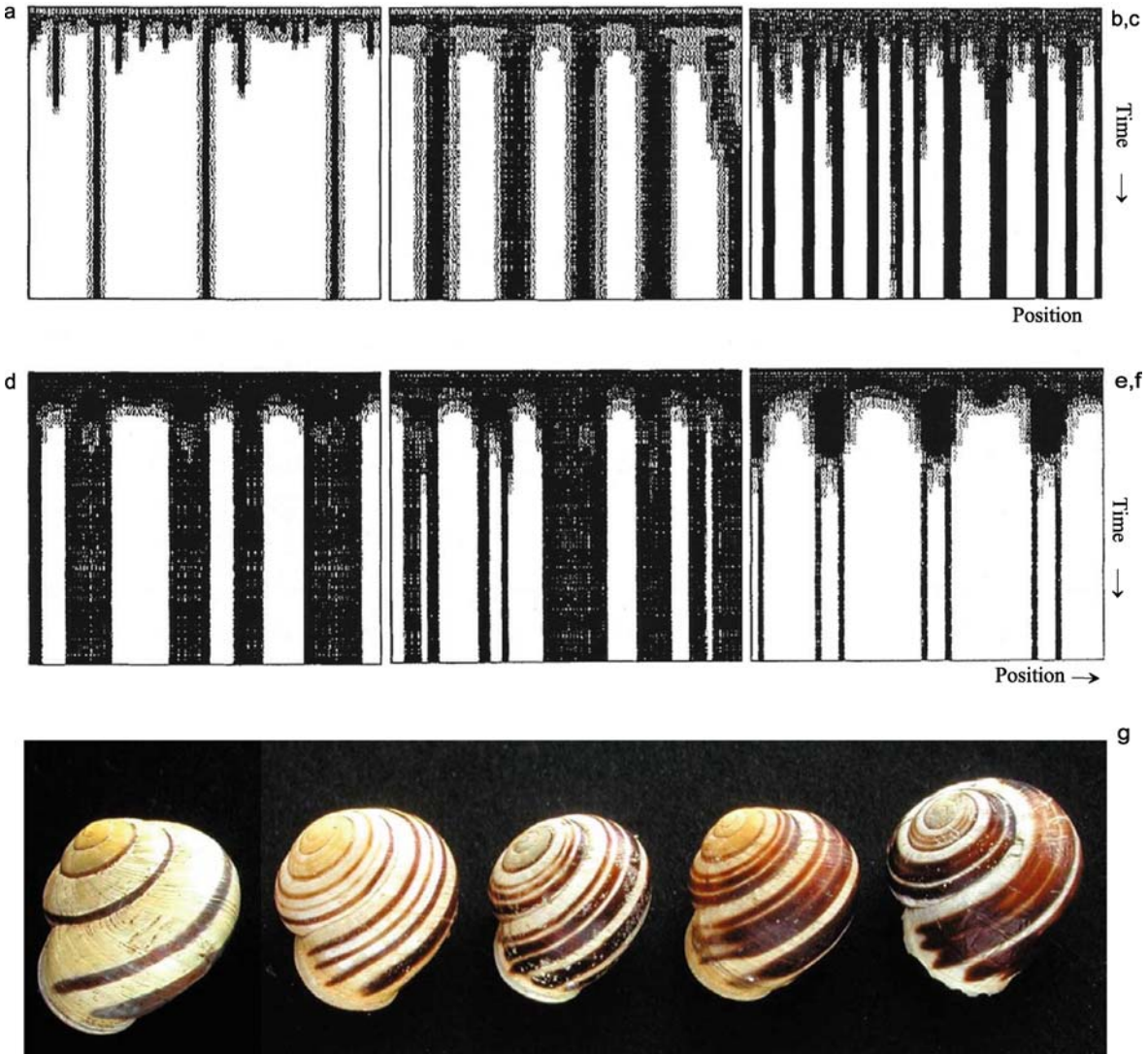


Figure 2.4. The width of stripes and the regularity of distances. (a) A short range activator and a long range inhibitor lead to narrow stripes at large distances. Since a maximum cannot be shifted, the distances are irregular. (b) Higher activator diffusion (D_a from 0.002 to 0.015) causes more regularly spaced broad stripes. (c) Saturation of the autocatalysis (s_a from 0.0 to 0.3) leads to broad stripes of irregular width and spacing. (d-f) Irregular stripes of different width and spacing will result if communication between the cells is switched off at an early stage. Pairs of stripes can arise (compare with Figure 2.1). (g) Stripes of different width on the garden snail *Cepaea nemoralis* [24a - 24d].

If the activator production has an upper bound due to saturation of autocatalysis, the activator concentration cannot surpass a certain level. Therefore, inhibitor production, and thus the inhibitory influence on neighboring cells, is limited as well. The activated region will increase in size until sufficient inhibitor is produced. In large activated regions, the accumulation of inhibitor at the center causes near-instability and the tendency to decay into two smaller maxima. The maxima can be broad although the range of the activator is small. Activator diffusion determines the minimum width of a stripe only. The individual maxima can have different widths. The transition between activated and nonactivated areas can be sharp since diffusion of the activator may be slow. Due to saturation, the ratio between activated and nonactivated cells becomes independent of the size of the field since, for instance, if less than the normal number of cells are activated, the inhibitor concentration will be too low and the activated regions will enlarge until the correct ratio is established. Thus, if activator production saturates, a pattern of broad but irregularly spaced stripes is expected. An example is given in Figure 2.4. With increasing saturation autocatalysis becomes less efficient until pattern formation is no longer possible. Therefore, the activated region cannot become much larger than the non-activated region due to saturation. If the pattern consists of narrow nonpigmented lines in a pigmented background, other mechanisms are expected to be involved (see Figure 2.8).

A further consequence of the saturation of autocatalysis is that a maximum can be shifted relatively easily to a more favorable location. If a portion of the maximum is disfavored, for instance by another activated region in the vicinity, this part of the maximum can become deactivated in favor of a portion that is not subject to this inhibition. An example is provided in connection with an increase in field size due to growth (Figure 2.6).

2.5 Early fixation of a pattern

The stripes on the shells shown in Figure 2.4 have very different widths at irregular distances although they belong to the same species and were found in the same place. This phenomenon could be based on the early fixation of an evolving pattern. Imagine that at an early state the exchange of substances by diffusion ceased, for instance, by closing the gap junctions between the cells. Usually, the nonactivated cells are no longer inhibited and return to the homogeneous steady-state activation. If, however, the inhibitor has an additional small activator - independent production term (b_b in Equation 2.1.b), a second stable steady-state exists at low activator concentrations. All cells above a certain threshold adopt the high steady-state concentration, while the remaining cells adopt the low. The activation of a cell will be faithfully transmitted to the progeny of each cell. During early phases of pattern formation, the pattern is much less regular and depends on accidental initial conditions (see Figure 2.3). If this pattern is frozen by the mechanism outlined above,

Equation 2.4: the activator - depleted substrate system

An antagonistic effect can result from the depletion of the substrate $b(x)$ needed for autocatalysis. The interaction may have the following form

$$\frac{\partial a}{\partial t} = sba^{*2} - r_a a + D_a \frac{\partial^2 a}{\partial x^2} \quad (2.4.a)$$

$$\frac{\partial b}{\partial t} = b_b(x) - sba^{*2} - r_b b + D_b \frac{\partial^2 b}{\partial x^2} \quad (2.4.b)$$

Usually this interaction is used with a saturation term s_a and

$$a^{*2} = \frac{a^2}{1 + s_a a^2} + b_a$$

The following is a description of some of the terms used in these equations:

sba^{*2} The production rate of the activator. The nonlinear autocatalysis is proportional to the substrate concentration b . This production leads to a decrease in b by the same rate $-sba^{*2}$.

b_a Basic activator production. A small activator-independent production can initiate the system at low activator concentrations. It is required for pattern regeneration or for sustained oscillations.

$b_b(x)$ Production rate of the substrate b . Usually this is the same in all cells. However, for the patterns discussed in chapter 4, different rates along the growing edge play a crucial role.

$-r_b b$ A destruction term independent of removal due to autocatalysis. It is not necessary for pattern formation. It limits the maximum substrate concentration in nonactivated regions. If significant, a spontaneous trigger at low activator concentration may no longer be possible, similar to the effect of the term b_b in Equation 2.1.b. It plays an important role in the transition between an excitable system and sustained oscillations (see Figure 3.3).

$s_a a^2$ This saturation term has similar consequences for the activator - inhibitor system as the one discussed in Equation 2.3: maxima become broader and the number of activated cells are a fraction of the total number of cells. For computational purposes, a small saturation term is also helpful in this interaction to avoid numerical instabilities.

it will be much less regular. Figure 2.4d-f show some simulations. Necessarily connected with such mechanisms is the loss of regulatory properties. For instance, the insertion of new maxima during growth is no longer possible. An example is given in Figure 2.6.

A further effect of ceasing diffusion may be the generation of pairs of stripes. Regions with high activator concentration also have high inhibitor concentrations. After an abrupt termination of diffusion, the center of a maximum may become deactivated. Activation survives only in the two marginal regions (Figure 2.4f). A natural example of such a pairwise arrangement of narrow stripes was given in Figure 8.1.

2.6 The activator - depleted substrate scheme

As mentioned earlier in connection with the sand dune example, the antagonistic effect can also result from the depletion of the substrate $b(x)$ that is consumed during production of the autocatalytic activator $a(x)$. A possible interaction is given in Equation 2.4. It is similar to the Brusselator reaction proposed by Prigogine and Lefever (1968) but is somewhat simpler. In order to allow stable pattern formation, sufficient substrate must be supplied to maintain a steady activator production, i.e. $b_b > r_a$. Again, the diffusion of the substrate must be much faster than that of the activator, i.e., $D_b \gg D_a$.

The formation of a periodic pattern by an activator - depleted substrate model is shown in Figure 2.5. For demonstration purposes, rather than random fluctuations in the source density s , a somewhat elevated activator concentration in the leftmost cell is assumed. This cell forms a full maximum, causing a depression in the substrate concentration. A second maximum can develop only at a distance, and so on. The patterning spreads like a wave and the spacing is regular.

As shown below, the activator - inhibitor and the activator - depleted substrate models lead to different patterns in some situations (see Figure 2.7). Although the two mechanisms appear so different in their molecular requirements, they may have ultimately the same basis. The interactions described by Equations 2.1 and 2.4 are idealized. In the activator - inhibitor scheme it is assumed that the activator is produced from a pool of precursor molecules that is infinitely large. Its depletion is assumed to be negligible due to the antagonistic action of the inhibitor. In the depletion scheme, on the other hand, the activator becomes degraded. It is conceivable that a degradation product acts as inhibitor in the autocatalysis due to competitive inhibition with the intact activator molecules. Thus, only minor evolutionary modifications may be required for a change from one regime to the other. We will use both schemes as well as combinations.

The activator - depletion mechanism has an inherent limit of maximum activator production since the activator production comes to rest if sufficient substrate is no longer available. Therefore, patterns generated using this mechanism show

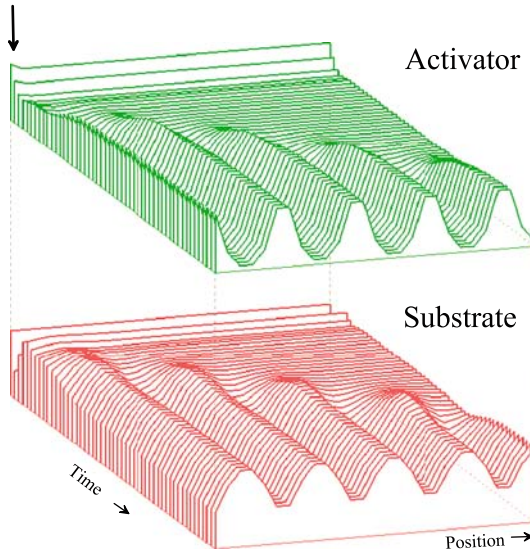


Figure 2.5. Pattern formation based on an activator - depleted substrate scheme. Initiation by a locally elevated activator concentration (arrow). This elevation grows to a full maximum at the expense of the substrate in the surroundings. A further maximum can be formed only at a distance. For demonstration purposes, the general activator concentration is higher than the steady-state. A rapid regulation back to the steady-state occurs [S25, 25a, 25b].

relatively broad maxima that tend to shift into regions in which high substrate concentrations are still available. Therefore, the spacing is generally more regular. The width of the maxima is of the same order of magnitude as the space that separates them. In contrast, in the activator - inhibitor system the activated region may be only a small portion of the total field (see Figure 2.7).

2.7 The influence of growth

In the generation of many shell patterns, the elongation of the margin due to growth cannot be neglected. By inserting new cells, the distance between pigment producing cells enlarges. This can either cause the insertion of new pigmentation lines or a broadening and branching of existing lines. In all such cases, the ratio of pigmented to nonpigmented regions remains more or less constant. Examples are given in Figure 2.6.

Insertion of new lines indicates the formation of a new activated region between existing maxima. Due to growth, the distance between the activated regions increases too. In the activator - inhibitor scheme large distances between existing maxima cause the inhibitor concentration to become so low that a small activator-independent activator production (b_a , Equation 2.1.a) is sufficient for the onset of autocatalysis (Figure 2.7).

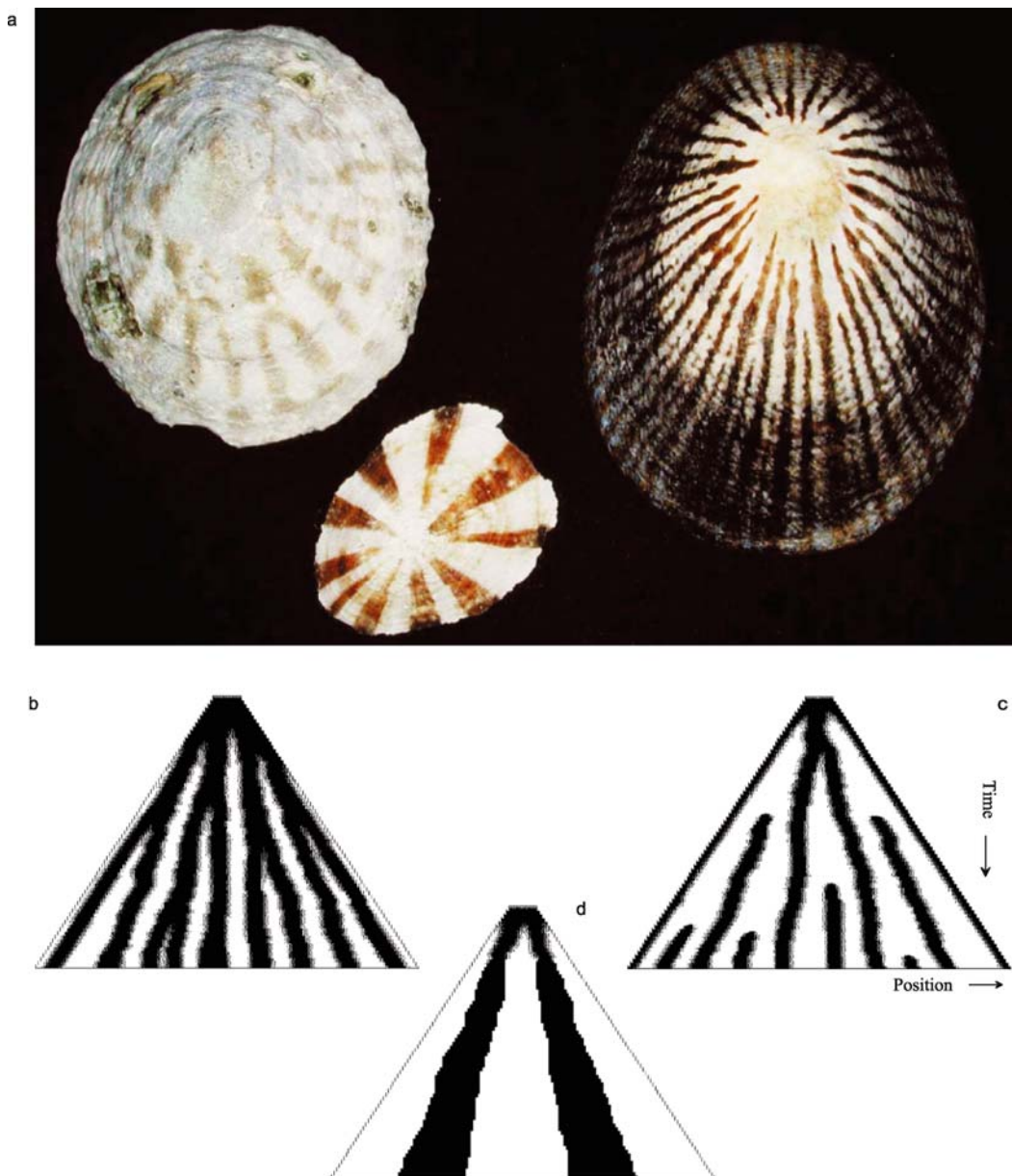


Figure 2.6. Pattern regulation due to growth. (a) Natural patterns: bifurcation of existing lines, insertion of new lines, or a wedge-like widening of existing lines. (b-d) Computer simulations of an activator - inhibitor model. Growth is simulated by the insertion of two new cells, one in each half after a certain time interval. (b) If activator production saturates, the broader maxima become still broader until a split and shift occurs. (c) Without saturation, new maxima become inserted if the distance between existing maxima becomes too large. (d) Wedge-like patterns result if once-activated cells propagate pigment production in a clonal way. In this simulation it is assumed that the activator - inhibitor system is bistable. After an early cessation of diffusion, all cells activated above a certain threshold remain activated while the remaining cells become completely nonactivated [S26b, S26d, S26m]

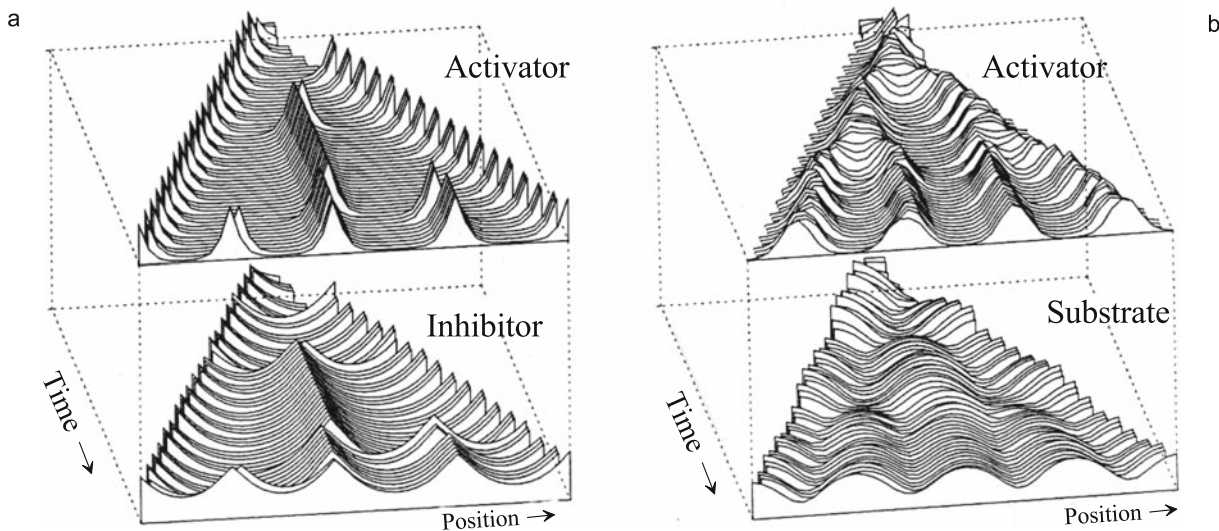


Figure 2.7. Different behavior during growth. (a) With the activator - inhibitor mechanism, new regions become activated if the inhibitor becomes too low to suppress the onset of autocatalysis in the enlarging space between the maxima. (b) By contrast, in the activator - substrate model, a tendency exists to shift existing maxima towards higher substrate concentrations. This shift may be connected with a split of a maximum. With saturation, an activator - inhibitor system behaves in a similar way (see Figure 2.6) [S27a, S27b].

As mentioned above, saturation of autocatalysis leads to a broadening of the stripes. A maximum that is too broad may become deactivated in the center, causing a split in a line. Thus, the shift and split of lines indicate either an activator - inhibitor scheme with saturation (Figure 2.6) or a depletion mechanism (Figure 2.7b) with its inherent saturation. Wedge-like structures emerge if a system is tuned to bistability and the communication by diffusion is switched off at an early stage since the state of activation is kept in the progeny of each cell.

2.8 Inhibition via destruction of the activator

An antagonistic reaction can result not only from the slowing down of the activator production rate, but also from an increase in its destruction rate. Turing (1952) used such a mechanism in his pioneering paper. An example is given in Equation 2.5. Segel and Jackson (1972) have proposed such a mechanism to describe the dynamics and pattern formation of two spreading populations in which one species acts as prey.

Such interaction has several drawbacks in normal pattern formation. If the inhibition results from increased destruction rather than reduced production, much energy would be required for the high turn-over of molecules. Moreover, the range of the activator, i.e., the mean distance between the production and the decay of the activator, changes with the formation of a local activator maximum, since the

Equation 2.5: inhibition via activator destruction

As an alternative to slowing down activator production, the inhibitor may also accelerate activator removal:

$$\frac{\partial a}{\partial t} = s(a^2 + b_a) - r_a b a + D_a \frac{\partial^2 a}{\partial x^2} \quad (2.5.a)$$

$$\frac{\partial b}{\partial t} = s a^2 - r_b b + D_b \frac{\partial^2 b}{\partial x^2} + b_b \quad (2.5.b)$$

$s a^2$ Production rate. In contrast to Equation 2.1.a, it is independent of inhibitor concentration.

$-r_a b a$ Rate of activator removal is proportional to the number of activator *and* inhibitor molecules.

inhibitor also increases and the lifetime of the activator becomes reduced. Therefore, the width of the peaks would shrink. As shown in the next chapter, a shortening of the activator lifetime may cause a transition to oscillating patterns. This is certainly not desirable for pattern formation during normal embryogenesis. But in shell patterning where oscillating patterns play an essential role, this mode cannot be ruled out.

2.9 Autocatalysis by an inhibition of an inhibition

The activator - inhibitor mechanism as given in Equation 2.1.a,b is, of course, only one example of the many possible molecular realizations that satisfy the general requirements of the theory. Pattern formation does not require a molecule with direct autocatalytic regulation. Autocatalysis can be a property of the system as a whole. For instance, if two substances, a and c exist and a inhibits c and *vice versa*, a small increase in a above an equilibrium leads to a stronger repression of c production by a . This, in turn, leads to a further increase of a , in the same way as a would increase if it were autocatalytic. The same holds for c . a and c together form a switching system in which either a or c is high. The switch of the λ phage between the lytic and lysogenic phase is based on such an inhibition of an inhibition (Ptashne et al., 1980). To allow pattern formation, a long range signal is required that interferes with the mutual competition, i.e., with the indirect self-enhancement of one or the other substance. For instance, if a has won the a - c competition in a particular region, c must win in the surrounding regions. A possible realization

Equation 2.6: indirect autocatalysis by an inhibition of an inhibition

Autocatalysis may result from the interaction of several molecules. In this case it results from an inhibition of an inhibition

$$\frac{\partial a}{\partial t} = \frac{s}{s_a + c^2} - r_a a + D_a \frac{\partial^2 a}{\partial x^2} + b_a \quad (2.6.a)$$

$$\frac{\partial b}{\partial t} = r_b a - r_b b + D_b \frac{\partial^2 b}{\partial x^2} \quad (2.6.b)$$

$$\frac{\partial c}{\partial t} = \frac{s}{s_c + a^2/b^2} - r_c c + D_c \frac{\partial^2 c}{\partial x^2} \quad (2.6.c)$$

- a,c Two substances that inhibit each other's production. Together they form a switching system in which one of the substances becomes fully activated.
- b The rapidly diffusing substance required for pattern formation. It undermines the inhibition of *c* production by *a* molecules and therefore acts as an inhibitor.
- s_a, s_c These constants determine the lowest level of *a* and *c* concentration. In this way they also determine the maximum concentration a substance may reach and function similar to the saturation term s_a in Equation 2.3. A more general discussion of possible mechanisms and their equivalences is provided by Gierer (1981).

would be that the *a* molecules control the production of a substance *b* which, in turn, either inhibits *a* or promotes *c* production. These modes are equivalent since self-limitation in competing systems is equivalent to support for the competitor. In Equation 2.6 an interaction is described in which the diffusible antagonistic substance *b* is produced under control of *a* molecules and undermines the repression of *c* production by the *a* molecules. The *b* molecules may be a decay product of the *a* molecules. No direct autocatalytic interaction is assumed.

As mentioned in the introduction, similar patterns may be formed with reverse pigmentation, i.e., white lines on a pigmented background. In the mechanism just described, *a* and *c* complement each other. In some mollusks *a*, while in others *c* may be used as a signal to induce pigmentation. With an otherwise unchanged mechanism, a pigmented pattern on a nonpigmented background would be formed, or *vice versa* (Figure 2.8).

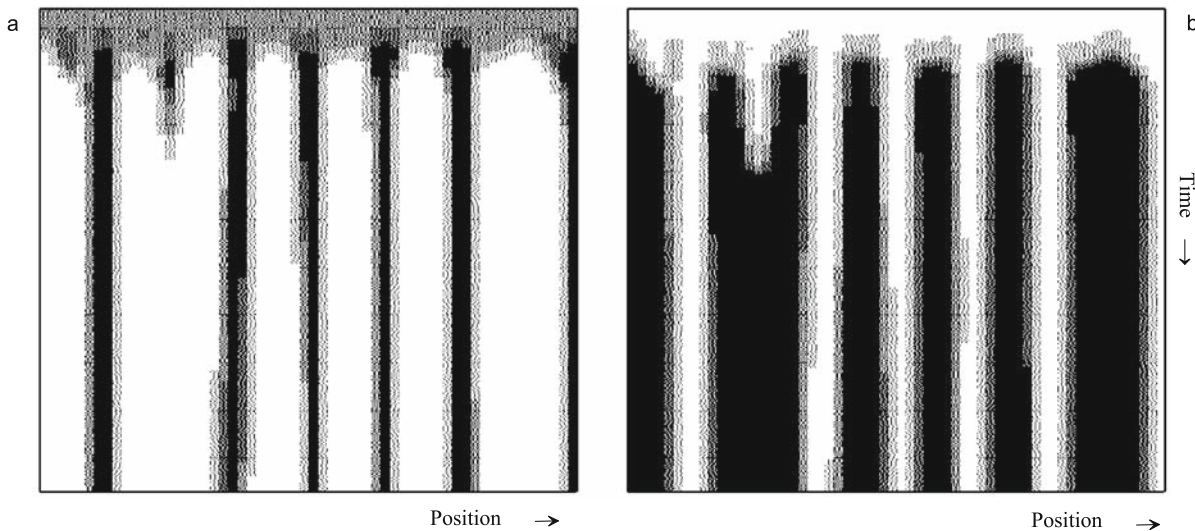


Figure 2.8. White pattern on a dark background. Two complementary distributions result if the autocatalysis is caused by the mutual inhibition of two substances (a and c in Equation 2.6). Depending on the substance that is used to trigger pigmentation, the pigmented region can be larger than the non-pigmented one [S28]. The formation of the famous Spemann-organizer can be explained by such a mechanism (see Figure 12.7 and GT127)

2.10 Formation of graded concentration profiles

The growing edge of a shell has been treated as a line and all cells along this line as equivalent. However, shells of snails are strongly asymmetric. One side usually forms the cone while the other side forms a finer tip and the opening for the siphon. The pattern formed along the edge frequently shows systematic nonuniformities, for example, two bands of stronger pigmentation at particular positions (see Figure 1.12). The cells, therefore, require some information about their position along the growing edge, where the shoulder or stronger pigmentation must be formed. This is a very general problem in early embryogenesis when the primary body axes are to be established.

Polar concentration profiles are formed if the range of the activator is comparable with the size of the field. A critical size must be exceeded in order for pattern formation to be possible since a rapid redistribution of the activator within a small field would wipe out any pattern. When this critical size is reached, only a polar pattern can emerge since a central maximum would require space for two slopes - a space that is not available at the critical size. Therefore, a high concentration appears on one side and a low concentration at the maximum distance (Figure 2.9). Thus, the mechanism allows the generation of a polar pattern even if the initial situation was almost uniform - a most-important step in early development of organisms. The local concentration of the activator and/or the inhibitor can provide positional information (Wolpert, 1969) about where a cell is located. A graded profile, once formed, can be maintained if the formation of secondary maxima is suppressed.

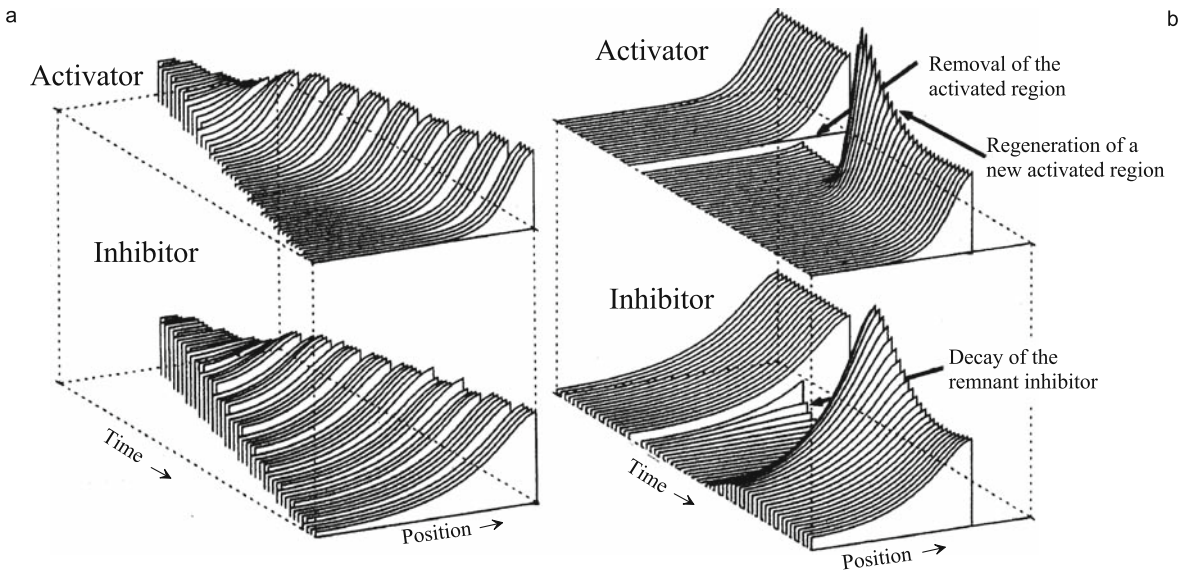


Figure 2.9. Generation of a polar pattern and its regeneration. (a) After the field has grown to a size comparable to the range of the activator, small random fluctuations in the cells performing the autocatalysis (the source density s in Equation 2.1) are sufficient to initiate pattern formation. At this critical size only one marginal maximum can be formed. The result is a polar pattern that can be used as positional information. For this simulation an activator - inhibitor mechanism was used; an activator - substrate model is less convenient for generating gradients due to the tendency of a maximum to shift towards higher substrate concentrations (see Figure 2.7). (b) After removal of the activated region, a new activator maximum can be formed once the remnant inhibitor has decayed [S29; GT29; program XY: S22c].

One possibility is that the basic activator production b_a is low and a basic inhibitor production b_b exists (Equation 2.1). This can suppress the trigger of a new activation. A more elaborate mechanism employs a feedback of the pattern on the ability of the cells to perform the pattern-forming reaction. Cells distant to an activated region lose the competence to perform the self-enhancing reaction. This enlarges dramatically the range of dominance of an existing maximum, and a polar pattern is maintained despite of substantial growth (see Figure 12.5).

Since a homogeneous activator - inhibitor distribution represents an unstable situation, any inhomogeneity can initiate pattern formation; even random fluctuations are sufficient. Any small asymmetry in the ability of the cells to perform the pattern-forming reaction (source density s in Equation 2.1) can orient the emerging pattern. The asymmetry can, but need not be, specific. A slightly higher oxygen supply, pH or temperature on one side would be sufficient. Local disadvantages cause the formation of the maximum at the opposite side. In many systems maternally supplied determinants impose rather strong asymmetries. According to the model, such asymmetries only orient the emerging patterns. Due to self-regulation, the resulting pattern is fairly independent of the initial stimulus. Therefore, no precision is required in the trigger. A stronger initiating asymmetry has the advantage that the pattern reaches the final steady-state much faster since no time-consuming competition is required between distant regions. A strong



Figure 2.10. Examples of shell patterns generated by a two-dimensional process. The mollusks engulf their shells with two ectodermal protrusions and impose a copy of the skin patterns onto the shell by secretion of pigment. The line where the two protrusions contact each other generates the seam-like structure on the top of both shells (*Cypraea scurra* and, at right, *Cypraea tigris*).

asymmetry makes sure that also in larger fields only polar patterns are formed (see the Guided Tour GT127).

An activator - inhibitor system exhibits substantial pattern regulation. By removing the site of high activator concentration, the site of inhibitor production is removed too. The remnant inhibitor decays until a new activator maximum is triggered in the remaining cells due to the low level of activator production (b_a in Equation 2.1). The pattern is restored in a self-regulatory way (Figure 2.9). This is, of course, a most-important feature to make development to a reproducible and robust process.

Mechanisms involving diffusion can generate graded distributions only in small fields. The organization of fields larger than about 2mm would require too much time (Crick, 1970). Wolpert (1969) has pointed out that all known biological systems are small at the stages at which pattern formation takes place; less than about 100 cells and less than 1mm across. For fields that grow to a larger sizes it is expected that diffusion-dependent concentration profiles become translated into stable patterns of position-dependent gene activations. The evoking signals, the graded distribution of the “morphogens”, are then no longer required. Corresponding models based on autoregulation and competition of genes will be discussed further below (see Figure 12.9, page 223).

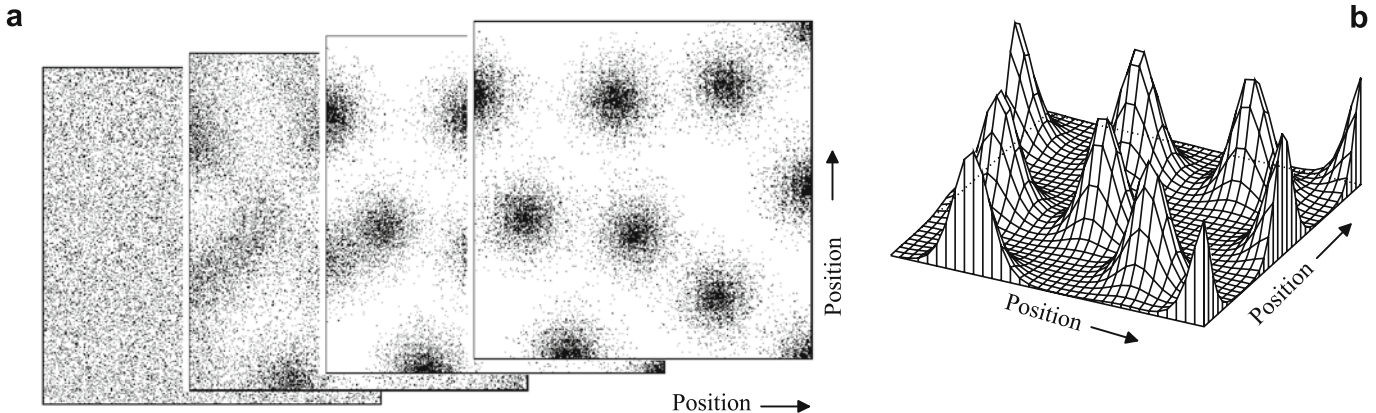


Figure 2.11. Pattern formation in two dimensions. If the range of the inhibitor is much smaller than the total field, a somewhat irregular pattern of patches emerges, but a maximum and minimum distance is maintained. (a) Stages. (b) Final distribution [Program XY: S211, GT1].

2.11 Pattern formation in two dimensions

Although pattern formation on shells can generally be regarded as a one-dimensional process that keeps a time record in the second dimension, some shells become decorated by a two-dimensional process (Figure 2.10). The mechanism outlined above produces activated regions at more or less regular distances in two dimensions. Figure 2.11 shows the emergence of such a pattern from random fluctuations.

As previously mentioned, saturation leads to a broadening of the maxima. In two-dimensional pattern formation this has a nontrivial effect: the formation of stripes. Stripes are very common in embryonic development. These stripes should not be confused with the stripes generated by the one-dimensional processes discussed earlier. Stripe formation in two dimensions is achieved by an activated region that has a large extension in one dimension and a small extension perpendicular to it. How could an activated region obtain a large extension in one direction and a short extension perpendicular to the first? In the model, due to saturation, activated cells have to tolerate other activated cells in their vicinity. If the activator shows a modest diffusion, activated regions tend to occur in larger coherent patches since the probability is high that an activated cell's neighbor will become activated too. On the other hand, activated cells must be close to nonactivated cells into which the inhibitor can diffuse or from which substrate can be obtained. These two seemingly contradictory requirements, large coherent patches and proximity to nonactivated cells are satisfied if a stripe-like pattern is formed (Figure 2.12). Each activated cell is bordered by other activated cells but is also close to nonactivated cells. If initiated by random fluctuations the stripes will also have random orientation and will exhibit some bending and bifurcations.

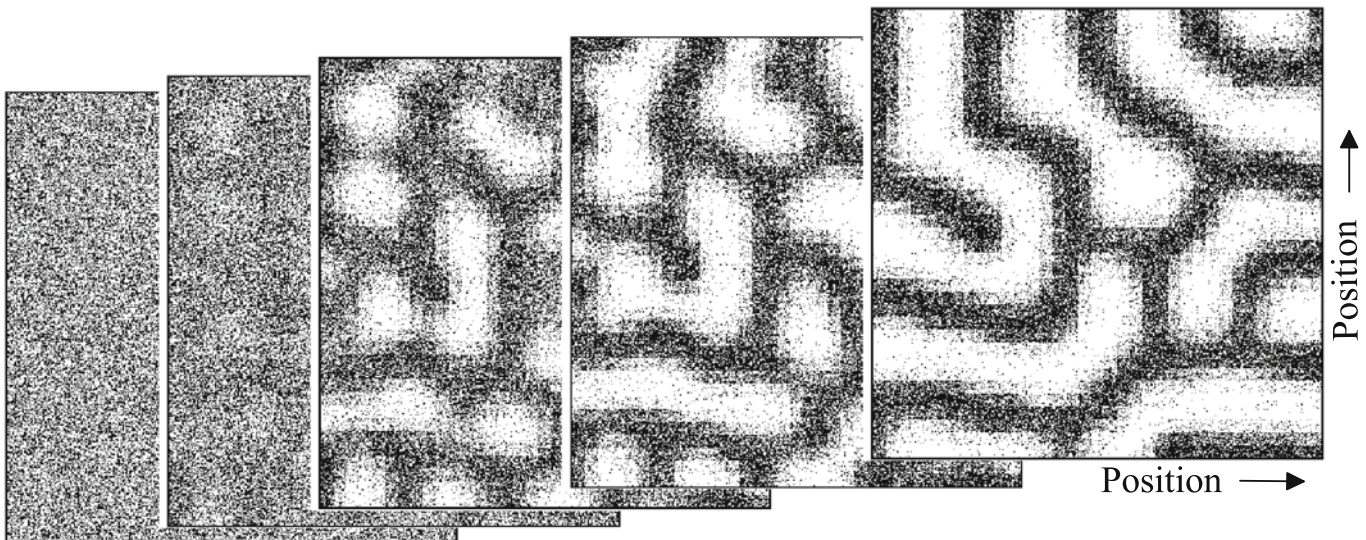


Figure 2.12. Stages in the formation of stripes. If the autocatalytic reaction saturates at low activator concentrations, more cells remain activated but at a lower level. Stripes are the preferred pattern since activated cells have activated cells as neighbors and nonactivated cells are nearby into which the inhibitor can diffuse [Program XY; S212]. In this mode of stripe formation, the width of the stripes is of the same order as the interstripe distance. This mechanism is, therefore, incapable to form a solitary straight stripe as it is required for the generation of the dorsal midline of vertebrates. A possible solution of this problem is a shifting spot-like organizer that elongates the stripe-like midline. The moving chick organizer, Hensen's node, is an example (see Figures 12.1, 12.7, and program XY, S134d)

In conclusion, relatively simple molecular interactions based on local self-enhancement and long range inhibition allow the formation of stable patterns starting from originally more or less homogeneous conditions. These patterns can be used to create particular structures at particular positions during development, for instance, to establish embryonic axes or to initiate periodic structures in space. Corresponding models and their biological background will be discussed in detail in Chapter 12. The formation of pigmentation stripes is only a very special case in which this type of interaction plays a central role.



Figure 3.1. Parallel and oblique lines, the traces of synchronous oscillations and traveling waves. On the shell of *Amoria ellioti* (top), the stripes are more or less perpendicular to the direction of growth. They result from an almost synchronous alternation between pigment producing and nonproducing phases. It is remarkable that the distance between the lines remains constant in regions of different shell diameter. Although the lower left pattern (*Nerita communis*) looks similar on the picture, it has a different origin. From the lower right figure it becomes clear that the stripes are oriented oblique to the direction of growth. Therefore, a pigmented region has triggered a neighboring region and so on, forming traveling waves at regular intervals. Minute irregularities and finer changes in the pigmentation indicate the orientation of the growing edge at the corresponding stage.

Oscillations and traveling waves

A very important class of shell patterning is caused by pigment productions that occur only during a short time interval, followed by an inactive period without pigment production. Stripes parallel to the growing edge and oblique lines belong to this class of patterns. Such oscillations can occur if the antagonist reacts too slowly. Then, a change in activator concentration is not immediately back-regulated since the antagonist reacts too slowly and the activation will proceed in a burst-like manner. Only after a sufficient accumulation of the inhibitor, or after a severe depletion of the substrate, will activator production collapse. A refractory period will follow with very low activator production in which either the excess inhibitor will degrade or the substrate will accumulate until a new activation becomes possible. The condition for oscillatory activations is the reverse of that given for stable patterns. In an activator-inhibitor scheme, oscillations occur if the decay rate of the inhibitor is smaller than that of the activator i.e., if the condition $r_b < r_a$ in Equation 2.1 (page 23) is satisfied.

In the activator-depleted substrate model, oscillations occur if the rate of substrate production is too low to maintain activator production in a steady state, i.e., if $b_b < r_a$ in Equation 2.4 (page 28). The onset of oscillations in a depletion-driven system can be observed using an everyday experiment. If a thick candle burns for a while, a deep hole will form in the wax and the flame will begin to flicker. The reason is that the oxygen supply becomes insufficient for a large flame. The flame shrinks, consuming less oxygen, thereby allowing the oxygen concentration to recover and the flame becomes larger again; and so on.

Depending on the parameter, this reaction can exhibit different behaviors. A cell may become activated with an internal periodicity. Or, it may be arrested in an excitable state. Small changes in a parameter can lead to a transition from one to the other mode. Figure 3.2a, for instance, shows the switch between oscillations and stable activation occurring in a single cell that is caused by a change in the decay rate of the activator. Theories on oscillations and waves in excitable media are well developed (see, for instance, Prigogine and Lefever, 1968; Winfree, 1980; Segel, 1984; Glass and Mackey, 1988; Murray, 1989). The different modes will be discussed here in some detail since they are the tools for deducing the parameters required for the patterns observed on shells.

Equation 3.1: Finite activator production at low inhibitor concentration: Michaelis-Menten kinetics

At very low inhibitor concentrations, inhibitor production must remain finite. This is accomplished using the Michaelis-Menten term s_b . Together with the saturation term s_a introduced in Equation 2.3, Equation 2.1a (page 23) would obtain the following form:

$$\frac{\partial a}{\partial t} = s \left(\frac{a^2}{(s_b + b)(1 + s_a a^2)} + b_a \right) - r_a a + D_a \frac{\partial^2 a}{\partial x^2}$$

s_b has an effect similar to the nonzero baseline inhibitor production b_b in Equation 2.1b. Both effects limit activator production at low inhibitor concentrations. This limitation can lead to a second stable state at low activator concentrations.

In an oscillating activator-inhibitor mechanism, inhibitor concentrations can become very low. So far, it has been assumed that the rate of activator production is inversely proportional to inhibitor concentration. This is a simplification since, of course, the production rate remains finite even if no inhibitor is present. At very low concentrations, a Michaelis-Menten term s_b , as introduced in Equation 3.1, must be considered.

If either the Michaelis-Menten constant s_b or the basic inhibitor production b_b is high, but the basic activator production b_a is low, a spontaneous trigger may not occur since the effective inhibition remains too high. Such a system will no longer oscillate but will remain arrested in an excitable state. The external addition of small amounts of activator can initiate either a single burst (Figure 3.2b) or a sequence of bursts, depending on the duration of the external activator supply. As shown below, this mode plays a crucial role in the formation of traveling waves.

A basic activator production b_a above the threshold leads to sustained oscillations. Whenever the inhibitor drops below a critical value, a new activator burst is triggered. A higher baseline activator production enables an earlier onset of the self-enhancing process. In this earlier phase inhibitor concentration is still higher. Thus, the bursting proceeds less dramatically (Figure 3.2c). This effect is well-known in economics as a means of dampening oscillations. By government investments in periods of economic depression, i.e., by artificial inputs into a process that hopefully becomes self-enhancing, attempts are made to make the depression less severe and to initiate the next upswing earlier. That the following boom is less exaggerated is another helpful side-effect of this strategy. From this modeling it is expected that the initiation of a self-enhancing cycle by governmental spending is only effective towards the end of a depression period. At initial phases, the antagonistic effects inherent in the system are too strong (see Figure 3.3b).

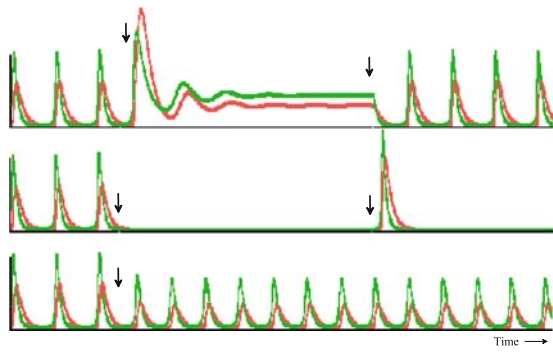


Figure 3.2. Oscillations in an activator - inhibitor system. Oscillations occur if the inhibitor has a longer half-life than the activator ($r_b < r_a$ in Equation 2.1); calculation in a single cell, concentrations of the activator (green) and inhibitor (red) are plotted as a function of time. (a) A temporary reduction of the decay rate of the activator ($r_a = 0.08 \rightarrow 0.03$) can lead to a transition into a stable situation. (b) If the basic activator production is too low ($b_a = 0.04 \rightarrow 0.01$) and either the basic inhibitor production b_b or the Michaelis-Menten constant s_b is sufficiently large, the autocatalytic cycle cannot be fired at low inhibitor concentrations. Oscillation stops and the system remains in an excitable state. A short, small increase in an external activator supply ($b_a = 0.01 \rightarrow 0.04$) can cause a single burst. (c) A higher basic activator production leads to smaller peaks in more rapid succession ($b_a = 0.04 \rightarrow 0.08$). Each sequence (a-c) begins with the same standard conditions. The time of the parameter change is indicated by an arrow [GT32].

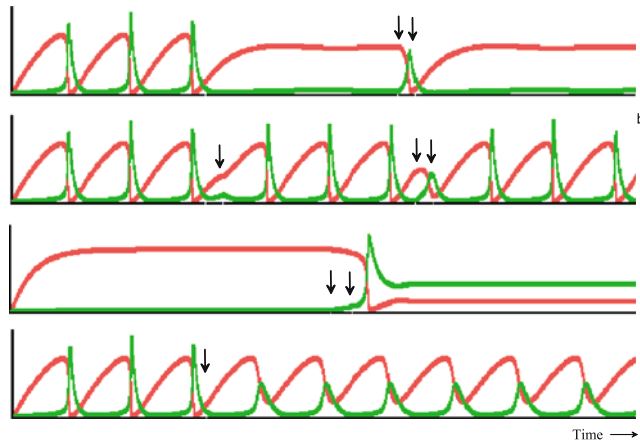


Figure 3.3. Oscillation in an activator-substrate scheme. If the substrate production is insufficient to maintain a steady state activation, the activator concentration (green) oscillates. The substrate concentration (red) collapses during activation. After sufficient accumulation of substrate, a new pulse can be fired. (a) A removal of substrate independent of activator production ($r_b = 0 \rightarrow 0.008$) leads to a reduced maximum substrate concentration. Oscillation may stop but the system remains excitable. A small external addition of activator for a short time interval ($b_a = 0.02 \rightarrow 0.06$) can initiate a single activation cycle. Due to the reduced substrate concentration, the pulse is somewhat smaller. (b) The result of an external activator pulse on an oscillating system depends on the phase. If the substrate concentration is low at this moment (arrow), no peak can be triggered. The additional substrate consumption may even delay the next peak. If activator addition occurs at a later phase, a premature peak with a lower amplitude (double arrow) will result. (c) The system becomes bistable if the substrate production is high enough to maintain a steady state activation but the loss of substrate via r_b suppresses the onset of a spontaneous activation. A short temporary increase in the external activator supply (double arrow) causes a permanent transition from low to high activation (and from high to low substrate concentration). (d) Saturation of the activator production ($s_a = 0 \rightarrow 1.0$) limits the height of the peak but elongates the duration of the pulses [GT33].

The same type of behavior may occur in an activator-substrate scheme (Figure 3.3). Substrate removal independent of consumption by the autocatalytic process ($r_b > 0$ in Equation 2.4b) limits the maximum concentration that the substrate may reach. This level may become insufficient to release a spontaneous trigger of activation. The sustained oscillations are suspended but the system remains in an excitable state similar to that accomplished by s_b or b_b in the activator-inhibitor system. Again, whether oscillations take place also depends on the basic activator production b_a required for the initiation of each subsequent burst. Depending on the phase of the oscillatory cycle, a short pulse of externally added activator can either advance or delay the next burst (Figure 3.3b). If the time constants allow a stable activation but the maximum substrate concentration is insufficient for a trigger the system becomes bistable. A short pulse of additional activator can accomplish a permanent transition from low to high activation (Figure 3.3c). Thus, small differences in parameters can cause very different behaviour within the system. The effects of these differences are basic to the understanding of different shell patterns.

3.1 The coupling between the oscillators by diffusion

In the overall pattern that emerges on shells, the coupling between oscillators is decisive. A strong coupling synchronizes the oscillations and the resulting patterns are stripes parallel to the growing edge (Figure 3.4). Since the total length of the edge is very long, even small phase differences between neighboring oscillators can accumulate such that distant regions are out of phase. At a given time pigment may be produced in some positions but not at remote locations. An example was given in Figure 1.4. This indicates that the synchronization of oscillations does not result from external influences, such as the seasonal changes that effect tree rings, since these would cause strict synchronization. The synchronization may fail between regions of larger and smaller circumferences on shells and lines may end blindly (Figure 3.4c). This phenomenon will be examined again later (Figure 4.14).

Synchronization can result not only from diffusion of the activator but also from diffusion of the antagonist. For instance, a cell that is activated somewhat later than its neighbors delays the neighboring cells by its later emitted inhibitor, thus enforcing synchronization. Therefore, a mere change in inhibitor lifetime may cause a transition from a stable pattern in time to synchronous oscillations. On shells, this corresponds to a transition from stripes perpendicular to the growing edge to parallel stripes (Figure 3.5c). Related transitions can be induced in shells. In a river polluted by salt-containing waste water from potassium mining, Neumann (1959a,b) observed corresponding changes on the shells of the freshwater snail *Theodoxus fluviatilis* as a function of the salt content. These changes can be reproduced in the laboratory (see Figure 1.11).

Very frequently shell patterns exhibit rows of dots (see Figure 4.13). It would appear straightforward to assume that these patterns result from a combination

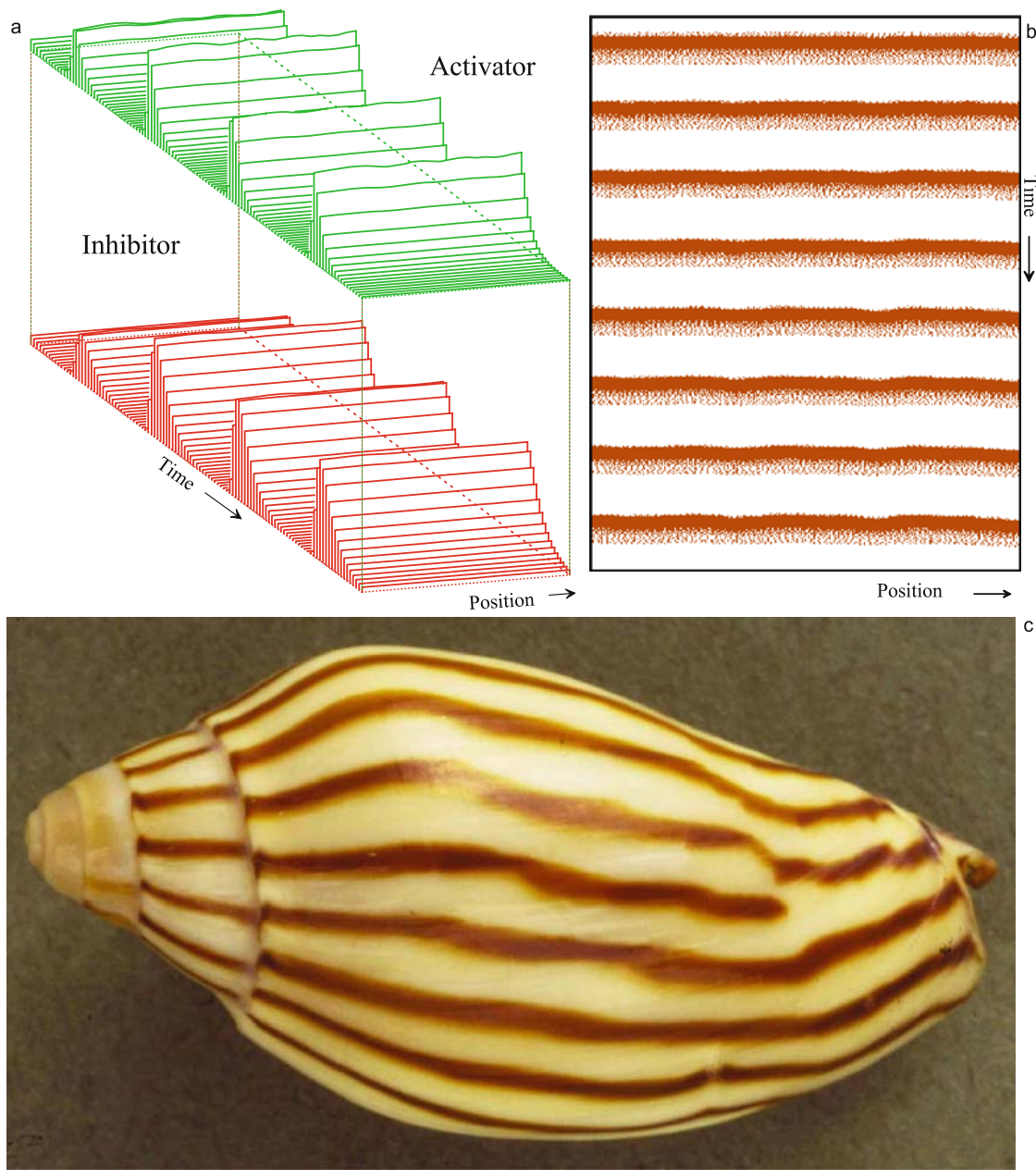


Figure 3.4. Stripes parallel to the direction of growth (perpendicular to the growing edge). This pattern indicates a nearly synchronous oscillation of pigment production. (a) Pattern formation by the interaction of an autocatalytic activator (top) and its antagonist, an inhibitor (bottom). Oscillations occur since the inhibitor has a longer time constant (lower decay rate) than the activator. High diffusion of the activator enforces a near-synchronization between neighboring cells. Nevertheless, a substantial phase difference can accumulate between distant cells. (b) The resulting pattern in a space-time plot analogous to that formed on shells. Activator concentration is indicated by the density of the dots. (c) Pattern on the shell of *Amoria dampieria*; [S34; S34a, S35a]

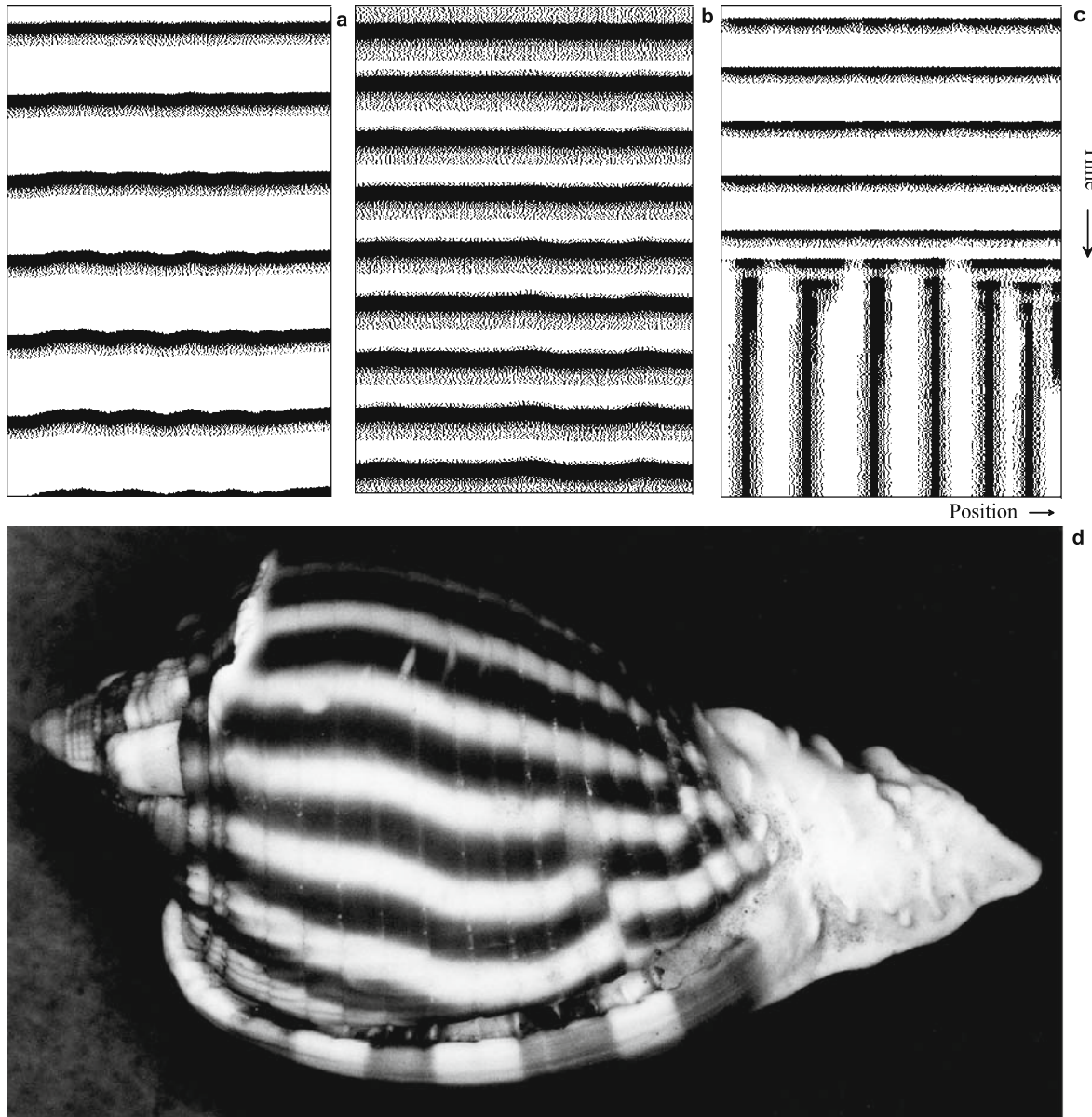


Figure 3.5. The width of stripes. (a) without saturation of the activator autocatalysis, a high activator concentration is present only for a short time interval. (b) With saturation ($s_a > 0$ in Equation 2.3), the width of the stripes becomes broader in relation to the interstripes. (c) A rapid diffusion of the inhibitor is insufficient for the formation of a pattern in space. However, a shortening of the inhibitor half-life is sufficient for a transition from a homogeneous oscillation to a stable pattern in space (see the experimental observation in Figure 1.11). This leads to a switch between stripes parallel and perpendicular to the growing edge. (d) *Phalium strigatum*, a shell with stripes and interstripes of about the same width. Note that at the bulge the pigment forms a pattern in space [S35a, S35b, S35c].

of the lateral inhibition scheme ($D_b \gg D_a$) localizing activations, and the oscillation scheme ($r_b < r_a$) enforcing periodic activations. However, lateral inhibition requires time for one region to suppress surrounding regions (see Figure 2.3). This time is not available if the activation proceeds in a burst-like manner. As shown earlier, the diffusion of the antagonist leads to synchronous bursts of activation. Before the excess of inhibitor produced in one region can reach the neighboring region *via* diffusion, full activation has already occurred there that will cause a down-regulation (Figure 3.5). As will be shown below, rows of dots require a superposition of two pattern-forming systems (see Figure 4.11 and 4.13).

3.2 The width of bands and interbands

On many shells with parallel stripes, the dark stripes have approximately the same width as the lighter regions in between. In the simplest model, however, the activation is a short burst followed by a long period without activation (Figure 3.5a). This changes if the autocatalysis saturates, a process introduced earlier to model the width of stable stripes (see Figure 2.4). By saturation, the maximum activator concentration is limited and it requires more time either to accumulate sufficient inhibitor or to consume all available substrate. Therefore, it takes longer for the activation to cease. Figure 3.5a,b provide simulations with and without saturation.

However, the actual mechanism by which broad stripes are generated may be more complex. The natural patterns show bands of a nearly constant density of pigmentation. In contrast, simulations involving saturation of the autocatalysis produce a slow increase followed by a slow decrease of activation (see also Figure 3.3d). One possibility may be that pigmentation depends in a nonlinear way on exceeding a certain threshold of activator concentration. It will be shown in chapter 7, however, that more complex patterns suggest the switching on and off of pigmentation are independent processes. This separation leads to periods of constant pigmentation density between the two signals (see Figure 7.4).

3.3 Oblique lines: traveling waves in an excitable medium

In many species pigmentation lines oblique to the growing edge are formed. An example is given in Figure 3.6. As mentioned, this type of pattern can be regarded as a time record of traveling waves of pigment production along the pigment-producing mantle gland at the growing edge. A cell with a high activator concentration “infects” its neighbor causing, with some delay, a burst of activation in this cell also, and so on. The chain of reaction can proceed only in one direction since after the collapse of activation the cells enter a refractory period. Either the excess of inhibitor must decay or the substrate becomes exhausted and must be replenished



Figure 3.6. Shell pattern generated by traveling waves: pattern on *Cymbiola nobilis* and *Lioconcha lorenziana*. The oblique lines result from a process that can be compared with an infection. Pigment-producing cells ‘infect’ their neighbors such that they also produce pigment, while pigment production is switched off in ‘infected’ (activated) cells after a short period. The cells become refractory, i.e., they become immune to another infection. Thus pigment production moves along the pigment-producing mantle gland like a wave. In the time record, this leads to oblique lines. A cell that starts spontaneously with pigment production gives rise to two diverging lines (\wedge -element). If two traveling waves collide, both waves become extinct since a wave cannot enter into the region made refractory by the counter wave. Such mutual annihilation leads to \vee -like pattern elements

(see Figure 3.3). The inclination of the oblique lines is determined by the ratio of the speed of the waves and the speed of shell growth.

After spontaneous activation in a small group of cells, both neighboring cells can be infected. At this point two waves are initiated that run in opposite directions. Such an event causes a \wedge -like pattern with two diverging oblique lines. Conversely, if two waves collide, they annihilate each other since waves cannot enter into a region made refractory by a counter wave. On shells, this leads to \vee -like pattern elements (Figure 3.6).

For traveling waves, activator diffusion must be within a certain range. If it is too high, an overall synchronization of the oscillations will occur and stripes parallel to the edge will result. On the other hand, if it is too low, oscillations of individual cells will become independent of each other and the phase relation among the cells will be lost. If the antagonist diffuses at all, the diffusion rate must be much lower than that of the activator, otherwise the faster spreading antagonist would arrest the wave.

A pure traveling wave mechanism for shell patterns seems to be more the exception than the rule. The shell in Figure 3.6, for instance, shows many details indicating that the actual mechanism is more complex. Oblique lines terminate without prior collision, and many of these terminations take place simultaneously, indicating some global influence. At other locations one of two lines terminate shortly

before wave collision takes place, indicating the long-range influence of one wave on another. While the upper boundary of the oblique lines appears smooth, the lower side can have small dents or a smear. Later we will see that these features are expressed even more strongly on other shells, providing important clues to the understanding of more complex patterns.

3.4 Traveling waves require a pace-maker region

In order for traveling waves to occur, the waves must be initiated at particular positions. Otherwise synchronous oscillations may occur even though the general conditions for traveling waves are satisfied (Figure 3.7a). One possibility to explain the initiation of traveling waves is that oscillation frequency depends on the position. Faster oscillating cells may become pace-maker regions. The pace-maker role of the sinoatrial node in the contraction waves of the heart muscle is a well known example (see Winfree, 1980, Glass and Mackey, 1988). Due to its higher oscillation frequency, a pace-maker region fires earlier than its surroundings, initiating traveling waves at specific positions. It may require many rounds of oscillation before the dominating role of a pace-maker region becomes fully established (Figure 3.7c). As discussed below the formation of a pace-maker region may require a separate pattern-forming process.

Pace-maker regions can also appear spontaneously if parameters slowly change the system from the excitable to more sustained oscillations. Those cells that first start to oscillate, trigger their still excitable but not yet spontaneously firing neighbors, initiating traveling waves. If the cells are on the borderline between an arrest in the excitable state and sustained oscillations (see Figure 3.2b), relatively minor fluctuations can lead to dramatic differences in oscillation frequencies and thus to pacemaker regions (Figure 3.7b).

Strong support for the suggestion that oblique lines are generated by traveling waves can be derived from pattern regulations as they are frequently seen on the shells of *Strigilla carnea* (Seilacher, 1972, 1973). The normal pattern consists of very regular oblique ridges that merge along a particular zone, producing a pattern of nested V's (Figure 3.8). In some specimens, the normal pattern has been perturbed, probably by an external event. Some neighboring waves become terminated causing a gap in the pattern of oblique lines. Pattern regulation occurs either by a bending of the remaining lines towards the gap and/or by the spontaneous initiation of new lines. The computer simulation in Figure 3.8 shows that the model correctly describes the essential features of this pattern regulation: the bending takes place only in an upward direction resulting from a speeding up of remaining waves; new initiation points lead to a W-like pattern, a pattern which is otherwise absent on the shell.

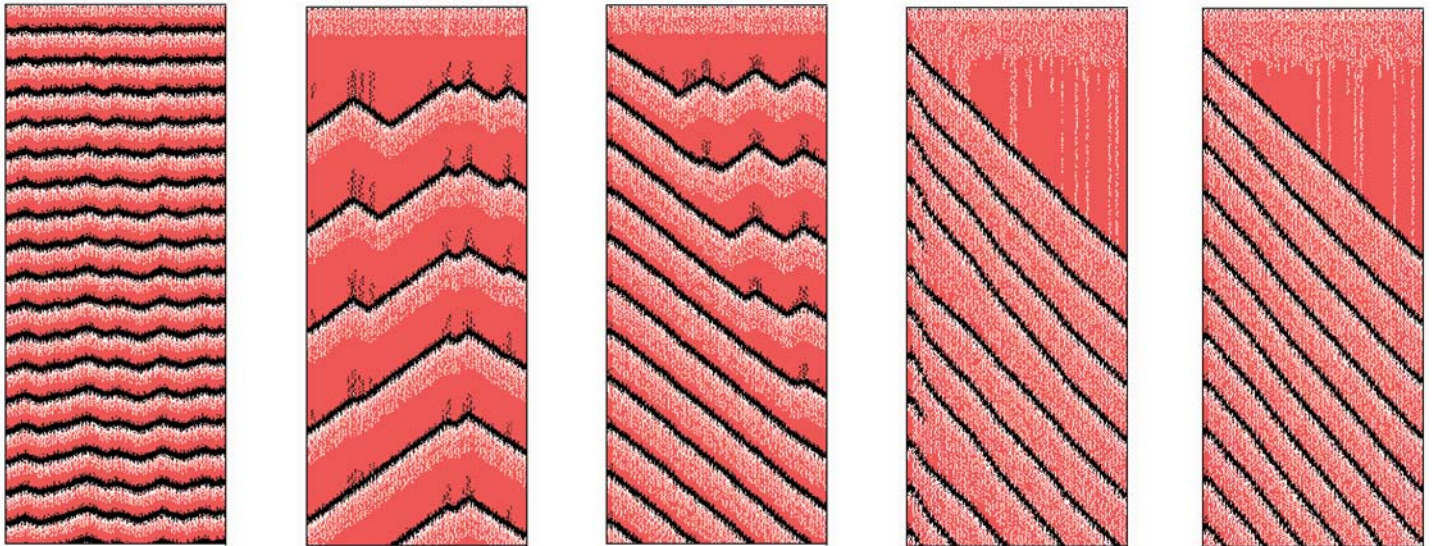


Figure 3.7. Role of pace-makers in the generation of traveling waves, calculated using the activator-depletion mechanism in Equation 2.4. (a) If the oscillation frequency is the same in all cells, oscillations can remain synchronous even though the conditions for traveling waves are satisfied. (b) If some cells at random positions oscillate somewhat faster than most other cells, these faster cells form pace-maker regions. These regions are the periodic initiation points of two diverging lines since a spontaneously activated cell can infect both neighbors (\wedge -like pattern element). (c-e) Reproducible and regular oblique lines emerge if a particular group acts as a pace-maker. (c) The substrate production b_b is 30% higher in the leftmost cell. It may require some time to bring a larger field under the control of a pace-maker region. (d) If a pace-maker fires too rapidly, not all initiated waves survive. This leads to termination of oblique lines. (e) Except for the pace-maker cells, the cells are unable to trigger spontaneously but they can propagate the excitation. Ordered traveling waves are formed from the beginning [GT37; S37A shows the situation in (c) in a movie-like manner]

The model predicts that the initiation zone of the traveling waves (\wedge 's) may have special properties indicating a pace-maker region. In contrast, the annihilation zones (\vee 's) are arbitrary and depend only on where the waves collide. This is supported by another pattern abnormality observed on these shells (Figure 3.9). Due to an interruption of some waves, the zone of mutual annihilation, i.e., the position of the tips of the \vee 's, can be shifted.

In conclusion, oscillations result when self-enhancing processes are antagonized by processes that are too slow to enable a stable balance. On shells, this can lead to stripes either parallel or oblique to the growing edge.

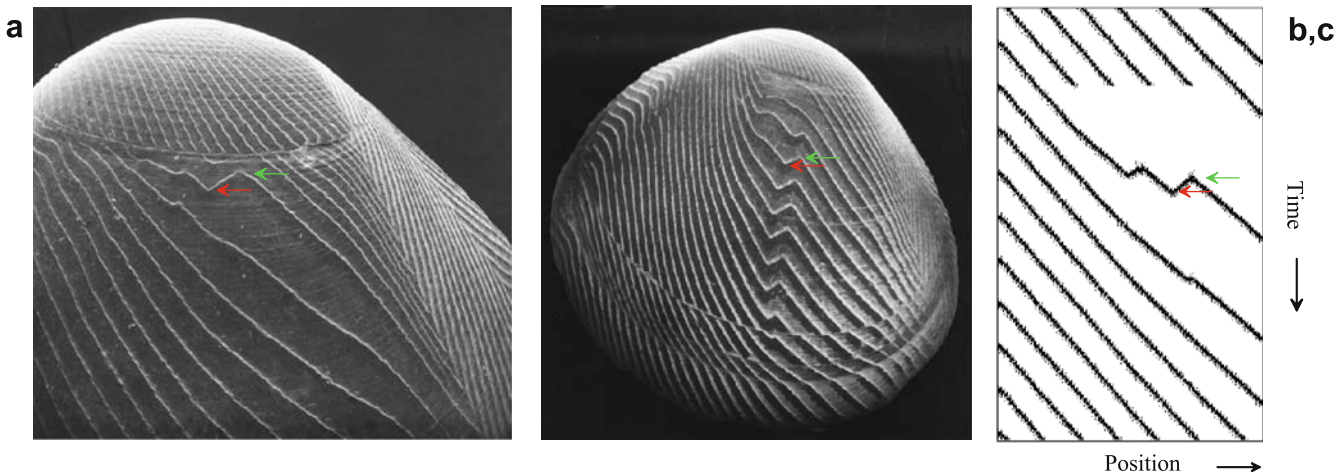


Figure 3.8. Pattern regulation: repair in the rib-like pattern of *Strigilla*. (a,b) Examples: after a perturbation of the normal pattern (caused presumably by an external event) some lines are interrupted but the pattern discontinuity disappears over the course of time. (c) Model: The oblique rib-like pattern is assumed to be generated in a similar way as the corresponding pigmentation pattern, i.e., by traveling waves. Interruption is simulated by an artificial lowering of activator concentration. Due to the absence of activation for a prolonged period, the substrate concentration (not shown) increases to such a level that a spontaneous activation becomes possible (\wedge -elements; green arrows). Due to the accumulating substrate, the cells become more and more susceptible to triggers from neighboring cells. This leads to a speeding up of the traveling waves causing the bending of the lines. The bending is unilateral since, of course, the waves on the other side of the gap are not retarded. Collision of two waves leads to their annihilation (\vee -elements, red arrows) [GT38].

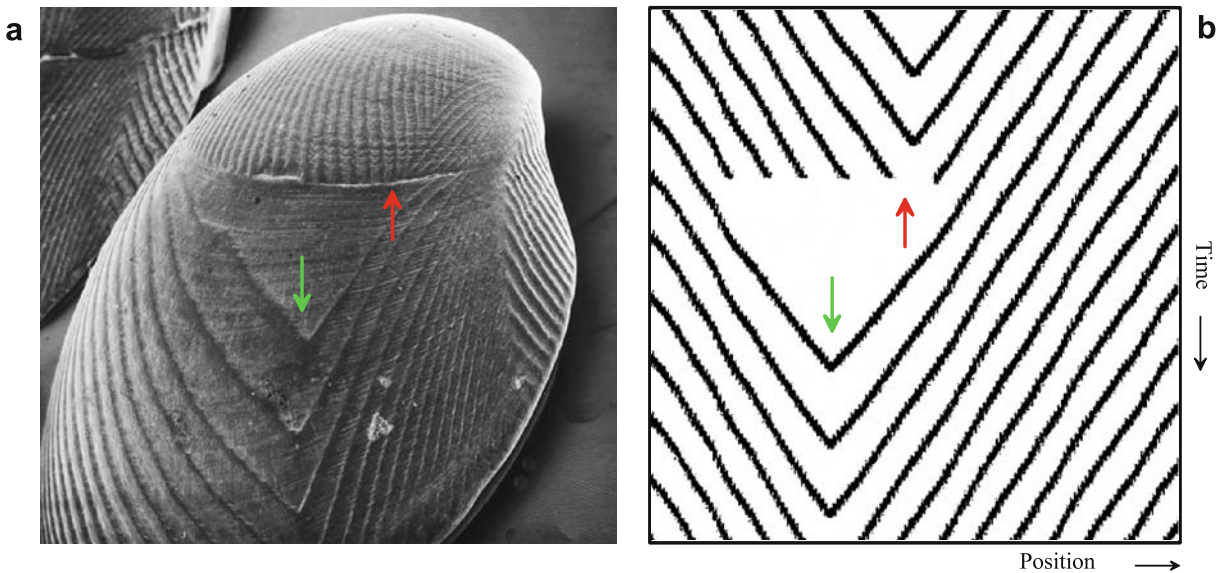


Figure 3.9. Shift of the annihilation zone. (a) A pattern irregularity that includes the annihilation zone (\vee -elements). A new annihilation zone forms at a new position. (b) Model: If the gap is asymmetrically located with respect to the normal annihilation zone, the new region of annihilation is shifted accordingly. This supports the view that the position of the tips of the nested \vee 's is determined only by where the waves collide, not by special properties of the corresponding cells. A bending of the ridges towards the gap can take place on both sides [GT38]; (Specimens kindly provided by A. Seilacher, see Seilacher, 1972, 1973)

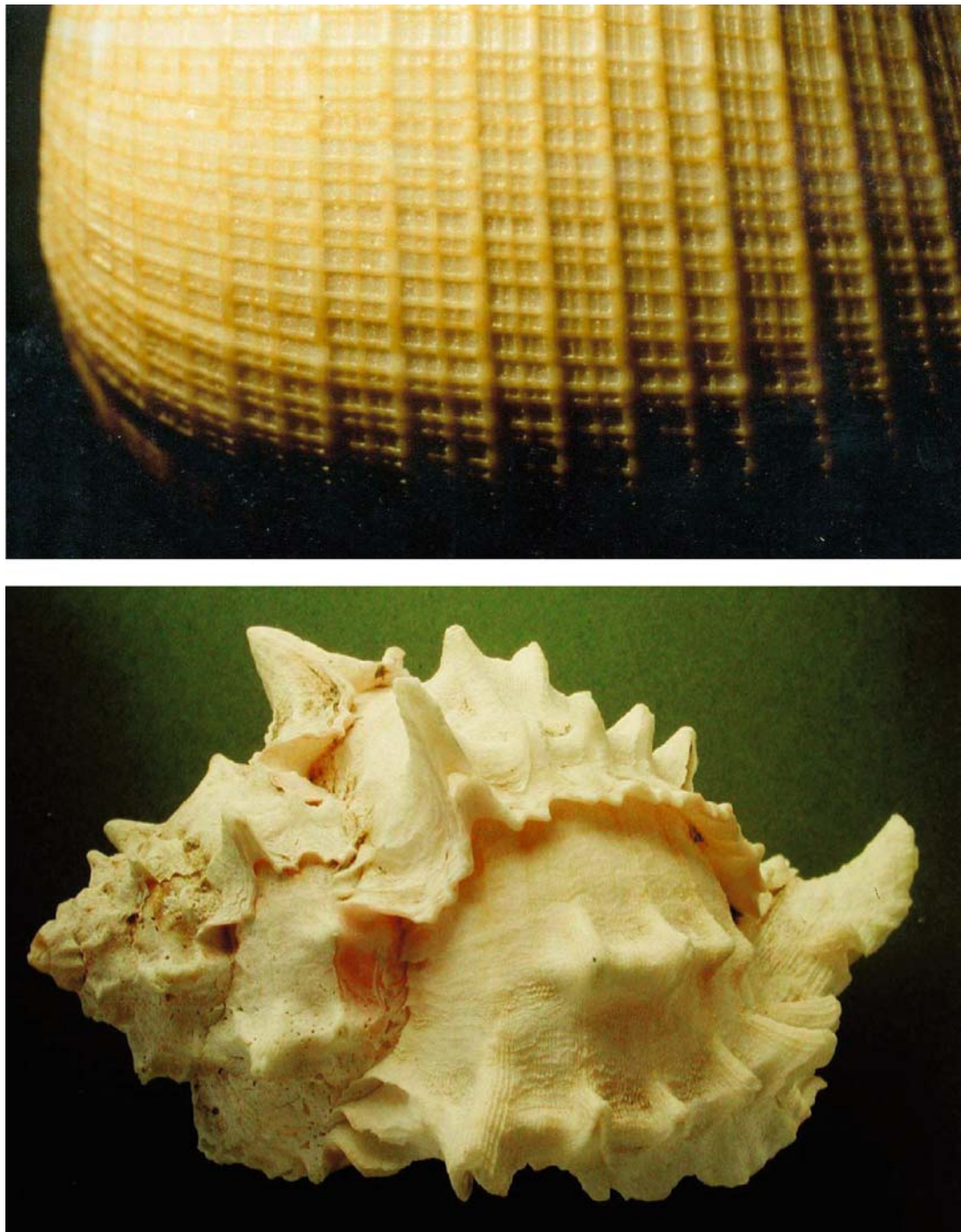


Figure 4.1. Superposition of two patterns, a periodic pattern in space that is stable in time and a periodic pattern in time that is spatially homogeneous. Top: *Ficus gracilis*; both patterns coexist without much interference. Bottom: *Bursa rubeta*. The pattern stable in time determines where, the oscillating pattern determines when the spines will be formed

Superposition of stable and periodic patterns

A widely distributed subgroup of shell patterns result from the superposition of a stable and a periodic pattern. The upper shell in Figure 4.1 shows two sets of parallel relief-like lines. One set is oriented parallel to the growing edge and results from a thickening of the shell at periodic time intervals. The other set is oriented parallel to the direction of growth and results from a permanently enhanced deposition of shell material at regularly spaced positions. In this example, the two patterns do not interfere with each other, a situation that is more the exception than the rule, but it shows that the assumption of two superimposed systems is reasonable.

More intriguing are systems in which one system modifies the other. The bottom shell in Figure 4.1 shows spines that have been formed at regular time intervals in defined positions. Evidently, a stable pattern must exist that determines the position of the spines, and an oscillating pattern must decide the time at which spine formation actually occurs. Another regular substructure can also be recognized. Every second row is different from the intervening row. The first spine, counted from the shoulder, appears only in every second row and is much larger. After every second row a discontinuity in the shell is formed. Thus, with their combinatorial possibilities, superpositions of two (or more) patterns can provide a rich source of complexity.

This chapter will discuss patterns that result from the modulation of parameters in an oscillating system by a stationary pattern. Usually the modulating pattern is not directly visible but has to be inferred from the space-dependent behavior of the oscillating system. The diversity in patterns results from differences in the actual form of the stable pattern, from its action on the oscillatory system, as well as from the particular properties of the oscillating system. The following cases will be considered:

- (i) The oscillation frequency is space-dependent resulting in a pattern of wavy lines.
- (ii) Steady-state activations occur in some regions while in other regions the system oscillates. Fishbone-like patterns result.
- (iii) Oscillations are restricted to particular regions, while in other regions they do not occur. The resulting pattern exhibits rows of dots or crescents.

4.1 The formation of undulating lines and the partial synchronization of cells by activator diffusion

A broad spectrum of patterns from very different species indicates that the frequency of the oscillations varies along the growing edge in a systematic manner. This feature is obvious on the shell of *Natica euzona* (Figure 4.2). For speed and simplicity in the following simulations, the stable pattern is not calculated but supposed to exist. Usually, it is shown on top of the simulation. The generation of stable patterns was discussed earlier in some detail (see Figure 2.3 and Figure 2.5). Its explicit integration into the models will be exemplified later in this chapter (Figure 4.13).

In the activator-substrate model higher substrate production rates lead to higher oscillation frequencies (until the system enters into a steady-state of activation). Thus, if a stable pattern exists that modulates the substrate production b_b (see Equation 2.4, page 28), the oscillation frequency becomes space-dependent. Initially, if all cells are in the same phase, subsequent pigment production will occur earlier in the faster oscillating cells due to the modulating pattern. Thus, the next line will have a wavy appearance. In the absence of any activator diffusion, the phase difference between neighboring cells will increase with each further oscillation until any phase relation is lost. Diffusion of the activator has the tendency to synchronize neighboring cells since cells activated earlier advance their delayed neighbors by activator exchange. Thus, traveling waves are possible. Cells in regions of high substrate supply act as pace-makers due to their faster oscillations.

Traveling waves can proceed only if the phase difference between neighboring cells is not too large. The cell to be triggered must be in a sensitive phase in order for the addition of small amounts of activator to release the autocatalytic burst. With the activator-substrate model, this means that substrate concentration must have reached a certain level. Otherwise the chain of triggering events will be interrupted and a pigment line on the shell will terminate. Figure 4.3 shows this process in detail. For example, the first wave will become slower as it enters a region of lower substrate production but it may find sufficient substrate to survive. However, the situation becomes more critical for subsequent waves. Since the speed of the fore-running wave is reduced, less time is available for the recovery of substrate concentration, especially since its production is reduced at this point. The available substrate may be insufficient and wave termination will occur. Thus, wave termination is expected to occur in regions where neighboring cells have different oscillation frequencies. The faster oscillating cells can no longer entrain the slower oscillating cells. In the model, a slowing down of the wave is expected before wave termination occurs. On the final shell this causes a bending of the pigmentation line towards the growing edge.

Connected with the termination of a pigmentation line is an interesting pattern irregularity on the subsequent pigmentation line. This line frequently shows a small \wedge -like bending towards the terminated line. The effect is reproduced in the model

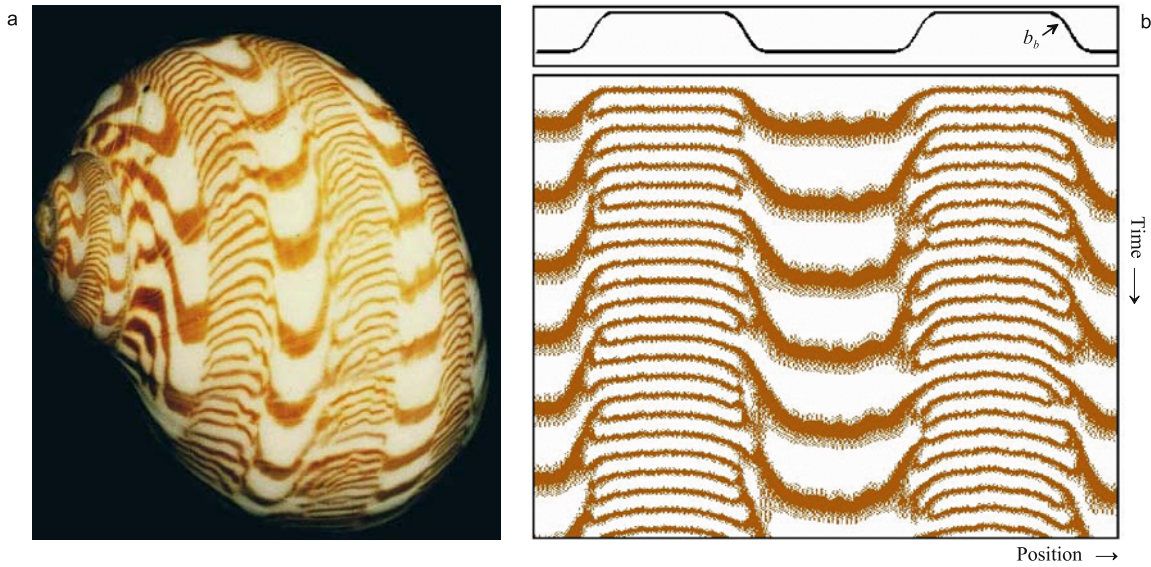


Figure 4.2. Shell of *Natica euzona*. The oscillation frequency is much higher in some regions, indicating the existence of a spatially stable pattern that influences the oscillation frequency. Model: space dependent substrate production (b_b ; Equation 2.4) leads to different oscillation frequencies. Lines of pigmentation are formed with different spacing. They merge or end blindly in the transition zone. To model the narrower bands in regions of high oscillation frequencies, the decay rate of the activator r_a and the source density s are assumed to have the same spatial pattern as the substrate production rate b_b [S42]

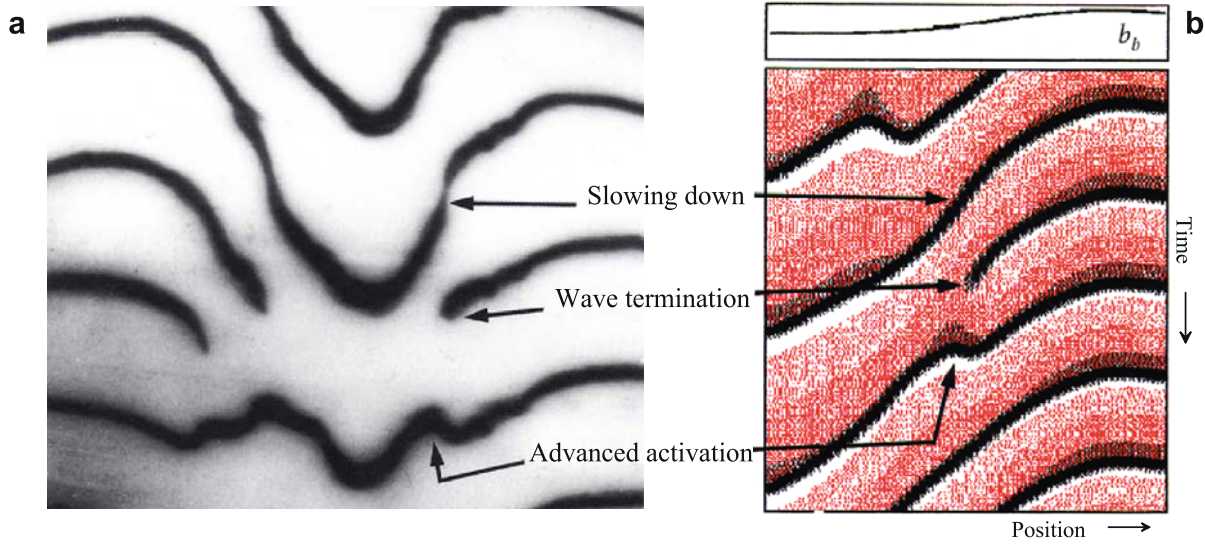


Figure 4.3. Termination of wavy pigmentation lines. (a) Example from *Amoria macandrewi*. (b) Model: after a traveling wave enters a region of low substrate production, the substrate concentration (red) may be too low for the wave to survive. The subsequent pigmentation line shows a characteristic irregularity due to an earlier trigger [GT44].

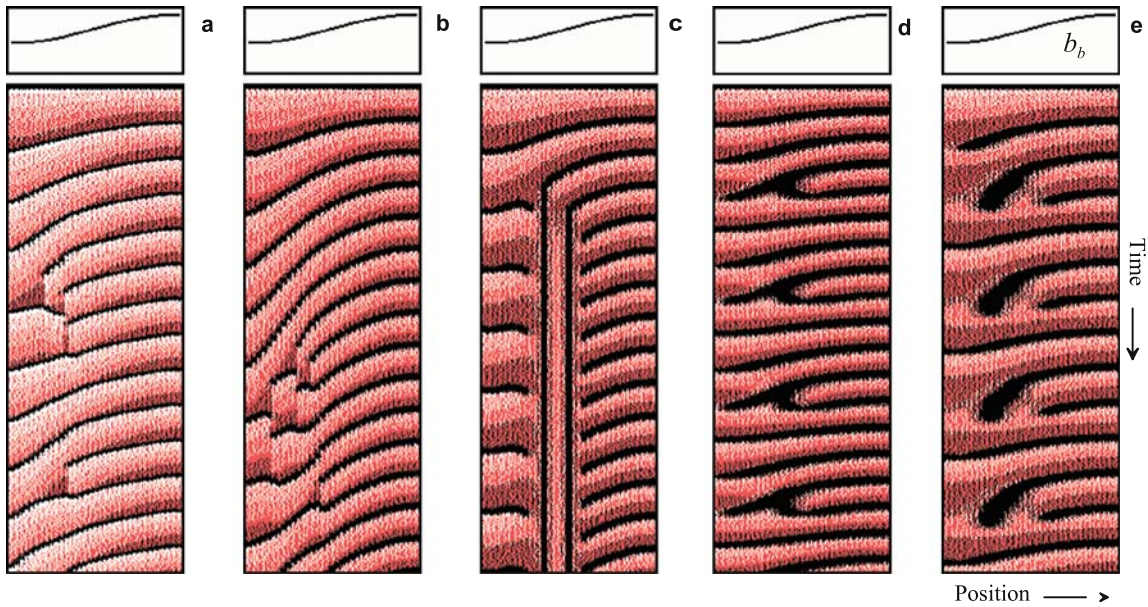
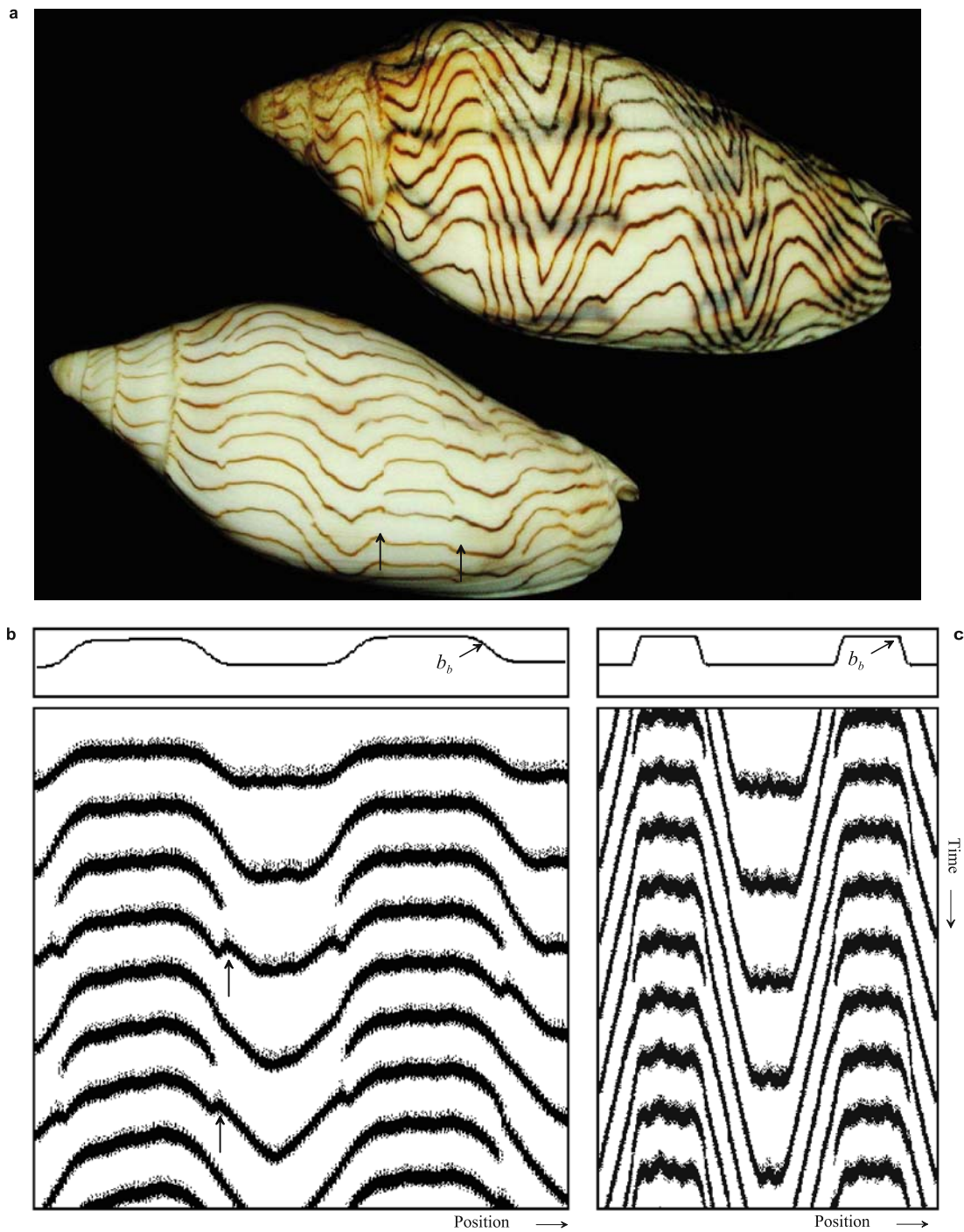


Figure 4.4. Modulation of an oscillating activator-substrate system by space-dependent substrate production (curve at the top), and the influence of diffusion and saturation. The region of higher substrate production acts as a pacemaker. (a) Low activator diffusion leads to waves that travel into a region of lower substrate production. The waves may terminate (see also Figure 4.3). (b) At higher saturation ($s_a > 0$) the activation period is longer (thicker lines). More time is available to infect neighboring cells. Slower waves (steeper lines) are possible. (c) Diffusion of the substrate can lead to the coexistence of stable and periodic activations. Stable activations occur preferentially in a region where neighboring cells show pronounced differences in the oscillation frequency. (d) Higher diffusion rates of the activator and the substrate can cause bifurcating pigmentation lines. (e) A lower substrate production causes more terminating lines and incomplete forks [GT44].

Figure 4.5. Wavy lines. (a) The shell of *Amoria undulata* (top) and *Amoria marcandrewi* (bottom). (b, c) Simulations: the faster oscillating cells entrain the slower oscillating cells. If the phase difference is not too large, a newly activated cell can accelerate the activation of its somewhat delayed neighbor. The steepness of the lines is an indication of the readiness of a cell to become activated. If the phase difference becomes too large, triggering neighboring cells is no longer possible and the pigmentation line will abruptly terminate. Neighboring cells skip one oscillation (Figure 4.3). After such a longer period without triggering, an advanced spontaneous activation may occur, in agreement with the natural pattern (arrows). (c) With a higher saturation, the tendency for line termination is reduced and long, steep oblique lines result [S45b, S45c].



and can be explained as follows. The substrate will not be used up in front of the wave that terminated. This locally higher substrate concentration leads to an earlier activation. The situation is illustrated in detail in Figure 4.3. Figure 4.5 shows a simulation on a larger field as a comparison with the corresponding shell.

4.2 Reducing wave termination with a longer activation period

Wave termination also depends on the relative length of the activated period. If activation persists for a relatively long fraction of the oscillatory cycle, the chances are good that enough activator will be transmitted to the neighboring cell by diffusion to activate it. If the increase in activator concentration is limited due to saturation, then the maximum substrate consumption is also limited. The same “fuel” is sufficient for a longer time period and the width of the pigmentation lines increases (see Figure 3.3d). As shown in the simulation in Figure 4.4b, saturation largely prevents line termination. Or, conversely, if the activation period is long, the exchange by diffusion can be much smaller and still maintain the chain of triggering reactions. In such cases, the pigment lines can be very steep. An example of this situation is given in Figure 4.6a,b. Figure 4.6c,d illustrates schematically the connection between line width and maximum steepness.

4.3 Interconnecting wavy lines and the formation of arches

In some species connections between subsequent lines do occur, either regularly (Figure 4.2) or occasionally (Figure 4.7, 4.8). As a rule, these connecting lines are steep and thin. The steepness indicates that the speed of the traveling waves in such regions is very slow. According to the model, these interconnections result from a moderate diffusion of the substrate (the antagonist). Low level activation can be maintained due to the influx of substrate from the surrounding cells when otherwise wave termination would occur. However, since some substrate has already been consumed by the cells into which the wave must spread, the activator concentration is low (and the pigmentation faint). More time is required before a neighboring cell is triggered, i.e., the speed of the wave is reduced and the line is steep. During this slow movement of the activated zone, the substrate concentration increases in neighboring cells. Later, full activation will be triggered again in those cells in which activation survived at low levels. On the final shell weak but steep lines are formed that connect two subsequent pigmentation lines (Figure 4.7).

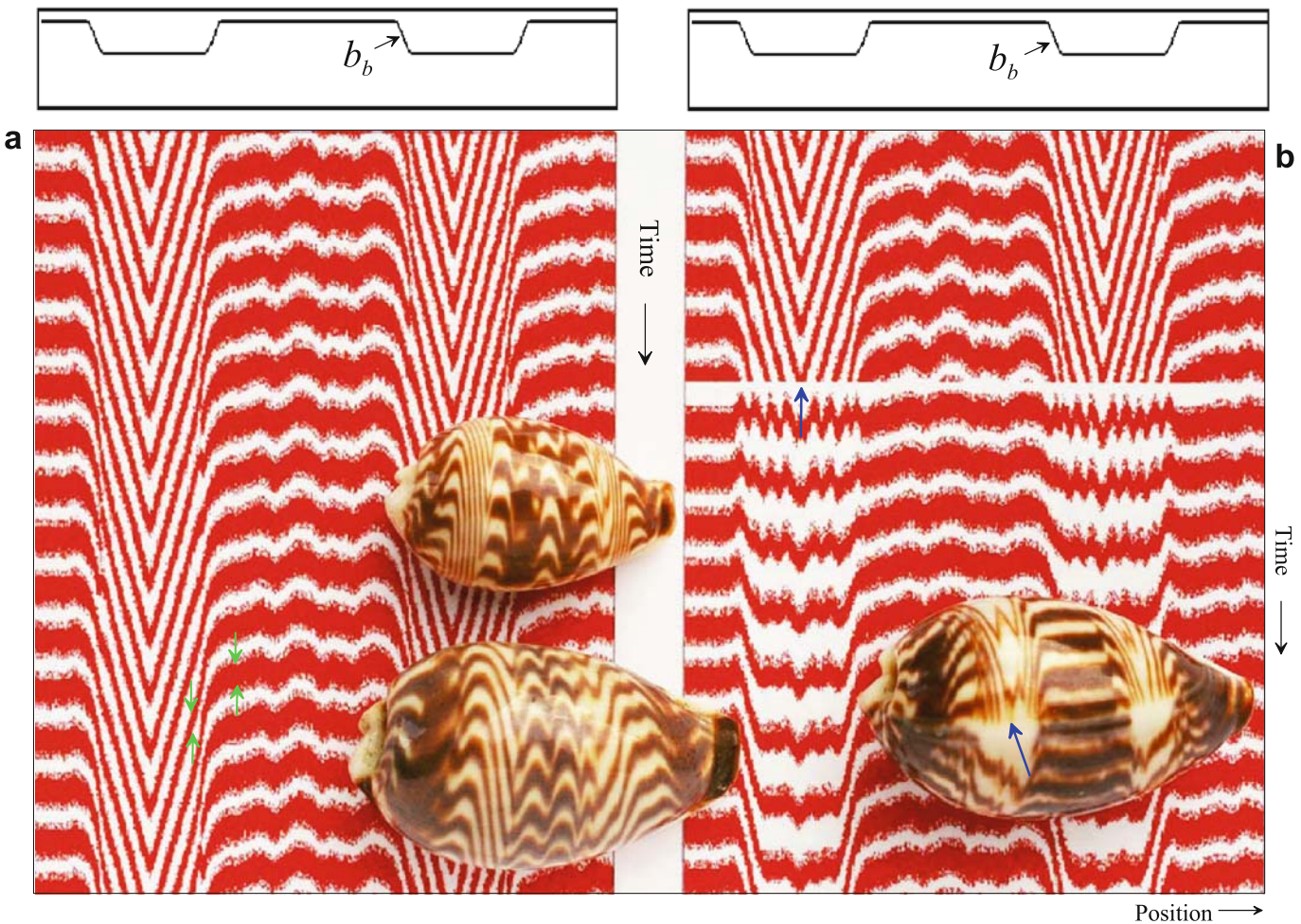


Figure 4.6. Steep lines. (a) Shell of *Cypraea diluculum*. Model: if the activator autocatalysis has an upper bound (saturation), the activated period within a cycle is relatively long and thick stripes result. If activator diffusion is low, the activation of one cell by its activated neighbor requires time. Due to the long persistence of the activation, this does not lead to wave termination. Large phase differences can accumulate between adjacent cells, giving rise to the steep lines in regions of lower oscillation frequencies. (b) According to the model, huge phase differences only accumulate in the course of time. Therefore, after a perturbation (blue arrows) and a new spontaneous trigger of the activation, the phase differences are reset. Steep lines are gone and reappear only in course of time. The horizontal and the steep lines seem to have different line width. Note, however, that the activation time in the regions of horizontal and steep lines is the same (green pairs of arrows); it is a system property of the oscillating system that does not depend on the phase difference between adjacent cells [S46]

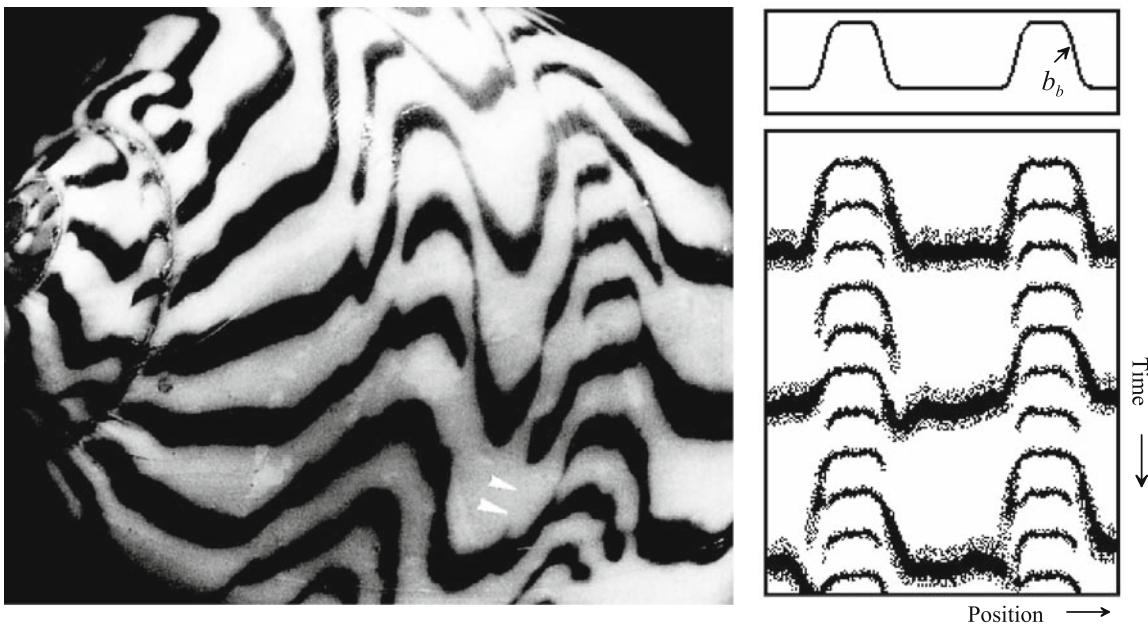


Figure 4.7. Connected arches: shell of *Natica undulata*. Model: if, in addition to activator diffusion, some substrate diffusion takes place, the connection of one line with the following line is possible. Due to substrate supply from the surrounding cells, the activation can be maintained almost locally. The traveling waves can come close to rest without becoming extinct. This “surviving” activation triggers activation of the surrounding cells as soon as their refractory period is over. The resulting pattern consists of a steep line forming a connection between subsequent pigmentation lines. The two arrowheads mark a hidden line [S47].

4.4 Hidden waves

On shells with arches, line termination may also occur occasionally. But the mode of re-activation indicates that the mechanism is somewhat different from the line termination mentioned above. The re-activation occurs at the elongation of a terminated line, i.e., at a displaced position (see the two arrows heads in Figure 4.7). This indicates that the traveling wave was still present, although the activator concentration was too low to evoke pigmentation. This observation suggests that pigment production is not by itself the autocatalytic process, since wave propagation can continue without (visible) pigmentation. Wave formation may be an independent process. Only if the signal is high enough would pigmentation be accomplished. Alternatively, it may be that wave propagation proceeds at two different levels (see Figure 8.8) and the lower level is insufficient to evoke visible pigmentation.

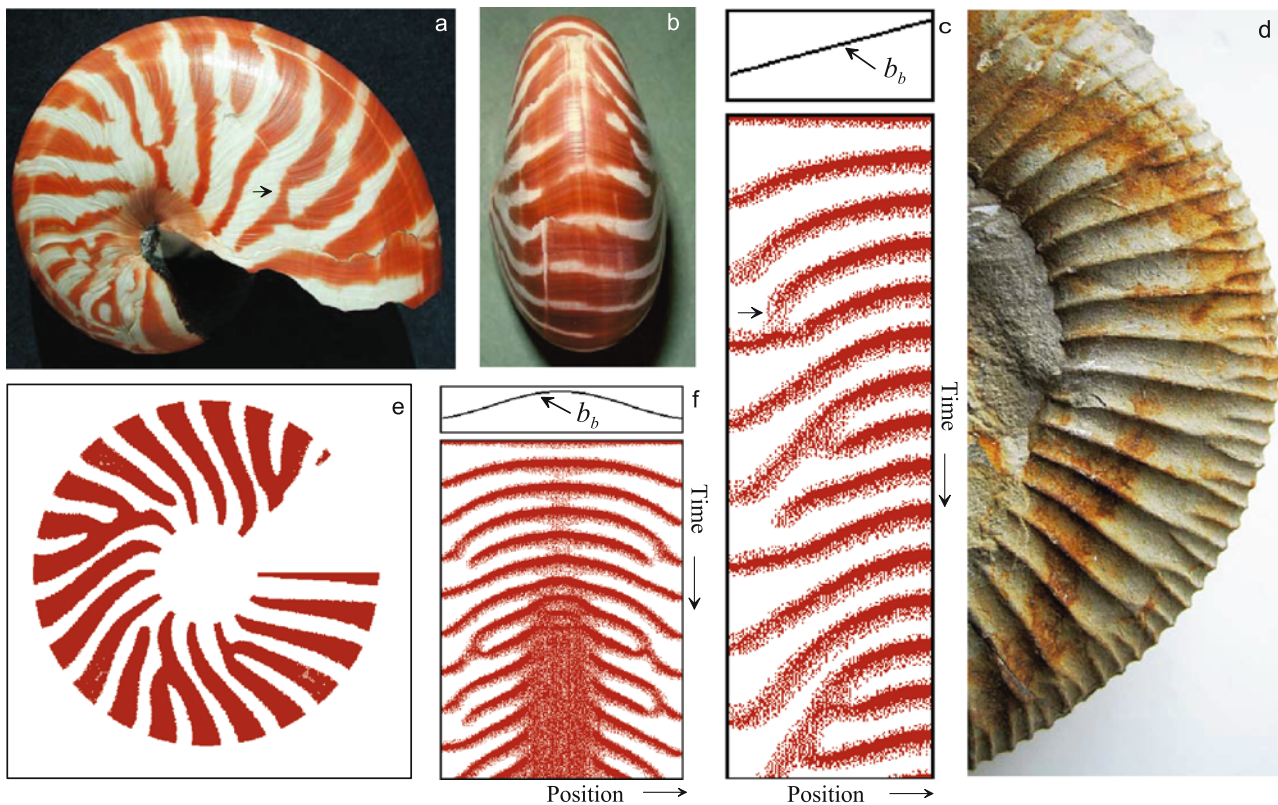


Figure 4.8. Shell of *Nautilus pompilius*. (a,b) Two views; the number of lines at the shell periphery is approximately double the number in the inner region, indicating a gradient in the oscillation frequency. (c) Model: an activator-substrate model with a graded substrate production $b_b(x)$ is assumed that leads to a gradient in the oscillation frequency. Blindly ending and merging lines appear as on the natural shell. Merging occurs if a wave comes to rest. It merges then with the subsequent wave. This coming to rest is also clearly visible at the natural pattern [compare arrows in (a) and (c)]. (d) Ammonites display a closely related pattern with bifurcations close to the periphery (Hammer and Bucher, 1999). (e) The activated phases are drawn as partial circles to demonstrate the similarities between the natural and the simulated patterns. (f) Simulation of a peripheral view. In the region of high substrate production, activator production attains nearly a steady-state. (Photograph (d) kindly supplied by Ulrich Heim) [S48c, S48d]

4.5 Pattern on the shell of *Nautilus pompilius*

The curled shape of the *Nautilus* shell results from different growth rates along the growing edge. Ward and Chamberlain (1983) have determined the growth rate of animals kept in the aquarium to be 0.15 to 0.25mm per day (or 7cm per year). Accordingly, the animal shown in Figure 4.8 produced about 8 pigmentation lines on the peripheral region of its shell in the last year of its life. At the same time only 4 lines have been formed on the inner region. This indicates roughly a factor of two in the oscillation frequency between the inner and outer side of the shell. Irregularities on the surface of the shell provide a record of the shape of the growing edge over

the course of the animal's individual history. These growth lines result neither from a daily nor a lunar rhythm. Saunders (1984) found a substantial variation of 4 to 15 days per growth line in the larger species *Pomphilus belanensis*.

A stable pattern must exist that controls oscillation frequency. It must have a graded distribution. For the sake of simplicity in the simulation in Figure 4.8c, a linear gradient has been assumed. To obtain the spiral shape of the shell, a similar gradient in the growth rate is required. Both oscillation frequency and growth rate may be under the control of the same gradient.

The pattern on the *Nautilus* shell shows pattern elements similar to those discussed in the previous section: interconnection of successive pigmentation lines, and terminating lines which are restricted to a region of high oscillation frequency. It is thus tempting to assume a similar mechanism to the one outlined above. In this case, moderate activator diffusion leads to partial synchronization among neighboring cells. High saturation causes the pigmentation lines to have about the same width as the space in between. Due to moderate substrate diffusion, two pigmentation lines can fuse. Termination of pigmentation lines also occurs. The similarity between the simulated and the natural pattern becomes especially striking if activator production is plotted as partial concentric circles corresponding to the actual mode of shell growth (Figure 4.8).

4.6 Stabilizing an otherwise oscillating pattern by diffusion

As outlined above, oscillations occur if either substrate production is too low to maintain a permanent activation or the inhibitor reaches equilibrium too slowly due to low turnover. However, the situation may change if the antagonist strongly diffuses, even though all time constants remain the same. An additional substrate supply from the surroundings via diffusion can be sufficient to maintain a steady-state activation. In the same way, a substantial loss of inhibitor by diffusion has an effect similar to shortening the inhibitor's life and can equally cause the transition to a steady-state. In such cases, lateral inhibition comes into play. The transition to the steady-state can occur only with a certain spacing. Figure 4.4 and Figure 4.7 illustrate the formation of connections between subsequent pigmentation lines based on substrate diffusion. Figure 4.9 shows that even stronger substrate diffusion can cause a localized transition into steady-state activation. On the shell this leads to lines parallel to the direction of growth. Between these lines the oscillations can continue. Line formation is expected to occur preferentially in regions with larger differences in oscillation frequency since the onset of stabilization requires a phase difference between neighboring cells. In this case an activated cell can profit from its nonactivated neighbor. The snail *Voluta musica* in Figure 4.9 produces a shell with a related pattern. Fine lines perpendicular to the growing edge are interspersed with periodic patterns of dots and fine lines parallel to the growing edge. These pattern elements are reproduced in the simulation. The simulation is certainly not perfect

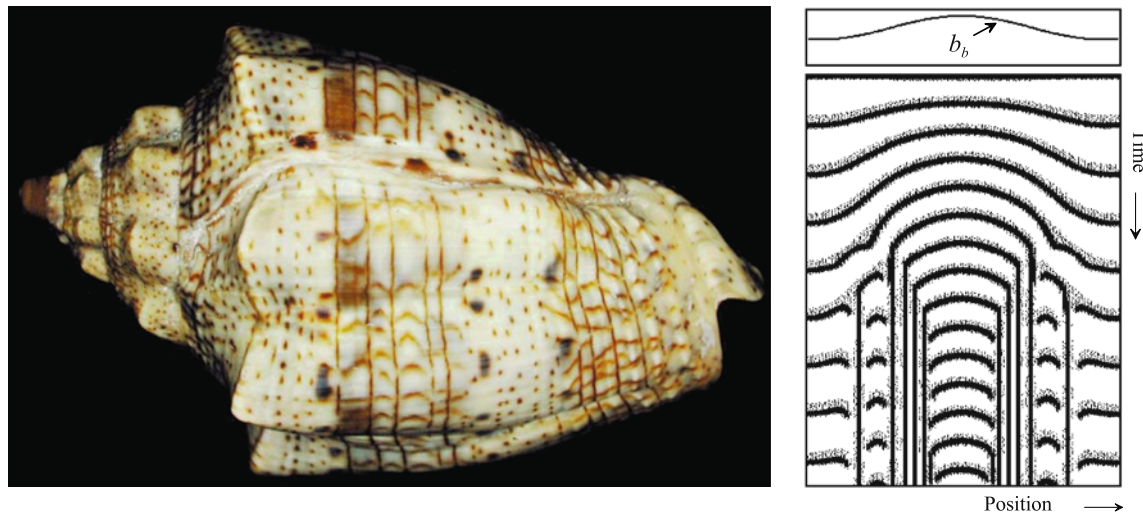


Figure 4.9. (a) Lines parallel and perpendicular on the same shell - the shell of *Voluta musica*. The pattern is characterized by two bundles of fine lines perpendicular to the growing edge, interspersed by periodic pattern elements. (b) Simulation. In regions of high substrate production (high b_b in Equation 2.4), the system is close to the transition from oscillating to steady-state activation. Diffusion provides an additional supply of substrate from neighboring nonactivated regions. In this way steady-state activation emerges at several sharply localized positions [S49].

since fine dots are formed on the shell between the bundles of lines while in the simulation more lines appear. The simulation merely illustrates the diffusion-based transition from an oscillatory regime to localized steady-state activations.

4.7 Combinations of oscillating and nonoscillating patterns

Very different patterns emerge if the stable pattern shifts groups of cells into a permanent steady-state. This occurs, for instance, if the local substrate production surpasses a certain level. Permanent pigment production by these cells leads to stripes parallel to the direction of growth. The cells in between these stripes are still able to oscillate. Traveling waves are initiated at regular distances by the permanently activated cells. The resulting pattern consists of nested V's between the stripes. Figure 4.10 shows a simulation together with the shell of *Cypraea ziczac* for comparison. The peripheral pattern of a *Nautilus* shell (Figure 4.8b,f) was an example of a system on the borderline between oscillation and steady-state.

4.8 Rows of patches parallel to the direction of growth

An even more common pattern is the reciprocal of that discussed above. Oscillations take place only in particular regions on the shells. Rows of patches,

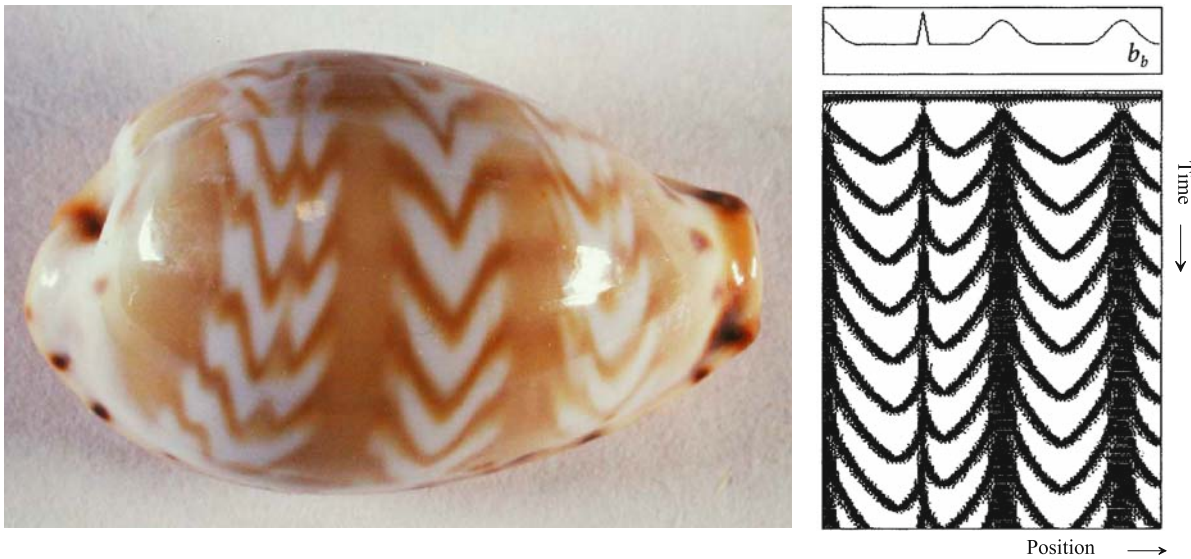


Figure 4.10. Fish-bone pattern resulting from a combination of permanent and oscillatory pigment deposition. (a) Shell of *Cypraea ziczac*. (b) Model: an activator-substrate model is assumed. In regions where substrate production is high, cells enter into steady-state activation, causing pigmented bands parallel to the direction of growth. These permanently activated cells periodically initiate waves traveling in the space between the bands. The V-like elements result from the annihilation of pairs of waves at the point of collision [S410]

dots, short lines or crescents result. They are separated by bands in which no pigmentation occurs.

It is tempting to assume that this pattern may be generated by an elementary system in which the antagonist has a high diffusion rate (pattern in space) and a long time constant (pattern in time). However, as mentioned, the mechanism for lateral inhibition requires some time before a particular region will dominate over a neighboring one. In oscillating systems with burst-like activation this time is not available (see Figure 3.5). Again, a stable pattern must be responsible for determining where activations will take place.

It is possible that a periodic pattern will generate its own stable pattern due to positive feedback from the activation on the source density, i.e., on the general ability of a cell to perform autocatalysis (s in Equation 2.1 and 2.4). Despite the initially sloppy separation of the patches due to a long-lasting influence on the source density, regions of slightly enhanced activation will obtain a stronger advantage in the next oscillation and so on until a stable periodic pattern in the source distribution emerges. A simulation is provided in Figure 4.11. Feedback by an activator pattern on the long lasting source density seems to be a general mechanism in development and is used, for instance, for the generation of stable tissue polarity. If a monotonic activator distribution is generated (see Figure 2.9) and the activator produces feedback on the source density, the source density will obtain a graded distribution too. In such a system, once the activated region is removed, a new activator maximum regenerates in the remaining tissue at the point of highest source density, i.e., at the side pointing towards the original activated region. Such a “memory” of the

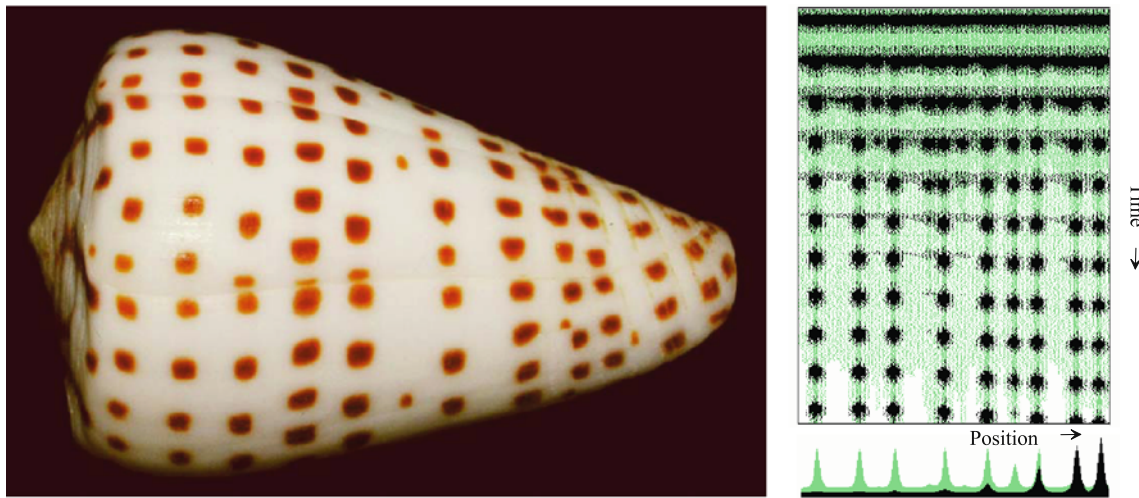


Figure 4.11. Generation of a stable pattern by feedback from an oscillating pattern on the source density. In an oscillating system rapid diffusion of the antagonist does not lead to well-resolved patches. With the feedback of activator concentration on the source density (green), a slightly stronger activation leads to an even stronger activation in the next cycle and so on until rows of patches emerge along the stable periodic pattern of the source density (curve at the bottom). However, as shown in Figure 4.13, the actual mechanism presumably involves two complete systems [S411].

tissue is suggested by classical experiments with the fresh water polyp *Hydra* (see Figure 12.5).

The types of patterns that can be generated by this mechanism are limited. For example, rows consisting of large patches in close proximity cannot be produced since the required saturation together with the required inhibitor diffusion would lead to continuous stripes instead of isolated patches. These restrictions disappear if, as in the examples discussed above, two patterns are superimposed. Two modes are conceivable for the action of the stable pattern. Either the stable pattern generates the precondition that allows oscillations to take place or, conversely, the conditions for oscillation are given everywhere except in those regions in which the stable pattern is in an activated state. One possible way to distinguish between these two modes is by the spacing between the rows. The activated region is usually smaller than the nonactivated region. On the shell shown in Figure 4.12 only very narrow pigment-free lines separate the much broader regions in which oscillatory pigment production actually occurs. The fact that the activated regions are usually smaller than the nonactivated ones, suggests that a localized suppression of oscillation by a spatially stable pattern is involved.

Figure 4.13 shows a simulation that assumes two activator-inhibitor systems. The stable system (the activator shown in red) acts as an additional inhibitor on the oscillating system (black). Thus, black patches can appear over the course of time only along the (nonred) interstices allowed by the stable system. Partial synchronization can take place such that several patches are formed at the same time.

On some shells the distances between the rows of pigmentation are irregular. A possible cause of these irregularities is that the interstices must have a certain width

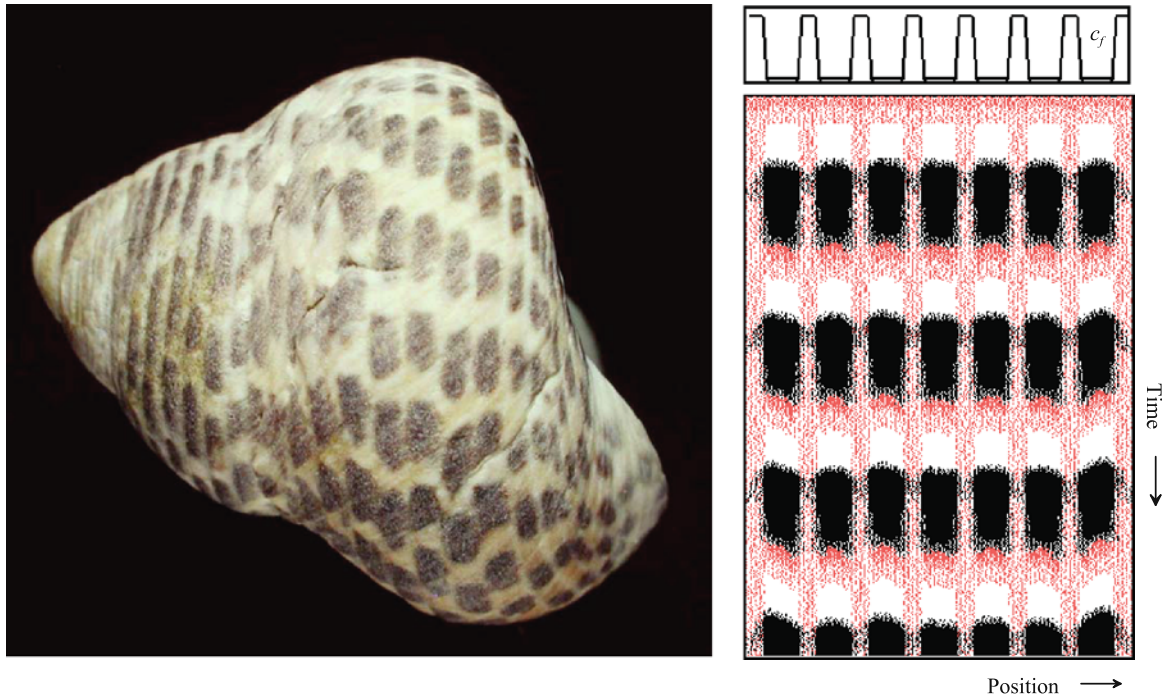


Figure 4.12. Narrow permanently unpigmented lines indicate an active suppression of the pigmentation reaction. Shell of *Austrocochlea adelaidae*. Activated regions are usually much smaller than the non-activated regions in between (see Figure 2.3). Therefore, the stable pattern must cause the suppression of pigmentation reaction and cannot function as a precondition for pigmentation. Simulation: constant pigmentation over a long period of time can be achieved if a separate extinguishing reaction is involved (shown in red) that terminates pigment production (see Figure 7.4); [S412]

in order for periodic activations to occur. If two maxima of the stable pattern are too close together, the inhibitory level in between is too high to allow the onset of oscillations. However, with the growth of an animal, the size of the interstices increases too and oscillations become possible. On a shell, such an event leads to the insertion of a new row of patches in a larger, formerly nonpigmented region. On the other hand, from a certain distance between the maxima of the suppressing pattern onwards, the insertion of new maxima is expected (see Figure 2.6 and 2.7). On the shell, a row with large patches of pigmentation will split into two smaller rows. Both the split and the insertion of pigmentation rows can be seen on the pattern of *Scaphella junonia* and are reproduced in the simulation (Figure 4.13). Such patterns demonstrate that the stable pattern is not fixed during an early stage of development, but that it is dynamically regulated in the growing animal.

4.9 The possible role of a central oscillator

Generation of the three-dimensional structure requires different growth rates along the mantle gland of the shell (see chapter 10). A very remarkable feature in many shell patterns is the constancy of the spacing between periodic pattern elements

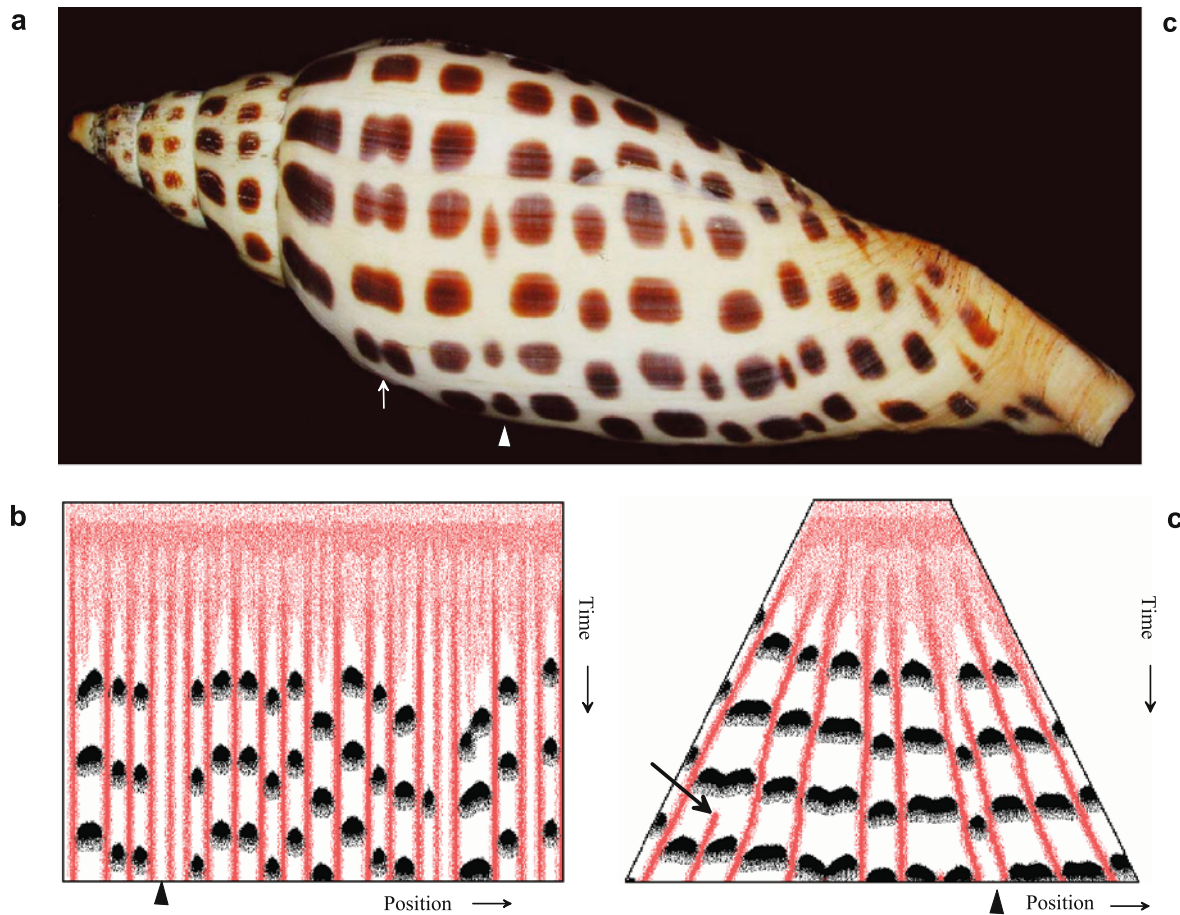


Figure 4.13. Rows of patches. (a) Shell of *Scaphella junonia* (b) Model: An oscillating activator (black) - inhibitor system is assumed to be responsible for pigment deposition. By cross-inhibition a stable activator (red) - inhibitor system restricts the oscillations to particular bands. Oscillations occur, nevertheless, essentially in synchrony. A minimum distance between suppressing stable maxima may be required for oscillations to occur; the arrowhead marks a too narrow and thus empty column. (c) Simulation of a growing system. After surpassing a critical size, a new maximum (arrow) is inserted into the suppressing pattern, causing a split of a row into two. If the distance between repressing maxima becomes large enough, oscillations starts in a previously empty column (arrowheads in the simulation and on the shell). Initially some oscillations may be skipped [S413b, S413c]

despite the different speed of accretion of new material at the shell's growing edge. One possible mechanism has been discussed already for the *Nautilus* shell (Figure 4.8): the growth rate and the oscillation frequency may be under the control of the same graded signal.

The constancy of spacing implies that more lines are inserted at positions with higher shell circumference. When, for instance, in a region of larger shell circumference ten, and in a smaller region only nine stripes are inserted in a certain time interval, there must be a zone of mismatch. An inspection of the shells tells us that these phase conflicts between neighboring oscillators are resolved in a very short time interval, within one or two oscillations. On the shells this causes, for instance, one line to end blindly while the preceding and subsequent lines make

connections (Figure 3.1 and 3.4). Remaining phase differences are resolved by a fast re-synchronization of the oscillators, as indicated by a sharp bending of the corresponding lines. Similarly, in Figure 4.14, a single line makes a sharp bend and fuses with the subsequent line.

Attempts to simulate this phenomenon turned out to be more difficult than expected. When the differences in the oscillation frequencies are small but the tendency to mutual synchronization is large (as indicated by straight parallel lines), it is expected that synchrony is maintained, as in the case of the shell shown in Figure 1.4 (page 8). Line termination as demonstrated in Figure 4.4 is difficult to obtain under these conditions. If a diffusing inhibitor is involved in the synchronization, line termination can occur due to lateral inhibition (Figure 4.14b). However, the resulting pattern differs substantially from the natural pattern. It requires several oscillations in the zone of conflict before synchronization is re-established.

An alternative possibility is shown in Figure 4.14c. In addition to the oscillating pigment system (black), an endogenous oscillating system is assumed (green) that is homogeneously distributed in the organism in a hormone-like manner. It oscillates with approximately the same frequency as the pigment system and has an enhancing influence on it. Therefore, the pigmentation system will be entrained by the central oscillator as long as the phase difference is not too large. Otherwise the pigmentation system will skip one pulse of the central clock and becomes entrained to the next pulse. As Figure 4.14c demonstrates, the simulation reproduces space-dependent reduction of line density much better. Re-synchronization is accomplished within one or two pulses. The synchronization remains through many more pulses until the next short relief of phase differences occurs.

Evidence for an oscillating system independent of the pigmentation system but with a stimulating influence on it was provided earlier in Figure 1.10 (page 14), where the periodic modulation of the background pigmentation and the locally restricted periodic pigment production can be easily distinguished. Both systems are in partial synchrony. With the analysis of triangular pattern elements in chapter 8, another example of the influence of global oscillations on pigment production will be discussed.

4.10 Conclusion

A large class of patterns can be explained by assuming that oscillating pigment deposition is modified by a stable and usually invisible pattern. Eye-catching bands appear on the shells. The oscillation frequency can be increased, decreased, or oscillations may be locally suppressed. Depending on the coupling between adjacent cells, some regions become pacemaker properties. Traveling waves may merge or terminate if the phase differences become too large. As discussed further below, the patterns become much more complex if the invisible modifying pattern is also oscillating. Few parameter changes are sufficient for such a transition.

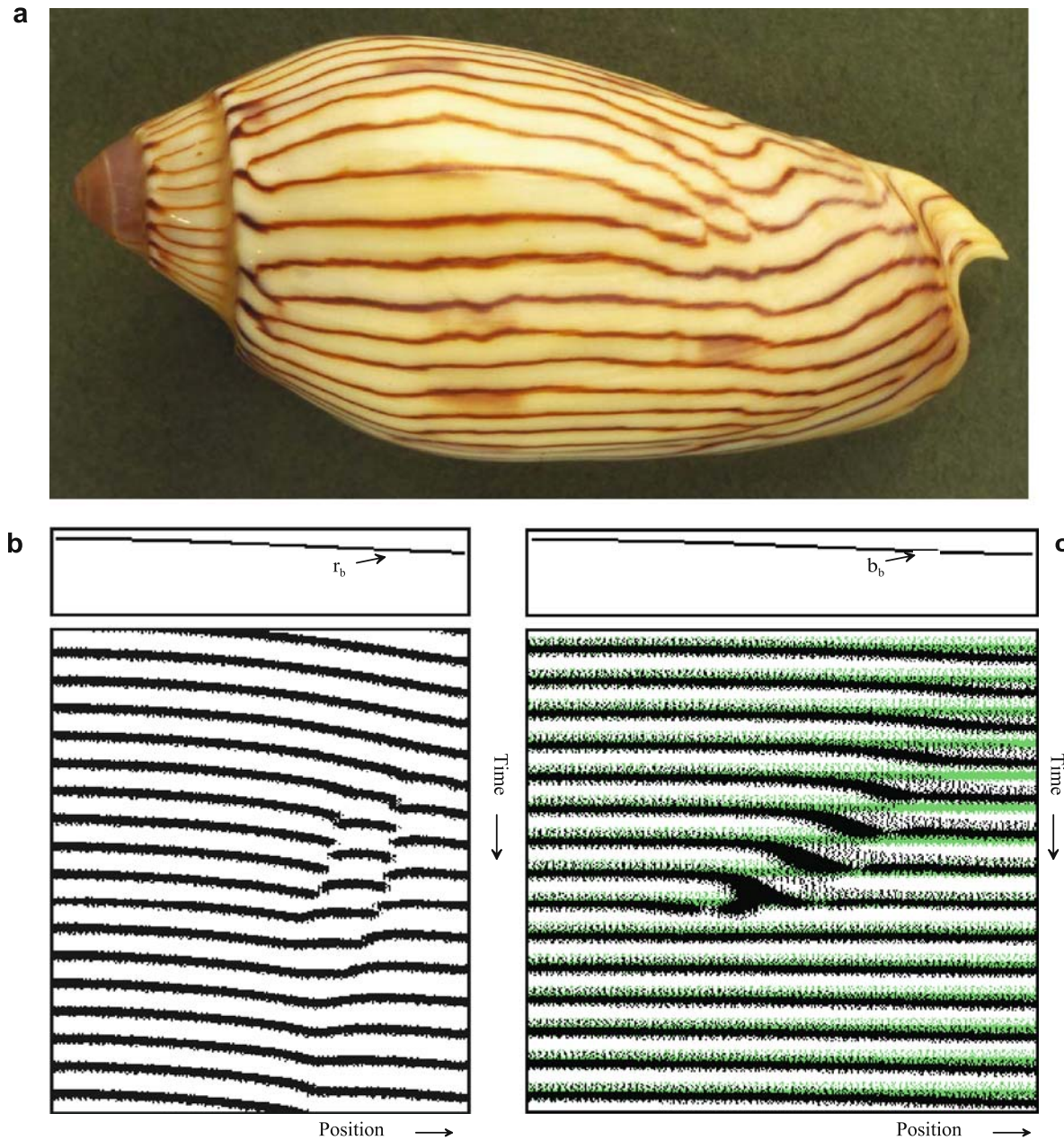


Figure 4.14. Synchronization of oscillating pigment deposition by an internal clock. (a) Shell of *Amoria turneri*. The lines have a constant spacing. The number of lines is reduced discontinuously in regions of smaller shell diameter. (b) With a diffusing inhibitor and a space-dependent oscillation frequency (lifetime r_b is space-dependent), accumulating phase differences between neighboring oscillators can cause periods of re-synchronization between adjacent cells. This would lead to extended zones of line mismatch. (c) A central oscillator (green) has a stimulating influence on the oscillating pigment system. Whenever the phase difference becomes too large, a local resetting is possible within one or two pulses, which is in much better agreement with the natural pattern (see also blue arrow in Figure 5.8 for a related phenomenon [S414b, S414c])

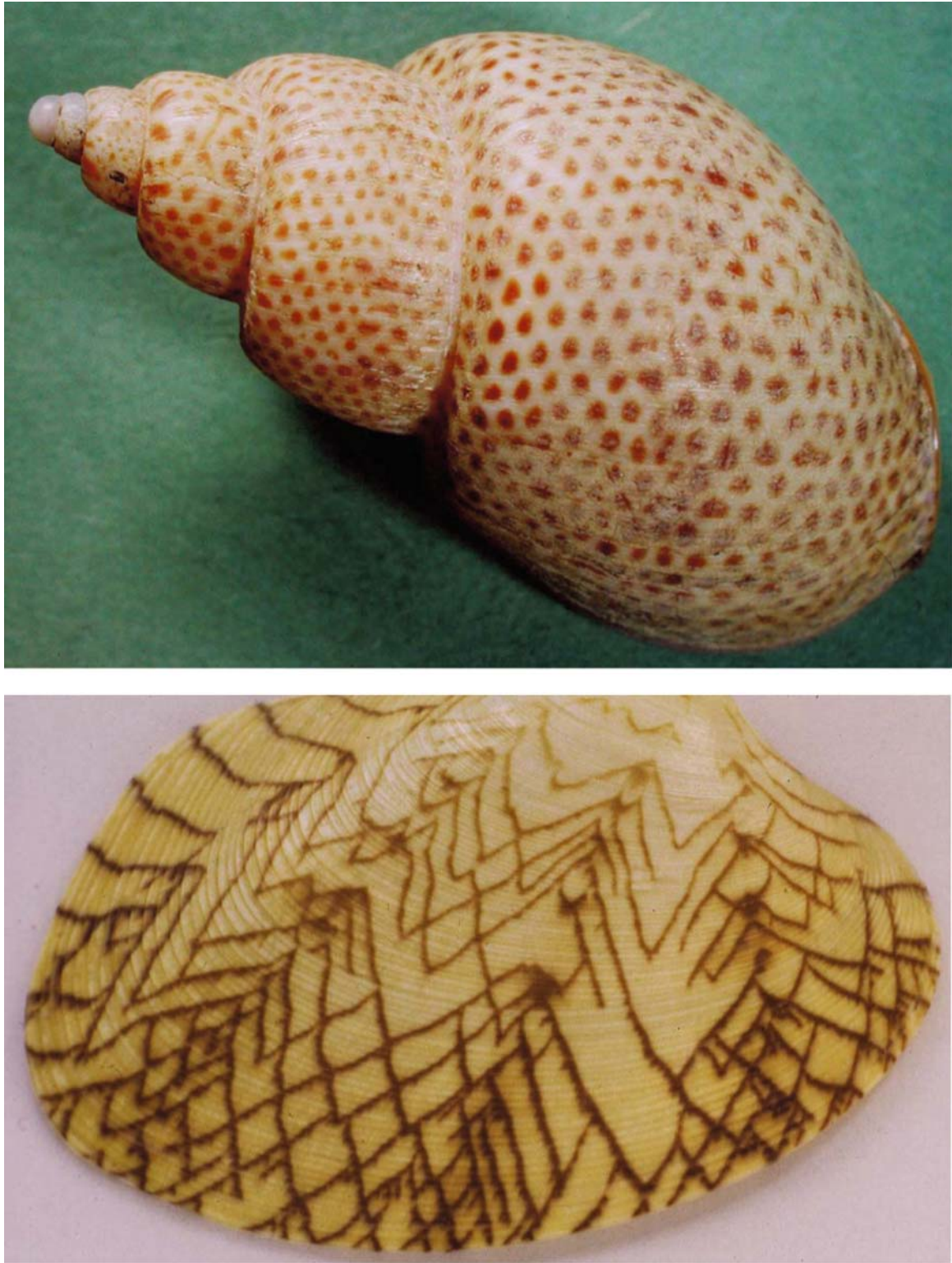


Figure 5.1. Staggered dots on *Babylonia papillaris* and oblique lines with crossings on *Tapes literatus*. Although the patterns look very different, it is proposed that both are based on a common mechanism. Two antagonists enforce a periodicity in space and time

Crossings, meshwork of oblique lines and staggered dots: the combined action of two antagonists

Many shells display simple periodic patterns that cannot be accounted for with the elementary mechanisms described so far. Patterns of staggered dots and meshworks belong in this class (Figure 5.1). These patterns are characterized by a periodicity along the time coordinate as well as along the space coordinate. This suggests that two antagonists are involved: a nondiffusible one that is responsible for the periodicity in time, and a second highly diffusible one that causes the pattern through space. The interactions described in this chapter are possible extensions of the activator-substrate and the activator-inhibitor model (see boxes). An important property of such mechanisms is that traveling waves can emerge without pace-maker regions and that colliding waves can penetrate each other without annihilation. In other words, crossings of oblique lines can occur.

5.1 Displacement of stable maxima or enforced de-synchronization by a second antagonist

For a more intuitive understanding of the role of the second antagonist let us first regard the elementary pattern on its own and then take the action of the second antagonist into consideration. If the primary system would lead to a stable pattern (highly diffusible antagonist), the local accumulation of the second antagonist would destabilize the maxima over the course of time. A neighboring region, not subject to the nondiffusible antagonistic effect, would become activated. Traveling waves would emerge.

Conversely, a system that is able to generate traveling waves (nondiffusible antagonist) may oscillate in a synchronous manner as long as no pace-maker region is available (see Figure 3.7a). An additional antagonist with a long range would enforce a de-synchronization. If a cell becomes activated somewhat later than its neighbors, this phase difference will increase during subsequent oscillations. The inhibitory influence that spreads from the advanced neighbors delays the somewhat retarded cells even more. The synchronism breaks down and traveling waves are formed. This type of transition is clearly visible in Figure 5.2.

Equation 5.1 and 5.2: extensions of the activator-depletion mechanism

For pattern formation involving two antagonists a third substance $c(x)$ is assumed that is produced at a rate proportional to the local activator concentration.

$$\frac{\partial c}{\partial t} = r_c(a - c) + D_c \frac{\partial^2 c}{\partial x^2}$$

It has the following inhibiting effect on activator-substrate interaction (Equation 2.4):

$$\frac{\partial a}{\partial t} = \frac{s b}{s_b + s_c c} a^{*2} - r_a a + D_a \frac{\partial^2 a}{\partial x^2} \quad (5.1.a)$$

$$\text{with } a^{*2} = \frac{a^2 + b_a}{1 + s_a a^2}$$

$$\frac{\partial b}{\partial t} = b_b - \frac{s b}{s_b + s_c c} a^{*2} - r_b b + D_b \frac{\partial^2 b}{\partial x^2} \quad (5.1.b)$$

s_b a Michaelis-Menten-type constant. If nonzero, c plays a role only at high c concentrations, while at low c concentration the system behaves the same as a standard activator-substrate system.

s_c efficiency of the additional inhibitor

a^{*2} subsumes activator production by autocatalysis, the baseline activator production b_a and its limitation by saturation

With this interaction, activator concentration (but not substrate concentration) is to a large extent independent of c , since a reduction of c also leads to a compensating decrease in substrate removal. Alternatively, the second antagonistic reaction may result from an additional substrate c that can maintain activator production:

$$\frac{\partial a}{\partial t} = s a^{*2} (b + c) - r_a a + D_a \frac{\partial^2 a}{\partial x^2} \quad (5.2.a)$$

$$\frac{\partial b}{\partial t} = b_b - s b a^{*2} - r_b b + D_b \frac{\partial^2 b}{\partial x^2} \quad (5.2.b)$$

$$\frac{\partial c}{\partial t} = b_c - s c a^{*2} - r_c c + D_c \frac{\partial^2 c}{\partial x^2} \quad (5.2.c)$$

In both cases, one of the antagonists (b or c) must spread rapidly, while the other should have a low diffusion rate (if any).

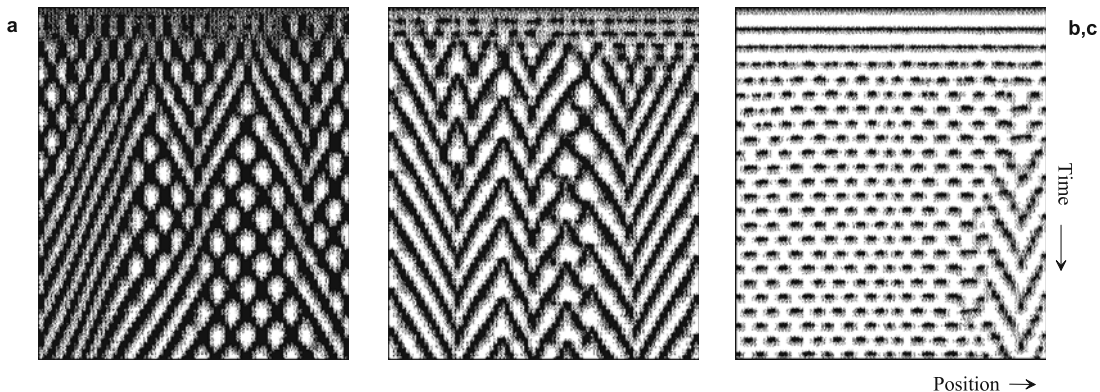


Figure 5.2. Meshwork, oblique lines and rows of dots: patterns resulting from an autocatalytic reaction coupled to *two* antagonistic reactions. A long-ranging antagonist generates the periodicity in space, the long-sating antagonist the periodicity in time. In these simulations the substrate is the diffusible antagonist. Simulated with Equation 5.1, using decreasing rates of substrate production ($b_b = 0.08, 0.06$ and 0.03). High substrate production leads to a more permanent activator production whenever the additional inhibitor is low enough, allowing a meshwork to form. At lower rates of substrate production only oscillations and thus traveling waves are possible. This produces oblique lines on the shell. At even lower production rates, the waves disintegrate to spots. [S52]

As shown earlier (Figure 2.7) when two maxima are too far apart, new maxima emerge in between. In a standard activator-inhibitor system, new maxima become preferentially inserted some distance from existing maxima. In contrast, in an activator-substrate model or in an activator-inhibitor system with saturation, new maxima result preferentially from a split and shift of existing maxima (Figures 2.6 and 2.7). This behavior is maintained if two antagonists are involved. As explained below in more detail, the combined action of two inhibitors preferentially leads to isolated patches in a staggered arrangement (Figures 5.11 and 5.12), while the involvement of a depleted substrate leads preferentially to shifting maxima and thus, in the time record, to oblique lines and meshworks.

5.2 Pattern variability

The characteristic patterns generated by two antagonists - meshworks, oblique lines and staggered dots - depend on the very different diffusion rates of the two substances. If, in contrast, both antagonists have similar diffusion rates, the overall patterns would be similar to the elementary patterns discussed in chapters 2 and 3, consisting of lines parallel, perpendicular or oblique to the axis. Therefore, the transition from an elementary pattern to a more complex pattern in related species does not necessarily imply the involvement of a different mechanism or an additional substance. Simply, it may be based on a change in the diffusion rate.

The resulting patterns are expected to show a high degree of variability from specimen to specimen. The variation of a single parameter can decide which of these patterns - meshworks, oblique lines and dots - will be formed (Figure 5.2).

Since the ranges of the parameters that form these different patterns will overlap, slightly different initial conditions or random fluctuations can lead to one or the other pattern.

Figure 5.3 shows two shells decorated with oblique lines and a meshwork. These shells were found in different layers of sediment in an ancient lake (Willmann, 1983). They belong to the same family. Although the patterns look so different, it is easy to understand why both patterns result from the same interaction. In both cases a regular alternation between pigmented and nonpigmented regions takes place along the time and space coordinates. In the model, a moderate increase in the decay rate of the diffusible inhibitor is sufficient to accomplish this transition (r_c from 0.022 to 0.033). Therefore, the model provides a rationale for assuming that either a change in environmental conditions or a genetic drift has led to the transition from one pattern to the other.

If the traveling waves are organized by pace-maker regions, the resulting pattern is very reproducible since wave initiation takes place at predictable positions (Figure 3.7). In contrast, if the traveling waves are enforced by a second antagonist their starting points and their direction of propagation is not fixed. These ambiguities are revealed in the diversity of patterns seen on different specimens of the same species. Of course, although not necessary, a pace-maker region may be involved in a reaction with two antagonists as well, causing more predictable patterns.

5.3 Global pattern rearrangements

On many specimens a global pattern perturbation can be seen that took place at a particular time. Such an event is indicated by an abrupt and simultaneous termination of a regular pattern that was prominent over a long period of time. A more or less complete rearrangement follows. Figure 5.4 shows two examples in which broad oblique lines disappear in favor of a series of zigzag or wavy lines. Such a global pattern rearrangement is easy to understand by the model. As can be seen in the simulation in Figure 5.3 it takes some time before the oblique line patterns become dominant. An unspecific perturbation, such as a general decrease in activation due to starvation or dryness, can wipe out such an established dominance. For instance, each region in which some activation survives can give rise to two diverging lines, temporarily causing a pattern of wavy lines (Figure 5.4). Somewhat later, lines with a particular orientation can emerge again and the dominating pattern of oblique lines may become re-established. However, the re-established pattern of oblique lines may have a different orientation. Figure 5.6f provides an example of such a situation.

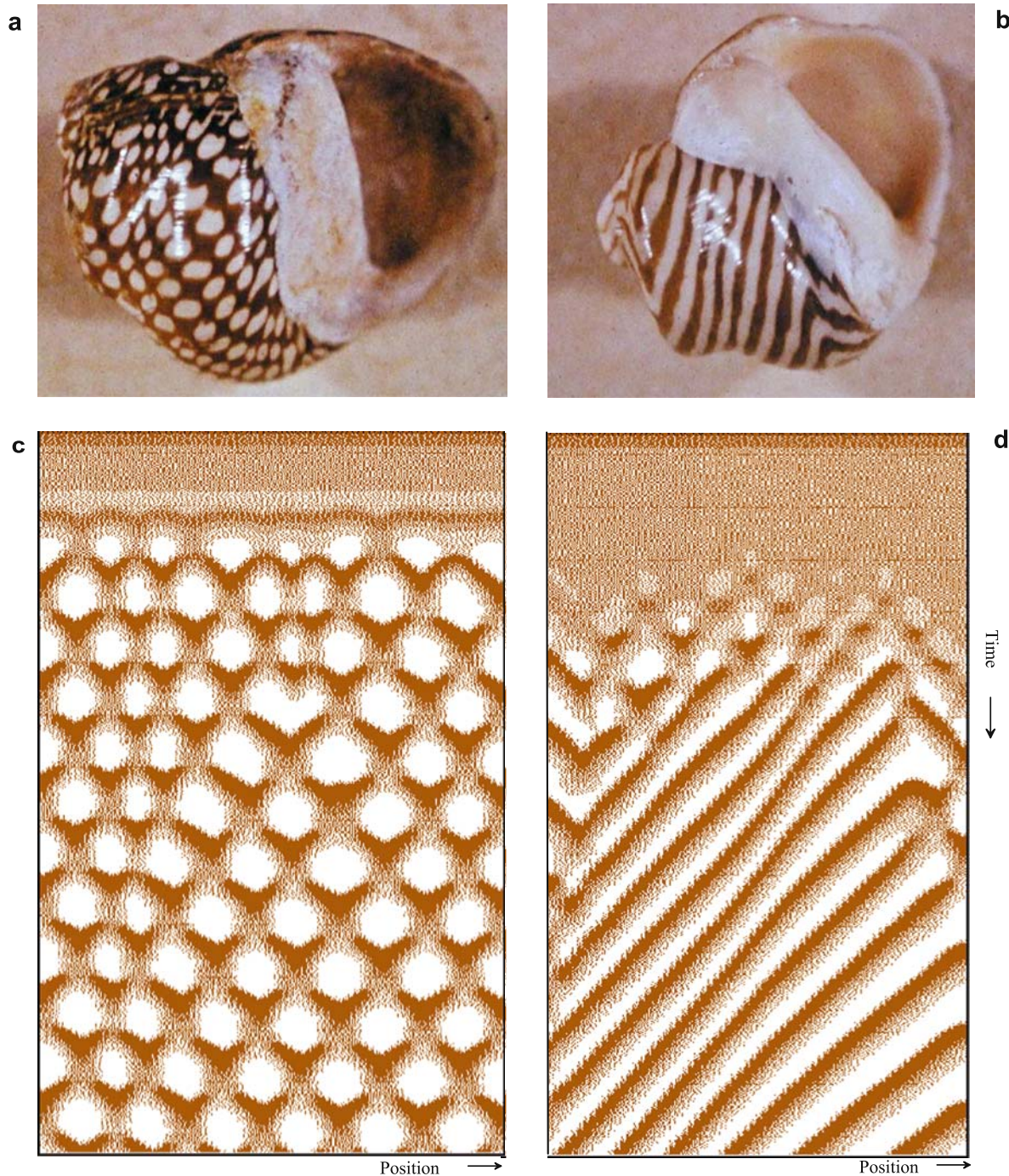


Figure 5.3. Variability of patterns. Shells of *Theodoxus dorus* found in different layers of an ancient lake on the Greek island Koos. Model: the meshwork and oblique line patterns can be generated by the same mechanism. A nondiffusible substrate is responsible for the periodic pattern in time, a diffusible inhibitor for the periodic pattern in space. A shorter half-life of the inhibitor leads to a more rapid alternation in space. In this way, the inhibitory action of one wave onto the subsequent wave becomes stronger and the meshwork degenerates into oblique lines. (Photographs kindly supplied by R. Willmann, see Willmann, 1983); [S53]

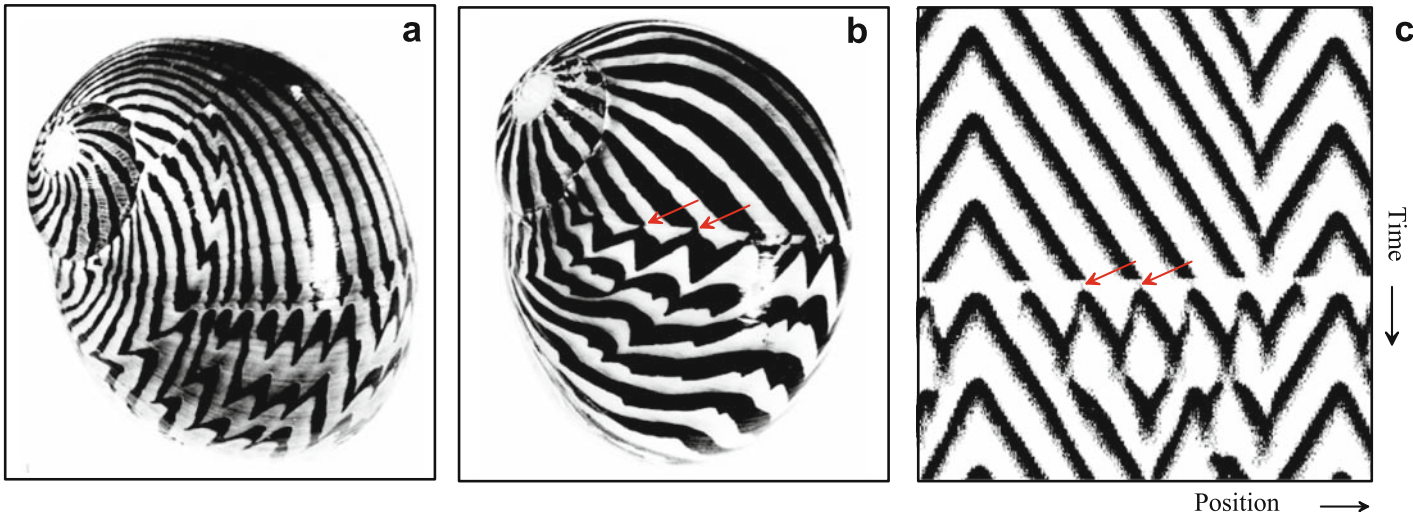


Figure 5.4. Pattern transition after global perturbation. (a, b) Two shells of *Neritodryas dubia* GMELIN with an abrupt global transition from oblique lines to a zigzag pattern. (c) In the simulation, a global reduction of the activator leads to the initiation of many new divergent lines (www-pattern). After a while, the oblique line pattern would be restored. The model describes correctly that faint connection between an unperturbed wave and the re-activation is restricted to the leading edge of the wave, i.e., to the regions where the activation is the highest (arrows). (Photographs kindly supplied by G. Oster); [S54]

5.4 Traces of the additional inhibition: oblique lines initiated or terminated out of phase

A species with an especially rich pattern variation on its shell is the small snail *Bankivia fasciata* (Figures 5.5 and 5.6, see also Ermentrout et al, 1986). These shells show peculiarities in their patterns that very conveniently illustrate the action of a second long-range antagonist.

If traveling waves are based on the elementary mechanism described earlier, no irritation is visible before two waves annihilate each other in a collision (see Figures 3.6-3.9). In contrast, traveling waves enforced by an additional inhibition can behave differently. Shortly before a collision takes place each wave enters a region of reduced substrate resulting from consumption by the counter wave. The result is a mutual retardation of the waves. After collision, survival is prolonged since substrate diffusing from the surrounding regions provides additional support for the activation (the local stabilizing effect of diffusion was discussed in detail in Figure 4.4). Together, the effects of retardation and elongation lead to a blob-like structure or a sharpening at the tip of the V's (arrows in Figure 5.5 a, b).

Although very different in its appearance, another phenomenon has presumably the same basis. Frequently a particular orientation of waves dominates because the waves in a small region that run in the opposite direction disappear (Figure 5.5 c, d). According to the model, the long-range antagonist causes a delay in the initiation of the short counter wave, the \wedge -like structure. Due to this delay, the counter wave will become shorter and shorter over the course of time until the dominating

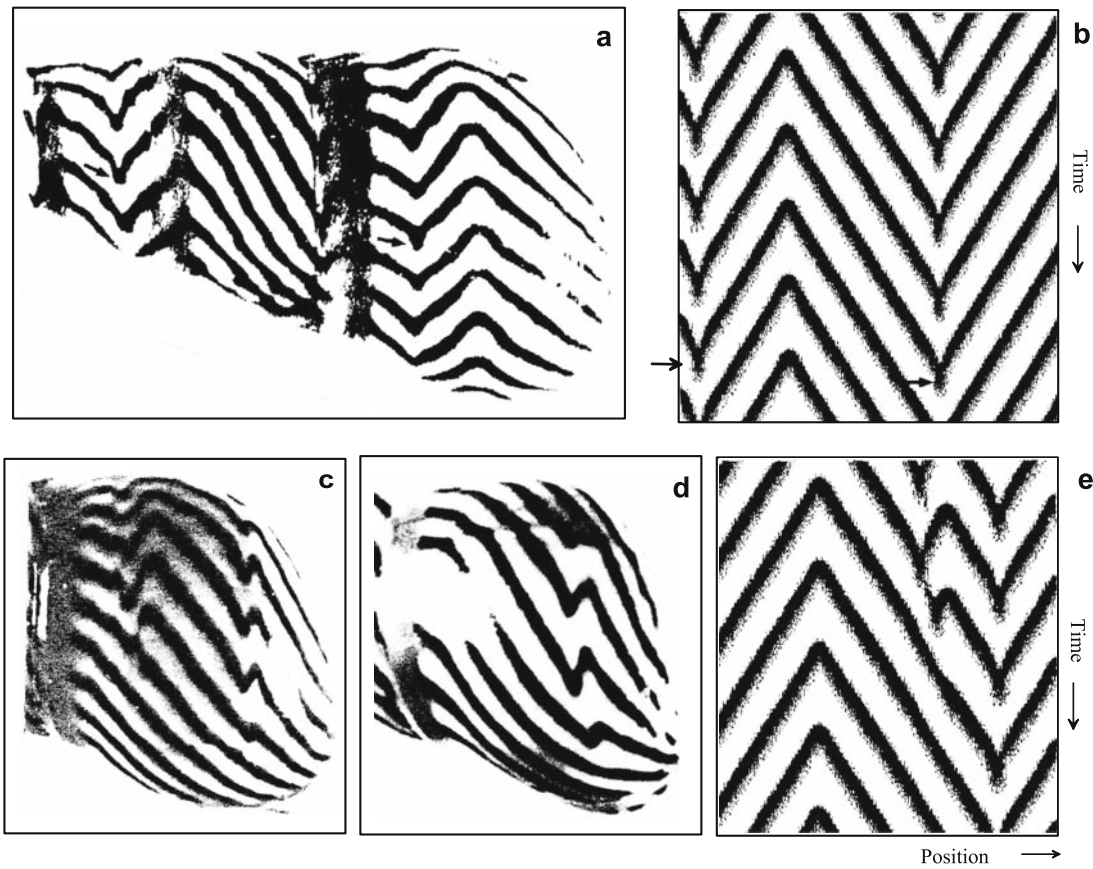


Figure 5.5. Traces of the diffusible antagonist in *Bankivia fasciata*. (a) The V-shaped zones of annihilation show some sharpening at the tip (arrow). (b) Model: The action of the long-range antagonist can lead to a reduction in the speed of the waves shortly before collision. After the collision, the local reduction of the antagonist due to its rapid diffusion elongates the active period, contributing to the tip formation. (c-d) Small irregularities on oblique lines disappear. (e) Model: the initiation of short counterwaves becomes delayed by the diffusible antagonist until no locally advanced trigger can take place. (Photographs kindly supplied by J. Campbell, see also Ermentrout et al., 1986) [S55]

wave reaches the initiation point before the spontaneous initiation can take place (Figure 5.5e).

The shell in Figure 5.6a exhibits a pronounced chessboard pattern decaying into oblique lines. As outlined earlier, if the autocatalysis saturates, the activated and nonactivated phase can be of the same length, causing thick parallel lines (see Figure 3.5). It is the second and diffusible antagonist that enforces the phase shift between parts of these lines. Or, to explain it other way round: the long-ranging antagonist on its own would lead to a stable pattern while the short-ranging but long-lasting antagonist poises these activations, causing their disappearance, which allows new activations in the former gaps. The saturation leads to the large extension of these activated regions in space and time. In the time record, this leads to the chessboard pattern. A higher substrate production causes the transition to oblique

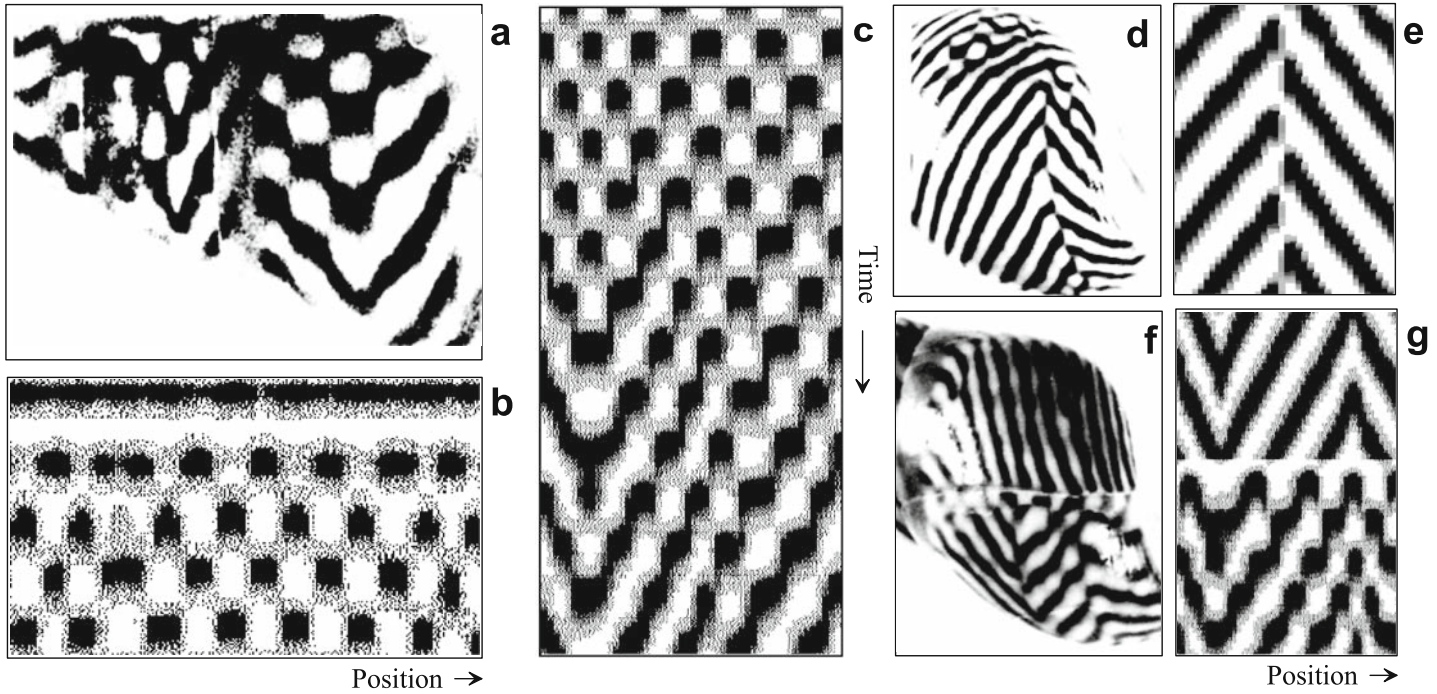


Figure 5.6. Chessboard pattern and its decay into oblique lines. (a) *Bankivia fasciata*. (b, c) Model: saturation of the activator autocatalysis leads to activation periods of the same length as the intervals in between. The highly diffusible antagonist (in this case, the substrate) causes the phase shift between parts of the resulting thick lines. Low inhibitor diffusion maintains the maximum phase difference and the coherence of the patches. An increase in substrate production leads to the tendency to form oblique lines. (d, e) Initiation and (f, g) termination of traveling waves may occur out of phase due to the long-range antagonist. In (f) a global perturbation took place, simulated in (g) by a temporary reduction of the activator concentration. The transient formation of a more meshwork-like pattern is reproduced. (Photographs kindly supplied by J. Campbell); [S56, S56m, S55]

lines, a transition that is analogous to that shown in Figure 5.2c-b for the nonsaturating case.

Even if the chessboard pattern resolves into oblique lines, some elements can remain that are reminiscent of this pattern. Either the initiation or the annihilation of waves may occur out of phase. Isolated columns of alternating black/white and white/black transitions can remain stable over a long period of time (Figure 5.6d-g). According to the model, the effect of the long-range antagonist is especially pronounced if two waves that run in opposite directions are close to each other. This is the case either at the initiation or the termination of waves. Waves can be generated in alternating directions, one to the right, one to the left, etc. since one wave inhibits the other. The small group of cells from which the waves spread maintains a nearly steady-state concentration.

The situation is similar during annihilation (Figure 5.6). The long-range antagonist stops the wave before a proper collision takes place. Again, the resulting black/white - white/black line can be regarded as a columnar fragment of the

chessboard pattern. The chessboard and out-of-phase patterns require similar ranges of parameters. Especially important to this type of handshaking are activated and nonactivated periods of about the same length.

5.5 Crossings and branching

The shells of some species are decorated with oblique lines that frequently cross each other. An example was given in Figure 5.1. Apparently, traveling waves can penetrate each other and enter into a region that should be refractory, in contrast to the normal rules for waves in excitable media. Survival of colliding waves is a feature of the meshwork patterns discussed above (Figure 5.3). However, patterns with general crossings are usually much less regular.

How can traveling waves survive a collision? One possibility is that during a collision cells remain activated until the refractory period of the neighboring cells is over. Thereafter, a re-infection of these cells can take place. A crossing can be regarded as the initiation of a new pair of waves at the point of collision. A signal must be available that enables the cells to remain activated. What can the signal be? What is different at the point of collision? In the normal chain of triggering events that leads to oblique lines, the activation of one cell is followed by a full activation of its neighboring cell. In contrast, after a collision, the activation breaks down, and no subsequent activated cells are available. Thus, for a group of cells, a possible signal that a collision took place at this position could be the absence of subsequent activation.

We have discussed the possible role of a second rapidly diffusing antagonist and we will see that the same mechanism (Equation 5.1) can be used to explain the formation of line crossings, although with a different range of parameters. Let us assume an activator-substrate system tuned to bi-stability, i.e., a low and a high steady-state exist (see Figure 3.3), and that the activator is diffusible while the substrate is not. The resulting pattern would not be very interesting. From a local initiation, the activation would spread until all cells are switched from the low to the high steady-state. Now let us assume in addition a highly diffusible inhibitor exists. During the spread of activation, each newly activated cell also produces a burst of diffusible inhibitor which shifts the recently activated cells back into the nonactivated steady-state. Traveling waves result that are very similar to those generated by the elementary mechanism. However, such waves behave differently upon collision. There, the decline of activation also causes a decline of the rapidly diffusing inhibitor. This creates a counter-regulation. If the time constant of the inhibitor is fast enough, this reduction will no longer allow the cells to shift from the high to the low state. The waves stop but a local activation remains. When the refractory period of the neighboring cells is over, two new waves are initiated that travel in opposite directions in much the same way as waves that penetrate each other, except for a small delay at the point of collision. The inhibitor that emanates from the

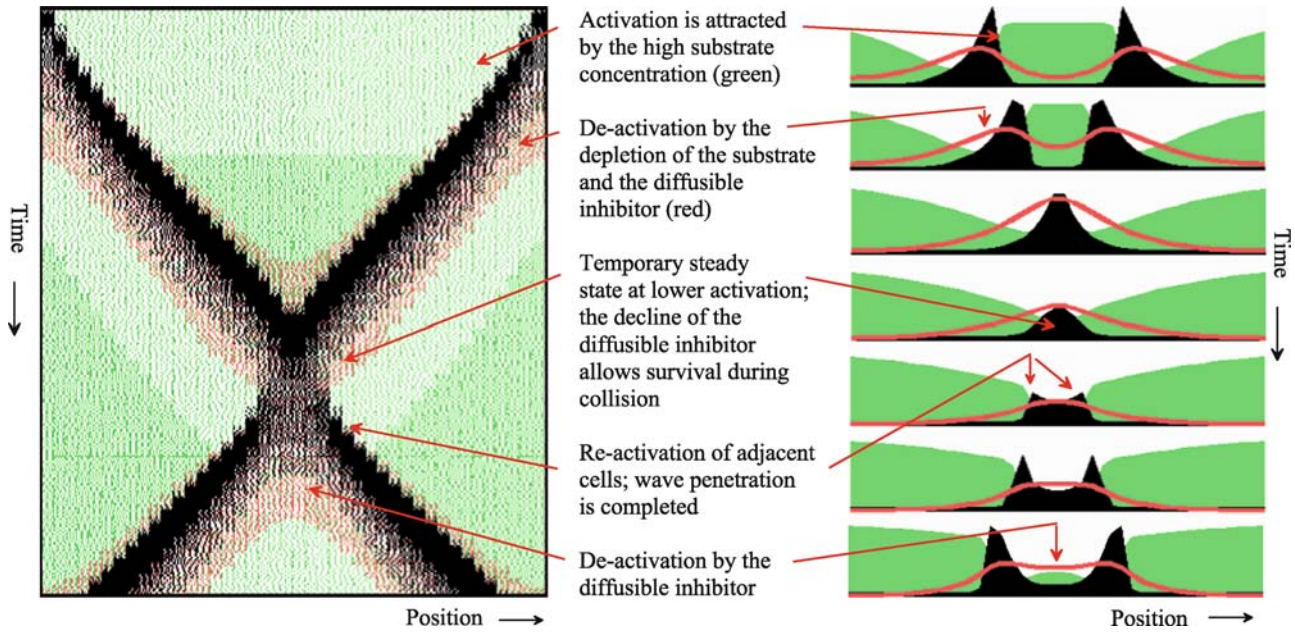


Figure 5.7. Formation of crossings by an additional diffusible inhibitor. An activator-substrate model is tuned to bi-stability. High activation spreads due to activator diffusion. The high state is reached with some overshoot. The additional diffusible inhibitor (red) causes each subsequently activated cell to down regulate the activation in previously activated cells. Apparently normal traveling waves result. However, at the point of collision the activation survives due to the rapid decrease of the additional inhibitor concentration. After recovery of the substrate (green), two new waves are initiated [S57, S57a, 57b, 57c]

reactivated cells suppresses the activation in those cells in which the activation has survived. Figure 5.7b shows a computer simulation and the presumed sequence of events.

A shell with crossings, as well as a simulation in a larger field, is shown in Figure 5.8. A comparison reveals that the model is able to account for fine details. Although, as a rule, both waves survive a collision, in some instances one of the new waves becomes extinct, causing a pattern like an amputated X. The initial attempt to form a second wave is clearly visible in most of these cases. In the model, most of the additional diffusible inhibitor is secreted after full activation of the two new waves. This leads to a competitive situation in which one of the two waves may not survive. Note that the competitive effect becomes critical only after a collision, not before, although in both cases the waves pass through a stage of comparable distances. After collision much less substrate is available for supporting the waves (see Figure 5.7). The situation is especially critical if another wave is nearby.

In addition to crossings, in the shell shown in Figure 5.8 also branching of the oblique lines do occur, indicating that occasionally wave splitting can take place. In terms of the model, a lowering of the activation for whatever reason also leads to a lowering of the long-range inhibition. The inhibition can become insufficient to enforce a rapid return to the nonactivated state. The activation remains temporarily

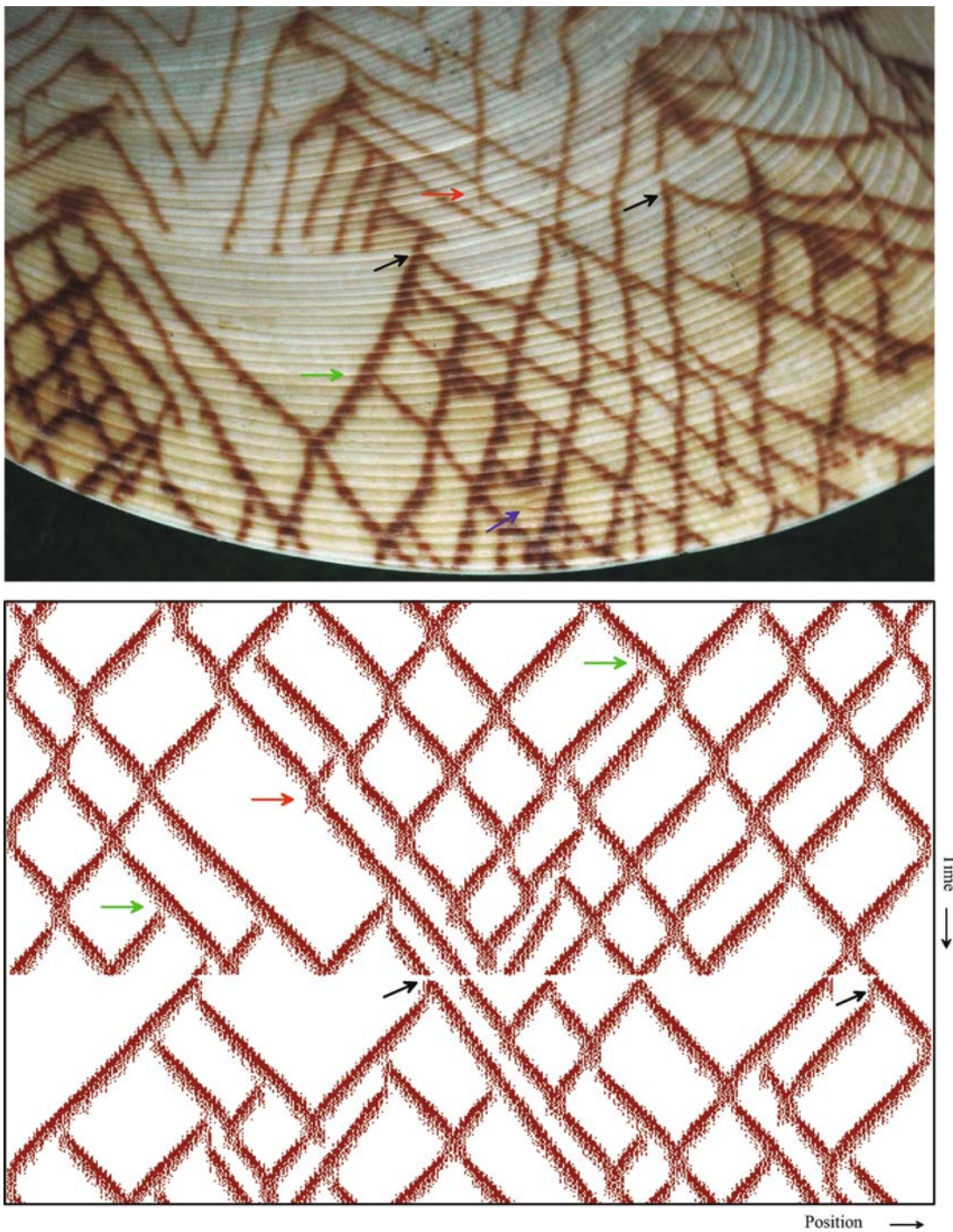


Figure 5.8. Formation of crossings: Patterns on *Tapes literatus*. Simulation calculated with an activator-depleted substrate model plus an additional inhibitor (Equation 5.1). The waves can survive a collision. The long-ranging inhibition assumed in this interaction accounts for the fact that occasionally only one wave survives the collision (red arrows). Wave splitting do occurs, leading to a branch on the shell (green arrows). The general pattern discontinuity visible on the shell is simulated by a reduction of the activator concentration to 20% of the current value in each cell. This leads simultaneously to the termination of waves and to the initiation of new pairs of waves (black arrows). The fusion of a growth line (blue arrow) indicates that an intrinsic oscillating process is involved in the generation of this rippling pattern (see also Figure 4.14) [S58, 58a; S57 provides a simulation without branching].

in a steady-state. After some times the refractory period is over and a wave is initiated that moves in the opposite direction, usually with the same speed. The elevated inhibition terminates the steady-state. This completes the formation of a branch.

The pattern on the shell shown in Figure 5.8 displays a global irregularity presumably, caused by a sudden external event such as dryness or lack of food. Many waves have vanished at the same time. However, other waves survived and even formed new waves by wave splitting. The model resolves this apparently contradictory behavior between the extinction of waves and the simultaneous generation of new waves. A temporary lowering of the activator can lead either to wave termination or, due to the concomitant reduction of the long-ranging inhibition, to the initialization of a new pair of waves, as during a normal collision. In some cases, the attempt to form two waves is clearly visible but one wave does not survive. This is another clear indication for the involvement of a long-range inhibition, an unusual feature of systems that form traveling waves.

The details on the shell in Figure 5.8 also reveal an aspect not yet included in the model. Relief-like structures separated by faint lines parallel to the growing edge can be seen. Between these lines, the pigmentation increases in width, but at the line this width is discontinuously reduced. The pigmentation has, in fact, a fine structure resembling a chain of triangles. Thus, the shift from the high to low steady-state is not, as assumed so far, a continuous process but depends on, or is enhanced by, an independent oscillatory process. One suggestion is that these fine lines result from an external periodic event such as a daily rhythm. However, sometimes two such lines merge, indicating that the synchronism of the oscillations is not absolute. Therefore, the periodic line formation must result from an internal oscillatory process. In other shells, the feature of chained triangles is more obvious (Figure 8.1) and we will come back to the underlying mechanism in Figure 8.5.

5.6 Changing the wave speed before and during collisions

Depending on how rapidly a system recovers after a collision, some time may be required before the two new waves can spread again. The local temporary steady-state after the collision leads to a thin line parallel to the direction of growth. Since the substrate concentration may not be fully recovered yet, the speed of the waves may be slow initially but may increase continuously until the next collision takes place. Figure 5.9 show this feature very clearly. The accompanying simulation was performed under the assumption that two substrates are available for maintaining the autocatalysis (Equation 5.2). The nondiffusible substrate is responsible for the movement of the waves. The diffusible substrate enables their survival after a collision. The resulting pattern on the shells is reminiscent of staggered wine glasses. The rounded shape at the top is followed by a thin stem below. On the shell shown in Figure 5.9, regions with different mesh size are visible, generated either by the initiation of an additional branch or by the failure of the waves to survive a collision.

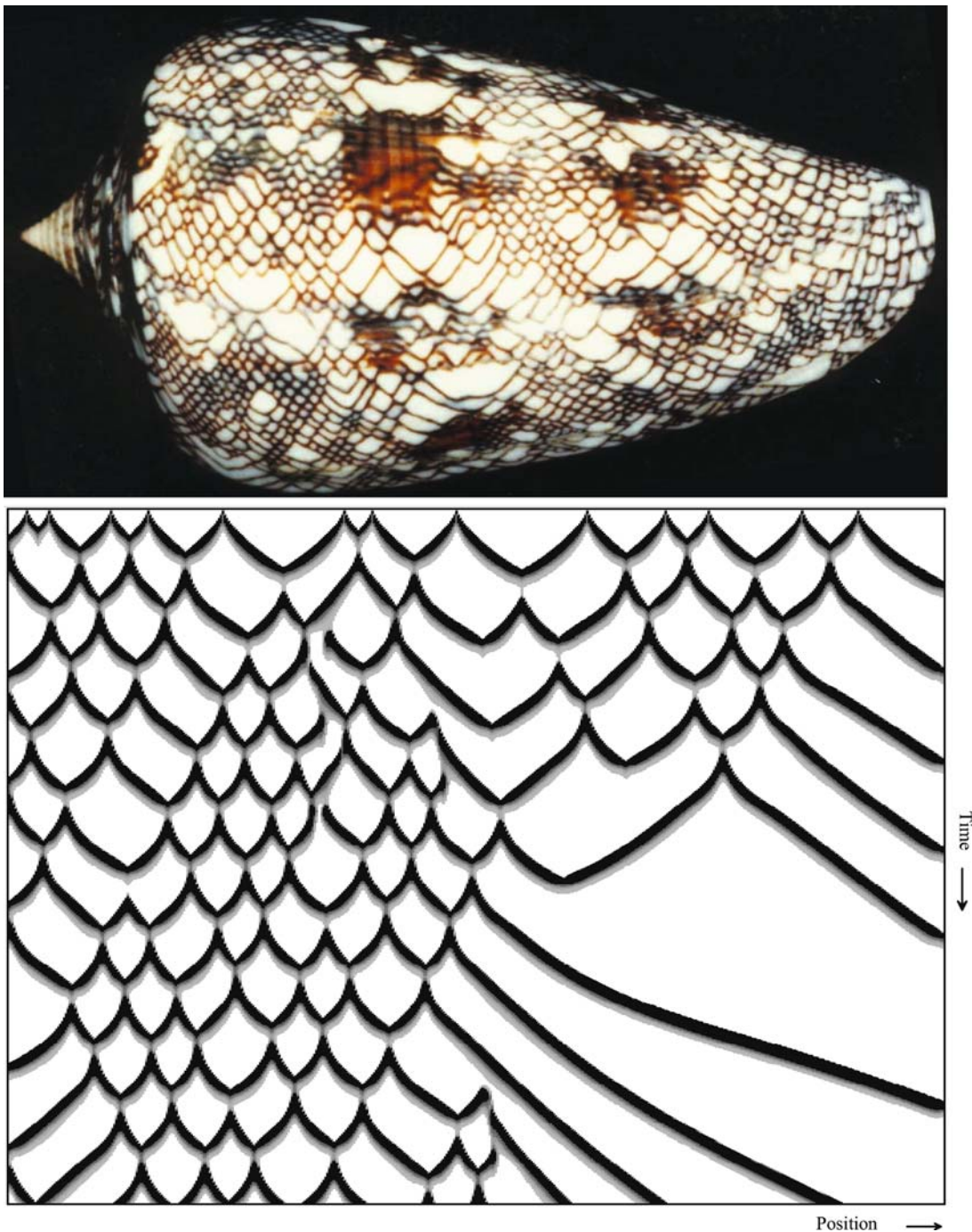


Figure 5.9. Changing wave speed during a collision: generating pattern elements reminiscent of staggered wine glasses. Shell of *Conus abbas*. One characteristic is the bending of the lines before collision indicating a speeding up. After the collision some time may be required before a wave starts moving. The simulation was calculated with a two-substrate model (Equation 5.2). The actual mechanism, however, is presumably more complex and involves two complete pattern forming systems (see Figure 7.3, page 109) [S59, 59m]

A stereotype mesh-like pattern with an oblique overall orientation can result. This feature is reproduced in the simulation. Later we will discuss evidence from related patterns indicating that not only a second antagonist but a complete additional pattern-forming reaction can be responsible for the alternation between the pulse-wise and the steady-state activation (Chapter 7).

5.7 Parallel and oblique rows of staggered dots

Another frequent pattern with a periodicity in space and time consists of rows of staggered dots. Activation in discrete patches suggests that both antagonists diffuse. This can cause patch-like activations separated along the space coordinate as well as along the time coordinate. This pattern occurs with a wide range of parameters if both antagonists are inhibitors (Equation 5.3). As mentioned, when an inhibitor is involved new maxima are inserted at some distance from existing activated regions (see Figure 2.7). This is precisely what happens in the staggered dot patterns, except that the maxima are no longer stable but disappear after a short time due to the second antagonist. In most of the simulations shown so far in this chapter, one antagonist has a high diffusion rate, the other was nondiffusible. However, when the second antagonist has a moderate diffusion rate, traveling waves are no longer possible if this slowly diffusing antagonist spreads faster than the activator. Under this condition and with the two antagonists having a time constant longer than the activator, activation occurs in separated patches. (If both antagonists were highly diffusible, stable stripes would result, as shown in Figures 2.3 and 3.5).

On some shells the dots appear to be arranged in oblique lines. On others the dots are in rows parallel to the growing edge but in staggered positions, i.e., each new dot appears exactly between two preceding dots. The simulations in Figure 5.10 illustrate the basis of this effect. Natural patterns of both types are given in Figure 5.11. Simulations have been performed with the two-inhibitor model. They differ only in the range of the slowly diffusing inhibitor which forms a forbidden zone after each activation (green in Figure 5.10). If its diffusion is more widespread, the subsequent activation will keep more distance from the previous activation. But this distance cannot be larger than half the distance between two previous activations since an activation cannot take place in the forbidden zone generated by the neighboring activation. Therefore, from a certain spacing onwards, subsequent activations will occur precisely in the gap between two preceding activations. This leads to a very regular pattern of dots out of phase. In addition to the regular spacing, a synchronization in time also takes place. Since the two new activations have the same distance from the previous spots of activation, the decline of the highly diffusible inhibitor is symmetric and the triggering of subsequent activations occurs simultaneously. Thus, neighboring dots appear on rows more or less parallel to the axis although a slight bending of these rows indicates that some phase shift may accumulate over the total length of the mantle gland.

Equation 5.3 and 5.4: extensions of the activator-inhibitor mechanism

A second inhibitor $c(x)$ is assumed to be involved in a normal activator-inhibitor interaction (Equation 2.1). The second inhibitor may have an influence on the production of the activator as well as on the production of the primary inhibitor $b(x)$:

$$\frac{\partial a}{\partial t} = \frac{s}{c} \left(\frac{a^2}{b} + b_a \right) - r_a a + D_a \frac{\partial^2 a}{\partial x^2} \quad (5.3.a)$$

$$\frac{\partial b}{\partial t} = \frac{r_b a^2}{c} - r_b b + D_b \frac{\partial^2 b}{\partial x^2} + b_b \quad (5.3.b)$$

$$\frac{\partial c}{\partial t} = r_c(a - c) + D_c \frac{\partial^2 c}{\partial x^2} \quad (5.3.c)$$

In this example the two antagonists are not completely equivalent. While the primary antagonist b has a direct influence on activator production but not on itself, the second antagonist also slows down the rate of inhibitor production. Similar to the description in Equation 5.1, this has the consequence that a is independent of c over a wide range. Therefore, the second inhibitor changes the region that will ultimately become activated but does not primarily change the absolute activator concentration.

Alternatively, the second inhibitor may have an additive inhibitory effect:

$$\frac{\partial a}{\partial t} = \frac{s(a^2 + b_a)}{(s_b b + s_c c)} - r_a a + D_a \frac{\partial^2 a}{\partial x^2} \quad (5.4.a)$$

$$\frac{\partial b}{\partial t} = r_b(a^2 - b) + D_b \frac{\partial^2 b}{\partial x^2} + b_b \quad (5.4.b)$$

$$\frac{\partial c}{\partial t} = r_c(a - c) + D_c \frac{\partial^2 c}{\partial x^2} \quad (5.4.c)$$

For instance, the diffusion of c does not allow a shift; the slowly accumulating inhibitor b chokes the activation and the activation soon stops. A new trigger is possible only at a displaced position. Oblique rows of dots or triangles results (Figure 5.12)

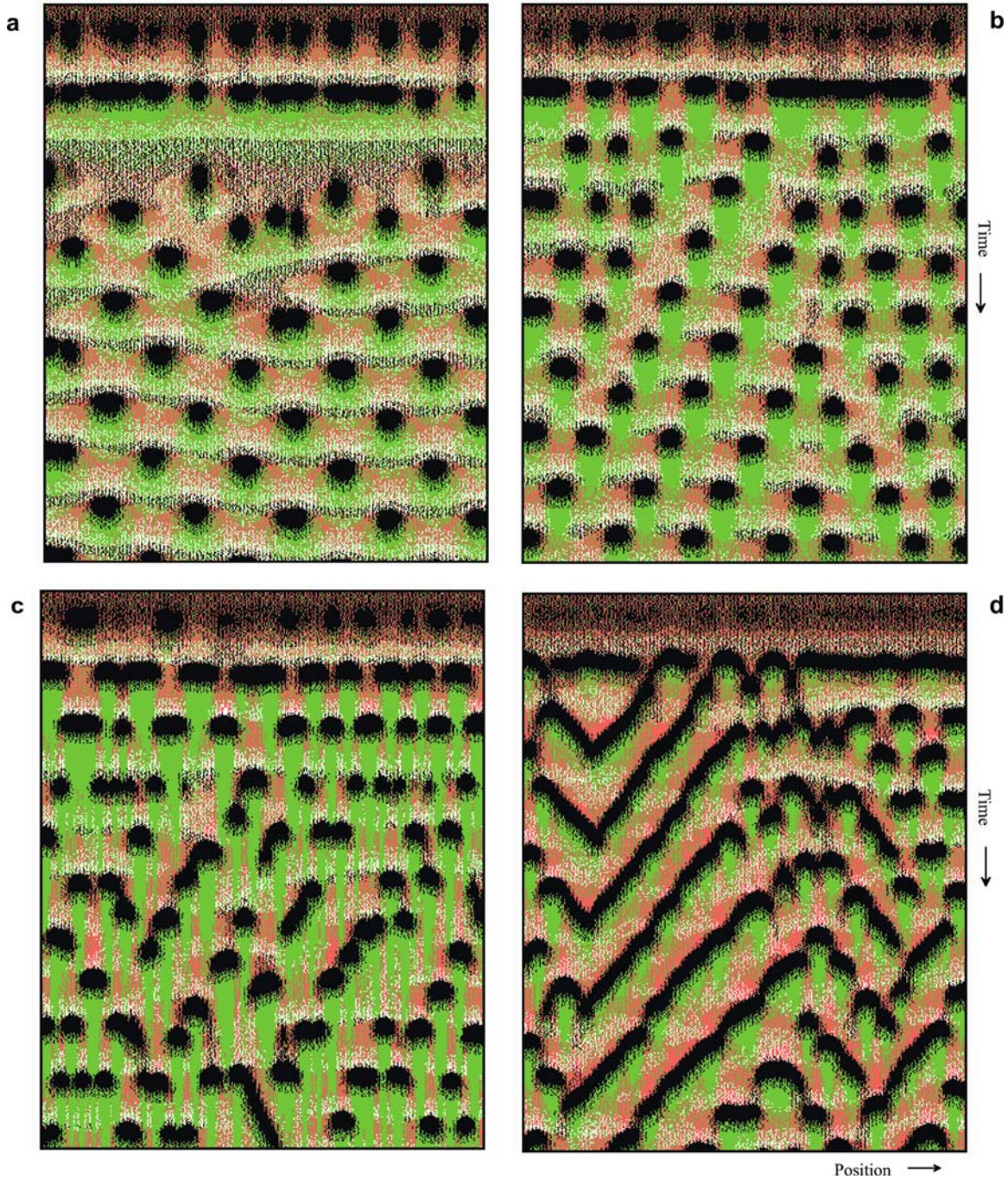


Figure 5.10. Horizontal and oblique rows of dots. Separate patches of activation occur if both antagonists diffuse; simulated with the two-inhibitor model, Equation 5.3. (a) If the rate of the slowly diffusing inhibitor (green) is above a critical level, the patches appear in horizontal rows and at positions precisely out of phase. (b) With a lower diffusion rate, the patches appear in oblique rows. (c) Without diffusion the patches partially merge. (d) When the low or nondiffusible antagonist has a shorter half life, a transition from patches to oblique lines occurs [S510]

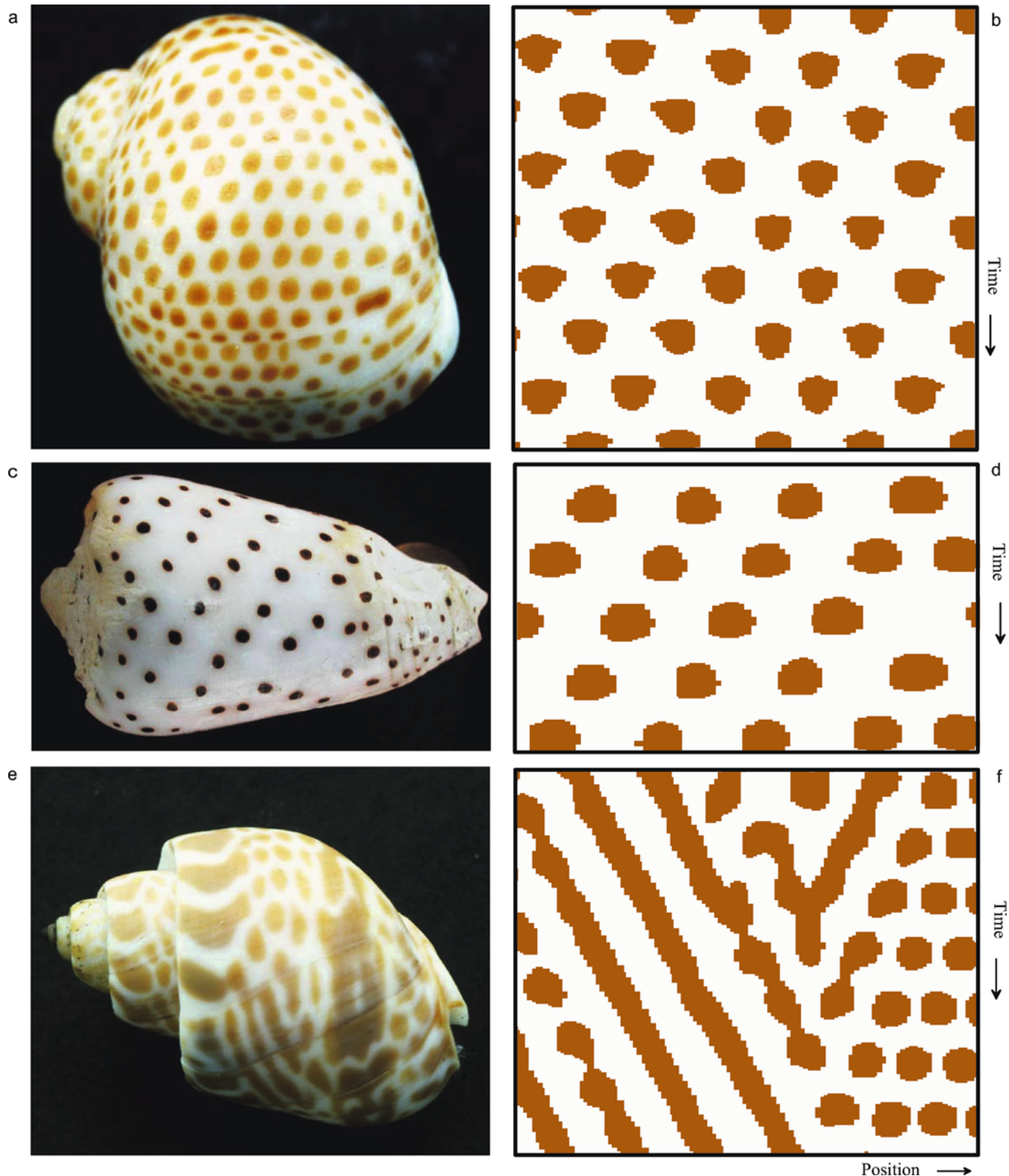


Figure 5.11. (a-b) Minor differences decide whether dots are arranged in horizontal or oblique rows. (Shells of *Natica stercusmuscarum* and *Persicula persicula*) (c) Shell of *Babylonia japonica*. The simulation reproduces the transition from isolated patches to oblique lines [S510]

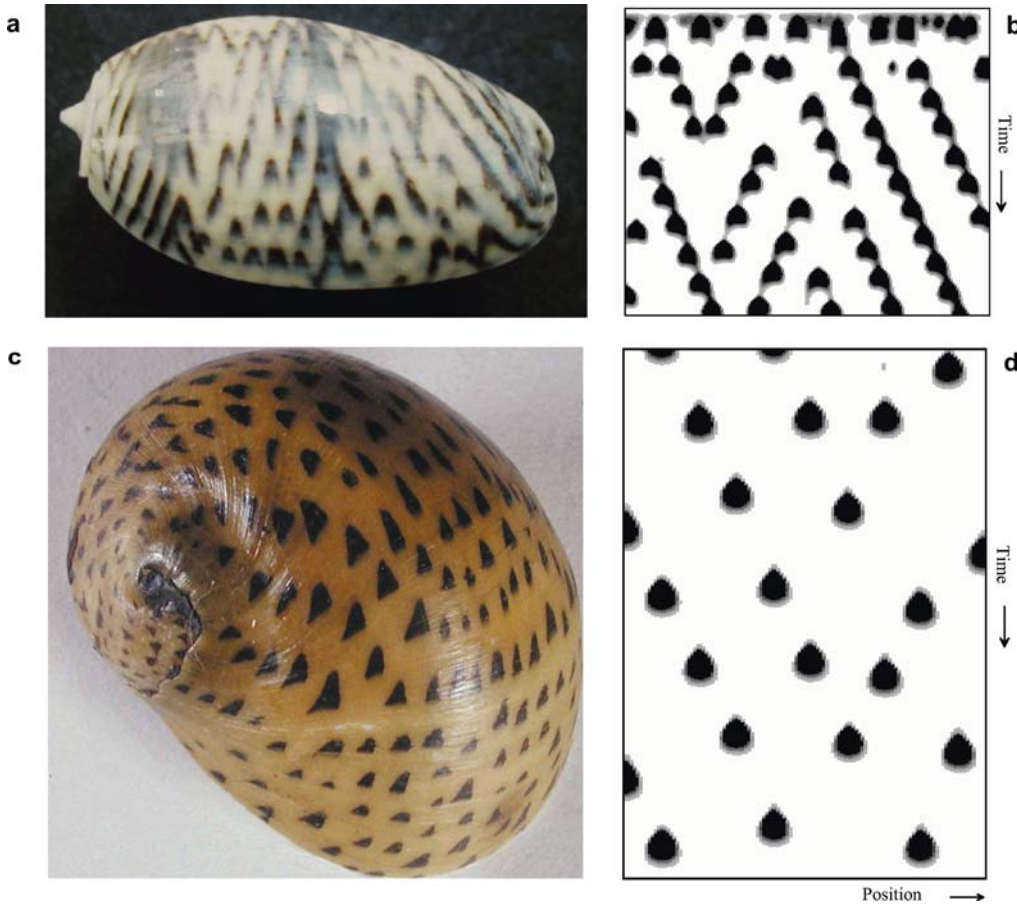


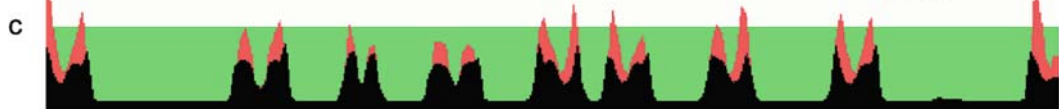
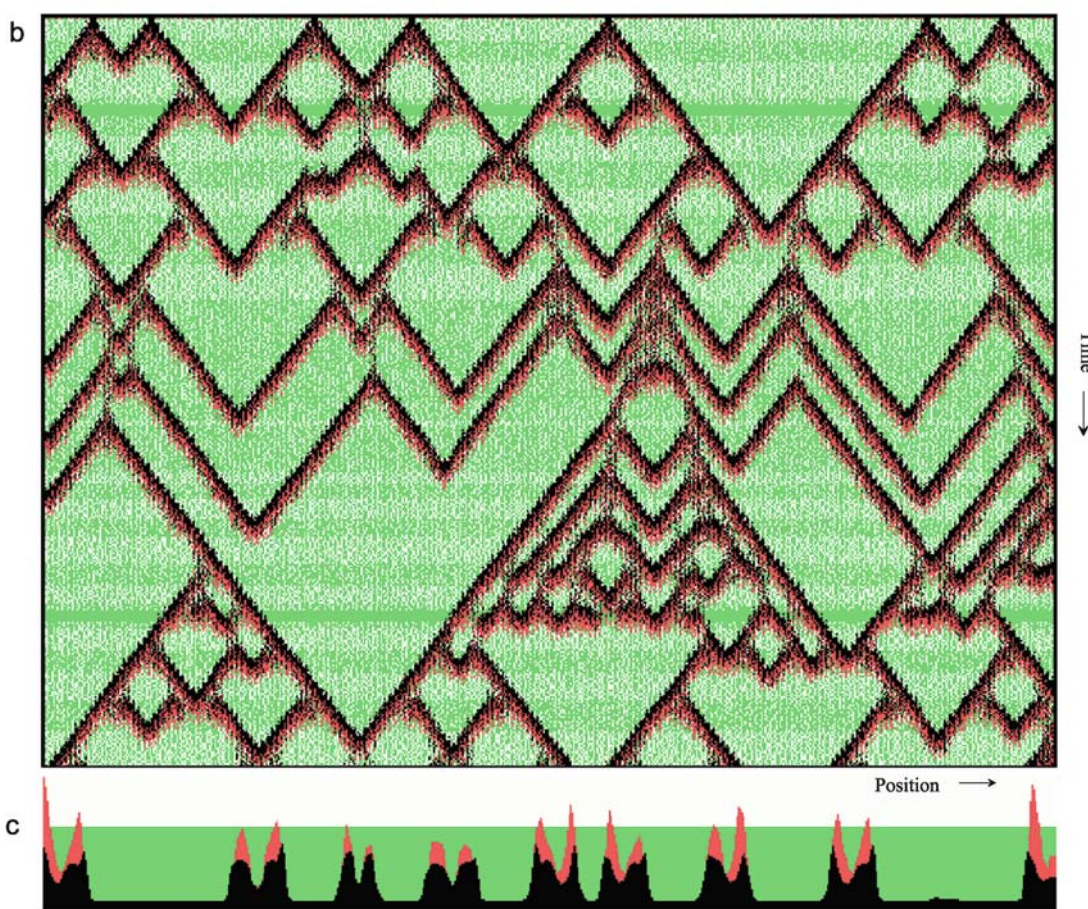
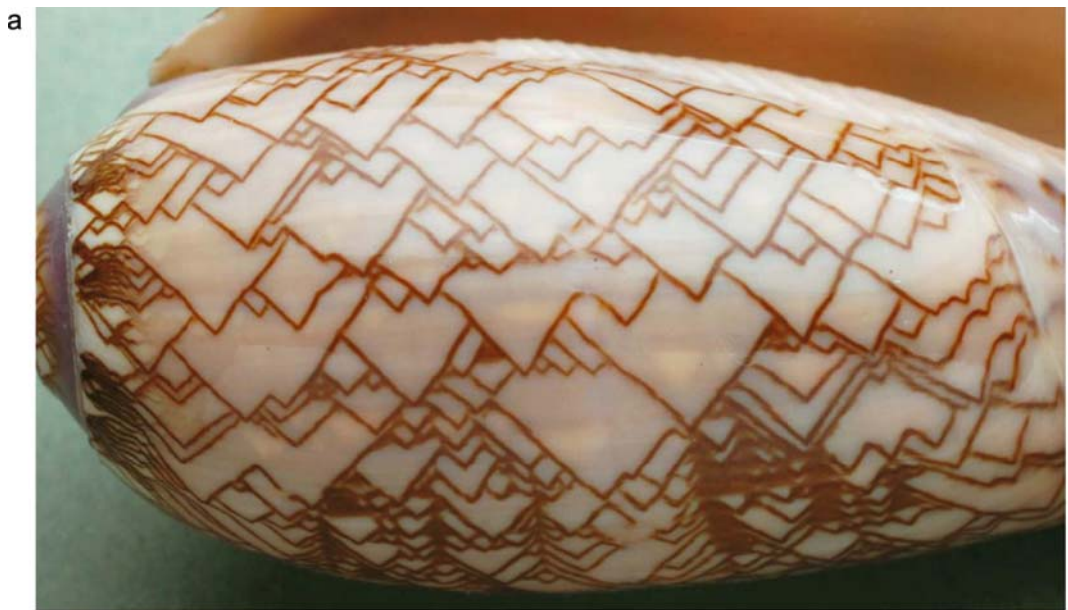
Figure 5.12. Crescents and triangles are the preferential pattern if two inhibitors act in an additive way. (a) Shell of *Oliva bulbosa*. (b) If the primary inhibitor is nondiffusible, the crescents can be connected by faint lines resulting from waves of low-level activation. (c) Shell of *Neritina penata*. (d) When the long-lasting inhibitor shows some diffusion, the patches are separated and isolated triangles are formed [S512]

In contrast, if the rate of the slowly diffusing inhibitor is lower, a pattern with patches arranged along oblique lines will emerge. Successive patches of activation appear with a slight offset in space, but only on one side of the forbidden zone. As will be shown further below, the helical arrangement of leaves is proposed to have a similar origin (Figure 13.3). An isolated activated patch gives rise to two diverging rows and two merging lines disappear, analogous to the behavior of traveling waves. At even lower diffusion rates, or without diffusion, the patches may fuse to become partially connected oblique lines. Figure 5.11 provides examples of the different modes of dot patterns. The range of parameters over which one or the other pattern is possible will overlap. In a critical range, both types may be formed. The system can lock into one or the other mode. Both types may even appear in different regions of the same shell and one mode may replace the other over the course of time. Therefore, neither pattern is exclusive.

On some shells, the patches have a triangular or crescent-like shape. Figure 5.12 shows two examples. According to the model, this pattern emerges preferentially if the two inhibitors work in an additive way (Equation 5.4). The inhibitor with the long time constant poises the activation in such a way that it terminates. Similar to the case with dots (Figure 5.11), a nondiffusible primary inhibitor allows a partial connection of the crescents (Figure 5.12a). The pattern has many of the features as those discussed above. Patches become partially connected to oblique lines that can cross or branch. Frequently, one or both waves terminate before a collision takes place, supporting the postulated feature of lateral inhibition. One remarkable feature is that the faint pigmentation lines that connect the crescent-like patches have the same inclination as the heavily pigmented regions. This seems to be counter-intuitive since cells with a lower activation should require more time to infect their neighbors.

5.8 Conclusion

By a second antagonist a system of many coupled oscillators may obtain unusual properties. Traveling waves can occur that penetrate each other, causing crossings of pigment lines in the shell patterns. Wave splitting and thus branching is possible as well. The second antagonist can enforce a de-synchronization of the oscillators. This is much in contrast with the behavior of many other coupled oscillators in biology that tend to synchronize. Flashing fireflies, the pace-maker cells of the heart, networks of neurons in the circadian pace-maker, and the insulin-secreting cells of the pancreas are examples for synchronizing systems. It has been postulated that this synchronization is a general feature of pulse-coupled oscillators (Mirolo and Strogatz, 1990; see also Stewart, 1991). As the staggered dot patterns on shells demonstrate, this rule is not universal. De-synchronization occurs if the antagonistic components have different time constants and ranges. Waves with unusual properties have been also observed in other systems. An example are waves of catalytic oxidation of Carbon oxide at the surface of Platinum crystals (Bär *et al.*, 1992). These authors assumed imperfections on the crystal structure as the cause of this phenomenon. For shell patterning, the systematic occurrence of wave penetration and splitting precludes an analogous explanation here. On the contrary, the shell patterns suggest considering long range inhibitory effects as an essential ingredient whenever penetrating or splitting waves are observed. In chapter 13 very different biological systems will be discussed that can be explained by mechanisms in which two antagonistic reactions are involved, too. The modeling of the sea shells were for me the key to find the corresponding explanations.



Branch initiation by global control

6.1 Branch formation: the trigger of backwards waves

Branch formation is a dominating pattern element of *Oliva porphyria* (Figure 6.1). Considering that the shell patterns resemble space-time plots, it is obvious that the formation of a branch is based on the sudden initiation of a backward-running wave. In the view of the normal behavior of waves in excitable media, this is a very unusual event. A new wave must spread into a region that should be refractory due to the primary wave. That regions are also refractory in *Oliva porphyria* after the passing of a wave is evident from the many \vee -like pattern elements: colliding waves annihilate each other in the usual way; the waves do not enter regions made refractory by the counter wave.

In the view that pigment deposition into the shell could resemble some sort of waste disposal, it appears reasonable to assume that a mollusk keeps the total number of traveling waves under control. Since with each collision the number of traveling waves becomes smaller, mechanisms must be at work that generate new waves to compensate for this loss. Wave splitting by the initiation of backwards waves is one possibility. Wave splitting is then expected to occur whenever the number of traveling waves became too low. By such a control, the average rate of waste disposal would remain approximately constant.



Figure 6.1. (a) Shell of *Oliva porphyria*. Branching occurs simultaneously at distant positions. (b) In the model, branching is regulated by a rapidly distributed hormone (green) that is produced by all activated cells. It is a measure of how many traveling waves are actually present in the mantle gland. Whenever the number of waves and, therefore, the hormone concentration becomes too low (light green regions) a temporary transition into a steady-state occurs that can cause the trigger of new waves; for details see Figure 6.2. (c) Distribution of the substances at the end of the simulation shown in (b). [S61; S62 displays the distributions shown in (c) in a movie-like manner]

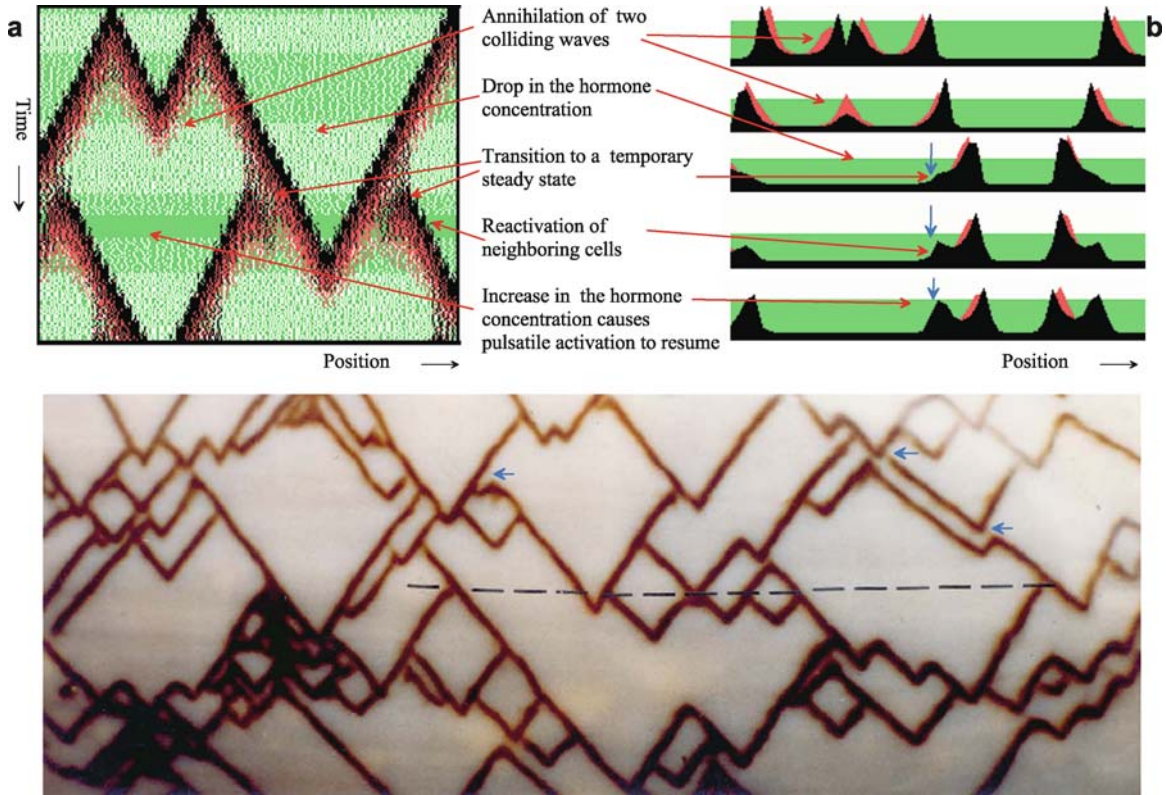


Figure 6.2. Backwards waves and branch formation. A branch indicates the sudden formation of a backward wave. In this model branching occurs whenever the number of traveling waves drops below a certain threshold value. The controlling agent is a hormone-like substance c (green) that controls inhibitor half-life. It is produced at a rate proportional to the local activator concentration. Its rapid distribution is simulated by averaging. Below a certain c concentration (light green) the activated cells switch from an excitable to a steady-state mode of activator production. Groups of cells remain activated longer than the refractory period of their neighboring cells. This initiates the backward waves. Since c is uniformly distributed, many oblique lines branch simultaneously. (b) The same simulation shown as a sequence of distributions. Shortly after its birth a backwards wave has a lower maximum concentration (blue arrows), which leads to the small gap at the branch points (see also Figure 6.4b,c) [S62]. (c) Details of a shell of *Oliva porphyria*. The dashed line marks a moment at which many branch formations took place

A closer inspection of Figure 6.1 and 6.2b shows the prerequisites for branch formation: the refractory period must be very short. Immediately after branching, the new oblique lines have the same inclination, indicating that the backwards waves start with the same speed. In other words, the system must return very rapidly to its former degree of excitability. Another feature points in the same direction. Two oblique lines can be very close together, indicating that one wave can be followed by a second wave after a very short time interval. Moreover, the straightness of the oblique lines next to large nonpigmented regions indicates that the excitability does not increase even if cells were non-activated for a longer period of time.

6.2 Simultaneous pattern change in distant regions

In the mechanisms discussed so far, only information exchange between adjacent cells has been considered. However, several patterns indicate that particular events occur simultaneously at very distant positions. For instance, the shell of *Oliva porphyria* tells us that many branches were initiated at distant locations at the same time. The dashed line in Figure 6.2b indicates such a moment. There would no time for a signal to travel by diffusion over such a long distance. However, not all lines branch at such a critical moment. This indicates that from time to time a situation is generated everywhere that greatly enhances the *probability* of branch formation. Such changes must be the result of a global control. This chapter will discuss the types of couplings that lead to global control of branch initiation.

For the global signal we will assume that a hormone-like substance, produced as a by-product of the patterning reaction, circulates within the animal (Meinhardt and Klingler, 1987). This signal is almost instantaneously available throughout the animal. Chapter 8 will discuss systems in which global signals result from an independent oscillating process. An instantaneous long-ranging signaling could be also achieved by neuronal signaling. By analogy with other secretory organs, Ermentrout et al. (1986) proposed a neuronal basis for controlling pigment secretion. So far, direct evidence for neuronal or hormone-like control is lacking. Only important for the further discussion is that a near-instantaneous signaling along the whole marginal zone exists.

The formation of a branch requires, for a short period, a modification of the simple serial triggering mechanism that generates oblique lines. A particular just-activated group of cells has to remain activated for a prolonged period such that the activation “survives” the (short) refractory period of their earlier activated neighbors. After this period a reinfection of previously activated neighboring cells is possible, causing the initiation of the backwards-running wave and thus a splitting of the primary wave. Therefore, the formation of branches requires a signal that causes an elongation of the activation period. The signal could be the hormone mentioned above. If each activated (pigment-producing) cell produces a hormone-like substance c that is rapidly distributed over the total number of n cells, the c concentration is proportional to the ratio of activated and nonactivated cells. New branches should form whenever c and thus the number of traveling waves becomes lower than a certain threshold.

How can the c concentration determine whether the activation is in a steady-state or a burst-like mode? In the activator-inhibitor model (Equation 2.1.b), pulse-like activations occur if the decay of the inhibitor is slower than that of activator, i.e., if $r_b < r_a$. In contrast, if $r_b > r_a$, the activation remains in a steady-state (see Figure 3.2). If the inhibitor is stabilized by the hormone c , a lower c concentration leads to more rapid inhibitor decay. Therefore, in the correct range, lowering the hormone concentration will lead to a shift from pulse-like to steady-state activator production - the precondition for branch formation. The substitution of r_b

Equation 6.1: Branch formation by changing time constants via a hormone-like substance

A slightly modified activator-inhibitor system (Equation 2.1) is assumed

$$\frac{\partial a}{\partial t} = s \left(\frac{a^2}{s_b [+ s_d d^2] + b} + b_a \right) - r_a a + D_a \frac{\partial^2 a}{\partial x^2} \quad (6.1.a)$$

$$\frac{\partial b}{\partial t} = sa^2 - r_{b_{eff}} b + D_b \frac{\partial^2 b}{\partial x^2} + b_b \quad (6.1.b)$$

In addition, the half-life of the inhibitor is assumed to be under control of a hormone-like substance. Each activated (pigment-producing) cell produces the hormone c that becomes rapidly distributed within the total number of cells n .

$$\frac{\partial c}{\partial t} = r_c \sum_{i=1}^n a_i/n - r_c c \quad (6.1.c)$$

All activated cells contribute to hormone production. The $1/n$ term results from the homogeneous distribution of the hormone c among all cells n . Due to this averaging, the c concentration is the same in all cells along the growing edge and decreases uniformly with a decreasing number of a -producing cells, i.e., with the number of traveling waves.

The hormone is assumed to modify the stability of the inhibitor. The decay rate of the inhibitor r_b in Equation 2.1.b has to be replaced by the effective decay rate of the inhibitor

$$r_{b_{eff}} = r_b/c$$

If the total number of traveling waves becomes too small, the inhibitor half-life becomes so short that the activated cells switch from a burst-like to steady-state activation. This enables wave splitting.

A lowering of the decay rate of the primary inhibitor r_b leads on average to fewer traveling waves and vice versa (see Figure 6.6a). A longer half-life of the hormone (reducing r_c) causes a dominance of long parallel lines (see Figure 6.6c) An increase in the Michaelis-Menten constant s_b in Equation 6.1.a leads to termination of traveling waves whenever a certain number of activated cells is obtained (Figure 6.8). The spontaneous trigger of new activations (arrows in Figure 6.4f) suggest the existence of a second long-lasting inhibitor d :

$$\frac{\partial d}{\partial t} = r_d (a - d) + D_d \frac{\partial^2 d}{\partial x^2} \quad (6.1.d)$$

Its inhibiting influence is described by the term s_d in Equation 6.1.a.

Branch formation would be possible also by a hormone-dependent elongation of activator half-life or by an increase in substrate production in an activator-substrate system. However, by a comparison of the details in the resulting patterns these possibilities can be excluded (see Figure 6.7).

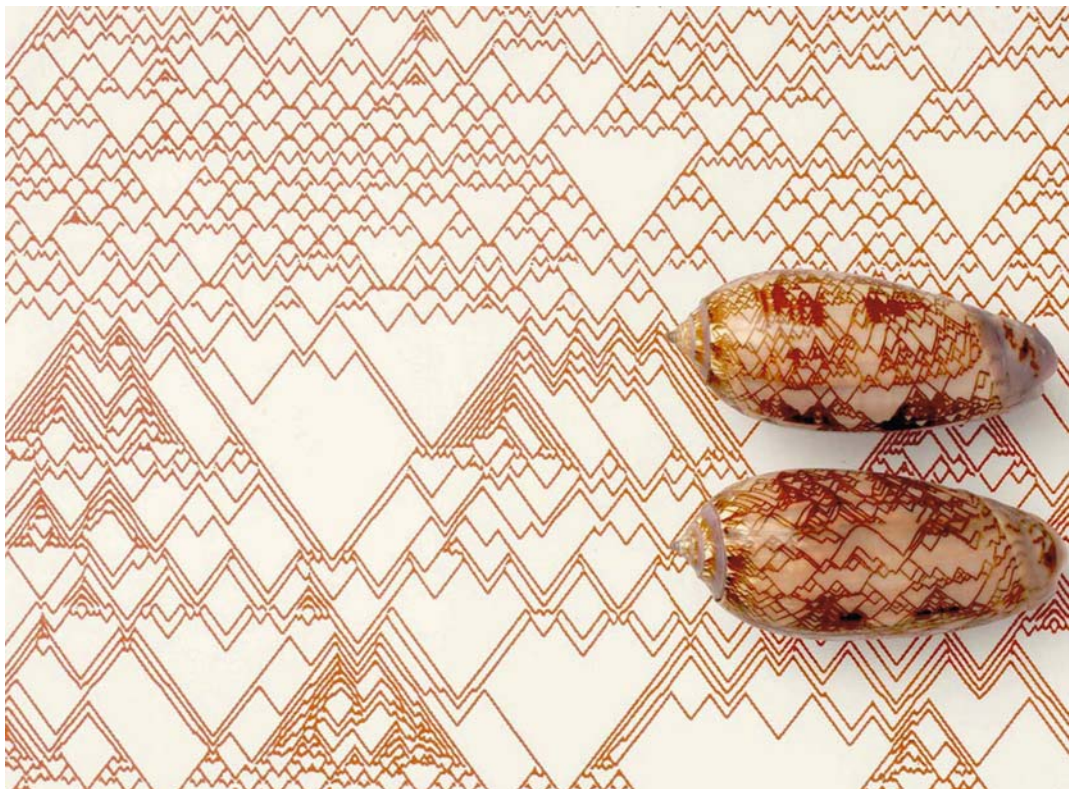


Figure 6.3. Pattern heterogeneity on the shell of *Oliva porphyria*. Phases showing normal branch formation alternate with phases in which dense oblique lines dominate. This is reproduced in the simulation, although its origin is not completely understood. In the simulation the long oblique lines occur only when the field size is large. Dense lines are expected if large nonpigmented regions are formed by chance [S63; depending on the random fluctuations the actual simulation may look quite different. The background was calculated with the short and well-documented minimum program OLIVA.EXE

by r_b/c has such an effect (see Equation 6.1). To reproduce the pattern of *Oliva porphyria* a further requirement is that cells become activated only by activated neighbors, not spontaneously. Cells must be excitable, but not oscillating. This is the case when a basic inhibitor production b_b or a high Michaelis-Menten constant s_b is given (Equation 3.1 and Figure 3.2). After several such simultaneous branch formations are completed in a short time interval, the number of traveling waves and thus the hormone concentration increases again, visualized in the light green - dark green transition in Figure 6.1. Cells switch back to the burst-like mode of activation. Thereafter, all oblique lines, including those just initiated by wave splitting, are elongated by the normal chain of triggering events. Figure 6.2 illustrates the formation of a single branch, while Figures 6.1 and 6.3 show simulations in a larger field of cells.

The simulations reproduce many details of the natural pattern (Figure 6.4). If, by accident, many waves become extinct almost simultaneously in a particular region, very dense pigmentation occurs in other regions due to the global control. While the original wave proceeds undisturbed, a branch frequently appears to be only loosely connected to the original line. According to the model, the pulse-like triggering of a new activation occurs with an overshoot. In contrast, the concentration is much lower during the temporary transition into the steady-state that gives rise to the backwards wave (see Figures 3.2 and 6.2b). Sometimes, a small hook appears close to the point of branch initiation. This is the result of an incipient wave initiated parallel to the primary wave after return to the burst-like mode of activation. The hook is a record that a wave did not survive because the cells were not yet excitable enough. If such a wave survives, a parallel line close to the original line results - a frequent pattern element on the *Oliva* shells.

Although many details are correctly described, a particular feature clearly demonstrates that an additional component must be involved. On many shells there are \wedge -like pattern elements visible that indicate a spontaneous trigger (Figure 6.4f). They occur in large nonpigmented regions, i.e., after a longer period without any activation. On the one hand, close parallel lines indicate a very rapid re-establishment of normal excitability. On the other hand, a spontaneous trigger is only possible after a long time interval. These two observations can only be reconciled by the assumption that two inhibitory actions exist that have very different time constants. According to the models, a new trigger occurs whenever the concentration of the second long-lasting inhibitor becomes sufficiently low. Such an inhibitor, if diffusible, solves another problem. In the simple model discussed so far, no lateral inhibition is assumed; the mechanism has no pattern forming capability on its own. The patterning has to be initiated from particular activated cells. If, however, the second long-lasting antagonist also has a longer range, the spontaneous trigger can be restricted in space, leading to new pairs of diverging lines (arrow in Figure 6.4g). Long-lasting inhibitions also play a role in many other shell patterns (e.g., Figure 8.8).

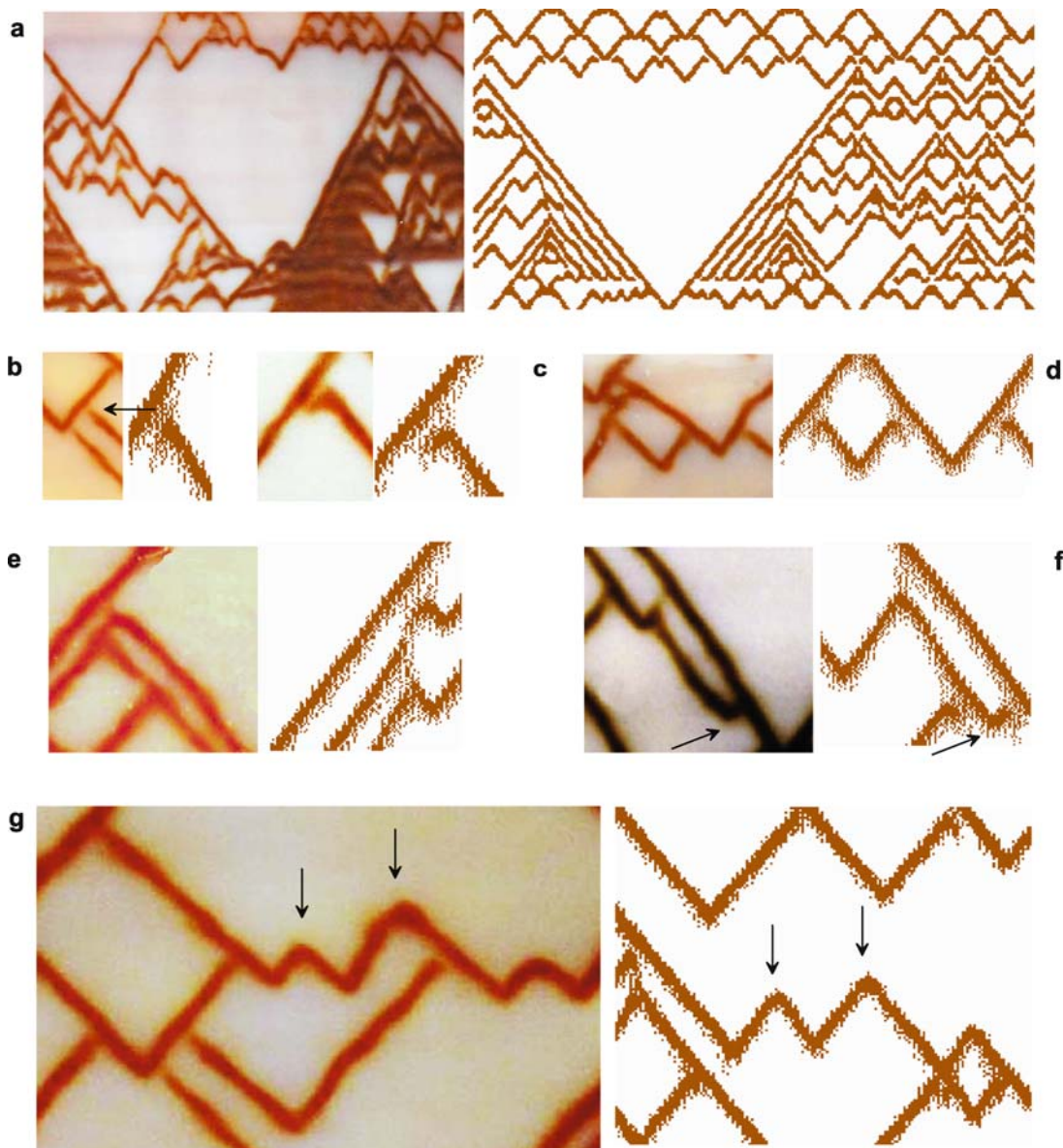


Figure 6.4. Correspondence between natural and simulated patterns. (a) If a larger wave-free area is formed accidentally by simultaneous annihilation of several wave pairs, a higher wave density is observed in other regions. According to the model, the dramatic drop in the hormone concentration causes the activation in other regions to remain close to the steady-state for a longer period, producing densely pigmented regions. (b) Sometimes a branch seems to be only loosely connected with the main line. The small gap results from the passage through the steady-state with its reduced concentrations (arrow; also see blue arrows in Figure 6.2b). (c) Sometimes a small hook appears close to the point of branch initiation. This is the result of an incipient wave initiated parallel to the primary wave. Usually this wave does not survive since the cells are not yet excitable enough. (d) The high probability of simultaneous initiation leads to many \vee -like elements with the same distance between the branch initiation points and the tip of the \vee 's. (e) Closely parallel lines can be formed, showing that the refractory period of the cells is very short. (f) A second branch from the main wave can terminate the following wave by annihilation (arrows). (g) The spontaneous initiation of two new divergent lines (arrows) indicates that a second long-lasting inhibitor is involved. After a prolonged nonactivated period a spontaneous activation can occur (\wedge -like elements, arrows)

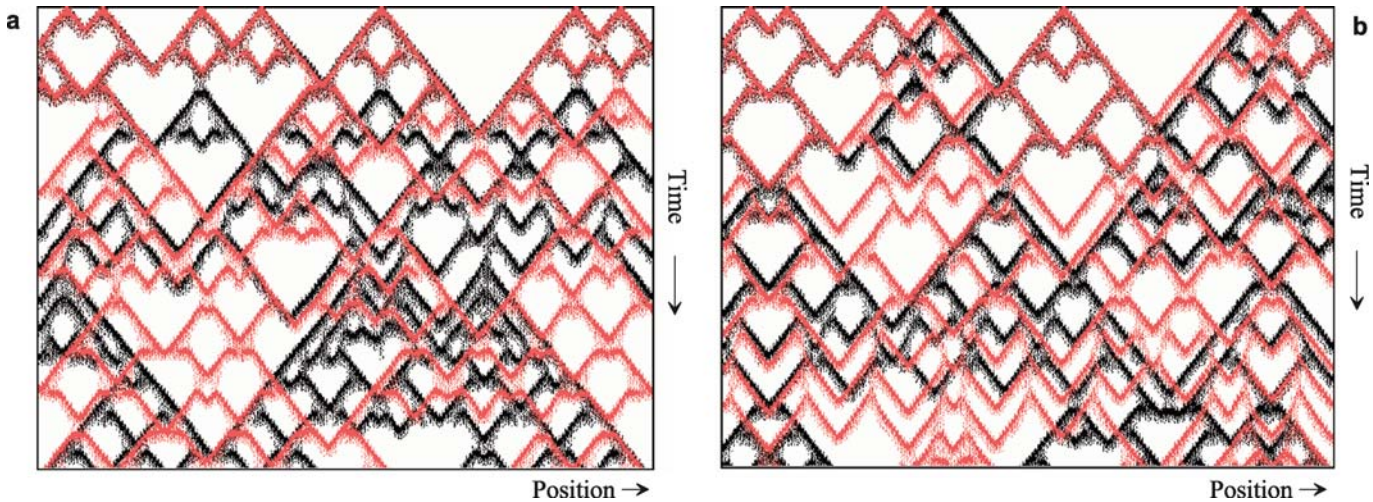


Figure 6.5. Chaotic character in the patterning of *Oliva* shells. Whether a backwards wave is initiated or not has severe consequences for the probability that subsequent branches are formed. In order to show that minute differences lead to different patterns two simulations are plotted on top of each other (black and red). (a) The same cells are activated initially but different random fluctuations exist. At early stages (top of the figure) the two patterns are very similar; the black pattern is largely covered by the red one. Small differences are decisive for whether branch formation occurs. After a few generations of branching, the patterns are completely different. (b) Two calculations with identical random fluctuations. Initially, however, some cells are activated at slightly different positions. Again, the pattern becomes different [GT65]

6.3 No *Oliva* shell is like another

If a particular species shows complex patterns, one will hardly find two shells with identical patterns. Simulations of *Oliva porphyria* can be used to demonstrate the origin of this pattern diversity. According to the model, minor differences can be decisive for whether a branch is formed. Any such decision has a dramatic effect on the probability of subsequent branch formation. Therefore, even if two systems are initially in an almost identical situation, this similarity is lost after a few generations of branch formation. This is a well-known behavior of chaotic systems. Therefore, unavoidable minor differences are sufficient to generate a diversity of patterns. To illustrate this feature, Figure 6.5 shows two simulations plotted on top of each other in different colors. Either random fluctuations or slightly different initial conditions have been assumed. Initially both patterns are nearly identical; the red pattern almost completely covers the black pattern. With each decision to form or not to form a branch, the patterns become more different. Due to the global effect of the hormone, whether a branch is formed has strong influence on the probability for forthcoming branching even at a distant position.

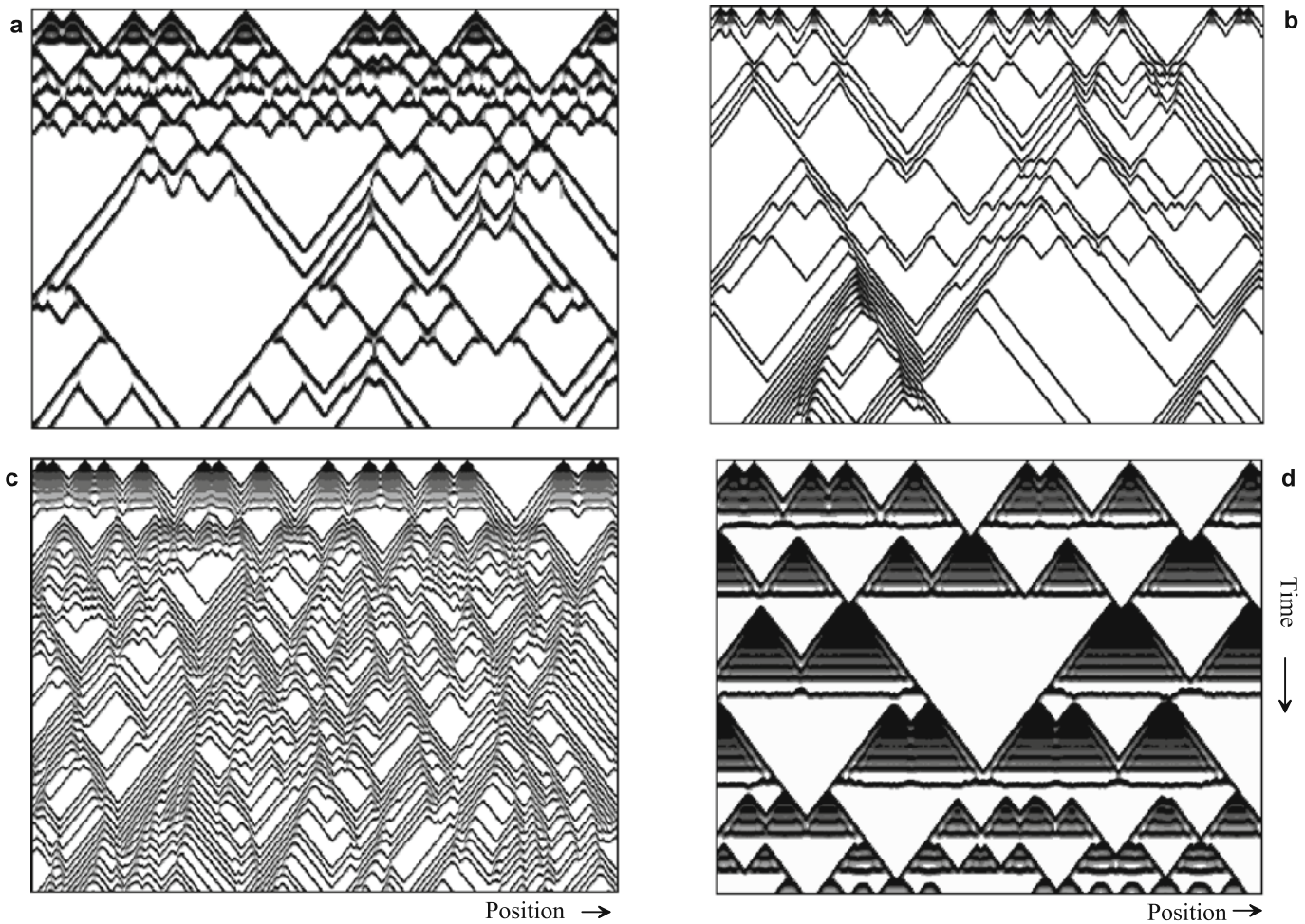


Figure 6.6. Types of patterns that can be generated by differing the parameter for hormone-like control. (a) The decay term of the inhibitor r_b determines the density of branching; r_b is lowered by a factor of 3 during the simulation. (b) A hormone with a longer time constant (smaller r_c) leads to clusters of branches and to longer, nonbranching lines in between. (c) As (b) with higher density due to an increase in r_b . (d) At even higher densities, triangles may be formed that can disintegrate into a pattern of dense lines. This transition may spontaneously revert back to triangles later on [S66a-S66d]

6.4 The influence of parameters

The overall appearance of patterns generated in this way depends on several factors. According to the model an equilibrium is maintained between the generation of new oblique lines by branching and their pair-wise termination by collisions. Important for the appearance of the pattern is the number of waves required to attain this equilibrium. This number depends on the hormone-controlled decay rate of the inhibitor. If this parameter is large, many waves are formed and a dense network of pigmented lines emerges. On the other hand, if the parameter is small, individual oblique lines are the dominating pattern element. Figure 6.6a shows the transition from high to low wave density due to a reduction in the parameter r_b .

If the time constant of the hormone is much larger than that of the activator, preferentially very dense bundles of oblique lines are formed that run parallel to each other. Many branches will then be formed in rapid succession since it takes a long time before the hormone concentration adapts to the elevated wave density. Conversely, it requires more time before the next set of backwards waves is triggered. Figure 6.6b,c shows simulations of low and high wave density. At still higher densities, a transition into triangles may occur. Although, as will be discussed in Chapter 8, triangles represent a frequent pattern, it is unlikely that they are formed by this mechanism. In the simulation in Figure 6.6d the upper tips of these triangles are in a permanent steady-state. With an increasing number of activated cells a continuous shift towards oscillations takes place. This is why the triangles resolve into stripe-like elements along the lower triangle border. However, when real shells have triangles with a stripe-like, fine substructure, they do not show this systematic evolution from tip to base (see Figure 8.10).

6.5 Alternative mechanisms

A change in the half-life of the inhibitor under hormone control is, of course, only one of the possible mechanisms for switching back and forth between burst-like and steady-state activation. An elongation of activator half-life or an increase in substrate production using an activator-substrate model would be appropriate as well (Figure 6.7). However, the details of the resulting patterns look very different from the natural pattern, making such mechanisms unlikely. An elongation of activator half-life leads to a characteristic thickening of the line shortly before and during branch formation, at variance with the natural pattern.

As mentioned, the fact that branches have the same inclination as the original wave indicates that the system returns to normal excitability very fast. In a depletion mechanism this would require very high substrate production *and* a high decay rate independent of the autocatalysis (r_b in Equation 2.4). These conditions appear unrealistic since they would require a considerable waste of energy just to produce and destroy molecules. However, if these conditions are not met, the waves that follow a primary wave would spread at a lower speed due to substrate consumption by the forerunning waves (Figure 6.7b). The resulting line would appear steeper and bent. No such features can be seen on the natural pattern.

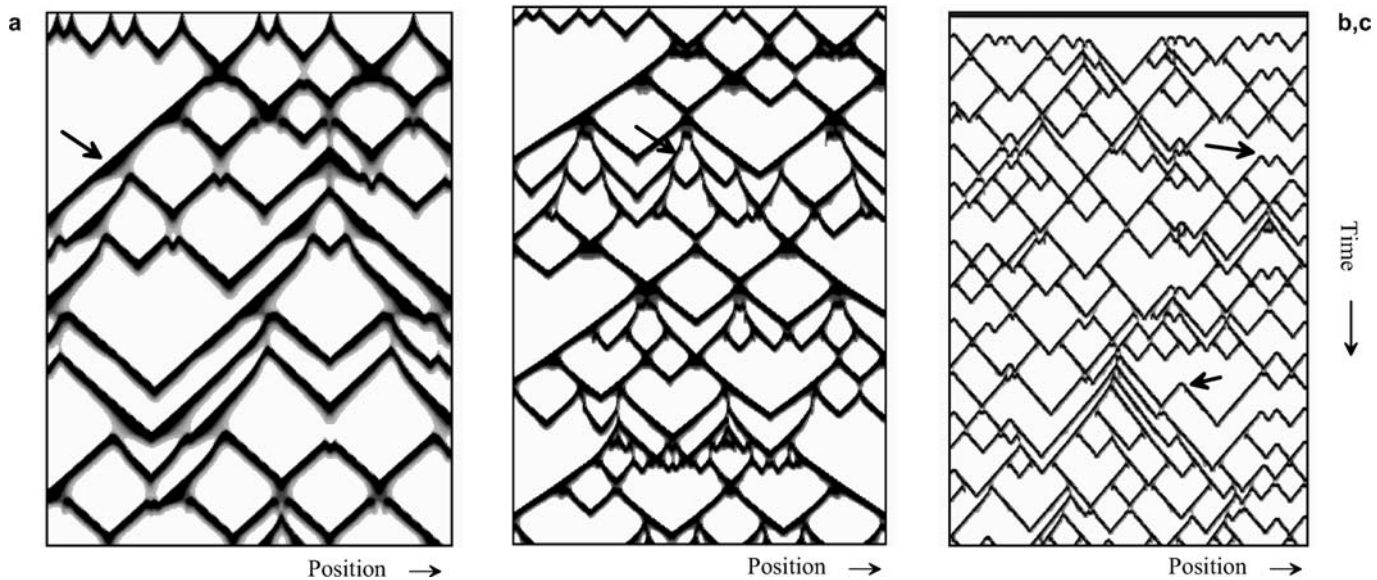


Figure 6.7. Alternative mechanisms for branch formation. (a) The hormone leads to an increased decay rate of the activator. The pigment lines show thickenings shortly before branching takes place (arrow). (b) The hormone increases substrate production. Waves that follow shortly behind a primary wave are retarded due to substrate depletion. The resulting lines are finer and steeper (arrow). Both features are absent on the natural pattern. (c) If a second long-range antagonist is involved, the system is capable of forming the proper pattern from homogeneous initial conditions. In addition, pairs of waves (arrows) can be spontaneously initiated [S67a-S67c].

6.6 A very different pattern generated by the same interaction

The pattern on the shell of *Conus thalassiarachus* (Figure 6.8) seems to bear no similarity to that of *Oliva*, as discussed above. However, in the model the change of one parameter is sufficient to account for the transition from the one to the other pattern. In the simulations of *Oliva* the excitability of the cells was always such that the adjacent cells could be triggered, leading to the long oblique lines. If the Michaelis-Menten constant s_b or the level of the basic inhibitor production b_b is increased in Equation 6.1.a,b, a higher activator concentration is required at least to trigger an adjacent cell. Due to the global control, whenever the number of activated cells surpasses a certain level, the chain of burst-like activations becomes interrupted. Oblique lines can terminate without a preceding collision. Since, on average, termination takes place after a relatively short time interval, the wave cannot spread very far. Regions appear spontaneously that do not form pigmentation for longer time intervals.

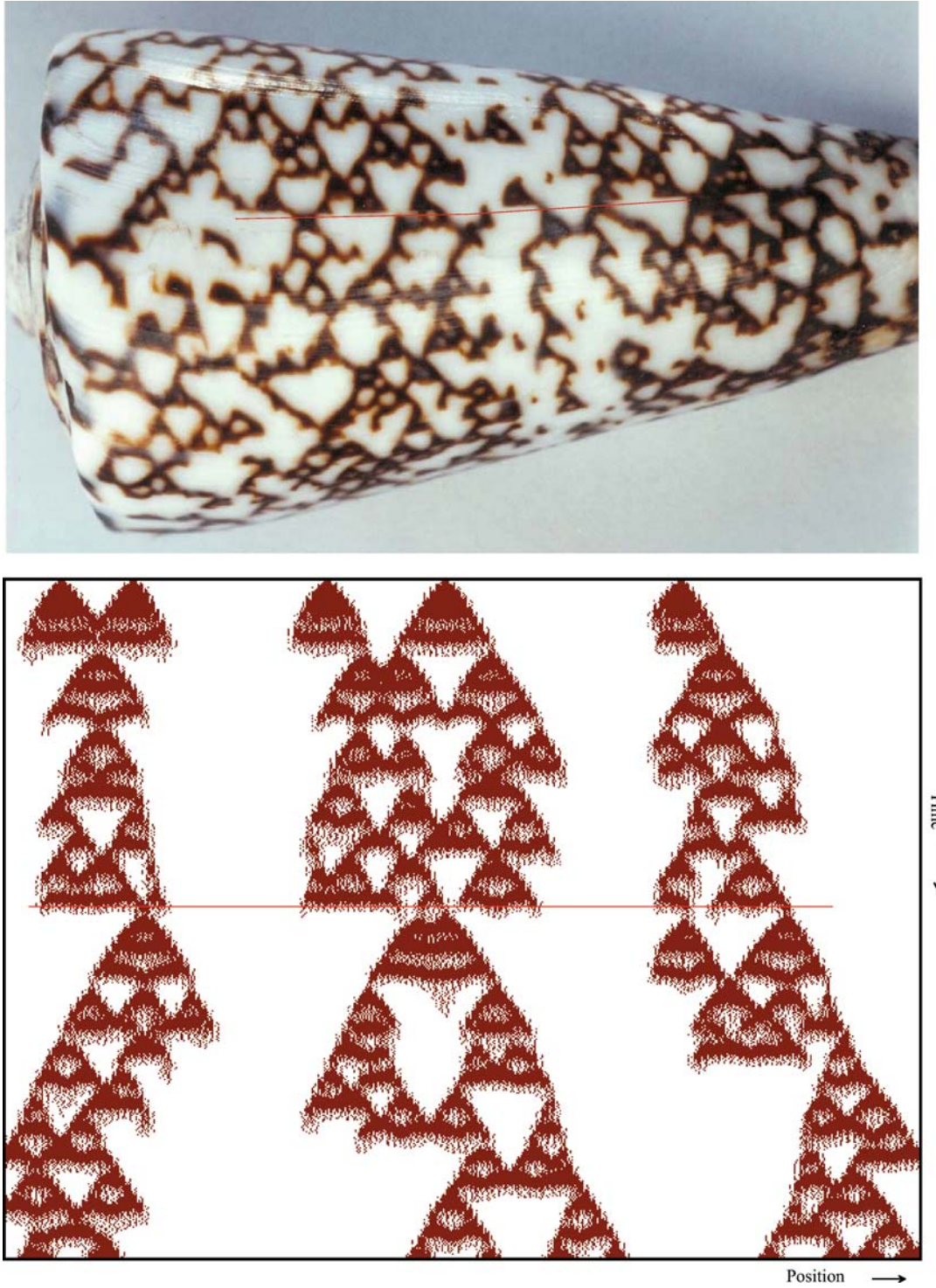


Figure 6.8. Global control and line termination. On the shell of *Conus thalassiarhus* line termination occurs without a preceding collision. In the model, when a high activator concentration is required to trigger neighboring cells (due to a high Michaelis-Menten constant s_b in Equation 6.1.a), oblique lines can also terminate without collision if a certain wave density is obtained. Since termination can take place after a short time interval, the wave may not proceed very far. Regions can appear that are free of pigmentation for a long time [S68]

The list of possible mechanisms that may cause branching under global control is certainly not exhaustive. The mechanisms outlined above should be regarded only as elements of a tool box for reconstructing shell patterns. Essential features include: (i) branch formation can be initiated by a temporary change in the time constant of one substance, and (ii) a simple feedback of the density of traveling waves on the half-life of the antagonist can lead to branching whenever the number of waves becomes too low. The result is an equilibrium between newly formed lines due to branching and the disappearance of waves after a collision.

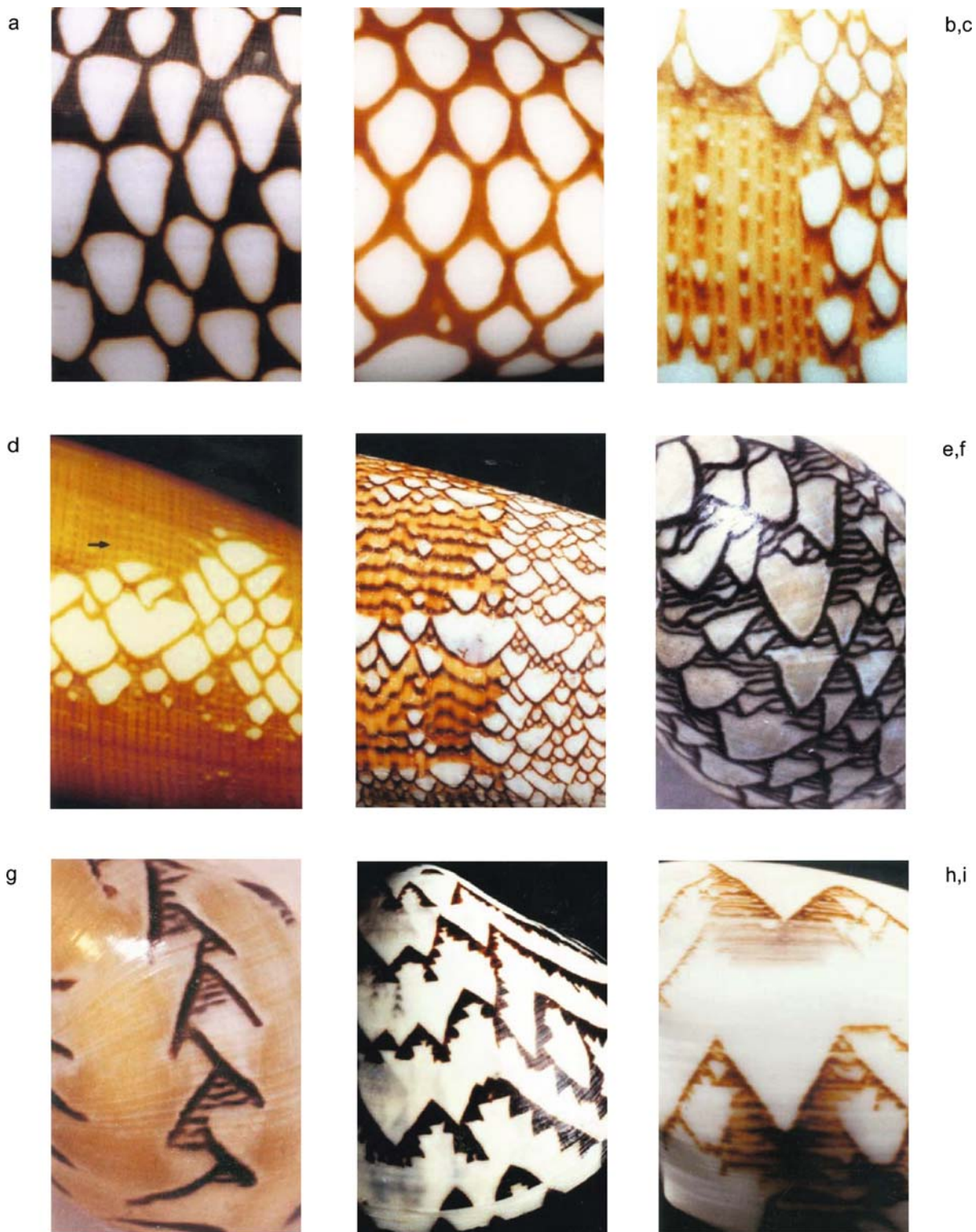


Figure 7.1. Inherent similarities in complex patterns. A collection of shells arranged such that each subsequent pattern contains elements of the preceding pattern

The big problem: two or more time-dependent patterns that interfere with each other

7.1 Inherent similarities in complex patterns

Many shells show patterns far more complex than those simulated so far. Figure 7.1 contains a collection of typical complex shell patterns. To show their inherent similarities, they are arranged such that each subsequent pattern contains elements of the preceding pattern as well as new features. *Conus marmoreus* (Figure 7.1a) shows white drop-like regions on a dark pigmented background. In *Conus marchionatus* (Figure 7.1b) the white drops are enlarged at the expense of the pigmented regions. The pattern is reminiscent of staggered wine glasses. *Conus pennaceus* (Figure 7.1c) shows, in addition, dark lines on a pigmented background, occasionally interrupted by small white drops. In *Conus auratus* (Figure 7.1d) the dark lines are maintained without the white drops. Instead, a periodic large-scale transition to oblique lines with crossings occurs. Shortly before this transition takes place the continuous background becomes modulated towards narrow lines parallel to the growing edge (arrow). Such axially oriented parallel lines on top of a pigmented background are a characteristic pattern element in *Conus textile* (Figure 7.1e). Non-pigmented regions with a drop-like shape occasionally appear. Their lower borders are formed by a dark pigmented line. In regions without a pigmented background the pattern consists of a fine meshwork including lines with the shape of a wine glass as mentioned above. Similar parallel lines with occasional loops (tongues) are characteristic of *Clithon* (or *Neritina*) *oualaniensis* (Figure 7.1f). Here, however, the regions with fine lines are missing. In the specimen of *Clithon* shown in Figure 7.1g narrow-spaced parallel lines are framed by oblique lines, causing the overall impression of connected triangles, a pattern that is characteristic of the bivalved mussel *Lioconcha castrensis* (Figure 7.1h). Similarly, in the shell of the snail *Cymbiola vesperilio* (Figure 7.1i) very fine but short parallel lines give the impression of oblique lines. The triangles that are occasionally formed may become starting points for branches.

The hidden similarities in these patterns that overtly look very different suggest that only a few basic mechanisms are at work. The diversity must result from

different parameter values or minor modifications. The perfect model would describe all these different patterns with a single set of differential equations. This is not yet possible, but a description of the basic elements and how they may arise will be given. The sequence as given in Figure 7.1 will be used as a guide for further analysis in this and the two subsequent chapters. A close examination of the shells will provide essential hints.

What could be the basis of this complexity? Chapter 4 discussed patterns resulting from modifications to the pigment-producing system by a second, not directly visible pattern. These cases were easy to see through since the pattern that accomplished the modifications remained essentially unchanged over the course of time. This unchanging pattern is certainly only a special case since the variation in a single time constant would be sufficient to switch from a stable to an oscillating pattern. Therefore, it is assumed that the complex patterns described in this and the following two chapters result from a pigment-producing system that is modified by one or more time-dependent, usually invisible, patterns.

To account for the different shell patterns that were governed by a stable modifying pattern, it was necessary to assume different modes of interference. Some shells indicated an enhancing or stabilizing effect, causing a locally higher oscillation frequency (Figures 4.2 and 4.5) or even a transition to steady-state pigment production (Figure 4.10). Other shells indicated an invisible pattern that had a suppressing influence (Figures 4.12 and 4.13). As will be shown in this chapter, similar modes of interference are required for time-dependent modifying patterns.

It is extremely difficult to decipher complex patterns. We do not know what the modifying pattern looks like, whether its influence is positive or negative, or which component of the modifying system interferes with which component of the pigment producing system - it could be either the self-enhancing or the antagonistic element. Does the modifying pattern change the production, the destruction, or the diffusion rate? Does the pigment-producing system, in turn, produce feedback for the modifying system? An enormous number of possibilities exist. And even if the correct mechanism is found, it is still difficult to find the range of parameter values in which the mechanism produces the expected patterns.

The similarities between complex patterns are very helpful in narrowing down the number of possible mechanisms. If two models describe a particular shell equally well but only one can also account for a related pattern, a correct decision can likely be made. Simulations of some apparently plausible models will be pro-

Figure 7.2. Shell patterns suggesting an extinguishing reaction: pattern on *Conus marmoreus* (see Figure 7.3 for mechanistic details). The logic of this pattern formation has formal similarities to that of blood coagulation (see Figure 13.12) [S72a, S72b; S72c shows a movie of the pattern along the growing edge]



vided in which the deviation between the simulated and the natural pattern indicate that the model can be ruled out.

On some shells, two distinctly different intensities of pigmentation are visible. These different pigmentation levels are presumably a direct expression of a modifying pattern and provide hints about its character. Thus, modulated background pigmentation can be a key to understanding the complexity of a pattern.

Modeling these complex patterns involves a much higher degree of uncertainty than the simulations given earlier. The models described here should only be regarded as a first attempt. It may require more words to describe the unsolved problems and the “if’s” and “but’s” of the models than the models themselves. This may make the reading of this chapter more cumbersome. On the other hand, it will show that many problems are open still exist and should be viewed as a challenge to find different and better solutions.

7.2 White nonpigmented drop-like pattern on a pigmented background

On *Conus marmoreus* (Figures 7.2 and 7.3a), it is difficult to determine what is pattern and what is background. Are white drop-like patterns formed on a dark pigmented background or are somewhat rounded, dark, pigmented triangles formed that are connected to each other? A decision in favor of the latter possibility is suggested by considering the related pattern on *Conus marchionatus* (Figure 7.3b). There, the red pigmented lines are much finer, indicating that traveling waves play an important role.

The oblique lines discussed so far (chapters 3 and 5) had a constant thickness. This told us that the time interval in which cells produce pigment remained constant during wave propagation. The switching off of activation spread with the same speed as its onset. In contrast, on *Conus marmoreus*, the spread of pigmentation proceeds relatively slowly while the termination of pigment deposition occurs almost simultaneously over a large region. It is, so to speak, a collective breakdown. Pigmented areas of nearly triangular shape result. The switching off occurs so abruptly and over such an extended region that there would be no time for a signal to spread by diffusion. Therefore, the signal for collective breakdown must be a sudden event at the end of a long preparation phase taking place during pigment production.

Some other features shed light on the underlying mechanism. Although pigment termination takes place simultaneously over a large region, this dramatic event obviously has no influence on the spread of activation. In other words, the cells become pigmented at the same rate, regardless of whether a collective breakdown takes place in the neighborhood. The breakdown only influences transition from an activated to a nonactivated state, but not *vice versa*. After a certain time interval pigment production becomes stable again and starts to spread in both directions.

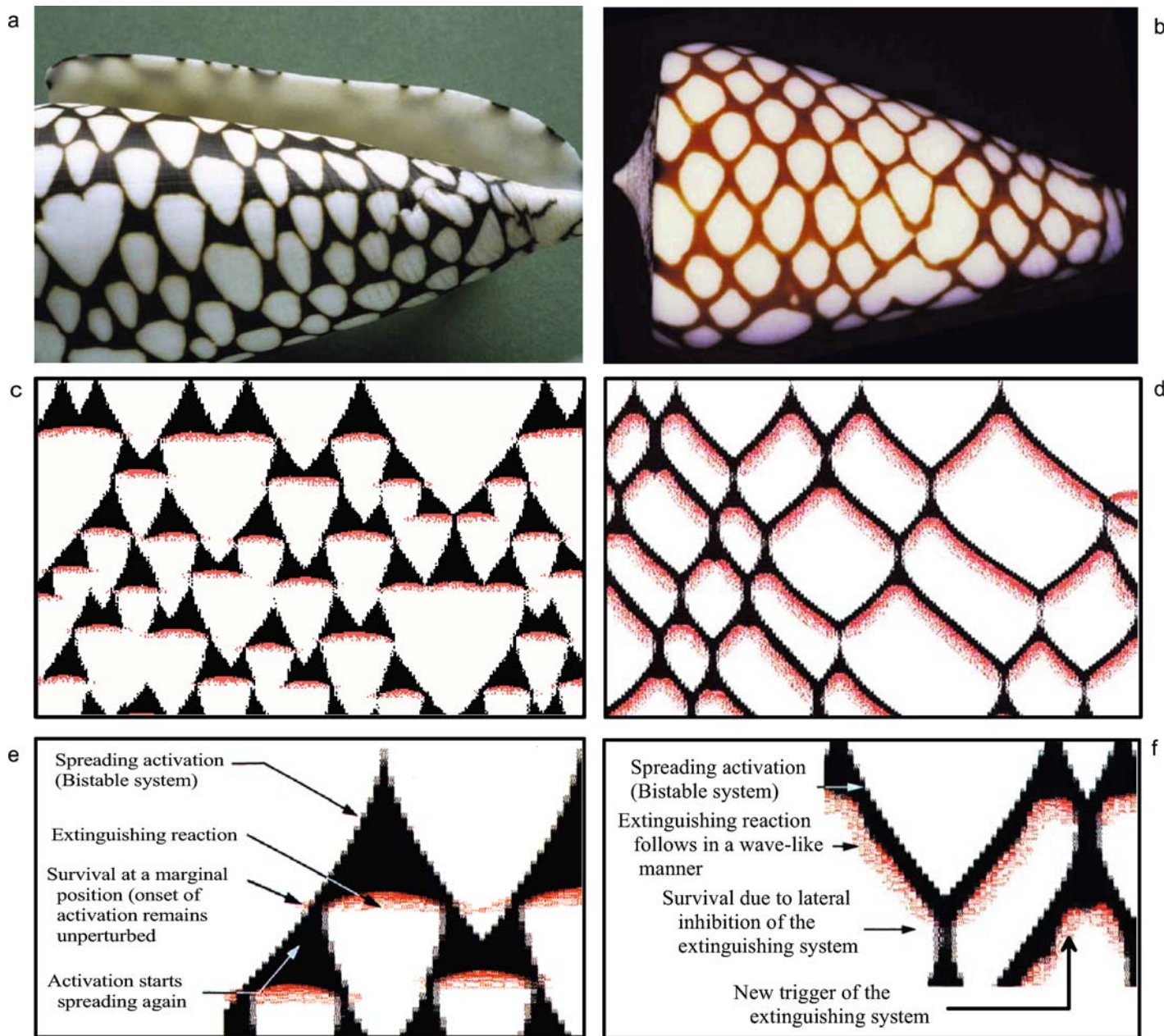


Figure 7.3. Complex patterning based on an additional extinguishing reaction. (a) Drop-like nonpigmented regions on *Conus marmoreus*; (b) a mesh-like pattern on *Conus marchionatus*. (c, d) Model: the activation of a bistable pigment-producing system (black) spreads slowly by diffusion, infecting adjacent regions. A second reaction (red) is triggered by the first and causes its extinction. In (c), pigmentation is produced for a certain period of time before the extinguishing reaction (red) is triggered, initiating the drop-like nonpigmented region. The pigment reaction survives at marginal regions where the activation was just triggered. From these regions the activation spreads again, until the next extinguishing reaction is triggered, and so on. (d) The extinguishing reaction follows in a wave-like manner. Since the antagonist in this reaction is diffusible, two extinguishing waves stop before collision and activation of the pigmentation system survives at the points of collision. (e, f) Details of the mechanisms. Calculated with equations 7.1.a,b and e, f (see page 113). In (c) the strength of the extinguishing reaction is between those used for the simulations in Figure 7.2, which is why occasionally the pigmentation reaction does not survive. The more complex patterns discussed later in this chapter indicate that local survival can be an active process. Calculated with Equation 7.1.a,b,e,f; [S72a, S73; see also S72c and S73b]

7.3 Evidence of a sudden extinguishing reaction

The pattern on *Conus marmoreus* (Figures 7.2 and 7.3a) can be simulated under the assumption that two pattern-forming reactions are superimposed on each other. One system produces the proper pigment and is characterized by a bistable mode of activation that spreads slowly. A second system extinguishes the first system when the first system has been in an activated state for some time. In Figures 7.2 and 7.3c this second system is shown in red. The red system is assumed to shorten the half-life of the activator of the pigment-producing system. Therefore, whenever the second system becomes active, the pigment system is shifted from a bistable to a pulse-wise mode of activation. To simulate the drop-like nonpigmented pattern, pigment production has to terminate almost simultaneously over a large region. Therefore, the components of the extinguishing system are assumed to spread much faster than those of the pigment-producing system. Due to the slow spread of pigmentation and large-scale termination, pigmented regions obtain a roughly triangular shape. The substrate in the extinguishing reaction is assumed to be produced only when a cell produces pigment. This causes the necessary delay between the onset of pigmentation and triggering of the extinguishing reaction. It also enables the pigmentation to survive at the wave front where substrate production began only shortly before the extinguishing reaction was triggered. The substrate concentration for the extinguishing reaction is, therefore, lower and the reaction is weaker at this point. The overshoot in the activation at the front of the spreading activation of the pigment system enhances the chance of survival (see movie S72c). After the extinguishing pulse is over, pigmentation spreads from these marginal zones of survival until the next extinguishing reaction is triggered. The pattern of black triangles and white drops results from the permanent interplay between the spread of activation, delayed large-scale extinguishing, and survival at the margins. The presumed sequence of events is shown schematically in Figure 7.3e. A stronger effect of the extinguishing reaction can lead to chains of triangles (Figure 7.2b).

The rapid destruction of the activator by the extinguishing reaction satisfies another requirement of the pattern: the absence of spontaneous reactivation. Because of the short time interval between collective breakdown and the onset of the spread of pigmentation, the extinguishing reaction must only last for a short period. In this short time interval the activator has to drop to a level so low that a spontaneous re-activation is impossible even though the system rapidly returns to a bistable mode of activation.

The longer and finer oblique lines in *Conus marchionatus* (Figure 7.3b) clearly underline the traveling wave mechanism. After collision, no spread of activation takes place at all for an extended period. Most remarkably, during collisions the two waves do not annihilate each other. However, in contrast to the crossings discussed earlier (Figure 5.8, page 81), the two waves do not simply penetrate each other. The activation remains sharply localized. After this quiet period the spread

of pigment deposition begins very slowly. As indicated by the curvature of the lines, it becomes progressively faster at later stages until the next collision occurs. The resulting pattern is reminiscent of tilings or a pattern of staggered wine glasses. To form the stalks, some type of local signal must be present, which sustains an activation period that is at least ten times longer in a stalk region than in regions that are directly adjacent. The assumed separate extinguishing reaction might represent the underlying mechanism for this. The two extinguishing waves may come to rest before they collide due to lateral inhibition. The trailing extinguishing waves do not collide if the substrate of this reaction is highly diffusible (Figure 7.3d, f). The waves cannot enter the region depleted by a counterwave and a gap remains. At this position the pigmentation system remains in the activated state. New pigmentation waves are formed after the refractory period of the neighboring cells is over.

Finer lines emerge if the substrate of the extinguishing reaction is produced not only by the pigment-producing cells but permanently everywhere. Under this condition the pigment reaction can trigger the extinguishing reaction without a longer delay. In the stalk regions pigment deposition is also switched off after some delay, as is the case in *C. marmoreus*. However, this does not occur simultaneously in a large region. Instead, pigment termination starts more locally but with greater speed, even from the beginning. It catches up with the pigmentation wave. Since it is triggered by the latter, it cannot pass it.

Like in stalk formation, the frequently observed branching of oblique lines also requires a temporary transition to a steady-state mode of activation. As discussed further below, this requires an additional mechanism.

7.4 Resolving an old problem with the separate extinguishing reaction

An additional extinguishing reaction has been introduced to account for large-scale breakdown. There are, however, much simpler patterns that indicate some sort of extinguishing reaction as well. Many shell patterns show a step-like rise and fall of pigmentation with a plateau at least as long as the intervals between the pigmentation periods. This is difficult to obtain with a single activator-antagonist system. If the duration of the pulse is elongated due to saturation, the pulse has a bell-shaped and not a step-shaped profile (see Figures 3.3 and 3.5). Step-like behavior is, however, a straightforward outcome if a bistable system is forced to switch back to the lower steady-state by a separate extinguishing reaction. An example is given in Figure 7.4. The accumulating substrate of the extinguishing reaction has no influence on pigmentation by itself. An abrupt change occurs only after a certain threshold level is exceeded and the extinguishing system is triggered. As discussed below, the bistability of the pigmentation reaction may in itself be the result of a composite process. The extinguishing feature, i.e., a hidden change over a long period culminating in a sudden overt change, may be used as a guide for designing models with more complex interactions.

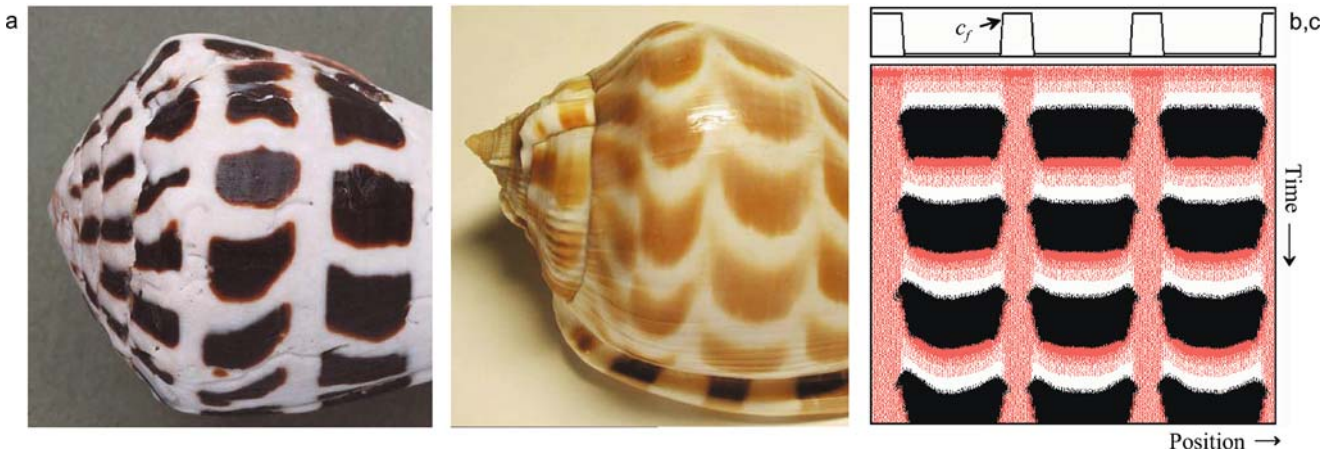


Figure 7.4. The possible role of a separate extinguishing reaction in simpler patterns. A plateau-like pigmentation can result from a bistable system that is switched off by a separate extinguishing reaction. This is in contrast to a system based on an activator and antagonist alone. In the simulation of *Conus ebbaeus* and *Phalium areola* pigmentation abruptly terminates due to the extinguishing reaction (red). At some positions the extinguishing reaction is stable and suppresses pigmentation there permanently. In the remaining regions it is triggered regularly after a certain period of pigment production or it can spread from regions in which the extinguishing reaction is permanently active. The result is, so to speak, a reversed fishbone pattern (see Figure 4.10, page 64), [S74]

A regular transition between a steady-state and an oscillating mode of activation could be also achieved by accumulating a substance produced in the pigment-producing phase that shifts the system into the oscillating mode (or vice versa). Interesting patterns can be generated in this way. These, however, do not show a strong resemblance to natural patterns (Figure 7.5).

7.5 The next step in complexity: an additional stabilizing pattern

The patterns on *Conus pennaceus* (Figure 7.6) and *Conus episcopus* (see Figure 7.10) display the same elements as discussed above, white drops and fine oblique lines with “stalks” where two lines merge. A remarkable new pattern element is that specific patterns can be seen in the regions with brown background pigmentation: darker lines perpendicular to the growing edge are clearly visible (darker lines parallel to the growing edge also occur, see Figure 9.8). Moreover, small white patches appear along the darker lines like pearls along a cord. The white drops may become larger and several drops may fuse, causing relatively large nonpigmented regions. The subsequent spread of pigmentation may result in two distinct patterns. Either narrow mesh-like pigmented lines are formed or the striped background pigmentation is re-established.

**Equation 7.1: Pattern formation involving three systems:
pigmentation, enhancing, and extinguishing systems**

The pigmentation system (an activator - substrate system):

$$\frac{\partial a}{\partial t} = s_b a^{*2} - r_a a + D_a \frac{\partial^2 a}{\partial x^2} - c_e e a \quad (7.1.a)$$

$$\frac{\partial b}{\partial t} = b_b (1 + s_b c + c_b d) - s_b a^{*2} - r_b b + D_b \frac{\partial^2 b}{\partial x^2} \quad (7.1.b)$$

The enhancing reaction (an activator - inhibitor system):

$$\frac{\partial c}{\partial t} = r_c a \left(\frac{c^2 + b_c}{s_d + d} \right) - r_c c + D_c \frac{\partial^2 c}{\partial x^2} \quad (7.1.c)$$

$$\frac{\partial d}{\partial t} = r_c a (c^2 + b_c) - r_d d + D_d \frac{\partial^2 d}{\partial x^2} + b_d \quad (7.1.d)$$

The extinguishing system (an activator - substrate system):

$$\frac{\partial e}{\partial t} = r_e f e^{*2} - r_e e + s_f a + D_e \frac{\partial^2 e}{\partial x^2} \quad (7.1.e)$$

$$\frac{\partial f}{\partial t} = b_f a + c_f(x) - r_e f e^{*2} - r_f f + D_f \frac{\partial^2 f}{\partial x^2} \quad (7.1.f)$$

$$\text{with } a^{*2} = \frac{a^2}{1 + s_a a^2} + b_a \quad \text{and} \quad e^{*2} = \frac{e^2}{1 + s_e e^2} + b_e$$

$-c_e e a$ describes enhanced a -activator destruction under the influence of the extinguishing system e .

$s_b c$ and $c_b d$ The increase of b -substrate production in the pigmentation system due to activator c or inhibitor d of the enhancing system.

$b_f a$ Substrate production in the extinguishing reaction caused by the pigment activator. This term plays a crucial role in patterns with large pigmented regions (Figure 7.3 c).

$c_f(x)$ Substrate production in the extinguishing system that is independent of the pigment activator. It plays a decisive role in patterns with fine pigment lines (Figure 7.3 d). It may depend on position (as indicated in Figure 7.10).

$s_f a$ The trigger for the extinguishing reaction caused by the pigment system. It is necessary when in the extinguishing system the substrate is produced independently of pigment reaction ($c_f > 0$, Figure 7.3d).

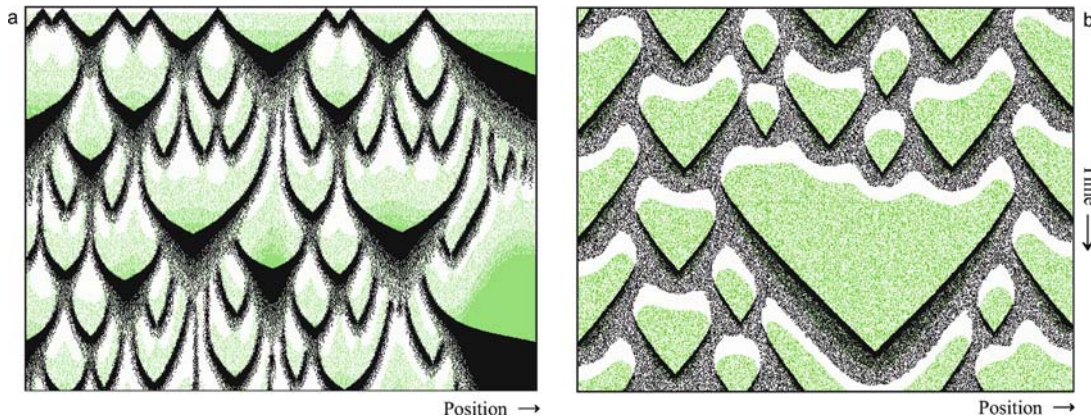


Figure 7.5. Two examples of patterns not found in nature. The alternation between steady-states and pulse-like activation is based on a single substance (shown in green). (a) The substrate of an activator-substrate mechanism receives feedback on its own production rate. During long nonactivated periods substrate production reaches a level sufficient for a temporary steady-state (note that the rate of substrate production, not its concentration, is decisive in determining whether oscillations or a steady-state will be formed, see Figure 3.3). At the end of nonactivated phases, activation is stable and local maxima arise which begin moving toward nonactivated regions. The gradual increase in line width and the resulting strong overshoot are arguments against such a mechanism. (b) Activation of pigment production reduces substrate production. After a certain period of steady-state pigment production, a transition into pulse-wise activation takes place and *vice versa*. Alternations between pigmented and nonpigmented phases occur but no tendency towards stalk formation exists. The white regions appear in columns since an overshoot during the onset of pigmentation increases the probability of another switch [S75a, S75b]

With a single autocatalytic reaction either full activation or suppression can be achieved. This is true even when two antagonists are involved (Chapter 5). Therefore, the three levels of pigmentation - very low in the white drops, higher in regions with background pigmentation, and even higher in the regions of enhanced pigmentation - require a further system that has an enhancing influence. Since the white drops appear preferentially along the darker lines, this enhancing reaction obviously has an influence on triggering the extinguishing reaction.

The existence of an enhancing reaction also resolves a problem remaining from the earlier model. Neither the bistable pigmentation reaction nor the extinguishing system are capable of initiating pattern formation. Simulations such as those shown in Figure 7.3 must be initiated from a set of specifically activated cells. Uniform activation would be wiped out by a single extinguishing reaction since the extinguishing waves only come to rest at a boundary between pigmented and nonpigmented cells, or by the near-collision of two extinguishing waves. Both features are absent when activation is homogeneous. The missing ingredient is a spatial pattern whose local maxima can act, for instance, as nucleation centers for the extinguishing reaction. The fine lines on *Conus pennaceus* (Figures 7.6, 7.7a) and in related patterns (Figure 7.10) indicate that such an enhancing reaction exists. Thus, the complete system would contain the following components:



Figure 7.6. *Conus pennaceus*. (a) Small drop-like patches and a pattern of “staggered wine glasses” on the same shells. In regions with coherent background pigmentation, darker lines appear that alternate with white drops. The white drops appear to have a shadow. The darker pigmentation results from an overshoot after the onset of the pigment reaction. (b-d) Details that restrict possible models (arrows). (b) On one side of a white region a fine line appears, on the other side background pigmentation. Stalks do not form. Obviously, the collision of two pigmentation waves is insufficient for stalk formation on its own. (c) A fine line ends in a “shadow.” Activation in the overshoot region lasts much longer than in the fine line region. This supports the view that either the fine lines result from an active shortening of activator half-life or the background pigmentation results from its active elongation. (d and b) Switching off pigment production in the stalk region may occur over several oscillations. On the shell this causes one or more ladder-like connections between the two diverging lines (large arrow). This argues against an enforced extinguishing reaction and in favor of a smooth change from a steady-state to an oscillating regime. After collision the narrow perpendicular lines occasionally end blindly (small arrows). Obviously, the refractory period of the neighboring cells can be so long that a reinfection is not possible before pigment production ceases. This phenomenon is also visible in *Conus episcopus* (see Figure 7.10)

- (i) The proper pigmentation reaction. It is responsible for the background pattern (light brown in Figures 7.6 and 7.10), and it can spread slowly into non-pigmented areas.
- (ii) An enhancing reaction (green in the simulations). If stable, it causes darker lines perpendicular to the growing edge. As shown further below, it is also responsible for branching.
- (iii) An extinguishing reaction (red) that accomplishes the sudden change from a bistable to a pulse-wise activation, as discussed above.

Some features of natural patterns restrict possible interactions. The darker lines are narrower than the spaces that separate them, suggesting that the stable pattern is active where the dark lines occur and that it enhances pigmentation. The reverse possibility, that the stable pattern reduces pigment production can be excluded. Since the dark lines are never observed to shift to neighboring positions, the enhancement system is more likely realized by an activator-inhibitor rather than by an activator-substrate system (see Figure 2.7 for the different properties of these two systems). Figure 7.7 shows that the enhancing reaction need not be stable in time. If oscillating, pigmentation lines parallel to the growing edge are formed. It is remarkable that patterns with oblique dark lines on a pigmented background seem not to occur.

7.6 Branch formation by a temporary stabilization

In the model outlined thus far, the formation of stalks results from the non-collision of two approaching waves of the extinguishing reaction. Correspondingly, branch formation would require a sudden decrease in an extinguishing wave. But what would cause such a decrease when no counterwave is present? This is only one of the problems with the simulation of stalk formation by noncolliding extinguishing waves. In the simulation of *Conus marchionatus* the stalks are very thin (Figure 7.3d), in contrast to the real pattern. This is not a question of parameters. If the extinguishing reaction is too weak, a direct spontaneous reactivation can take place; if it is too high, stalk formation is not possible. Moreover, in many shells the level of pigmentation increases shortly before branch or stalk formation - again, a feature incompatible with the assumption that stalk formation results from an arrest of extinguishing waves.

The enhancing reaction introduced above resolves these problems. Imagine that the pigment-forming reaction generates traveling waves. The enhancing reaction can be triggered along these waves with a certain spacing due to the long-range inhibition. For instance, if the enhancing reaction increases the local substrate supply of the pigmentation reaction, the system shifts into a temporary steady-state. Further, if the elongation of the pigment-producing period lasts longer than the refractory period of neighboring cells, branch formation is initiated (Figure 7.8a,b). Otherwise

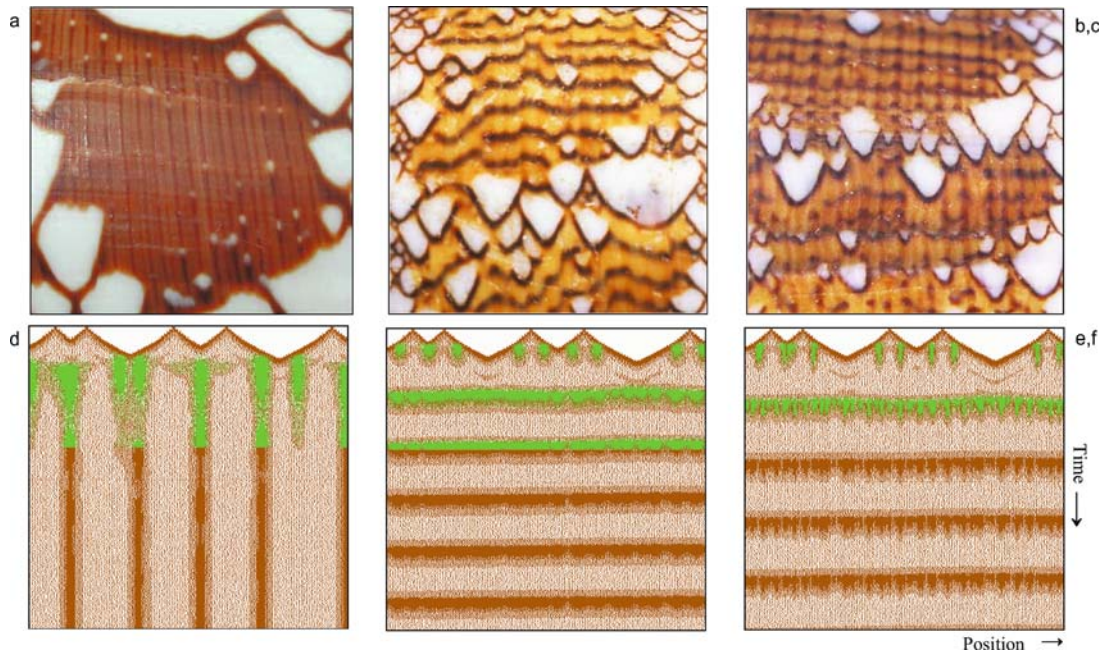


Figure 7.7. Evidence for an enhancing reaction: Elementary pattern on a background. (a) *Conus pennaceus* with dark lines perpendicular to the growing edge. (b,c) *Conus textile* with dark lines parallel to the growing edge; in (c) these lines partially disintegrate into spots. (d-f) Simulations: the character of the resulting pattern is very different, depending whether stable or oscillating enhancing reactions (green in the upper part of the simulation) are involved and whether the pigmentation reaction is stable or oscillating. The partial disintegration into spots (f) is assumed to be based on a lateral inhibition component in the enhancing reaction. Calculated with Equation 7.1a-d; [S77a - S77f]

it makes an attempt to branch, resulting in an irregularity on the lower edge of an oblique line, a feature visible on many shells (Figures 7.8c,d; see also 7.10). In this view, stalk formation is just a special case in which the trigger of the enhancing reaction occurred at the point of collision. In addition, the transition from a steady-state mode back into an oscillating mode at the end of stalk formation is a more continuous process and ensues with the fading of the enhancing reaction. This accounts for details on some shell patterns. In *Conus pennaceus* there are several instances of ladder-like connections between two diverging lines (Figure 7.6b, d). This suggests that the steady-state causing the stalks smoothly changes to an oscillating mode. Such a ladder-like pattern is never observed in simulations in which stalks are terminated by a nonlinear extinguishing reaction and is not observed on the corresponding shells (Figure 7.3).

In the simulation of the white drop pattern (Figure 7.3), steady-state pigment production was an essential ingredient. The formation of branches by a temporary transition into a steady-state under the influence of a stabilizing enhancing reaction suggests the following generalization: steady-state pigment production in complex shell patterns results from the interaction of two patterns that mutually depend on

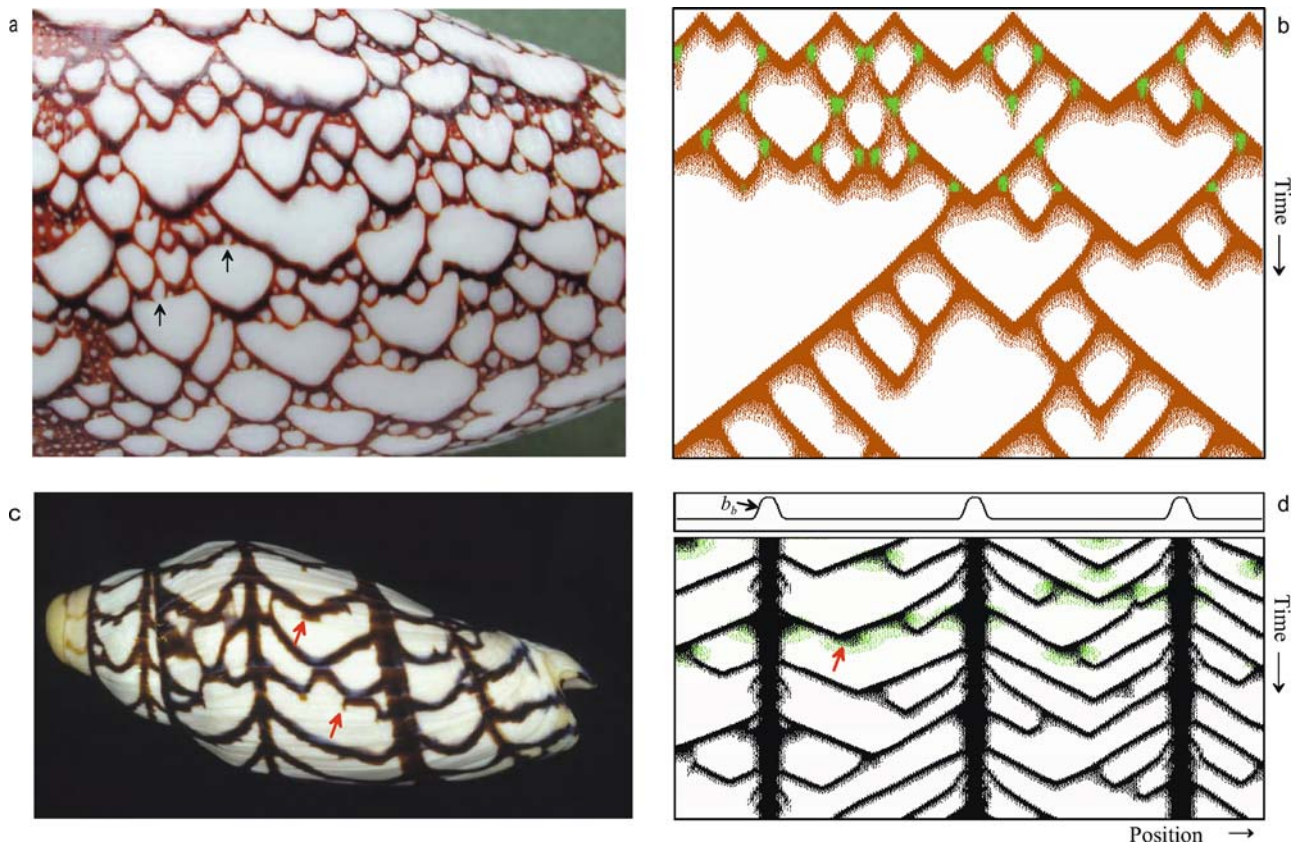


Figure 7.8. Branches initiated by an enhancing reaction. (a, b) *Conus pennaceus* BORN. In the simulation an additional pattern-forming system is assumed (green in the upper part of the simulation) that enhances substrate production. The locally elongated activation of the pigment reaction allows the initiation of backwards-running waves. Although the model employing local enhancement accounts for branch initiation, the abrupt termination (black arrows) indicates that an extinguishing reaction is also involved. (c,d) *Voluticonus bednalli*. The stripes perpendicular to the growing edge indicate that in this region the pigment-forming reaction is in a steady-state. From these regions traveling waves spread that lead to the oblique lines. The enhancing reactions triggered by these waves (green) can lead to the initiation of branches. Unsuccessful attempts of branch initiation are also clearly visible (arrows); [S77b, S78]

each other. The pigment reaction acts as a precondition for the enhancing reaction, which, in turn, shifts the pigment reaction towards a steady-state. This mechanism accounts for very different patterns, depending on the character of the two systems involved. The following cases can be distinguished:

- (i) Both the pigmentation and the enhancing patterns oscillate: branches are formed (Figure 7.8a,b).
- (ii) The pigmentation pattern oscillates but the enhancing pattern is stable in particular regions: separate lines parallel to the direction of growth are formed from which traveling waves spread in both directions (Figure 7.8c,d).

- (iii) At least for a certain time interval the pigmentation and the enhancing reaction are in a steady-state: dark lines perpendicular to the growing edge can emerge on a pigmented background (Figure 7.7a,d).
- (iv) An oscillating enhancing reaction maintains the pigmentation reaction at least temporarily in a steady-state: dark lines parallel to the growing edge can emerge on a pigmented background (Figure 7.7b,c,e,f).
- (v) The pigmentation and the enhancing systems are at the border between a steady-state and oscillations. Large but irregularly sized pigmented regions and finer oblique lines may appear on the same shell. This type of pattern will be discussed in the next two chapters (e.g., Figures 8.11 and 9.5).

Several interactions between the enhancing and pigmentation reactions are conceivable. Either component of the enhancing system, the activator or the inhibitor, can mediate the increase in the substrate production of the pigmentation reaction. The branches have slightly different shapes. If the inhibitor is involved, the enhancement is less localized due to the inhibitor's longer range and half-life. The initiation point for a branch has a more triangular shape. In contrast, the more localized activator produces a sharper line from the beginning. A comparison with natural patterns indicates that the inhibitor solution corresponds more closely. Later we shall encounter more evidence for the involvement of antagonists in the interference between two reactions (Figure 8.7).

7.7 Intimate coupling of an enhancing and an extinguishing reaction

Although the use of an enhancing reaction for local survival describes branch formation very well, the situation appears to be unsatisfactory because two different modifying reactions have to be assumed to model closely related patterns. On the one hand, for the white drop pattern, we are assuming that the pigmentation reaction remains in a steady-state and the *extinguishing reaction* creates the white drops (Figure 7.3). On the other hand, for branches it is assumed that the pigmentation reaction produces traveling waves on its own and a special *enhancing reaction* is required for the temporary transition to a steady-state. Do we need both modifying reactions, enhancement *and* extinguishing? The shells of *Conus pennaceus* (Figure 7.6) and *Conus episcopus* (Figure 7.10) provide a clear answer. There, the darker lines in front of a background pigmentation regularly alternate with white drops. This cannot be the result of a periodic enhancing reaction alone since this would only cause an alternation between darker and normal background pigmentation. Hints of an extinguishing reaction also exist in patterns that are ruled mainly by branching, i.e., in patterns where enhancement is the prevalent element. In *Conus pennaceus* abrupt large-scale pigment termination takes place within a short time period after the formation of many branches (arrows in Figure 7.8a). Therefore, both elements are necessary.

Since the white drops preferentially appear along the darker lines, the enhancing and the extinguishing reactions must be coupled. Several observations indicate that the periodic alternation between enhancing and extinguishing phases do not result from a single process. In Figure 7.6 the white drops are definitely wider than the lines of enhanced pigmentation. Therefore, a breakdown can occur without having been exposed to a preceding enhancing reaction. Similarly, the irregular alternation between dark and white patches on a pigmented background (see Figure 1.9, page 13) excludes the possibility that the two processes resulted from different phases of a single cycling reaction. Grüneberg (1976) postulated, on the basis of his investigation of shells of the *Clithon* family (see Chapter 9), that two pigmentation systems exist, the leuko-pigment and the melano-pigment system. The two exclude each other and depend on each other. This schema is very similar to the mechanism derived here from the dynamic properties of the system.

It may appear reasonable to assume that there is interference from a fast enhancement reaction and, on a larger time scale, a destabilization after sufficient accumulation of a “poison.” This, however, will not work. All destabilizing influences (shortening activator half-life, elongating inhibitor half-life, or reducing substrate production) also decrease the activator concentration. As a rule, negative feedback causes homeostasis. Rather than alternating between enhanced pigmentation and white drops the consequence would be a permanently reduced steady-state. As mentioned earlier, it is crucial for the extinguishing reaction that hidden changes occur without any visible alterations until sudden triggering occurs.

The situation appears to be paradoxical. A modifying reaction must be involved that has both an enhancing *and* a destabilizing influence. The nature of this coupling is the central problem in modeling complex patterns and will be a constant theme throughout the remainder of this book. Again, the problem is that many possible implementations are conceivable. One of them is used in the simulation of *Conus episcopus* (Figure 7.10): the stable enhancing system increases substrate production and thus the activator concentration of the pigmentation reaction. This produces the darker lines. For the extinguishing reaction it was assumed that its substrate is produced proportionally to the activator concentration of the pigment-producing system. Therefore, the extinguishing reaction is fired more frequently along the lines of highest pigmentation. This model describes correctly that the white patches are usually larger than the dark lines on which they are formed. Due to some diffusion of the substrate of the extinguishing reaction, regions adjacent to an enhanced stripe are also prone to breakdown.

In this example, both modifying reactions were complete pattern-forming systems and only loosely coupled. In the next section another reaction will be discussed in which the two features result more naturally from a single reaction. Before doing so, a very remarkable feature of these patterns should be mentioned that is not yet reproduced by the models. On many shells, the width of bended pigmentation lines remains approximately constant, although very different processes contribute to the line width (Figure 7.9). The width of the lines more perpendicular to the

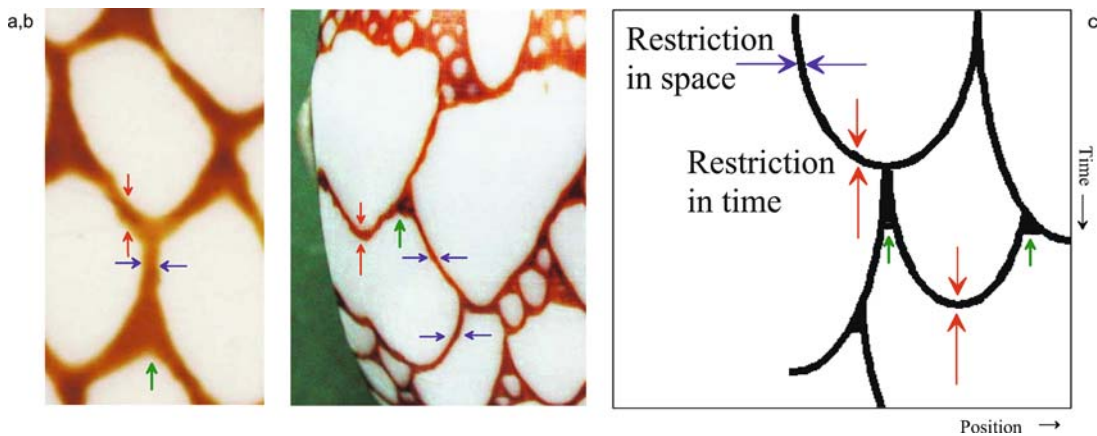


Figure 7.9. The nontrivial feature of constant line width of curved lines. The thickness of more vertical lines depends on a restriction in space (blue pairs of arrows). In contrast, the thickness of more horizontal lines depends on a short duration (red pairs of arrows). The resulting patterns are reminiscent of “staggered wine glasses” and indicate a sudden temporary transition from a burst-like into a steady-state activation, in which the spread of the activation is strongly reduced. A temporary transition into a steady-state (green arrows) is also required to initiate branching

growing edge - the “stalks” of the wine glass pattern - is determined by a restriction in *space*: the width in which activation survives. Later, after the wave speeds up, the width of the oblique lines is determined by a restriction in *time*: the duration of the pigment-producing phase, which becomes successively shorter. Both processes are, in principle, independent of each other. A similar phenomenon is also displayed by other shells. For instance, the round patches of pigmentation or the round holes in pigmentation (Figure 1.8) are also based on a comparable extension of a time- and a space-dependent process. The same phenomenon can be seen in the pigmentation patterns of some avian feathers (Figure 13.10c).

7.8 Extinguishing that results from a depletion of resources due to an enhancing reaction

One key to solving the aforementioned problem may be found in the patterns of *Conus pennaceus* (Figure 7.6a) and *Conus auratus* (Figure 7.11), which show long enhanced lines rarely interrupted by white drops. These phases of coherent background alternate with phases in which the background pigmentation disappears and only narrow oblique lines with crossings remain. White drops are formed more in the zones of transition between the two phases. In other words, white drops occur only when the system is near the border between a steady-state and a pulsating mode of pigment production. This suggests that the enhancing reaction is accompanied by a depletion of resources, causing an earlier breakdown. The situation may be compared with doping in sport. Doping releases the available resources

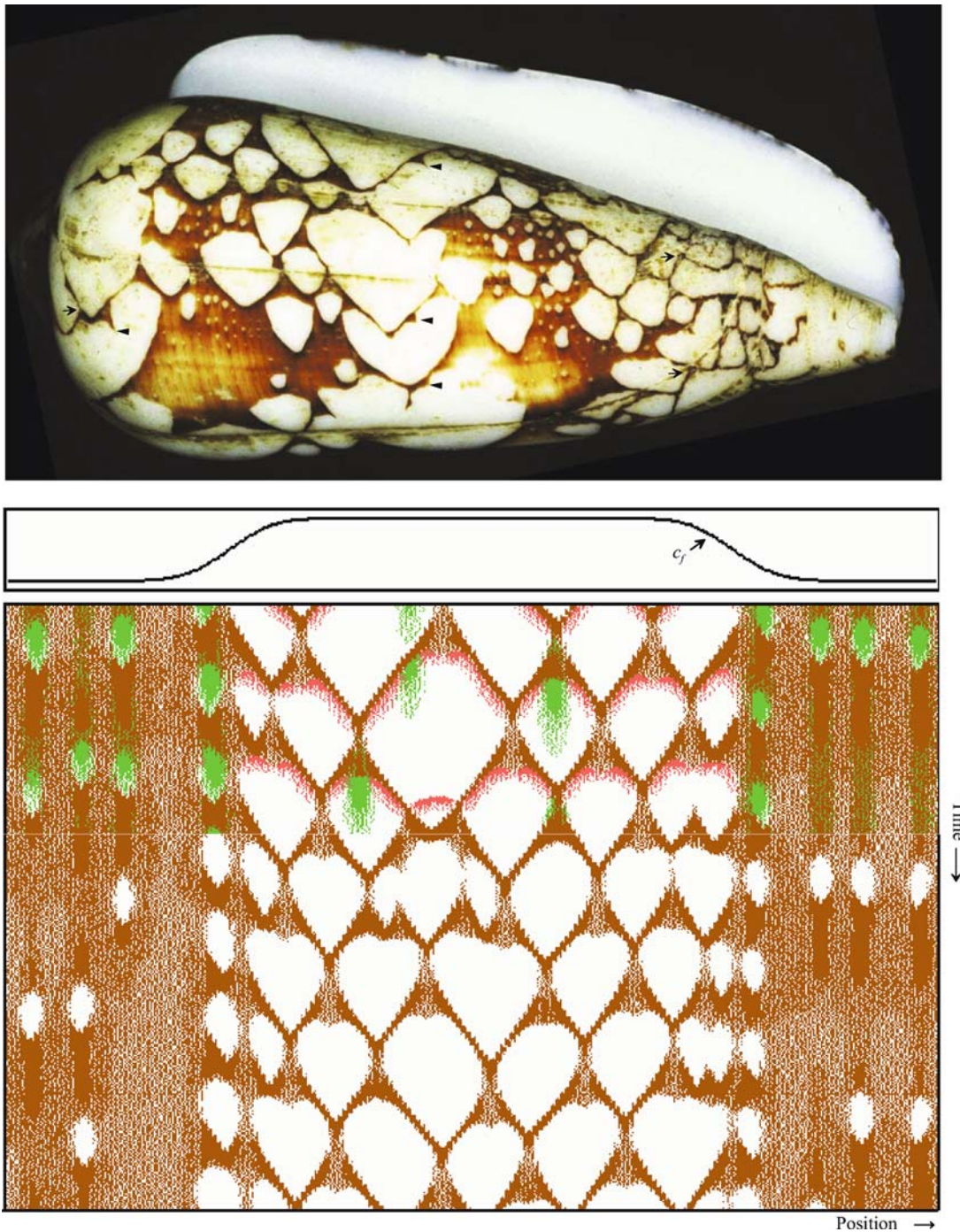


Figure 7.10. *Conus episcopus*. Large pigmented areas display darker lines with small white drops. The fine oblique lines form branches (arrow) or attempt to branch (arrowheads). In the simulation three interacting pattern-forming systems are assumed: the pigmentation (brown), the enhancing (green), and the extinguishing system (red). The upper part shows all activators, the lower only the expected pigmentation. The simulations are calculated with Equation 7.1, page 113. The graph above the simulation indicates the substrate production for the extinguishing reaction independent of pigmentation, $c_f(x)$. The higher rate in the center leads to larger nonpigmented regions. Calculated with Equation 7.1;[S710, S710a]

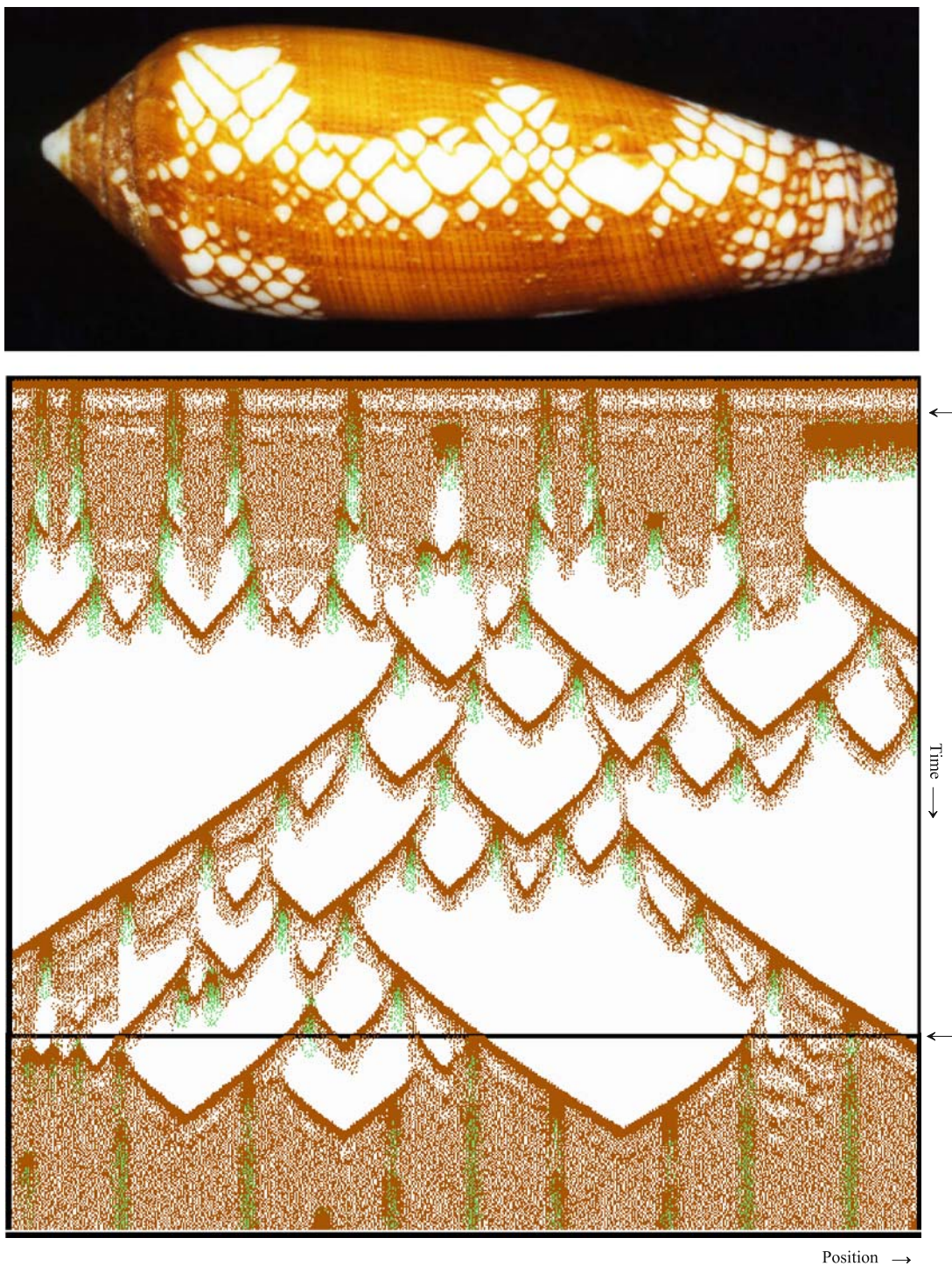
of the body, temporarily enabling high output of power. This, however, can cause a breakdown in the body when resources become exhausted. Without doping, a continuous output of power is possible over a longer period of time although at a lower level. Exhaustion comes into effect only if the system is at the border where continuous activation is just possible. In contrast, if the ability to replenish resources is sufficiently high, no enhancement-induced breakdown will take place.

Several implementations of this idea are conceivable. For instance, a pool may exist from which the substrate for the autocatalytic reaction is obtained. The enhancing reaction would promote increased utilization of this pool and corresponding depletion. The dynamics of such a system, however, are difficult to understand. For instance, it seems reasonable to assume that in a normal activator-substrate system (Equation 2.4), the rate of substrate removal in a cell depends on whether the cell is activated or not. However, this is not the case. This is most easily understood by realizing that, by definition, the concentration change is zero in the steady-state. Since the production rate b_b is the same in all cells, the sum of all processes that lead to substrate removal (consumption during the reaction, loss by diffusion, and independent decay) must balance constant production. It must also be the same in all cells and independent of local activation. Therefore, if a pool exists from which substrate is drawn, utilization of the pool would be independent of local activation. If, however, a lower substrate concentration leads to an increased transfer from the pool to substrate production, the pool would be depleted.

The system satisfies the requirement that accumulating changes must be hidden. As long as sufficient precursors are available, the system works normally. The situation can be compared with a car whose power output is independent of how much fuel is in the tank. Of course, the situation changes suddenly when the tank is empty. The substrate pool differs from the car analogy though because there is a constant influx into the pool even when it is almost empty. However, this supply may be insufficient to maintain the steady-state. Figure 7.11 has been calculated using this scheme. It can be seen that the first white patches appear in those regions that were previously exposed to the enhancing reaction. However, the correct simulation of white drops along dark lines using a single modifying reaction has not yet been achieved.

7.9 Related patterns reveal unsolved problems

The patterns on related shells demonstrate a wide range of variations. The shell of *Conus ammiralis* (Figure 7.12a) shows the usual patterns of white drops and of dark stripes on a pigmented background in some regions. In other regions, however, the coherent background pigmentation is replaced by a meshwork of fine lines. It is quite remarkable that the size of the large white drops, their frequency, and the spread of the pigmentation are not affected by the transition from one region to another. This is not expected from the models outlined above. It was assumed



that enhanced pigmentation preferentially triggers the extinguishing reaction. This accounts for chains of white drops along the dark lines (Figure 7.10); however, in *Conus ammiralis*, pigment termination seems to work normally even if much less pigment is produced. A similar problem exists with another pattern discussed earlier (Figure 7.6). Increased pigmentation occurs in the “shadow” of the white drops resulting from an overshoot of the pigmentation reaction. Why does this not immediately trigger an extinguishing reaction?

Figure 7.12b shows a shell of a closely related snail, *Conus ammiralis archithalassus*. In addition to the normal lines of enhanced pigment production perpendicular to the growing edge, dark lines parallel to the edge are also visible. The large white drops are more irregularly arranged but, especially the finer ones, appear preferentially at a crossing of the two types of enhanced lines. This underlines the intimate coupling between enhancement and termination of pigment production. The fine meshwork suggests that steady-state pigment production is in itself a composite process and is based on an enhancement. If this enhancement is insufficient to maintain an overall steady-state, its oscillation causes a rapid sequence of branching. Given this interpretation, the thickness of the fine lines would be a measure of activator half-life without enhancement.

The rounding of white drops at their lower tip is a special problem (compare, for instance, the collision of waves in Figure 5.1 and Figure 7.6). These roundings indicate that two approaching waves are speeding up. Two mechanisms can be envisioned: (a) The cells become more excitable the longer they have not been activated. The excitability of the cells, and thus the speed of the wave, is correlated to the length of the nonactivated period. (b) Alternatively, two approaching waves are attracted to each other; the speed would correlate with the remaining distance between the two waves. From the pattern one can infer that the rounding is roughly the same in large and small white drops, giving more support to the second possibility.



Figure 7.11. *Conus auratus*. Periods of coherent background pigmentation alternate with meshwork-like structures over long time intervals. Dark lines of enhanced pigmentation are clearly visible on the light brown background. Small white patches are only formed in zones of transition. Model: a pool of precursor molecules for the production of the substrate is assumed. If the influx into this pool is sufficiently high, pigmentation reaction is in the steady-state; otherwise traveling waves are formed. The enhancing reaction (green in the upper part) is responsible for the stripes of increased pigmentation in the steady-state as well as for branching in the traveling wave mode. Regions exposed to the enhancing reaction are the first to terminate pigment production. To simulate the transition from a steady-state to oscillatory behavior, the influx into pool b_e has been changed from 0.06 to 0.035 and back to 0.06. The time of each change is indicated by an arrow. In reality, this is certainly accomplished by an independent oscillation; [S711]



Figure 7.12. Pattern variations in related species. (a) *Conus ammiralis*. Its most remarkable feature is the transition from regions of pigmented background with dark stripes to light narrow meshwork-like pigmentation. The size of the white drops and the spread of pigmentation remains the same in both regions. (b) Shell of a related species, *Conus ammiralis archithalassus*. Darker pigmentation lines parallel and perpendicular to the growing edge are visible. The fine meshwork pattern is restricted to narrow stripes. They are almost free of white drops

7.10 Apparently different patterns can be simulated by closely related models

Several shells that overtly look very different can be described by basically the same mechanism. The shell of *Cymbiola pulchra wisemani* (Figure 7.13), for instance, shows nonpigmented patches. Some of them have dark dots at the top. No fine lines or stalks are present. However, a closer inspection reveals that the same elements are involved here as have been discussed earlier. The white patches appear as a result of abrupt large-scale termination and slow repigmentation. The dark dots at the beginning of the white patches underline the postulated intimate coupling between enhancing and extinguishing reactions. Again, the latter extends further. Both events, enhancement and extinction, follow each other rapidly. It is difficult to decide whether a local increase in pigment production enhances the probability of a large-scale extinguishing reaction or whether it is a part of the extinguishing reaction itself. The pigment production must be in the ON state for some time before the enhancing reaction, and thus the destabilization, can be triggered. It is quite remarkable that large-scale pigment termination can occur without an enhancing reaction beforehand, especially in regions of high background pigmentation. Again, the enhancing reaction is not a prerequisite for pigment termination. The main difference for the patterns discussed above is that the enhancing pattern obviously only has a destabilizing effect on background pigmentation.

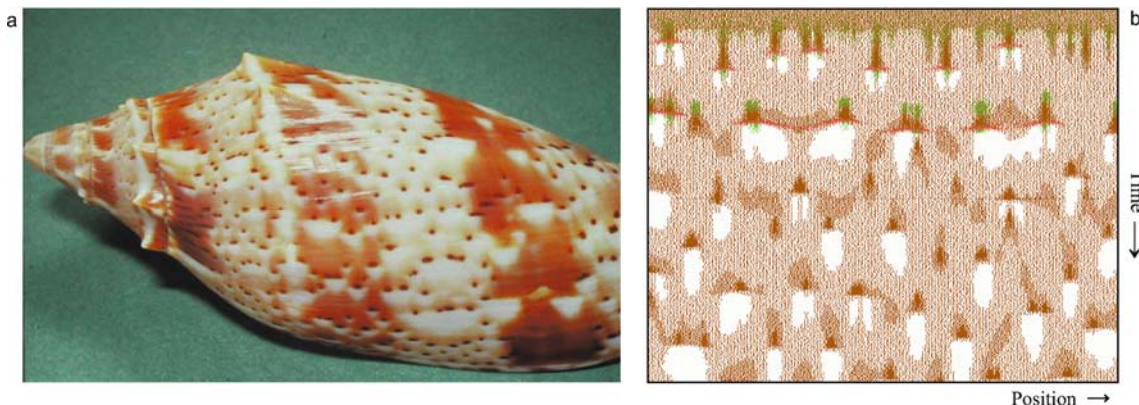


Figure 7.13. Nonpigmented patches with an i-dot, the shell of *Cymbiola pulchra wisemani*. The same pattern elements are involved: local enhancement and concurrent large-scale breakdown. An enhancing pattern that leads to staggered dots (see Figure 5.10) is assumed in this simulation. Increased pigmentation accelerates the trigger for the extinguishing reaction. [S713]

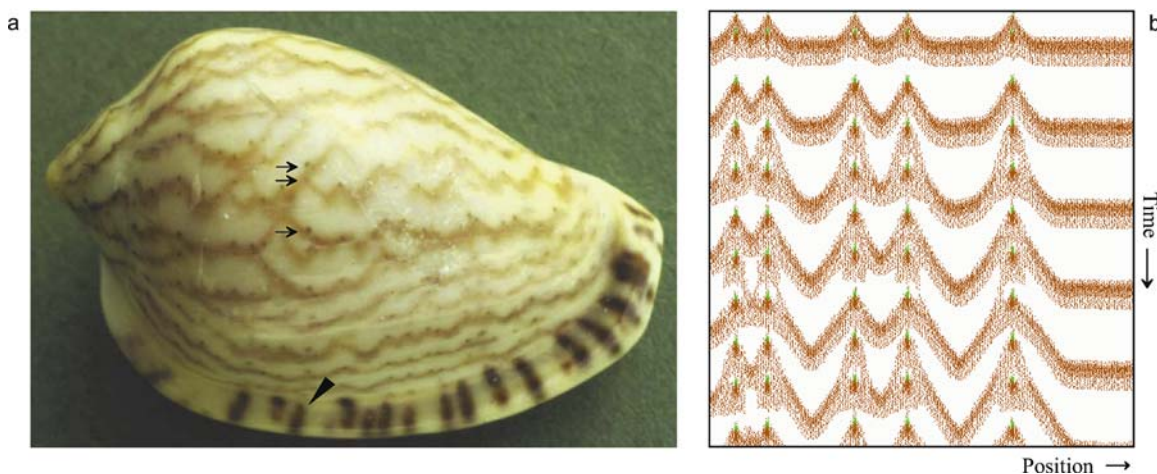


Figure 7.14. Traveling waves and rows of fine dots: *Marginella limbata*. Model: The coincidental activation of both a stable and a wave-generating system can trigger a third system, an enhancing reaction, for a very short time. Small dots are formed in rows. Sometimes two such dots are formed within the passage of a single wave (arrows). This pattern indicates that a stable system may be a prerequisite for the enhancing reaction, but since it switches off so rapidly it seems that activation of the enhancing reaction has its own dynamics. [S714]

The shell of *Marginella limbata* (Figure 7.14) shows common traveling waves. In addition, very fine dots are visible that are strictly arranged in rows. Patches of dark pigmentation at the growing edge mark some of these rows. Three pattern forming systems must contribute: the first forms an invisible but permanently stable pattern that acts as precondition for the fine dots. The second forms the waves and the third is triggered only by the simultaneous activation of the first two systems, i.e., if a wave

passes an active region in the stable pattern. The third system must have very short time constants since pigmentation rises and declines very rapidly. The short time constants and the required presence of the two other systems lead to the formation of dots. A very low concentration of the wave system is sufficient to trigger the dots. Therefore, the dots appear to arise shortly before the wave passes. Sometimes two such bursts fit into one stroke of the wave. This can be the origin of a wave running in the opposite direction. The most important feature in the present context is that switching off the enhancing reaction is an independent and very rapid process. This shell supports the view that the superimposition of waves on a stable pattern leads to pigment enhancement. It is special in that the enhancing reaction has two clearly separable components, one with a long and another with a very short time constant. The mechanism of spine formation shown in Figure 4.1 (page 52) presumably has a similar basis.

7.11 Conclusion

The complexity of many shell patterns results from superimposing two types of modifying reactions onto the pigmentation system. An enhancing reaction increases pigment deposition and frequently shifts the pigmentation system from an oscillating to a temporary steady-state. Branches, the formation of darker lines on a pigmented background, and the formation of patches with increased pigmentation are traces of this reaction. A second modifying influence has the opposite effect, causing an abrupt and often large-scale termination of pigmentation.

The number of possible interactions between these three systems is extremely large. Deducing the most likely form of interaction from the details of a shell pattern is a very difficult task. The interactions given here should be regarded only as examples.

The postulated systems have different properties - a feature that makes further simplifications difficult. The pigment system requires a slowly diffusing activator and a nondiffusible antagonist in order for the pigmentation reaction to spread. The components of the extinguishing reaction must spread rapidly to enable the large-scale breakdown. In turn, the enhancing reaction must have a rapidly spreading antagonist with a short time constant in order to generate at least temporarily a stable pattern. Since this pattern may change after long inactive periods, presumably it depends on the background system. It is not yet clear whether the extinguishing reaction is based on an independent system or results as an implicit consequence of the enhancing system. Arguments for both versions have been discussed. In any case it requires some type of large-scale action.

On the other hand, both modifying influences are not always required in order to generate interesting patterns. Without the enhancing reaction simple white drop patterns are obtained (Figure 7.3). With the enhancing but without the extinguishing reaction, the huge class of patterns discussed in chapter 4, the net-like patterns

in Figure 7.8, and the pattern characterized by large pigmented areas and finer oblique lines in irregular arrangement (see Figure 8.11) are obtained.

To generate higher organisms, many pattern-forming reactions must be superimposed upon each other. Although biological systems handle this complexity without any problems, it makes theoretical analysis very difficult and the result, even if correct, may not be elegant. Inelegance, however, only represents an aesthetic problem for theorists.



Figure 8.1. Different shells bearing triangles as their basic pattern element

Triangles

Several mollusks display triangles as their basic pattern element. The triangles may be connected to each other to form oblique lines with a triangular substructure. If both corners of the lower edge give rise to new triangles, the white regions in between also have a triangular shape although with opposite orientation. The triangles may cover different portions of the shell. If they are densely packed, it appears as if white triangles are arranged on a black background. The triangles can also be of very different sizes. On some shells they are a prominent pattern element, on others they appear more as a roughness in the oblique lines but are clearly visible on closer inspection. The triangles themselves may have a fine structure of lines parallel to the growing edge or they may resolve into bundles of lines parallel to the direction of growth. On some shells an almost continuous transition from triangle to branch formation can be recognized. The occurrence of triangles on very different mollusks, on bivalved mussels and on snails, indicates that the possibility of forming triangles is a basic feature of shell patterning. Figure 8.1 gives some examples. In this chapter, an attempt will be made to find a unified explanation for this diversity. I will begin with the basic features and how they can be modelled within the framework of the theory. Discrepancies with natural patterns will be used as guides to develop more complex models.

As mentioned in chapter 7, formation of triangles requires a bistable system. From a small activated point, activation spreads in both directions and the cells remain in an activated state. While in the patterns discussed in the previous chapter termination of pigmentation spreads more rapidly than the onset of pigmentation (Figures 7.2 and 7.3), the sharply straight lower edge of triangles indicates that termination occurs strictly simultaneously. This excludes the possibility of a signal being initiated at a particular position spreading by diffusion. Therefore, it is assumed that the signal for pigment termination in triangle formation does not result from a metabolic product of the pigment producing system but from an independent central oscillating system. The substances responsible for the extinguishing reaction can be distributed within the animal in hormone-like fashion. In this way concentrations of the oscillating system are constant along the growing edge of the shell. More or less synchronous oscillations as shown in Figure 3.4 (page 45) are conceivable as well.

The most surprising feature of connected triangles is the almost immediate spread of pigmentation after a collective breakdown. Usually there is no lag between the breakdown and the spread of pigmentation into the same region again. Thus, the signal that causes the transition from the steady-state to the burst-like mode of pigment formation must be very short. The system returns very rapidly to the normal mode of bistability. In connected triangles, one side should be in the shadow of a previous activation while at the other side, pigmentation spreads into a region that was not activated for a long period. Nevertheless, the shape of most connected triangles is symmetric, suggesting that the spread of pigmentation is independent of the time that the cells were not activated. In other words, the system does not become more excitable as time progresses from the last activation. A similar feature was mentioned in chapter 6 in connection with the branching of lines. In that case, backward waves proceeded immediately after their birth with the same speed as the original wave, although they were in the shadow of the primary wave (Figure 6.1). The inherent similarities between triangle and branch formation will be discussed again later.

Figure 8.2 shows simulations of triangle formation using simple models. An oscillating system (red) shifts a bistable system from active to inactive state for a short period. This transition can be accomplished either by a reduction of substrate production (Figure 8.2b) or by additional removal of the activator. The first mechanism is less convenient for producing symmetric triangles since it requires time for the recovery of substrate concentration. If the extinguishing reaction is short and of moderate strength it may require several pulses before the activator no longer recovers instantaneously. The result is a pattern similar to the famous Sierpinsky triangles with their fractal geometry. It closely fits the pattern on the shell of *Cymbiola innexa* (Figure 8.3).

8.1 The crossing solution through the backdoor

The models developed so far are parameter-sensitive. A small increase of the efficiency in the extinguishing reaction leads to a considerable change in the resulting pattern. Nevertheless, this may correspond to the actual situation since a single shell can exhibit a variety of analogous patterns (Figure 8.2). However, several distinct features of natural patterns are not reproduced by minimal models. Although pigmentation spreads with the same speed in both directions, activation often survives only on the outer side of the triangles. There must be a memory feature that does not affect the spread and comes into play only at the time of collective breakdown. A region recently activated would remain more prone to the extinguishing reaction. Figure 8.4 illustrates this situation.

Another problem is the spontaneous initiation of new chains of connected triangles. This is impossible to simulate by using the minimal model described above. The symmetric shape of the triangles requires almost instantaneous recovery of the

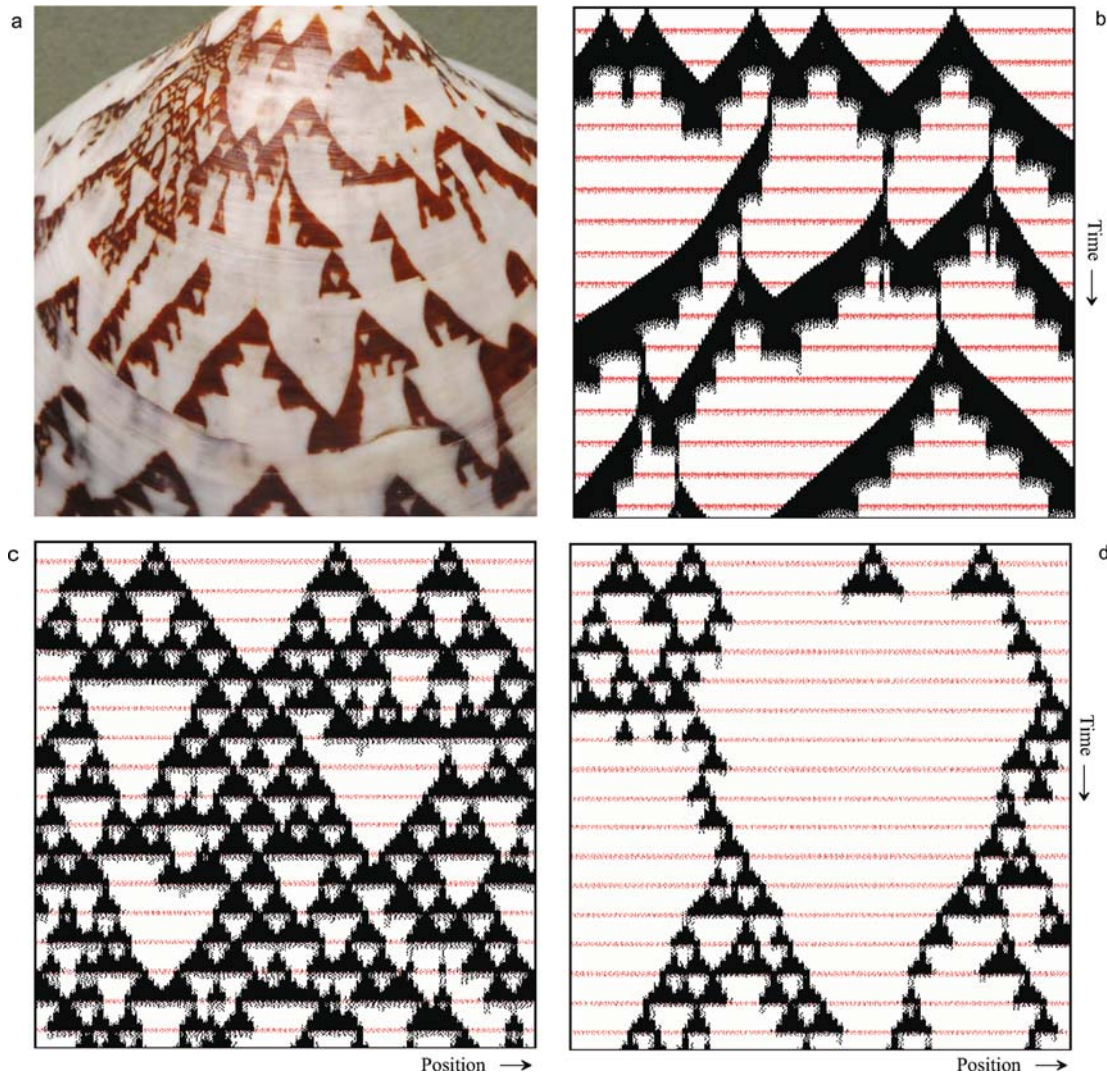


Figure 8.2. Simple model of triangle formation. (a) Details of *Lioconcha castrensis*. (b-d) A bistable reaction is assumed. Activation (black) can spread in both directions due to activator diffusion. An oscillation (red) is superimposed that blocks pigment reaction, either (b) by suppressing the necessary substrate production, or (c, d) by increasing activator removal. For a short time the activation is shifted from a bistable mode to a mode with short pulses. Activation can survive at the margins of the resulting triangle since here sufficient substrate is still available. Both models are parameter-sensitive. An increase of 10% in the rate of activator removal by the extinguishing reaction leads to a dramatic change in the pattern (c versus d). A similar pattern alteration from bilaterally connected triangles to separate chains of triangles is also visible on the shell (a) [S82a, S82b, S82c].

system and thus very short time constants. In contrast, a spontaneous trigger occurs only after a long time interval. Both the unilateral survival mentioned above and the delayed spontaneous trigger indicate that a second antagonist, for instance an inhibitor with a long time constant, is involved. This inhibition is higher in cells that have recently been activated, lowering the chances that the pigmentation system

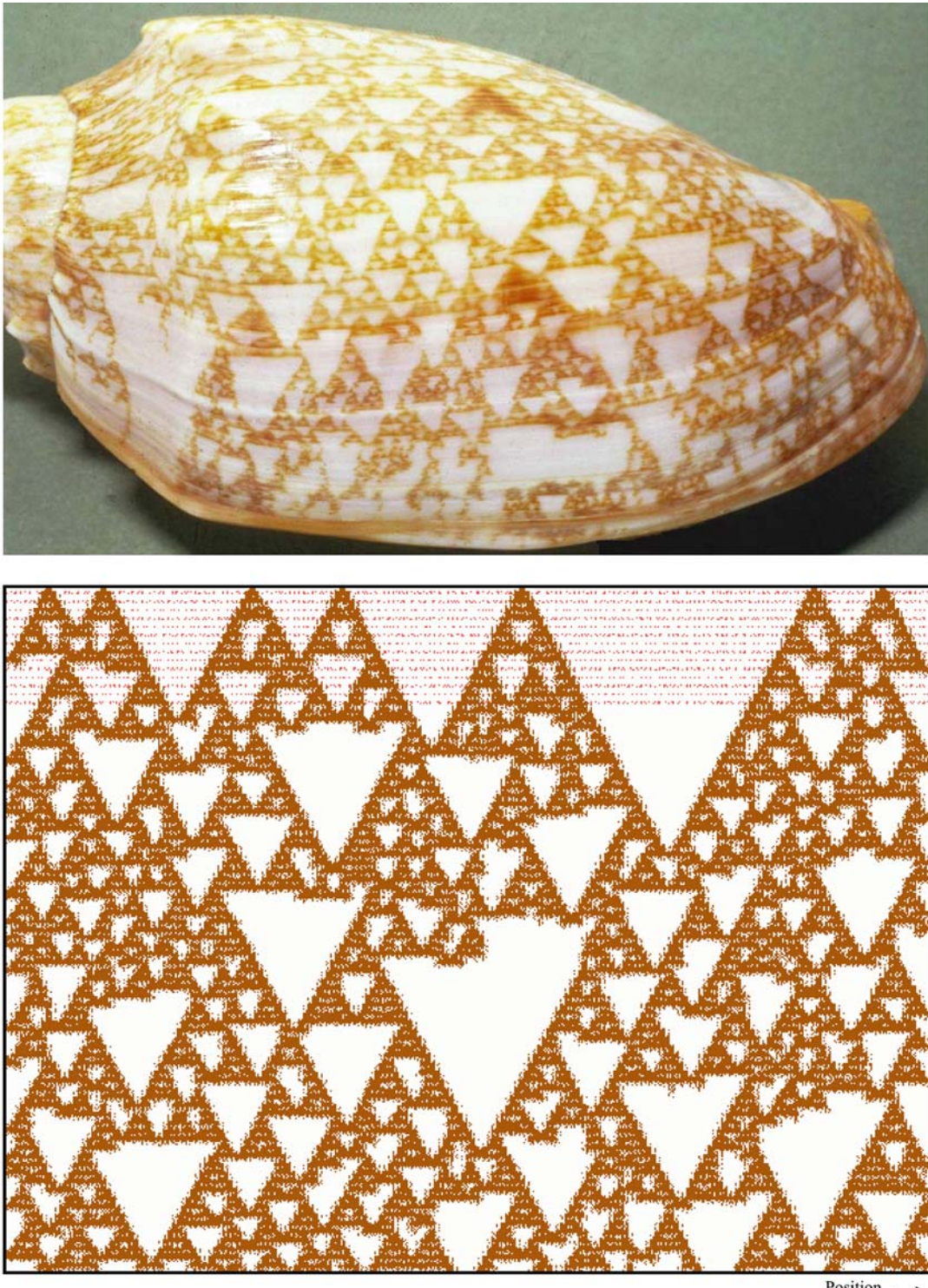


Figure 8.3. Sierpinsky triangles: the pattern on *Cymbiola innexa* REEVE. The signal for the transition into pulse-like activation (red) may be so short that activation (brown) reappears immediately. Occasionally however, this may fail. This is relatively frequent in small areas, forming many small triangles. It may also occur, although more rarely, over a larger area leading to large triangles. The pattern is similar to the well-known Sierpinsky triangle with its fractal geometry; [S83]

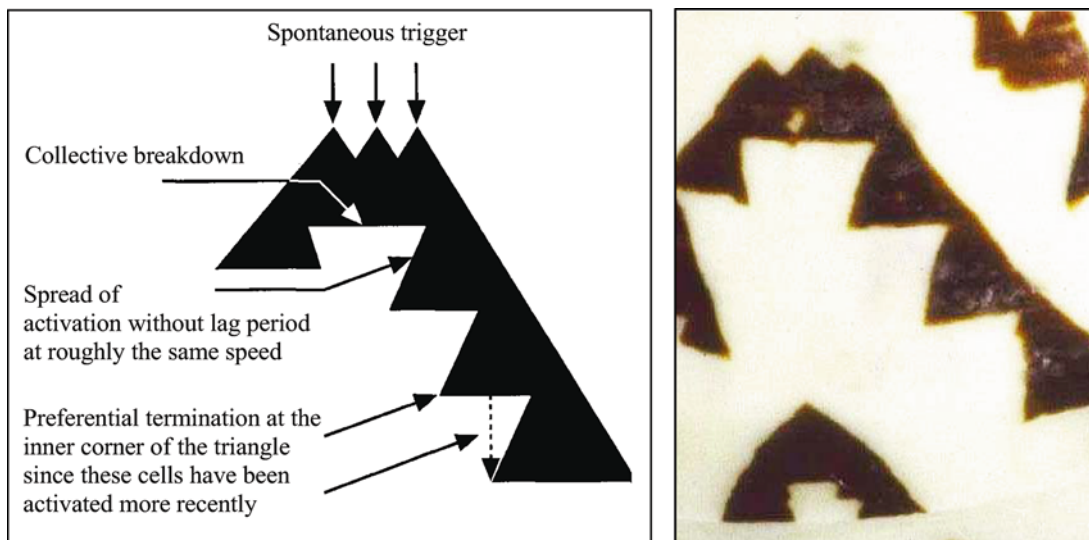


Figure 8.4. The problem of unilaterally connected triangles. Although pigmentation spreads with the same speed in both directions after a breakdown, termination occurs preferentially on the side that produced pigment more recently.

will survive the extinguishing reaction at the inner margin. A spontaneous trigger is possible after the decay of this second inhibitor. Figure 8.5 shows examples of different shells of the *Lioconcha* family and corresponding simulations.

A system with two different time constants was already employed for the formation of crossings (see Figure 5.8, page 81). It was mentioned that the oblique lines in these crossings show a fine substructure of connected triangles. The assumption of a second antagonist for these systems was based on the survival of activation during collisions. Now, to model triangle formation the same mechanism is used for a different reason. The first antagonist is required for fast recovery after collective breakdown. The second one is responsible for the memory feature that leads to preferential termination of pigmentation on the inner side of the chain of triangles. Later we shall see that a third inhibition must also exist.

8.2 Triangle versus branch formation

Although the occasional branching and the crossing of the chained triangles is correctly reproduced, finer details indicate that even this model is too simple. The triangles in the simulations are too regular when compared with natural patterns. Pigment termination is sometimes incomplete causing a fuzzy lower edge to the triangles. The time interval between termination may also vary.

Other shells of the *Lioconcha* family and related shells show further interesting modifications (Figure 8.6). In parts of *L. castrensis* (8.6a) that were formed at

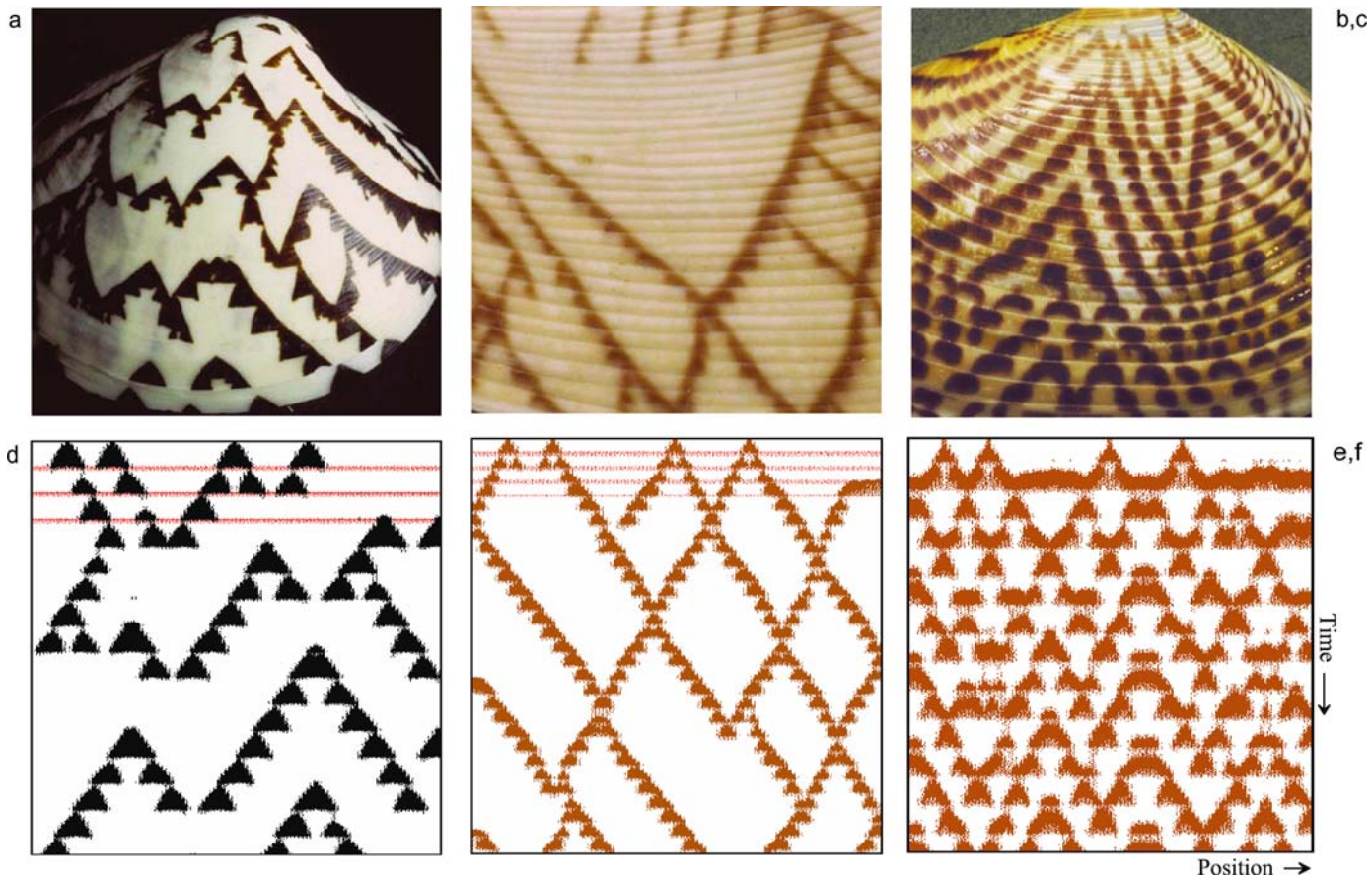


Figure 8.5. Chains of connected triangles. (a-c) Patterns on *Lioconcha castrensis*, *Tapes literatus* and *Sunetta meroe*. (d-f) Simulations using Equation 5.1 together with a global oscillating system. The activator of the oscillating system (red in the upper parts) shortens the activator half-life of the pigmentation reaction for a short time interval. Depending on the parameter values used, the triangles may be either the dominating pattern element or more a fine structure. Occasional branching, crossing and annihilation after a collision are reproduced. In (f), the inhibitor of the oscillating system increases the substrate production of the pigment system (see Figure 8.7); [S85a, S85b, S85c]

younger stages, triangles and branches visibly coexist. In *L. ornata* (8.6b) branching is the dominating structure. In *L. hieroglyphica* (8.6c), branching lines frequently terminate without collision or form triangles that have an internal structure of

Figure 8.6. The diversity of patterns on related mollusks. (a) Transitions from branching lines to triangles on *Lioconcha castrensis*. (b) Branching lines can form a dense meshwork (*L. ornata*). (c) Branching lines can terminate blindly or fade away (*L. hieroglyphica*). (d) A specimen of *L. hieroglyphica* that has formed branched lines at younger stages (top) but larger triangles consisting of fine parallel lines at later stages. (e) Triangles, branchings, crossings and large-scale breakdown on the same shell. Occasionally pigment production can be locally maintained in small regions for a relatively long period. (f) In *Lioconcha lorenziana* pigmentation can remain at an elevated level after passing of a wave. The oblique lines have a fuzzy lower border.



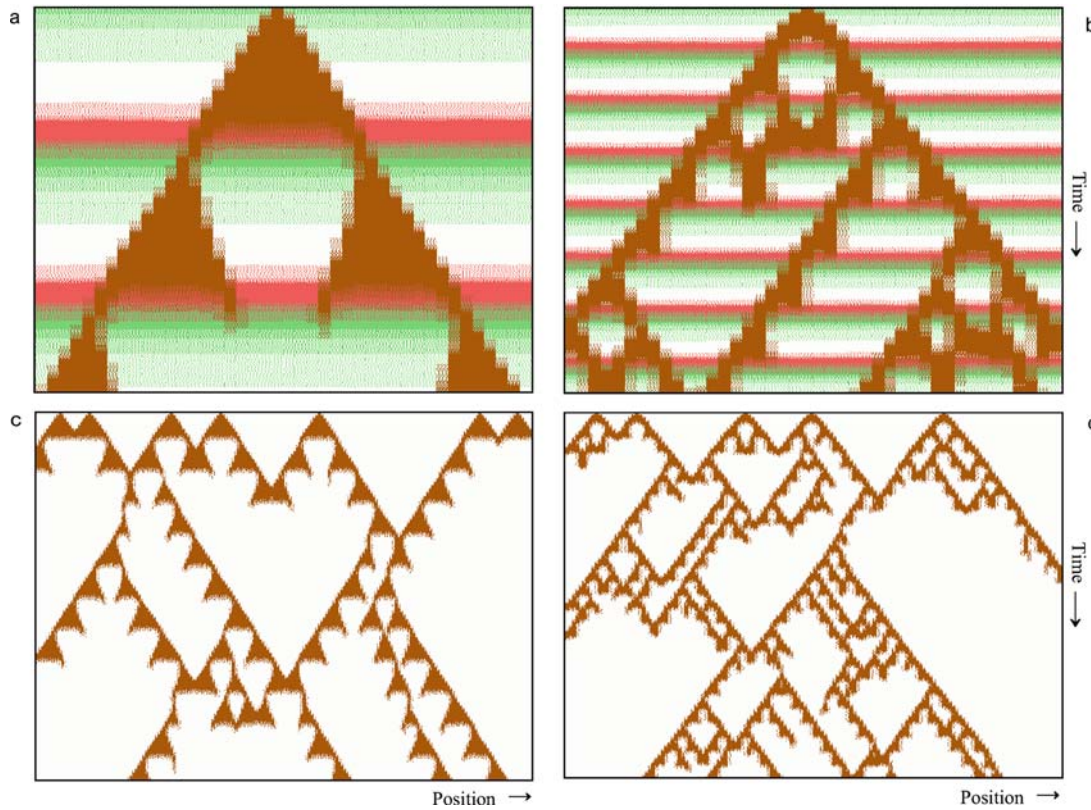


Figure 8.7. Triangle *versus* branch formation. Triangle formation requires an abrupt termination of a spreading steady-state pigment production. In contrast, branch formation requires a temporary transition into a steady-state pigment production to allow the formation of backwards-running waves. Both requirements can be met if the activator (red) and the inhibitor (green) of the modifying system have antagonistic influences on the pigmentation system. (a, c) The extinguishing effect of the activator dominates: triangles result. (b, d) The enhancing effect of the inhibitor dominates: branches result [S87a, S87b]

fine parallel lines (8.6d). The lines may become thicker and smeared (8.6e). In *L. lorenziana* (8.6f), pigmentation fades away rather than forming branches. In the remaining sections of this chapter, possible origins of this diversity will be discussed.

The simultaneous formation of branches and triangles on the same shell (Figure 8.6a) is very remarkable since, as explained above in detail, the two patterns require opposite sets of parameters. Branches are formed by a system of traveling waves in which a short temporary transition into a steady-state takes place. The transition enables the survival of activation until the refractory period of the neighboring cells is over. In contrast, triangle formation needs a pigmentation system in a steady-state with short temporary transitions into pulse-like activations.

These conflicting requirements can be resolved under the assumption that both modifications, extinguishing and enhancement, occur in rapid succession. So far,

we have assumed that the activator of the modifying system shortens the half-life of the pigment activator, causing a transition from a steady-state to pulse-like activation. The branching phenomenon suggests that the antagonist of the modifying reaction, for instance an inhibitor, plays the opposite role in this modification. While the short pulse of the activator acts as an extinguishing signal to form the lower border of the triangle, the longer-lasting inhibitor that immediately follows brings the pigment system towards a steady-state. Depending on whether the unperturbed pigmentation system forms traveling waves or tends to bistability, and on how strong the extinguishing and/or enhancing influences are, either triangles or branches will be formed. Simulations of both modes are shown in Figure 8.7. The upper figures provide a close-up of how the system works showing the pigmentation system (brown), the extinguishing activator (red) and the enhancing inhibitor (green) of the modifying reaction. The lower two panels provide simulations using the same parameter values over a larger field of cells to demonstrate the overall pattern. With this modification, triangle formation becomes even more similar to the extinguishing and branching patterns discussed in chapter 7 (see, for instance, Figure 7.2, page 106).

In order to maintain the two stable steady-states, one at low and one at high concentrations, high substrate production and a high decay rate independent of the autocatalytic process are required (see Figure 3.3). In other words, much of the substrate produced would not contribute to pattern formation. The branching phenomenon suggests a more economic method of substrate production. It would increase only temporarily when required, i.e., immediately after an enforced breakdown.

8.3 The involvement of three inhibitory reactions

The shell of *L. hieroglyphica* (Figure 8.6c) shows oblique branching lines that terminate without any collision with counter-waves. This phenomenon is also visible in a milder form in Figures 8.6a and 8.6f. Termination of this type is not announced by a retardation in the spread of pigmentation. This suggests that activation is near the lowest level at which the chain of triggering events can be maintained. Any additional lowering causes termination even in cells that have not been activated for a long time. What can cause wave termination? Termination occurs preferentially if two waves approach each other. Either one or both waves terminate. In the latter case, a nonactivated gap remains. This suggests that a rapidly spreading inhibition emanates from the activated cells. Sensing this inhibition, a counterwave may terminate. If the time constant of this inhibition is long, an overall poisoning occurs. (In contrast, if the time constant of this rapidly diffusing inhibitor is short, crossings can occur, see Figure 5.8).

After some delay, a spontaneous trigger of new activations occurs preferentially in the gap left untouched by the two terminated waves (arrows in Figures 8.6a, c

and 8.10). This seems to be a curious behaviour. On the one hand, the inhibition is so strong that wave termination takes place even without collision. On the other hand, a spontaneous activation is possible somewhat later in the same cells that could not be triggered earlier by activated neighboring cells. A very long-lasting, nondiffusible inhibitor must exist that provides a measure of the time since the last activation. Only when most of this inhibitor has decayed is spontaneous activation possible again. (The diffusible inhibitor is almost completely gone by this stage). If this inhibitor were diffusible, information on the location of the gap would be lost. The long-lasting inhibitor also has another function. Similar to the discussion in chapter 5, local accumulation of this inhibitor also forces pigment activation to move into a neighboring region even though this region is already poisoned by the diffusible inhibitor. By itself, the rapidly diffusing inhibitor would lead to spatially stable patterns, in contrast to observations. The pushing effect of the nondiffusible inhibitor and the poisoning effect of the diffusible inhibitor together may cause a situation in which activation can no longer be maintained. On the shell this leads to the spontaneous terminations of an oblique line.

Considering all these features, at least three inhibitions must be involved to generate a pattern of fine branching lines that terminate but re-trigger spontaneously in the gaps left by wave that disappeared before collision (Figure 8.8)

- (i) A very rapid and nondiffusible inhibition that causes activation to last for a short time interval only. It determines the thickness of the oblique lines. Its diffusion (if any) must be much smaller than that of the activator; otherwise no traveling waves would form.
- (ii) A rapidly diffusing inhibitor with a long time constant whose overall accumulation poisons a region. This causes wave termination when two waves approach.
- (iii) A very long lasting, nondiffusible inhibition responsible for the shift of activation despite the diffusible inhibitor. It also makes spontaneous activations possible again after an interval of nonactivation. This occurs preferentially in the gaps left by earlier waves.

Several of the shells display a second pattern at lower pigmentation levels. In Figures 8.6c and 8.8 this faint pattern maintains the character of the main pattern while in Figure 8.6f it has more of an area-filling character. It is not clear whether this background pattern results from a partially independent system that forms in a deeper layer of the shell, or whether pattern formation can proceed at such a reduced level. The systematic decrease of pigmentation levels in Figure 8.6c, for instance, suggests the second possibility. If this is true, the next question would be how pigmentation can spread with the same speed even though activation is reduced.

A system with three inhibitory effects has interesting features of its own and the resulting pattern elements can be recognized on the collection of shells given



Figure 8.8. Interrupted lines and branches - the involvement of three antagonists: *Lioconcha hieroglyphica* with a simulation in the background. A first antagonist is responsible for the duration of the pigment production, i.e., for the width of the oblique lines. A highly diffusible inhibitor (red) causes frequently a termination of one or both approaching waves before a collision occurs (red arrows). After the decay of a third long-lasting and nondiffusible inhibitor (blue), a spontaneous new activation is possible. This occurs preferentially in the gap left by two waves that terminated before a collision occurred (white regions; green arrows); [S88]

in Figure 8.6. That crossings become possible due to a diffusible inhibitor was discussed earlier. The third and nondiffusible inhibitor allows spontaneous activation to occur whenever no pigment was produced for a long period (Figure 8.9a). This is a feature clearly necessary for *L. hieroglyphica* (Figure 8.6c). If, in contrast, the second inhibitor is much less diffusible and has a longer time constant, neighboring regions are much less affected and pigmentation slowly fades away. The oblique lines have a sharp upper boundary but a fuzzy lower one (Figure 8.9b), a feature characteristic for *L. lorenziana* (Figure 8.6f).

Other specimens of *Lioconcha hieroglyphica* display triangles that have a fine structure of parallel lines (Figure 8.10). Of course, the mechanisms leading to one or the other pattern within the same species cannot be very different. This is underlined by an even higher degree of similarity at younger stages. One possibility for the generation of these fine lines, therefore, is a less effective extinguishing reaction.

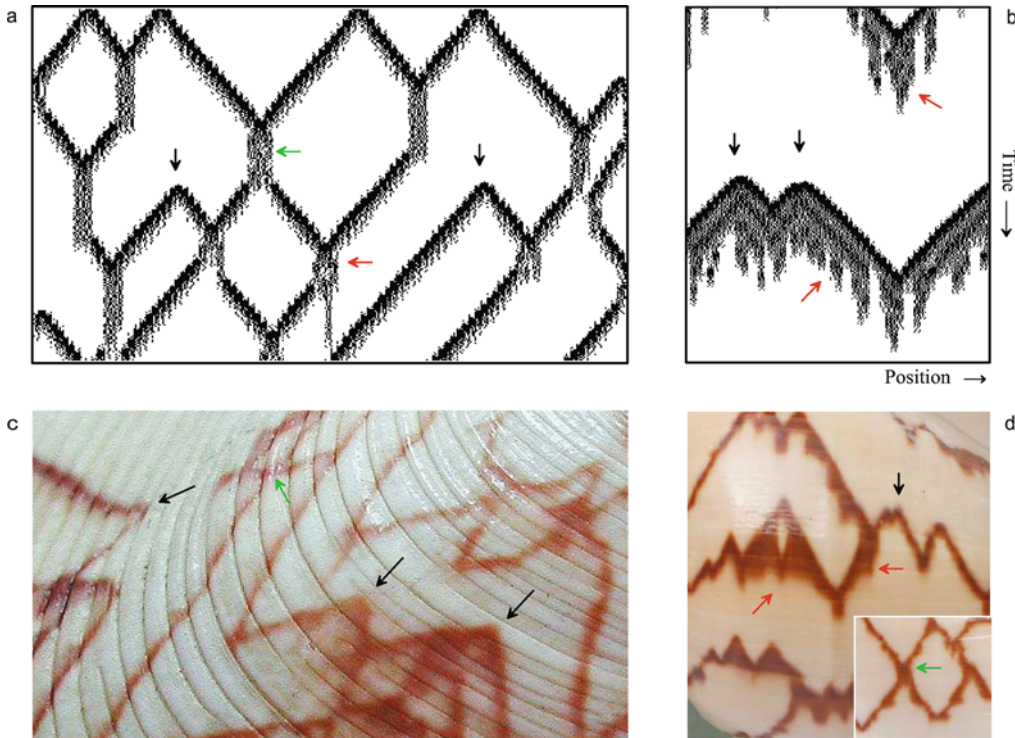


Figure 8.9. Patterns generated by a system with three inhibitions. (a) Formation of crossings (green arrows) and spontaneous initiations of two diverging lines (black arrows). Occasionally one of the waves does not survive the collision (red arrows). (b) Oblique lines with a sharp upper but a fuzzy lower border. (c, d) These pattern elements are displayed on *Tapes literatus* (c), *Cymbiola nobilis* (d), and other species of the *Lioconcha* family (Figure 8.6) [S89a, S89b]

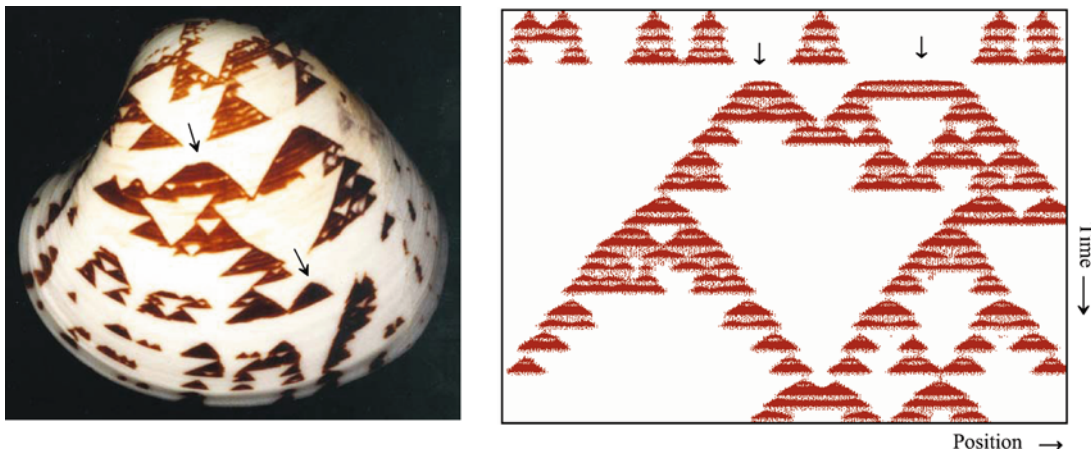


Figure 8.10. *Lioconcha hieroglyphica*: large triangles with a fine structure. The simulation is based on a two inhibitor model (Equation 5.4) plus a hormone for simultaneous termination of many triangles. Oscillations cause the fine structure of triangles [S810]

If sufficient activator remains when the extinguishing reaction is over, an immediate re-activation is possible. The periodic extinguishing reaction shapes the fine structure. Triangles result since each newly reactivated area is a bit larger due to survival and spread at the margins.

In the specimen shown in Figure 8.10, the lower edges of several triangles are formed at the same time. Obviously, termination of triangle formation can be a global event (see chapter 6). The simulation assumes the presence of a hormone produced by all pigment producing cells. An increase in this globally distributed hormone makes the system more sensitive to the actions of the extinguishing reaction. As discussed above, if, by chance, all activations terminate, a spontaneous new trigger occurs preferentially in the gap between two triangles since the concentration of the nondiffusible inhibitor with the long time constant is lowest in this region.

Although the main features are reproduced, there are still discrepancies. In natural patterns, many more parallel lines can appear in series, forming larger coherent triangles. This causes problems in the simulations since, due to the accumulation of the long-lasting inhibitor, the center is more sensitive to the extinguishing reaction. But the very pronounced feature of spontaneous activations in the gaps left by preceding triangles (Figure 8.10) indicates that such an inhibition must exist.

The occurrence of pigment termination at the outer edge without previous termination at the center suggests that the reaction causing the coincident termination of many triangles is much stronger than the usual oscillating reaction that causes the fine parallel lines. An interaction between two oscillating systems is conceivable. The first system would produce the fine lines. Interference with the second system is decisive where termination occurs (see Figure 4.14). Occasionally this can be so strong that regions at the center and at the tip of a triangle are affected simultaneously. In the next chapter, an alternative model for the generation of fine parallel lines with interruptions will be explored. At present it is difficult to determine whether these models will be helpful in overcoming the problems.

8.4 Breakdown as a failure of the enhancing reaction

Shells of *Cymbiola vespertilio* (Figure 8.11) typically have large but irregularly pigmented areas that are partially connected by oblique lines. The lower edges of these lines usually have a fuzzy appearance. In large pigmented regions a stripe-like modulation is frequently visible. These are very similar to the pattern elements discussed above for *L. hieroglyphica* (Figure 8.10). The pattern varies considerably among shells of the same species. To illustrate an alternative possibility, these patterns are simulated not by an explicit extinguishing reaction but by an enhancing reaction that brings the system close to a steady-state. This simulation uses the same interaction as the meshwork pattern shown in Figure 7.8b, although the patterns look very different. If this mutual stabilization causes a situation in which

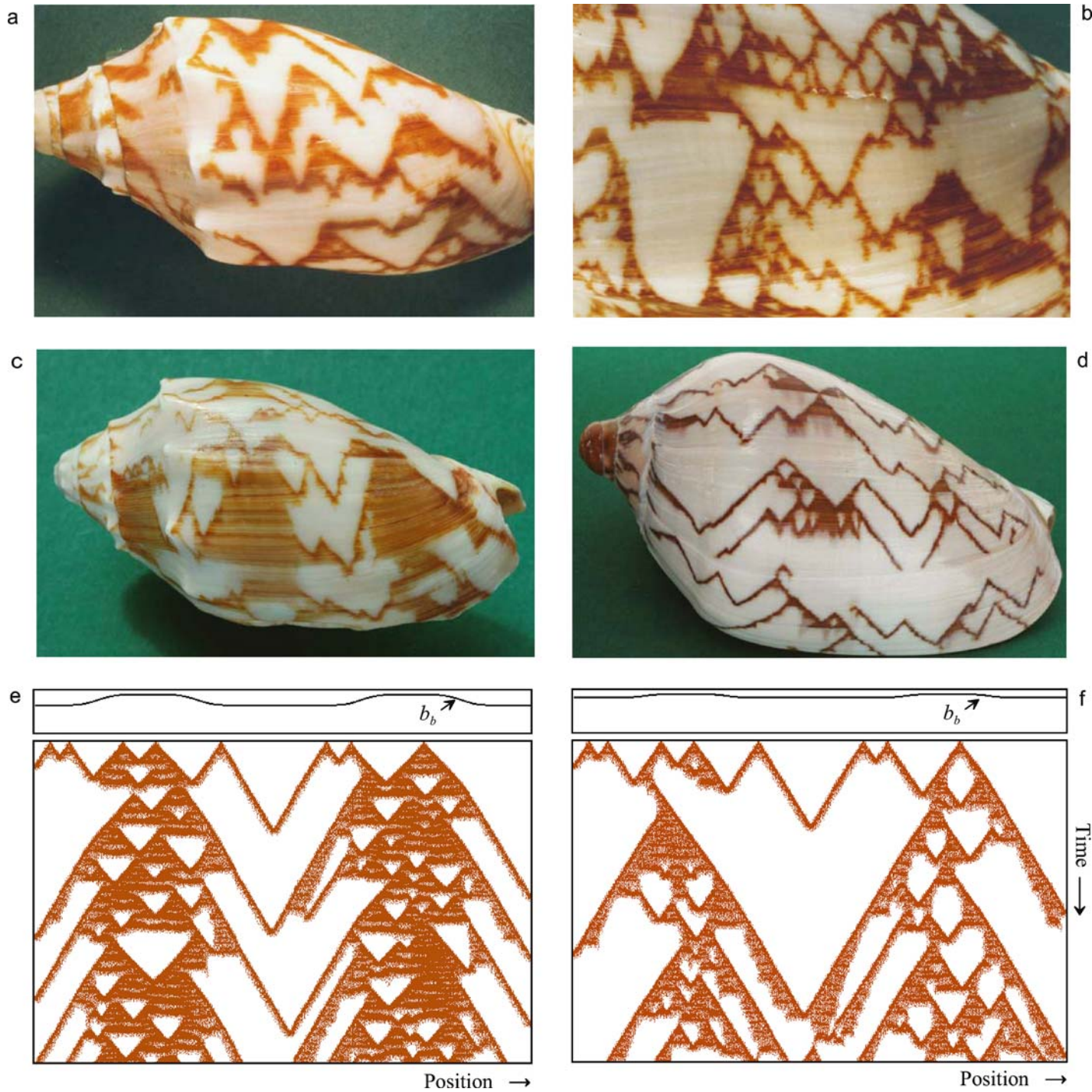


Figure 8.11. Irregular arrangement of large pigmented areas and isolated oblique lines. (a-c) *Cymbiola vespertilio*, (d) *Cymbiola nobilis*. (e, f) Model: the enhancing pattern is not restricted in space but is on the border of oscillations. Over large time intervals the mutual stabilization is sufficient to maintain a steady-state. Minor fluctuations can amplify over the course of time such that large scale breakdowns occur. If mutual stabilization is interrupted, it may take some time before it is established again. The simulations are performed by using equations 7.1 a-d. To simulate the two darker bands visible on most shells, substrate production in the pigment reaction is assumed to have some modulation (b_b) [S811e, S811f]

both the pigmentation and enhancing systems are on the border of maintaining a steady-state, minor fluctuations can become amplified over the course of time until a breakdown occurs. Since the enhancing reaction is assumed to spread more rapidly, this breakdown can occur over a large region due to the synchronization of these fluctuations. Pigmentation eventually survives at the borders of activated regions and form traveling waves. After variable time intervals the stabilization again becomes sufficient to allow a steady-state pigment production. The simulations include only the pigment and enhancement reactions (Equation 7.1 a-d, page 113). This model introduces a different possibility for large scale breakdown. The extinguishing reaction is replaced by the failure of a rapidly spreading enhancing reaction. As it has been discussed, this simple form is relatively parameter-sensitive. This sensitivity could be an origin of the large variation in the observed patterns. The mechanisms become more robust if additional regulatory processes are included. As discussed above, a global control or an additional long-lasting inhibition would be a possibility.

8.5 Conclusion

Triangles underline once more the intimate coupling between the extinguishing and enhancing effect of a modifying reaction. In the case of triangles, the extinguishing reaction is followed very rapidly by the enhancing reaction, causing rapid recovery after a large scale breakdown. In many mollusks shell growth is not a continuous process but occurs in phases, indicated by distinct growth lines. The frequent coincidence between these lines and the lower edges of the triangles (as seen in Figure 8.5b) suggests that the oscillations required for triangle formation may be part of a general physiological process taking place in the mollusks.



Parallel lines with tongues

The upper shell in Figure 9.1 is decorated with many fine parallel lines. This pattern suggests the same synchronous oscillations as described earlier (see Figure 3.4). However, at particular positions, the parallel lines are deformed into U- or V-shaped gaps. The pattern on the lower shell is based on the same principle; only the size and regularity of the gaps are different. On the upper shell the gaps are restricted to particular positions. On the lower shell two broad bands are nearly free of parallel lines while smaller gaps appear at more scattered positions. The shells belong to the species *Clithon ovalaniensis* (in older literature also termed *Neritina* or *Theodoxus ovalaniensis*). These small brackwater snails are frequent on shores around India and Sri Lanka and display an incredible richness of patterns. Grüneberg (1976) made a careful study of the polymorphism of these shells. He termed the deviation from parallel straight lines “tongues”. His article contains many examples of different types of patterns, transitions from one type to another, and pattern regulation after perturbation.

What is the basis of tongue formation? Obviously, a tongue results from the temporary suspension of otherwise almost synchronous oscillations. A non-pigmented area results that is re-pigmented from neighboring regions in which oscillations survived. The V- or U-shaped oblique lines that border the tongue indicate that traveling waves move into the region of interrupted oscillation, filling the gap. After the waves meet, normal oscillation usually continues, at least for a certain interval.

9.1 Survival using a precondition pattern

An important hint in determining the underlying mechanism comes from a background pigmentation that is visible between the parallel lines on some shells (Figure 9.2a). This is most clearly visible on parts of the shell of *Conus textile*



Figure 9.1. Parallel lines with tongues: Patterns on *Clithon* (or *Theodoxus*) *ovalaniensis*. The parallel lines indicate synchronous oscillations. These may be interrupted both in smaller (top) or larger regions (bottom). The resulting gaps, the “tongues”, are slowly filled by waves that have spread from regions in which the oscillation survived.

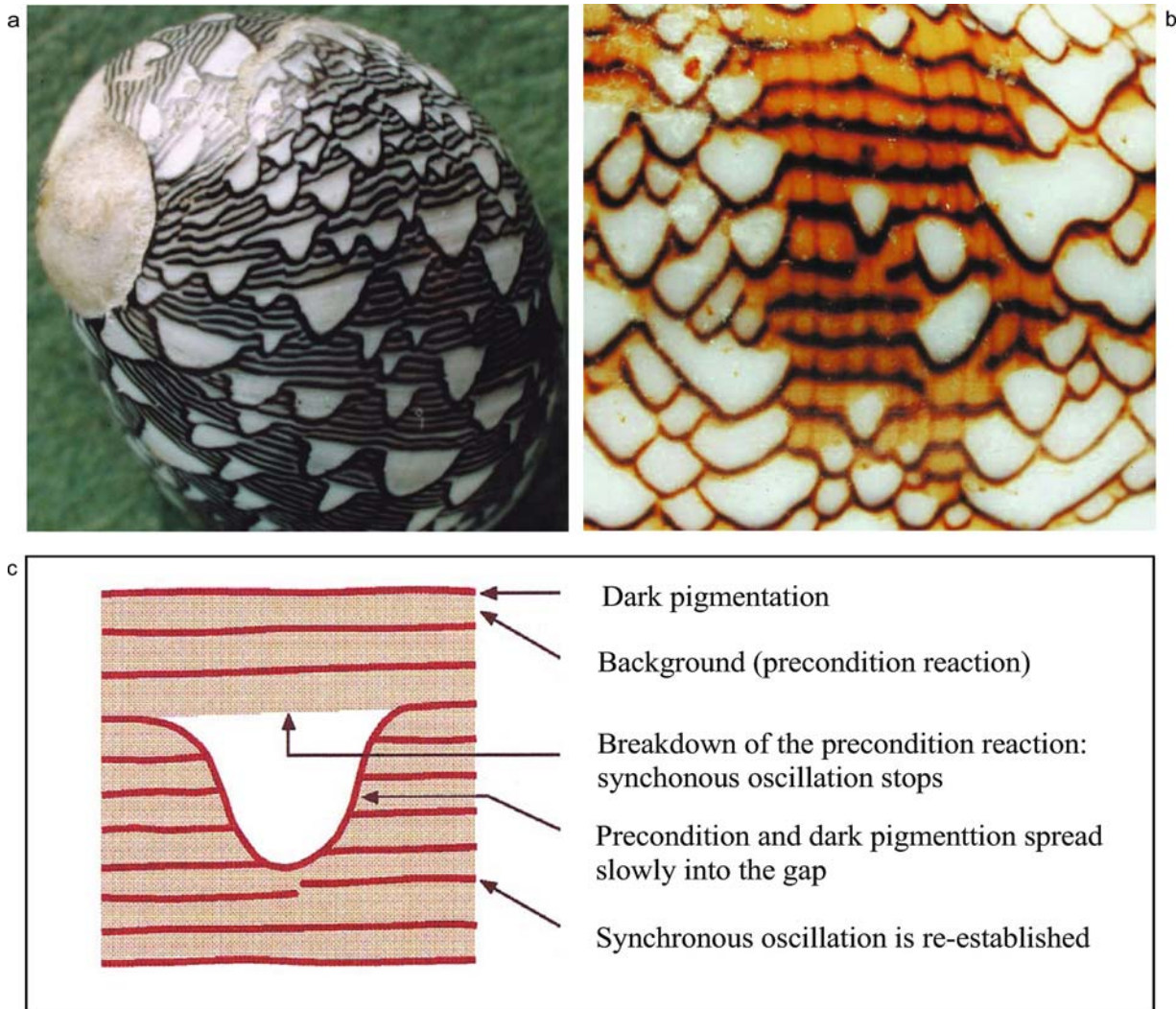


Figure 9.2. Temporary interruptions in synchronous oscillations causing gaps in a pattern of parallel lines - the tongues. (a) Details of *Clithon oualaniensis*. A grey background pattern is visible between the parallel lines. It is absent in the tongues but remains active for a while after the last pulse at the beginning of a tongue. As far as can be seen, the background system switches off abruptly, suggesting that its survival does not depend on the half life of a substance but results from the property of a non-linear reaction. (b) The same pattern elements in the more complex pattern of *Conus textile*. The beginning of a tongue is more variable in respect to the last unaffected line. In addition, finer oblique lines with branches are formed. (c) Schematic drawing of a possible mechanism that leads to the formation of tongues. Two systems are superimposed, an oscillating system that forms dark parallel lines and the background system. Oscillations are only possible when the background pattern is in an active state. The oscillating system has a role in maintaining the background system. Whenever an oscillation comes too late to refreshes background system that provides the precondition for the oscillations, a tongue would be formed

(Figure 9.2b) because of the light brown pigmentation that is absent in the tongues. Thus, three different levels of pigment production can be distinguished: a high level causing the dark pigmented lines, a lower level causing background pigmentation between the lines, and a zero level inside the tongues. Shells with three distinct levels of pigmentation have been discussed earlier (Figure 7.10 and 7.6) and a case has been made that this involves two pattern forming systems. The present pattern suggests that the background system acts as a precondition. It must be in the “ON” state in order for the pigmentation system to oscillate, forming the dark parallel lines. Whenever the precondition disappears locally, for whatever reason, the oscillations are interrupted (Figure 9.2c). It is worth mentioning that, in contrast to the shell shown in Figure 9.2a, the background pattern is not visible on the shell shown in Figure 9.1b. Reconstruction of the underlying mechanism of such shells would be much more problematic without hints from related specimens.

According to this view, the present pattern is similar to the complex patterns with branching discussed in chapter 7 in which the pigment system is modified by a second auxiliary system. The difference, however, is in the function of the auxiliary system. In the former case, branch and stalk formation result from a temporary shift of the pigmentation system from an oscillating mode to a temporary steady-state under the influence of an enhancing system: survival by locally elongated pigment deposition time. In contrast, the parallel lines discussed here result from a rapid re-triggering of the pigmentation system under the influence of a precondition system: survival by revival. Minor alterations in the mechanism are sufficient for this change. It may be that during the diversification of the species the need of an enhancing pattern became so strong that it began to act as precondition, i.e., that without the enhancing pattern no pigmentation was possible. While in branch formation the pigmentation system is (presumably) a precondition for the enhancing system, in the present pattern the background pattern between the lines indicates that the precondition can survive for a certain period without the pigmentation system. The coexistence of both parallel lines with tongues and oblique lines with branches on the shell of *Conus textile* (Figure 9.2b) suggests that a nearly continuous transition from one mode to another exists.

The simultaneous formation of two different elementary pattern elements, lines parallel and oblique to the growing edge, is another indication of the involvement of two patterning systems since they require conflicting sets of parameter values. Parallel lines result when synchronization is enforced by a strong coupling between neighboring cells (see Figure 3.4). In contrast, oblique lines are caused by a moderate diffusion of the self-enhancing agent combined with an almost nondiffusible antagonist. Slow infection of neighboring cells and thus traveling waves are the consequence (see Figure 3.7). This conflict disappears if two systems are involved. The precondition/background system spreads slowly causing the time-consuming filling of the tongue. In contrast, the rapid spread of the dark pigmentation system leads to a synchronization of the oscillations. Despite the fact that its spread is

rapid, it cannot invade the tongue immediately because the precondition must be re-established first.

If two patterns are superimposed, it is difficult to determine whether both reactions are directly involved in pigment production or, as was assumed in chapter 7, only one reaction produces pigment and the second causes its enhancement. In the case of parallel lines with tongues background pigmentation may result from a baseline activation required for the rapid triggering of the oscillating system. It is naturally restricted to regions in which the pattern is active.

9.2 Tongue formation: refresh comes too late

This section will describe several models but will conclude that the shape and arrangement of the tongues are very restrictive for possible mechanisms. In Figure 9.3a it is assumed that the substrate of the oscillating reaction is only produced when the background reaction is in an active state. The background pattern is, therefore, a precondition for the sustained oscillations and can spread slowly into nonactivated regions. A breakdown in the background pattern inter-

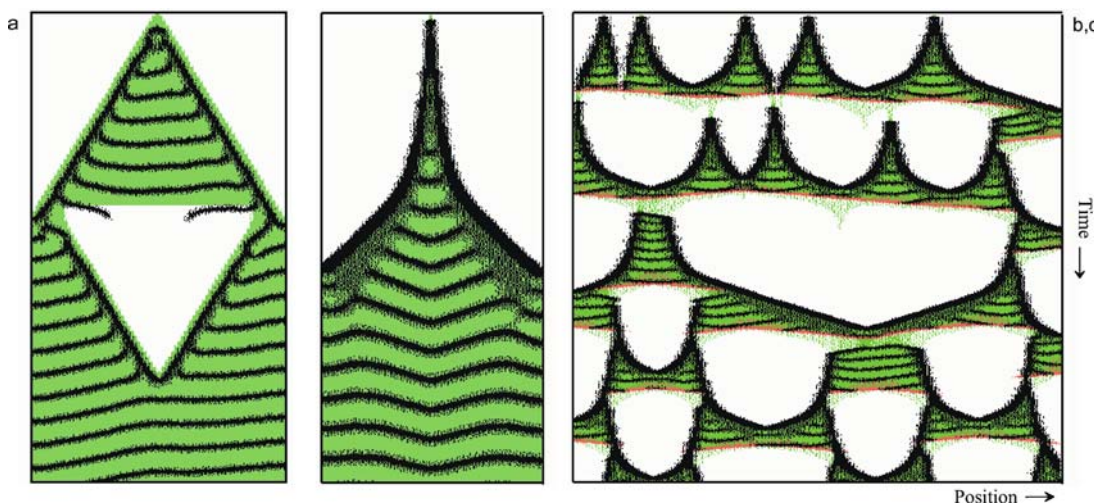


Figure 9.3. Models for parallel and oblique lines on a single shell. A background system (green) forms the precondition for the oscillating pigment-producing system (black). (a) The substrate of the oscillating pigment system is only produced when the background system is active. The near-synchronous oscillations are restricted to regions in which the precondition pattern is active, which leads to the parallel lines. The pigment system follows the slowly spreading background-precondition system. This leads to the dark oblique lines at the border to white regions. A gap in the precondition pattern - artificially introduced in this simulation - interrupts the oscillation and causes tongue formation. (b) An alternative possibility: the precondition pattern is required as a co-factor in the autocatalysis for pigmentation production [and not for the substrate production as in (a)]. (c) A model that can be excluded: Gaps in the background system are produced by a separate extinguishing system (red). This leads to interrupted pigment lines, in contrast to the natural patterns [S93a, S93c]

rupts the oscillations and leads thus to a gap in the patterns of oblique lines. Such a gap becomes re-activated from adjacent regions in which the background pattern survived. With such a model one would expect a certain time lag between the re-activation of the background pattern and the onset of dark pigmentation, since the substrate for the oscillatory reaction must be produced first. Grüneberg (1976) concluded from his microscopic inspection of *Clithon* shells that two pigmentation systems are involved: a leuco-system that produces a white pigment and a melano-system that produces the dark pigment. He observed that the activity of the leuco-system always precedes that of the melano-system. In Figure 9.1b a lighter pigmentation is clearly visible in front of the dark oblique lines and may be attributed to the second pigment system. In contrast, in *Conus textile* (Figure 9.2b) the spread into the gap is headed by a dark line, not by background pigmentation. This suggests that oscillations can be triggered immediately once the precondition is re-established. This is the case when the precondition pattern acts as a co-factor. Figure 9.3b provides a corresponding simulation in which, in addition, the background system is assumed to be nondiffusible. Its spread results from a cross-reaction with the oscillating system. Due to its rapid diffusion, the oscillating system spills over the ON-OFF border of the background system. The cross-reaction triggers activation of the precondition system and allows it to extend into a formerly nonactivated region. This system provides a better description of the acceleration of the waves, i.e., of the rounded shapes of the tongues.

What could lead to the breakdown of the background (precondition) reaction that initiates tongue formation? One possibility would be a separate extinguishing reaction that would produce gaps in the background pattern, similar to the simulation in Figure 7.3. However, the corresponding simulation (Figure 9.3c) shows clearly that this cannot be the case. The sudden de-activation of the precondition/background pattern would lead to interruptions in the parallel lines, a feature that is rarely observed on real shells. Or, conversely, the fact that the beginning of a gap is usually parallel to a dark line, suggests that the oscillatory system is involved either in maintaining or switching off the precondition system.

One could imagine that the oscillating system has an extinguishing influence on the background pattern, and that sometimes the background pattern does not survive. However, especially in patterns of the *Clithon* type, the background pattern remains in the ON-state for some time after the last oscillation (Figure 9.2a). If the oscillating system had an extinguishing influence, the probability of killing the background pattern would be highest when the oscillating system reaches its highest level. This is not the case. An overshoot of the antagonistic reaction is equally unlikely since this would also appear immediately after a pulse.

The lengthy survival of the background pattern suggests another mechanism: the oscillating system may act to refresh the background system. When a pulse of the oscillating system appears too late, the background system dies out along with the prerequisite for sustained oscillations. After each pulse, a type of race takes place to determine whether the next pulse will arrive early enough to accomplish the

Equation 9.1: parallel lines and tongues

The pigmentation system (an activator-substrate system) in which the precondition system c acts as co-factor:

$$\frac{\partial a}{\partial t} = s_c b a^{*2} - r_a a + D_a \frac{\partial^2 a}{\partial x^2} \quad (9.1.a)$$

$$\frac{\partial b}{\partial t} = b_b(x) - s_c b a^{*2} - r_b b + D_b \frac{\partial^2 b}{\partial x^2} \quad (9.1.b)$$

The precondition system (an activator-inhibitor system):

$$\frac{\partial c}{\partial t} = r_c \left(\frac{c^{*2}}{d + c_c b + s_e e} \right) - r_c c + D_c \frac{\partial^2 c}{\partial x^2} \quad (9.1.c)$$

$$\frac{\partial d}{\partial t} = r_c c^{*2} - r_d d + D_d \frac{\partial^2 d}{\partial x^2} \quad (9.1.d)$$

$$\text{with } a^{*2} = \frac{a^2}{1 + s_a a^2} + b_a \quad \text{and} \quad c^{*2} = \frac{c^2}{1 + s_c c^2} + b_c$$

The production rate of the metabolic product, the “poison”:

$$\frac{\partial e}{\partial t} = b_e(x) c - r_e e \quad (9.1.e)$$

$c_c b$ The substrate of the pigment system has an inhibitory influence on the precondition pattern. It is at its lowest immediately after a pulse and increases thereafter.

$s_e e$ The inhibitory influence of the poison on the precondition reaction. Both inhibitory effects bring the precondition system c to the border of stability.

$b_e(x)c$ The production rate of the poison depends on the presence of the background system. Either this production rate or the sensitivity s_e may be space dependent, producing large tongues at regular distances (Figure 9.5).

refresh. The mutual dependence of a steady-state system and an oscillating system may be illustrated with an analogy. The living state of a higher organism depends on a beating heart. But the heart can only beat if the organism is alive. If a single heart beat comes too late, the organism may die. Of course, if the organism dies for other reasons, the heart will also stop beating.

The repetitive breakdowns of the background system suggest that the latter is close to the border of stability. On some shells the tongues are arranged in a scattered way, on others they appear at more staggered positions. In the first case, their initiation may depend on statistical fluctuations. In the second case, however, a signal must be present that establishes a time interval between the close of one tongue and the trigger for the next tongue. During tongue formation a substance may be produced that stabilizes subsequent oscillations. Or, either the oscillating or background system may produce a poison that eventually terminates the precondition system early, making the next breakdown more likely. A decrease in oscillation frequency would have the same effect. Occasionally somewhat larger spacing between the parallel lines is visible at the onset of tongue formation (arrow in Figure 9.1b) which is an argument in favor of the latter possibility.

Modeling the generation and action of this tongue-inducing signal turns out to be very difficult. With most of the models envisioned poisoning would lead to longer and longer intervals between pulses (larger and larger distances between lines) until breakdown occurs. In terms of the heartbeat analogy, dying does not happen from one heartbeat to the next. In shells, however, breakdown is not announced by a preceding modification in the oscillating pattern, except for the possible minute increase in the line spacing mentioned above. The build up of the signal must proceed in a hidden way – a puzzling feature that was also required in earlier simulations (chapter 7). There does not seem to be any visible structure to the background pattern. If the probability for breakdown increases over time one would expect the background pigmentation to have a graded profile. This is, however, not the case.

The delay between the last pulse and the breakdown of the background system suggests that the refresh function lasts longer than the pulse width of the pigmentation reaction. Oscillations require a longer time constant for the antagonist (substrates or inhibitors). Thus, it is presumably the antagonist and not the activator of the oscillating pigmentation system that is involved in refreshing the background system.

The simulations in Figures 9.4 - 9.6 have been made with equation 9.1 (page 152) which assumes that the background/precondition system is generated by an activator-inhibitor interaction (green in the simulations). An additional long-lasting inhibitor functions as the poison mentioned above. It is produced whenever the precondition system is active. Its accumulation initiates tongue formation while its decline during the tongue-phase has a stabilizing effect on the background system and thus on the subsequent synchronous oscillations. The precondition system is close to the border of stability. Therefore, small changes that do not influence

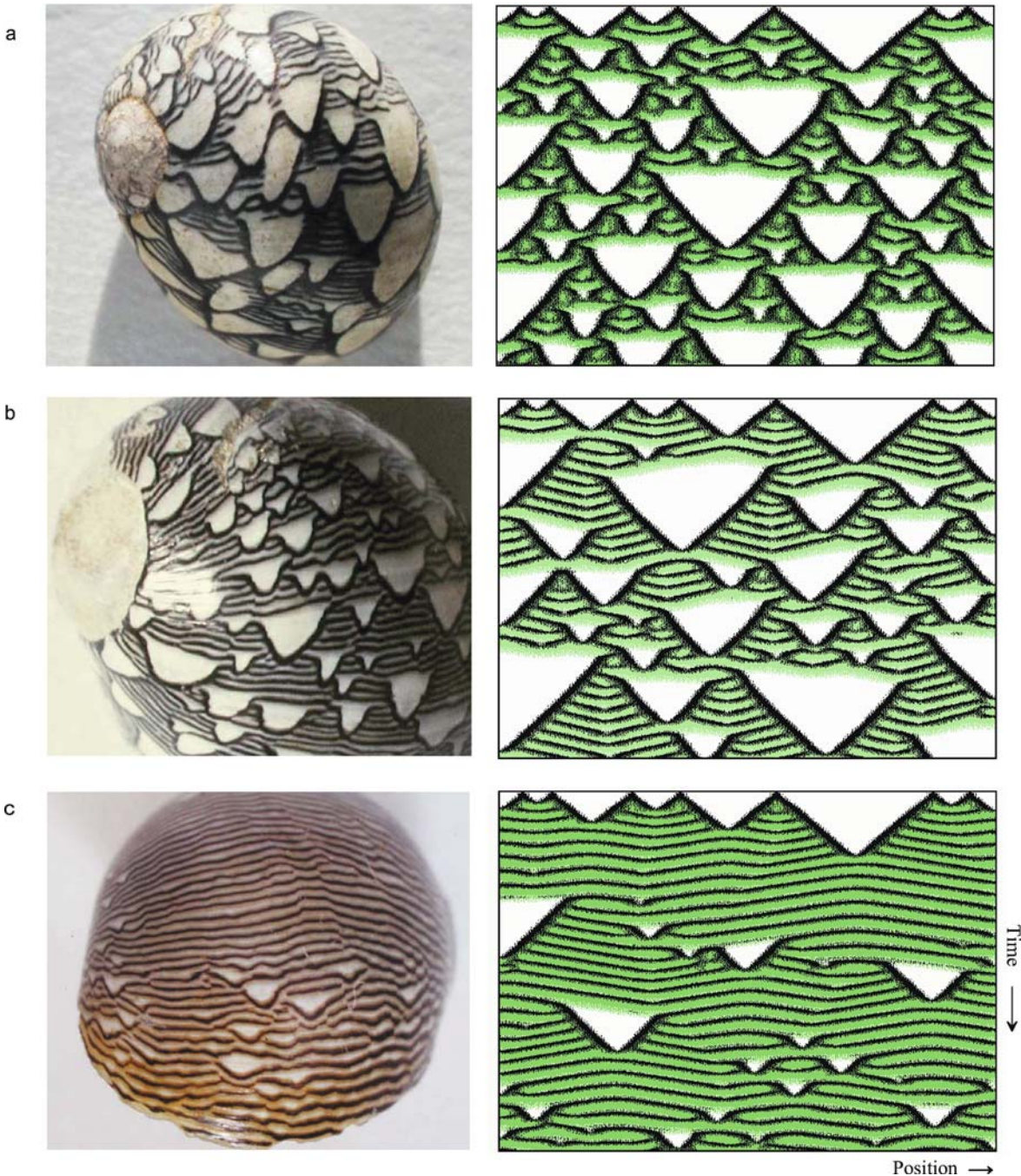


Figure 9.4. Parallel lines and tongues on *Clithon ovalaniensis*. Model: a precondition pattern (green) is required in order that synchronous oscillations can take place (dark parallel lines). The oscillating system, in turn, acts to maintain the precondition system in an active state. Due to the accumulation of an inhibitory metabolic product, a pulse may arise too late to maintain the precondition pattern. Nonpigmented regions emerge that are filled by traveling waves. The frequency of these tongues depends on sensitivity against the poisoning product. Calculated using Equation 9.1 [S94].

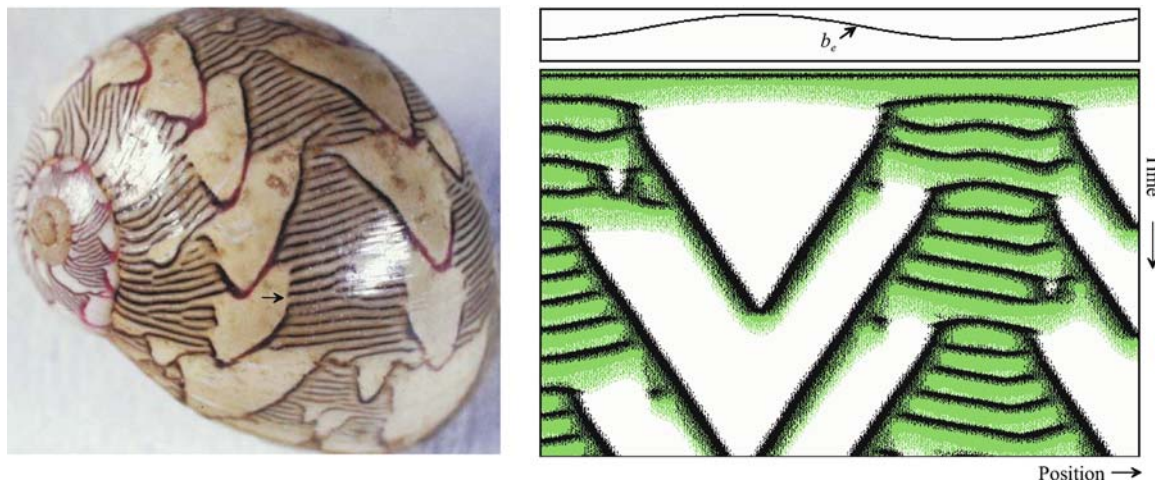


Figure 9.5. The restriction of the parallel lines into bands, a characteristic feature of many *Clithon* shells. These bands are frequently connected by oblique lines. Model: in regions with a higher production rate of the poison (b_e in equation 9.1), activation of the precondition pattern is too short to allow several oscillations. Isolated oblique lines (traveling waves) result that have their origin in one of the parallel lines. Note that these lines do not branch [S95].

the overall pattern are sufficient to switch it off. For the oscillating pattern (black), an activator-substrate interaction is employed. In the simulations an activator-substrate system is more convenient for both the spread into the tongues and for the synchronization. The precondition system is required as a co-factor for the oscillating system. The refresh function of the oscillating system has been implemented in the following way: In an activator-substrate model, the substrate concentration declines dramatically with each pulse and recovers slowly afterwards (see Figure 3.3, page 43). The substrate is assumed to have a cross-inhibitory influence on the precondition system. This inhibitory effect is, therefore, very low immediately following a pulse and increases thereafter. With time, the stability of the precondition system becomes more and more endangered. Either the next pulse arises in time to refresh the system or a sudden breakdown occurs. From this model it is expected that the breakdown would occur very shortly before the next pulse is due to appear, which agrees with the natural pattern.

In many specimens of *Clithon ovalaniensis* the parallel lines are restricted to three or five bands. These bands may be connected by oblique lines (Figures 9.5 and 9.1b). According to Grüneberg (1976), the separation of a coherent field of parallel lines into bands occurs more frequently in older animals. The bands are created by small tongues formed in rapid succession at particular positions (see Figure 9.1a) and becoming larger and larger. This process is not necessarily irreversible. In the model, isolated oblique lines suggest that the period in which the precondition is active is too short to host more than one pulse of the pigmentation system (Figure 9.5). In other shells, the inhibition is so strong that even these con-

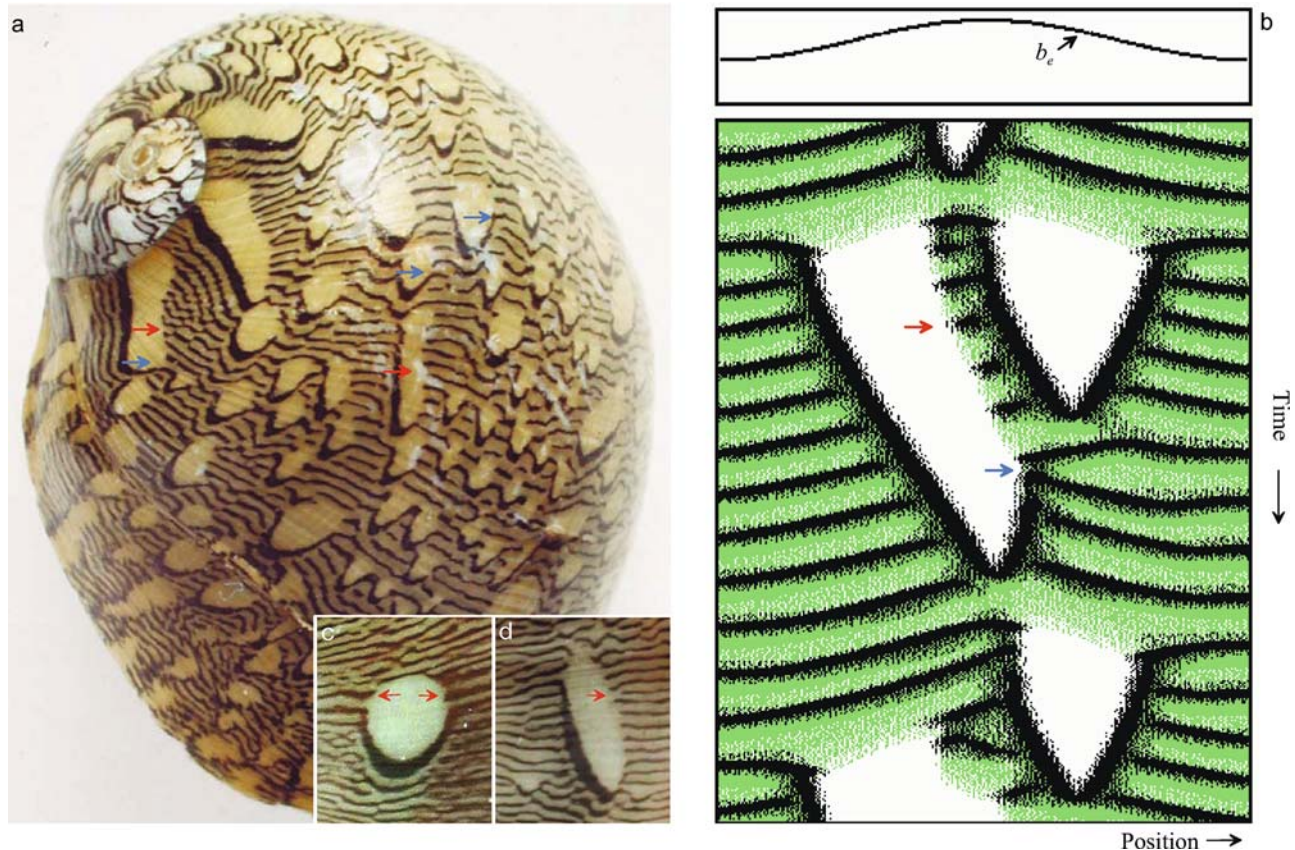


Figure 9.6. Enlarging and shifting tongues. (a) *Neritina virginea* (b) Model: after initiation of a tongue, the precondition system (green) may retract further on one or both sides, enlarging the oscillation-free area (red arrows). The reinforcing action of the pigmentation system has a counteracting influence. It allows a wave-like spread of the precondition system (dark oblique lines); the tongue shrinks. If the tongue enlarges on one side and shrinks on the other, its position shifts. A trigger of a traveling wave on the retracting side (blue arrows; V-like black line) causes the closure of the tongue. (c) A circular tongue results from a symmetrical enlargement that is followed by a symmetric closure. (d) A closeup of a shifting tongue [S96]

nctions are no longer formed. Examples were given earlier in another context (see Figure 1.10).

In *Clithon*, isolated oblique lines never branch, in contrast to the situation discussed in chapter 7. According to the model, the oblique lines in *Clithon* result from a wave-like spread of both the precondition *and* the pigmentation system. In contrast, in patterns with branching, the oblique lines are formed by one system only, while the occasional triggering of the second system may cause the formation of a branch (compare the black-green line in Figure 9.5 with the green dots along black lines in Figure 7.8). In the present pattern, when the precondition remains active for a long period, the result is not a branch but two successive lines or small patches of parallel lines (see Figure 9.7f).

After tongue initiation, the next dark pigmentation is usually involved in filling the gap immediately. Occasionally, however, several oscillations are required before a traveling wave (oblique line) is formed (arrows in Figure 9.5). The formation of a wave seems to be correlated with the spread of the oscillations, but it is difficult to determine which the cause is and which is the effect. On some shells a gap can be formed that enlarges on one side and shrinks on the other, thus moving across the field (Figure 9.6). This phenomenon is reproduced in the simulation. The moving gaps shed light on the interplay between the two systems. On its own, the precondition system may have a tendency to retract. In contrast, the pigmentation system has a tendency to move into the gap since more substrate is available there. Gap formation and its closure is thus a fight between the retraction of the precondition system and the spread of the oscillating pigmentation system, pulling the precondition system with it by its refresh function. Accordingly, the probability that enlarging or traveling gaps are formed increases with decreasing diffusion of the substrate; the attraction of the substrate that accumulated in the gap on the pigment-producing activation becomes lower. As in the real pattern only the lower side of such an oblique gap is bordered by a dark oblique pigmentation line. The shift of the gap terminates when the dark system is also triggered at the crumbling side, causing a bilateral spread into the gap and thus its closure.

9.3 Variations on a common theme

Related species display a large variety of patterns. Examples are given in Figure 9.7, although detailed modeling of this diversity has not been accomplished. The shell in Figure 9.7a displays round nonpigmented patches on a more densely pigmented background. This pattern may appear as a complement to the staggered dot pattern in Figure 5.11. However, the patches are less regularly arranged and have a dark crescent-shaped line at their lower edge. On closer inspection the impression of a background free of textures emerges because the parallel lines are extremely fine and very close to each other. The shell in Figure 9.7b displays a similar pattern with a somewhat larger spacing between the lines. The white drops are tongues and the dark crescents result from an overshoot of the pigment reaction. The steps that lead to circular tongues are clearly visible in Figure 9.6c: a symmetrical enlargement that is followed by a symmetrical shrinking.

One remarkable feature of the shell in Figure 9.7a is the long faint shadows under the white patches (arrow) which are distinctly different from the overshoot phenomenon. This suggests that when pigment deposition is interrupted, background pigmentation becomes enhanced for an interval at least as long as the nonpigmented period. This enhancement suppresses the onset of tongue formation and is thus responsible for the staggered position of the white patches. New patches can appear only outside these shadows. According to the model, the shadows result from the stabilizing influence of the gap on successive oscillations. In the example



given in equation 9.1 the stabilization is caused by a decline in poison concentration during tongue formation. Since a shadow does not change its lateral extension over the course of time, the poison must be nondiffusible. To obtain the rounded shape in the upper parts of the patches, the breakdown of the background pattern must retract, similar as seen on the shells shown in Figure 9.6). Moreover, the nearly circular shape of the patches requires the breakdown to spread with about the same speed as the re-population of the gaps. Since both processes presumably depend on different mechanisms, these equivalent speeds are nontrivial.

In Figure 9.7c the oblique lines that border the tongues are much broader, suggesting either a strong overshoot or an active process (see Figure 7.5a). In Figure 9.7d, only the oblique lines that border the tongue are darkly stained, while the closely spaced parallel lines are pale. The oblique and parallel lines in Figure 9.7e have also different colours, black and red. In *Puperita pupa* (Figure 9.7f) two oblique lines frequently appear close together, followed by a larger region free of pigment. In terms of the model, this suggests that the precondition reaction is active for a relatively short period in which only two pulses of the oscillating pattern can fit. Transitions into patches with parallel lines are also clearly visible. In the model this would occur when the precondition pattern is active for a longer period.

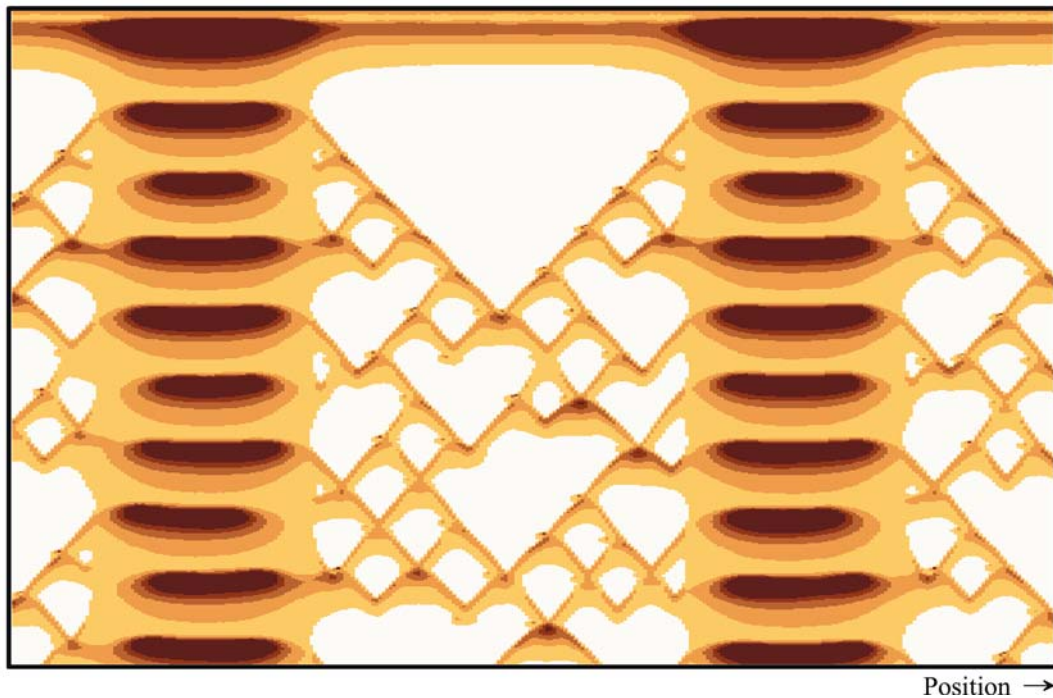
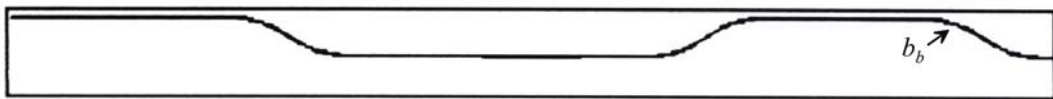
9.4 *Conus textile*: tongues and branches on the same shell

The highly poisonous snail *Conus textile* forms much larger shells (up to 7cm) that are decorated with similar pattern elements. Some examples were given earlier (Figures 1.12 and 9.2). Figure 9.8 shows another specimen. The dark parallel lines, the light brown background pigmentation and the tongues are usually restricted to two bands. Between these bands fine lines are formed that occasionally branch. Therefore, these patterns provide a link between the complex branching patterns discussed in chapter 7 and the parallel lines with tongues discussed above. The occurrence of branches suggests the use of the model developed earlier (equation 7.1). In the simulation the dark bands with parallel lines and the oblique lines with branches are reproduced using this model (Figure 9.8).

What are the common features in this and the *Clithon* patterns, and what causes the differences? According to the models, one difference is the pattern that oscillates. In the *Clithon* model, the pigmentation pattern oscillates while the auxiliary (precondition) pattern remains in a steady-state as long as no tongues are formed. The latter pattern provides the ingredients for a rapid re-trigger. In the branching model used for the simulation of *Conus textile* (Figure 9.8) the reverse is true. The pigment pattern may obtain a steady-state while the auxiliary (enhancing) pattern oscillates. This leads to large pigmented areas with parallel stripes of enhanced



Figure 9.7. Variation in patterns of the *Clithon*



pigmentation. If the pigment pattern does not remain in a steady-state, traveling waves are formed and the periodic enhancement causes branching. In the *Clithon* model, oblique lines result from joint waves of both the pigment and auxiliary system. No branches can be formed since, during this spread, the auxiliary pattern is already in the ON-state. The background pigmentation results from residual activation of the pigment system by the auxiliary system. In contrast, the background in the branching model results directly from the pigment reaction. This provides a rationale for the much stronger background pigmentation on shells like *Conus textile* or *Conus episcopus*, (see Figure 7.10) in contrast to shells of the *Clithon* type.

As shown in Figure 9.8 the branching model correctly describes the parallel lines, which are much thicker than the oblique lines. This results from the influence of the enhancing pattern which elongates the period of pigment deposition. This was a necessary condition for branch formation. In this view, branch formation and the thick lines are two manifestations of the same interaction.

On the other hand, *Conus textile* displays many features that cannot be explained by the branching mechanism but suggest the actual mechanism is closer to that developed for *Clithon*. For instance, the oblique lines have variable thickness and degrees of pigmentation. This is most obvious when an oblique line has a light-brown band at its lower edge. The dark parts of these lines are distinctly thicker than lines without these bands (compare the two lines marked by a double arrow in Figure 9.8). This suggests that joint waves from the pigmentation and the auxiliary system are possible and that the trigger of the latter does not necessarily lead to branch formation. It is very remarkable that increased intensity does not lead to waves with a higher velocity.

Furthermore, branch formation is not the only mode of generating new waves within the white region (see symbols in Figure 9.8). Occasionally the light-brown background pattern is triggered and remains active long enough to trigger the dark system again (arrowhead and arrow). Therefore, *Conus textile* shows both modes of survival on the same shell: elongation of lifetime (branching) and revival (a rapid re-trigger *via* a second system). Often the trigger of the oscillating system occurs somewhat earlier at the border between a white and light-brown region (asterisk). Thinner light-brown bands cause the next trigger to occur sooner (arrow 2). Obviously, proximity to a nonpigmented region can accelerate the next pulse of the oscillating system.



Figure 9.8. Tongues and branches on the same shell: *Conus textile*. The simulation uses a pigment and an enhancement system (equation 7.1a-d). The first produces the background or the traveling wave patterns. Whether the system is in a steady-state or burst mode depends on the rate of substrate production b_b . The enhancing pattern is responsible for the dark lines on top of the background pattern and for the branching of oblique lines, depending on whether the pigmentation system is in the steady-state (high b_b or in the traveling wave mode (lower b_b). For arrows see text; [S98]

The background reaction cannot spread on its own. On the contrary, it may rapidly retract (arrowhead), a situation analogous to that of *Clithon* (Figure 9.6). The white triangles or tongues are described much better by the *Clithon* model and retraction is certainly an integral part of tongue formation in *Conus textile*.

The tongues in *Conus textile* are much less regularly arranged than in *Clithon*. This makes it difficult to design models for their initiation. Moreover, this initiation does not have a strict phase relation with respect to the last dark line. The breakdown may also appear immediately after the dark line. Therefore, in contrast to *Clithon*, the dark lines in *Conus textile* presumably serve no maintenance function.

The light-brown background is also modulated by stripes parallel to the direction of growth which may resolve into a fine meshwork-like pattern (arrow 3). In other specimen (see Figures 7.1e and 1.12) longer nonpigmented phases may give rise to branches in quick succession, creating a fine bubble-like pattern. The similarity between these patterns and the complex patterns discussed earlier (Figure 7.12) is easily recognizable.

9.5 Missing elements, missing links

The models developed in this book are certainly only first approximations. Many details of the patterns have not been described. Chains of white drops (Figure 7.6), irregular alternations between dark and white patches (Figure 1.9) and the transition into fine meshworks (Figure 7.12) are examples. However, these problems are discovered only when a theory is available. The models help to uncover elements that are not fully understood, and discrepancies become apparent only when models are formulated mathematically.

Figure 9.9 contains a collection of shell patterns that may stimulate further model building. *Conus marmoreus nigrescens* (Figure 9.9a) displays the same white drops on a black background as *Conus marmoreus* (Figure 7.3). However, the black region has a substructure of closely packed parallel lines and the white drops are unmistakably analogous to tongues. It is thus a missing link and suggests that the formation of white drops in *Conus marmoreus* (Figure 7.3a) and of tongues in *Clithon* may have the same basis. Unification of the corresponding models is certainly the biggest challenge in the future modeling of shell patterns.

Conus nicobaricus (Figure 9.9b) shows fine branching lines superimposed with cloudy patches of dark black-blue pigmentation. As far as one can observe through this cloud, the number of branches but not the thickness of lines increases tremendously in these regions. The nonlinear models employed in the simulations tend to produce regions of all-or-none activations with sharp demarcations. How do the cloudy patches arise? How do they influence the probability of branching?

Conus vicweei (Figure 9.9c) displays the usual oblique lines but the lines are white on a pigmented background. Does this result from a normal reaction that either causes the deposition of white pigment or suppresses (extinguishes!) the

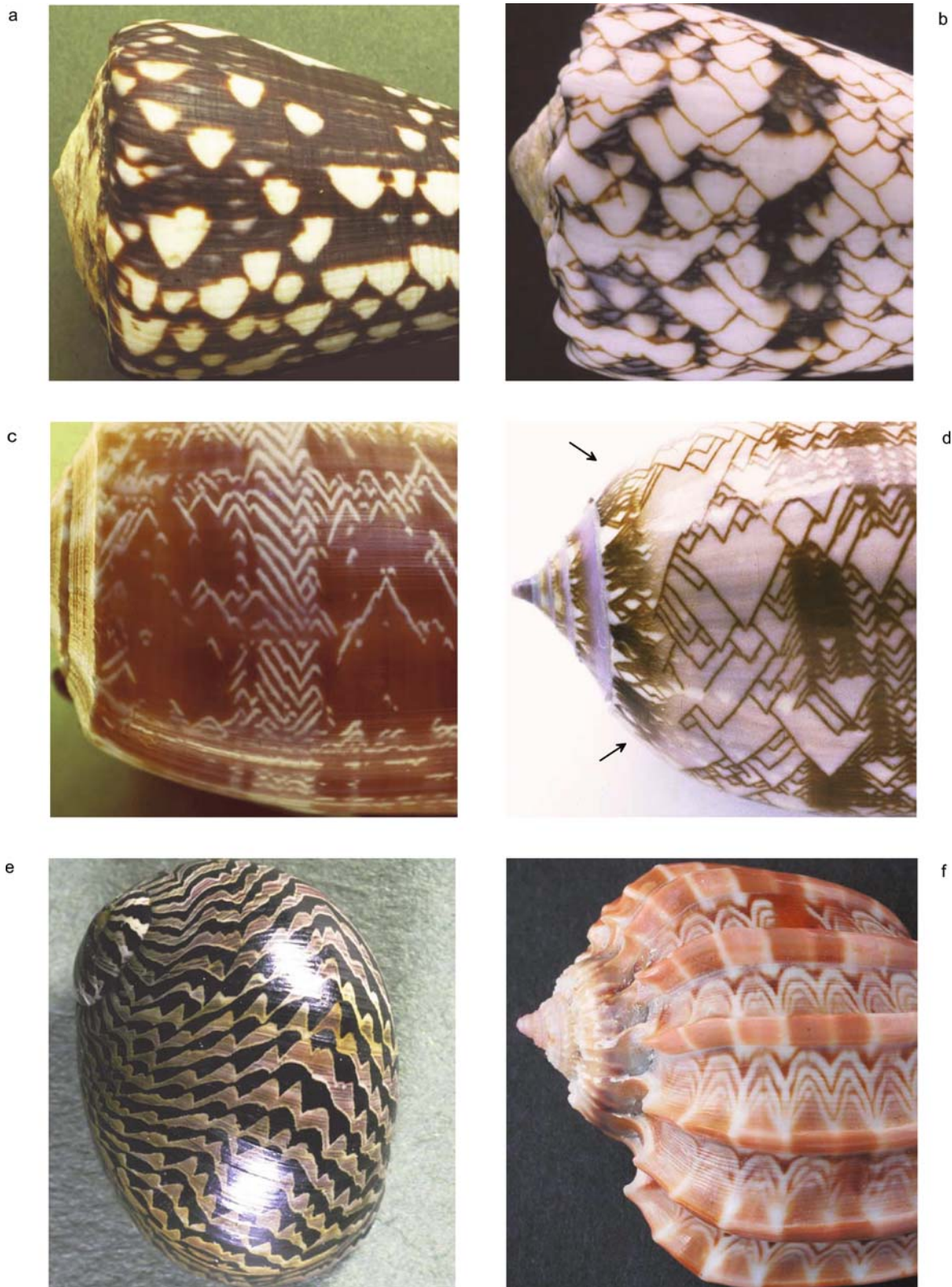


Figure 9.9. Some of the many patterns that await modeling

pigmentation reaction locally? Alternatively, are reactions conceivable in which the self-enhancing process leads directly to a traveling local collapse of pigment production?

Many specimens of *Oliva porphyria* have a second pattern in the background. This is most clearly seen between the two arrows in the specimen in Figure 9.9d. The two patterns merge into each other without much interference. Normal background pigmentation obviously results from this underlying system. Is this caused by another layer of cells in the mantle gland that behaves similarly but is partially uncoupled? Furthermore, what is the origin of the columns of densely packed parallel lines on this shell? Does this have a similar basis to the dense branching underneath the dark patches in Figure 9.9b?

Other patterns await modeling as well. In *Neritina communis* (Figure 9.9e) the oblique lines have a zigzag pattern. How does this arise? Is it a smoothed chain of triangles? The last example, *Harpa major* (Figure 9.9f), shows a regular pattern of parallel ribs. After each rib a space-dependent oscillatory pigment deposition takes place. The first stroke is the most vigorous; further strokes are more damped until a transition into steady-state pigmentation occurs. Soon after this stage is reached, a new rib is formed. This oscillation is modulated by a spatial pattern, showing that more complex superpositions of stable and oscillating patterns can be realized. These examples certainly do not exhaust the list of shells yet to be simulated but it is hoped that they will stimulate further attempts.

Epilogue

Stable patterns, oscillations and traveling waves are the basic building blocks of shell patterns. These phenomena have a common base: the coupling of self-enhancing and antagonistic reactions.

Shell patterns have been used to demonstrate the general principles of mechanisms that generate stable patterns, oscillations and traveling waves. By comparing these mechanisms with everyday experiences such as pattern formations caused by erosion, waves of influenza or the flickering of a candle, the universality of these principles has been illustrated. Of course, shell patterns are only a very special case of pattern formation in space and time. The same mechanisms also play a decisive role in more important biological and nonbiological processes. The development of higher organisms from a single cell, the fertilized egg, requires a cascade of at least temporarily stable patterns. Traveling waves are crucial for the organized contraction of the heart muscle. Neither thinking or sensing would be possible without nerve pulses that travel along a nerve fiber. The patterns on sea shells may not be convenient for investigating the molecular basis on which pattern formation is based. But their unique feature of maintaining a historical record and their incredible diversity recommend shell patterns as a natural picture book for study-

ing dynamic systems. I hope that a reader coming across a shell will start to read the pattern just like a fascinating book.

In his novel “Doctor Faustus”, in the same chapter quoted in the preface, Thomas Mann describes Jonathan Leverkühn’s thoughts on the creative irregularity and beauty of frost flowers. He speaks about the “*creative dreaming of Nature*”. And further, “... *what occupied him was the essential unity of the animate and so-called inanimate nature, it was the thought that we sin against the latter when we draw too hard and fast a line between the two fields, since in reality it is pervious and there is no elementary capacity which is reserved entirely to the living creature and which the biologist could not study in an inanimate subject.*”¹

In this book I have tried to listen to the creative dreaming of nature and I hope I have contributed a little to a reconciliation between the animate and inanimate worlds.

The remaining chapters of this book will deal with the generation of the three-dimensional shell shape - an essay kindly provided by Przemysław Prusinkiewicz and Deborah R. Fowler -, with the handling of the computer programs provided on the CD enclosed and with pattern-forming processes during development of higher organisms.

¹ Thomas Mann, Doctor Faustus, translation by H. T. Lowe-Porter, Penguin Books, p. 23



Figure 10.1. Trophon shell. Inspiration for this sculpture-like view came from shell photographs by Andreas Feininger (see Feininger and Emerson, 1972)

Shell models in three dimensions

Przemyslaw Prusinkiewicz and Deborah R. Fowler[†]

Department of Computer Science
The University of Calgary

[†]now at Hi Tech Toons

Inspired by the models of pigmentation patterns developed by Dr. Meinhardt, we pursued a further goal — to create a comprehensive model of seashells that would incorporate these patterns into three-dimensional shell shapes. Our motivation was twofold. On the one hand, in the absence of a formal measure of what makes two forms and patterns look alike, it is often necessary to rely on visual inspection when comparing models with nature (Prusinkiewicz, 1994). Realistic presentation adds credibility to such comparisons by removing potentially misleading artifacts. On the other hand, we consider visual simulations a celebration of nature’s beauty similar to painting, sculpture, or photography (Figure 10.1). Our results are described here according to the paper (Fowler *et al.*, 1992).

10.1 Mathematical descriptions of shell shape: a brief history

The essence of shell shape is captured by the logarithmic spiral, characterised mathematically by Descartes in 1638 (see Thompson, 1952, page 754) and first applied to describe shell coiling by Moseley (1838). By the beginning of the twentieth century, the logarithmic spiral was observed in many artificial and organic forms (Cook, 1914). Thompson (1952) presented careful measurements of a wide variety of taxonomic and functional shell types, and showed their conformity with the logarithmic model.

The application of computers to the visualisation and analysis of shells was originated by Raup. In his first paper devoted to this topic, he introduced two-dimensional plots of longitudinal cross-sections of shells as a blueprint for manually drawing shell forms (Raup, 1962). Subsequently, he extended his model to three dimensions (Raup and Michelson, 1965) and visualised shell models as stereo pairs to emphasise the three-dimensional construction of the shells (Raup, 1969). His models were plotted as a collection of dots or lines.

In the pursuit of realistic visualisations, Kawaguchi (1982) enhanced the appearance of shell models using filled polygons, which represented the surface of shells more convincingly than line drawings. Similar techniques were used subsequently by Oppenheimer (1986), and Prusinkiewicz and Streibel (1986b). A different approach was adopted by Pickover (1989, 1991), who approximated shell surfaces using interpenetrating spheres. They were placed at carefully chosen distances from each other and rendered using periodically altering colours to create the appearance of a ribbed surface with stripes.

Recent work on the modelling of shells has been characterised by an increasing attention to detail. Illert (1989) introduced Frenet frames (see Bronsvoort and Klok, 1985; do Carmo, 1976) to precisely orient the opening of a shell. His model also captured a form of surface sculpture. Cortie (1989) allowed independent tilting of the opening in three directions, presented models with apertures defying simple mathematical description, and extended the range of surface ornamentations captured by the model.

10.2 Elements of shell shape

Our model of shell geometry is similar to that introduced by Raup and developed further by Cortie. The underlying ideas, however, were already present in the work of Thompson (1952, chapter XI). We quote his observations in a slightly edited form.

The surface of any shell may be generated by the revolution about a fixed axis of a closed curve, which, remaining always geometrically similar to itself, increases its dimensions continually. [...] Let us imagine some characteristic point within this closed curve, such as its centre of gravity. Starting from a fixed origin, this characteristic point describes an equiangular spiral in space about a fixed axis (namely the axis of the shell), with or without a simultaneous movement of translation along the axis. The scale of the figure increases in geometrical progression while the angle of rotation increases in arithmetical, and the centre of similitude remains fixed. [...] The form of the generating curve is seldom open to easy mathematical expressions.

The construction of models derived from this description is presented below.

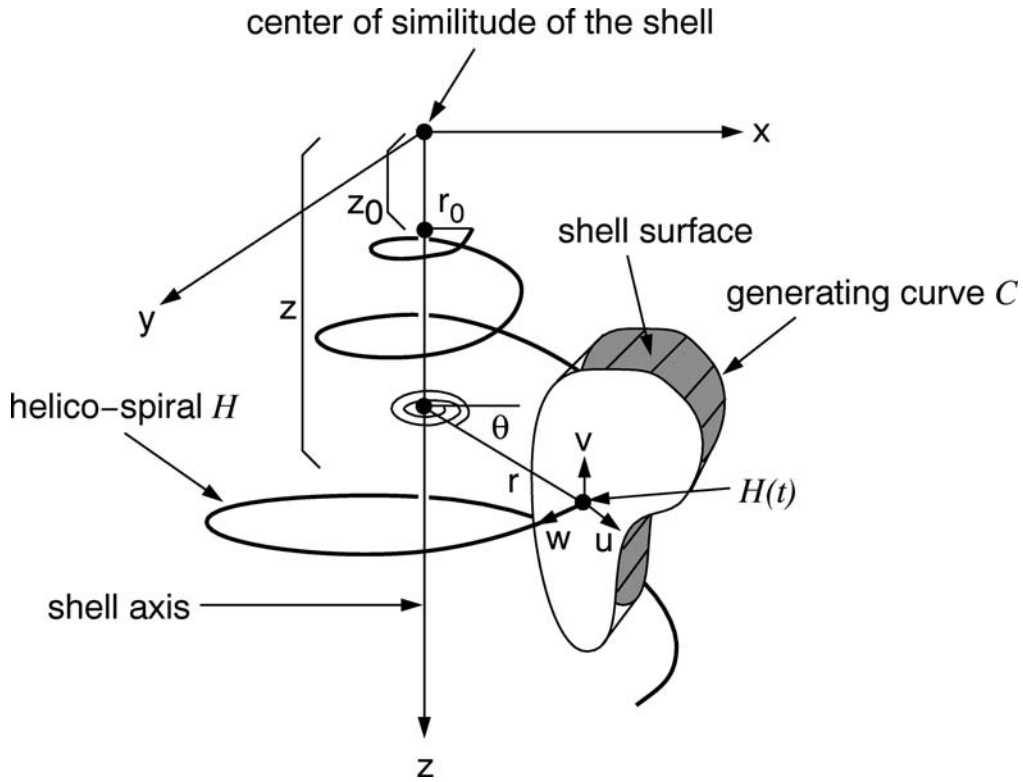


Figure 10.2. Construction of the shell surface

10.3 The helico-spiral

The modeling of a shell surface starts with the construction of a logarithmic (equiangular) helico-spiral \mathcal{H} (Figure 10.2).

In a cylindrical coordinate system (shown in Figure 10.2 as embedded in the Cartesian xyz system) it has the parametric description (Coxeter, 1961):

$$\theta = t, \quad r = r_0 \xi_r^t, \quad z = z_0 \xi_z^t. \quad (10.1)$$

Parameter t ranges from 0 at the apex of the shell to t_{max} at the opening. The first two equations represent a logarithmic spiral lying in the plane $z = 0$. The third equation stretches the spiral along the z -axis, thus contributing the helical component to its shape.

Distances r and z are exponential functions of the parameter t , and usually have the same base, $\xi_r = \xi_z = \xi$. As a result, the generating helico-spiral is self-similar, with the center of similitude located at the origin of the coordinate system xyz . Given the initial values θ_0 , r_0 , and z_0 , a sequence of points on the helico-spiral can be computed incrementally using the formulae:

$$\begin{aligned} \theta_{i+1} &= \theta_i + \Delta t = \theta_i + \Delta\theta, \\ r_{i+1} &= r_0 \xi_r^{t_i} \xi_r^{\Delta t} = r_i \lambda_r, \\ z_{i+1} &= z_0 \xi_z^{t_i} \xi_z^{\Delta t} = z_i \lambda_z. \end{aligned} \quad (10.2)$$

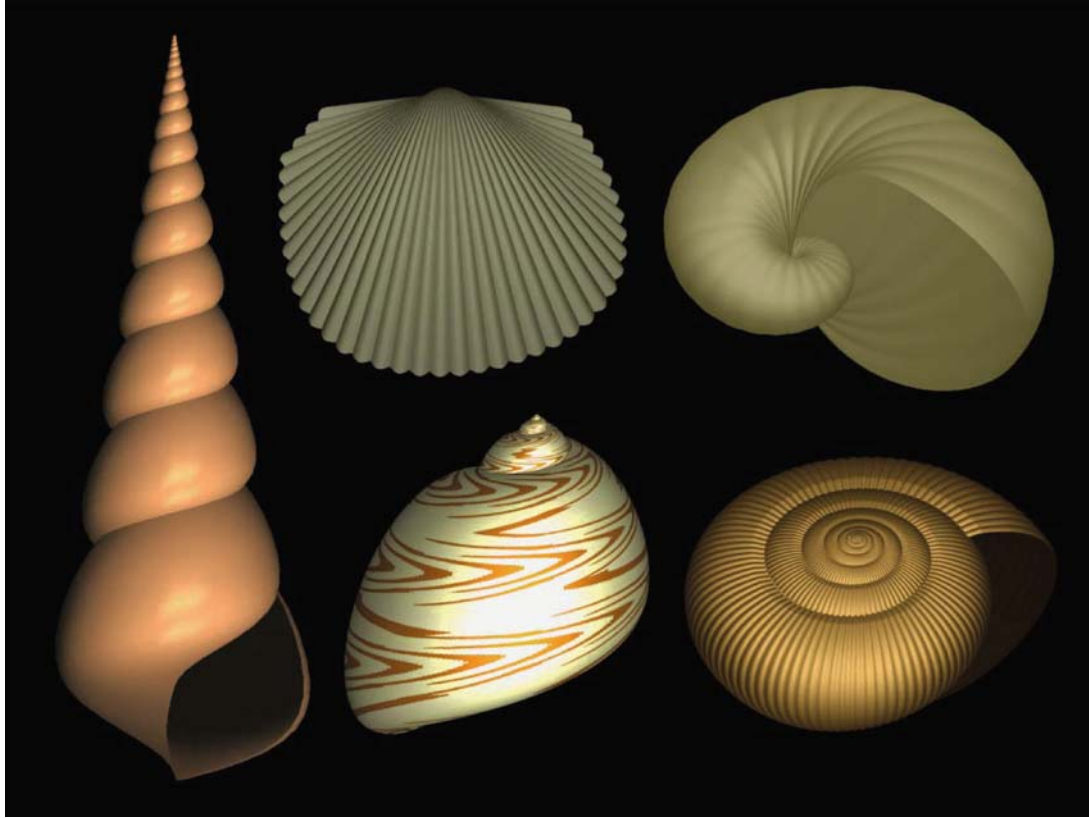


Figure 10.3. Variations in shell shape resulting from different parameter values characterising the helico-spiral. Leftmost: turbinate shell ($z_0 = 1.9$, $\lambda = 1.007$). Top row: patelliform shell ($z_0 = 0$, $\lambda = 1.34$) and tubular shell ($z_0 = 0.0$, $\lambda = 1.011$). Bottom row: spherical shell ($z_0 = 1.5$, $\lambda = 1.03$) and diskoid shell ($z_0 = 1.4$, $\lambda = 1.014$). Values of $\lambda = \lambda_r = \lambda_z$ correspond to $\Delta\theta = 10^\circ$.

While the angle of rotation θ increases in arithmetic progression with the step $\Delta\theta$, the radius r forms a geometric progression with the scaling factor $\lambda_r = \xi_r^{\Delta t}$, and the vertical displacement z forms a geometric progression with the scaling factor $\lambda_z = \xi_z^{\Delta t}$. In many shells, parameters λ_r and λ_z are the same. Variations in shell shape due primarily to different parameter values characterising the helico-spiral are shown in Figure 10.3. They correspond closely to the shell types identified by Thompson (Thompson, 1961, page 192).

The parameters introduced in this section provide a convenient means for generating the logarithmic helico-spiral. Other mathematically equivalent families of parameters have been described in the literature (for example, see Cortie, 1989, Lovtrup and Lovtrup, 1988).



Figure 10.4. Variations in shell shape resulting from different generating curves. From left to right: turreted shell, two fusiform shells, and a conical shell.

10.4 The generating curve

The surface of the shell is determined by a generating curve \mathcal{C} , sweeping along the helico-spiral \mathcal{H} . The size of the curve \mathcal{C} increases as it revolves around the shell axis. The shape of \mathcal{C} determines the profile of the whorls and of the shell opening. In order to capture the variety and complexity of possible shapes, we construct the generating curves from one or more segments of Bézier curves (Foley *et al.*, 1990). This method makes it easy to design an almost unrestricted range of generative curves using an interactive three-dimensional modelling program. The impact of the generating curve on the shape of a shell is shown in Figures 10.4 and 10.5.

10.5 Incorporating the generating curve into the model

The generating curve \mathcal{C} is specified in a local coordinate system uvw . Given a point $\mathcal{H}(t)$ of the helico-spiral, \mathcal{C} is first scaled up by the factor ξ_c^t with respect to the origin O of this system, then rotated and translated so that the point O matches $\mathcal{H}(t)$ (Figure 10.2). The axes uvw are used to orient the generating curve in space. The simplest approach is to rotate the system uvw so that the axes v and u become,

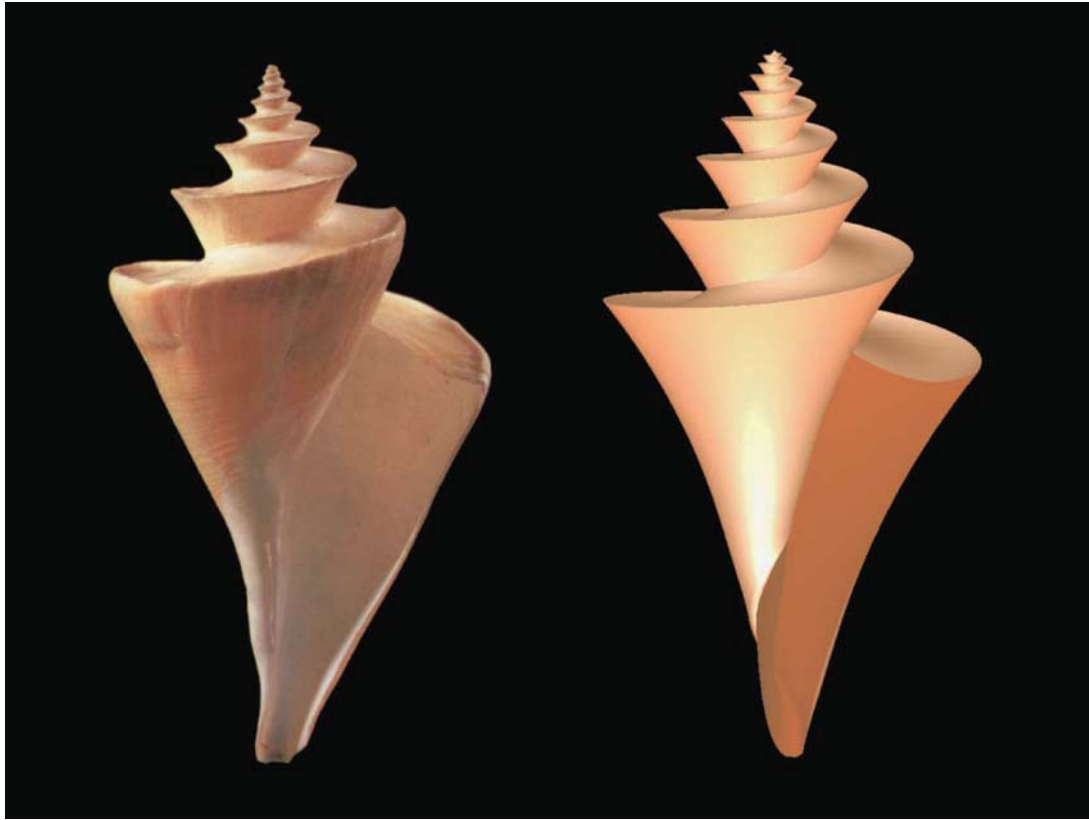


Figure 10.5. A photograph (Gordon, 1990, page 97) and model of *Thatcheria mirabilis* (Miraculous Thatcheria). The unusual shape of this shell results from the triangular generating curve. Photograph courtesy of the Natural History Museum, London, England.

respectively, parallel and perpendicular to the shell axis z . If the generating curve lies in the plane uv , the opening of the shell and the growth markings (such as the ribs on a shell surface) will be parallel to the shell axis. However, many shells exhibit approximately *orthocinal* growth markings, which lie in planes normal to the helico-spiral \mathcal{H} (Illert, 1989). This effect can be captured by orienting the axis w along the vector \vec{e}_1 , tangent to the helico-spiral at the point $\mathcal{H}(t)$. The curve is fixed in space by aligning the axis u with the principal normal vector \vec{e}_2 of \mathcal{H} . The unit vectors \vec{e}_1 and \vec{e}_2 can be calculated as follows (Bronsvoort and Klok, 1985):

$$\vec{e}_1 = \frac{\vec{\mathcal{H}}'(t)}{|\vec{\mathcal{H}}'(t)|}, \quad \vec{e}_3 = \frac{\vec{e}_1 \times \vec{\mathcal{H}}''(t)}{|\vec{e}_1 \times \vec{\mathcal{H}}''(t)|}, \quad \vec{e}_2 = \vec{e}_3 \times \vec{e}_1. \quad (10.3)$$

Symbols $\vec{\mathcal{H}}'(t)$ and $\vec{\mathcal{H}}''(t)$ denote the first and second derivative of the position vector $\vec{\mathcal{H}}(t)$ of the point $\mathcal{H}(t)$, taken with respect to the parameter t . Vectors \vec{e}_1 , \vec{e}_2 and \vec{e}_3 define a local orthogonal coordinate system called the *Frenet frame*. It is considered a good reference system for specifying orientation, because it does not



Figure 10.6. A photograph (Gordon, 1990, page 47) and two models of *Epitonium scalare* (Precious Wentletrap). Photograph courtesy of Ken Lucas, Biological Photo Service, Moss Beach, California.

depend on the parametrisation of the helico-spiral \mathcal{H} or on the coordinate system in which it is expressed (do Carmo, 1976). The Frenet frame is not defined at points with zero curvature, but a helico-spiral has no such points ($\mathcal{H}''(t)$ is never equal to zero). The impact of the orientation of the generating curve on the shell shape is illustrated in Figure 10.6.

The opening of the real shell and the ribs on its surface lie in planes normal to the helico-spiral. This is properly captured in the model in the center of the figure, which uses Frenet frames to orient the generating curve. The model on the right incorrectly aligns the generating curve with the shell axis.

In general, the generating curve need not be aligned either with the shell axis or with the Frenet frame (Cortie, 1989, Illert, 1989). In the case of non-planar generating curves, it is even difficult to define what “alignment” would mean. It is therefore convenient to be able to adjust the orientation of the generating curve with respect to the reference coordinate system. We accomplish this by allowing the user to specify a rotation of the system uvw with respect to each of the axes \vec{e}_1 , \vec{e}_2 , and \vec{e}_3 .

Although, in a mathematical sense, the surface of a shell is completely defined by the generating curve \mathcal{C} sweeping along the helico-spiral \mathcal{H} , we represent it as a

polygon mesh for image synthesis purposes. The mesh is constructed by specifying $n + 1$ points on the generating curve (including the endpoints), and connecting corresponding points at consecutive positions of the generating curve. Such a polygonal representation can be easily rendered using standard computer graphics techniques (Foley *et al.*, 1990).

10.6 Modeling the sculpture on shell surfaces

Many shells have a sculptured surface. Common forms of sculpturing include ribs more or less parallel to the generating curve or to the direction of growth. Both types of ribs can be easily reproduced by displacing the vertices of the polygon mesh in a direction normal to the shell surface. Ribs parallel to the generating curve result from a periodical variation of the value of the displacement d according to the position of the generating curve along the helico-spiral \mathcal{H} . The amplitude is proportional to the current size of the generating curve. A striking example of such ribs can be observed in Precious Wentletrap (Figure 10.6). A shell with more gentle corrugation is shown in Figure 10.7.

In the case of ribs parallel to the direction of growth, the displacement d varies periodically along the generating curve. As previously, the amplitude of these variations is proportional to the current size of the curve. Examples of this type of sculpturing are shown in Figures 10.8, 10.9 and 10.10.

More dramatic departures from the “basic” shell shape can be reproduced by combining several generating curves in the same model. For example, the knobs on the surface of a triton shell (Figure 10.11) were generated by interpolating between two periodically exchanged generating curves: one smooth and one undulating. A similar method was used to model the trophon shell in Figure 10.1. In this case, one of the curves had cusps, which produced the spikes on the shell surface.

Three generating curves can be found in the model of the pelican shell shown in Figure 10.12. Two alternating curves were used to generate most of the shell body, as in the triton shell. The third curve, with large cusps, captured the shape of the shell opening.

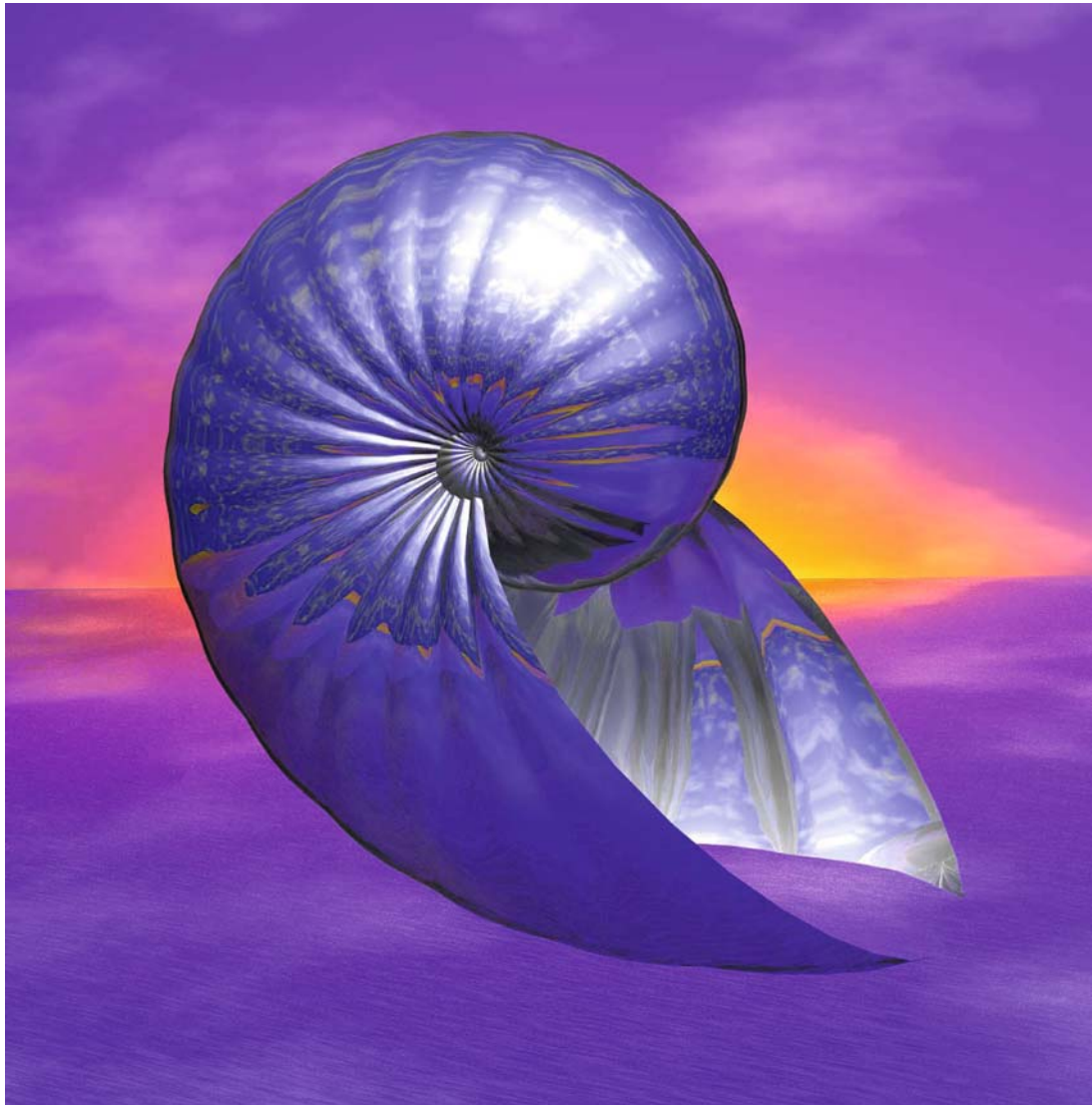


Figure 10.7. A corrugated shell

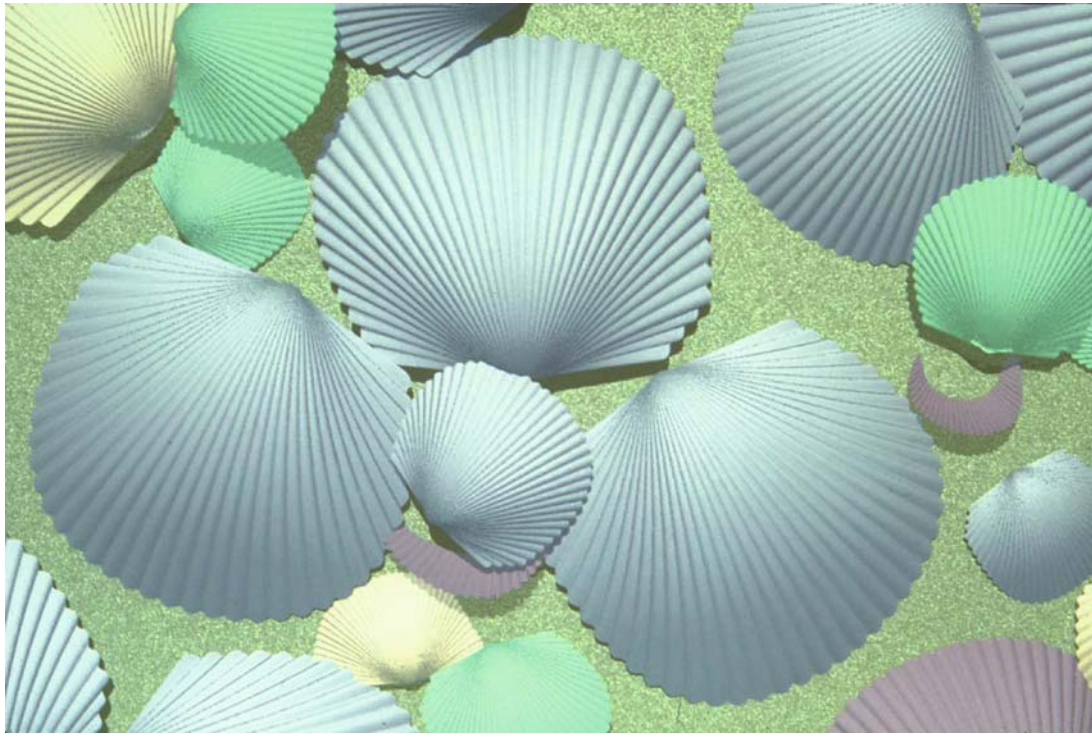


Figure 10.8. Clam shells provide a simple example of surface sculpturing with ribs orthogonal to the generating curve



Figure 10.9. A photograph (see Sabelli, 1979) and model of *Rapa rapa* (Papery Rapa) showing surface sculpturing with ribs orthogonal to the generating curve. The shape of the ribs in the model is captured by a sine function uniformly spaced along the edge of the shell.



Figure 10.10. Surface sculpturing with ribs orthogonal to the generating curve. A photograph (see Sabelli, 1979) and three models of *Turritella nivea* illustrate the effect of decreasing the frequency of the modulating function.

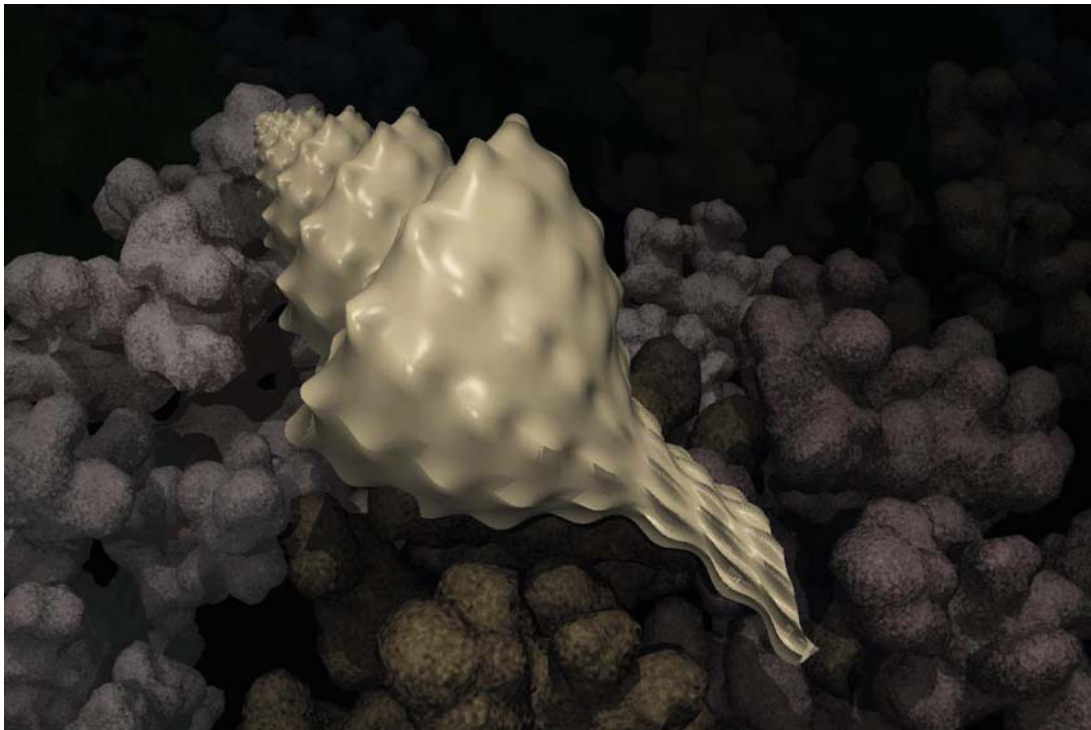


Figure 10.11. A triton shell. The corals in the background were modeled by Jaap Kaandorp, using a method described in his book (Kaandorp, 1994; chapter 5).

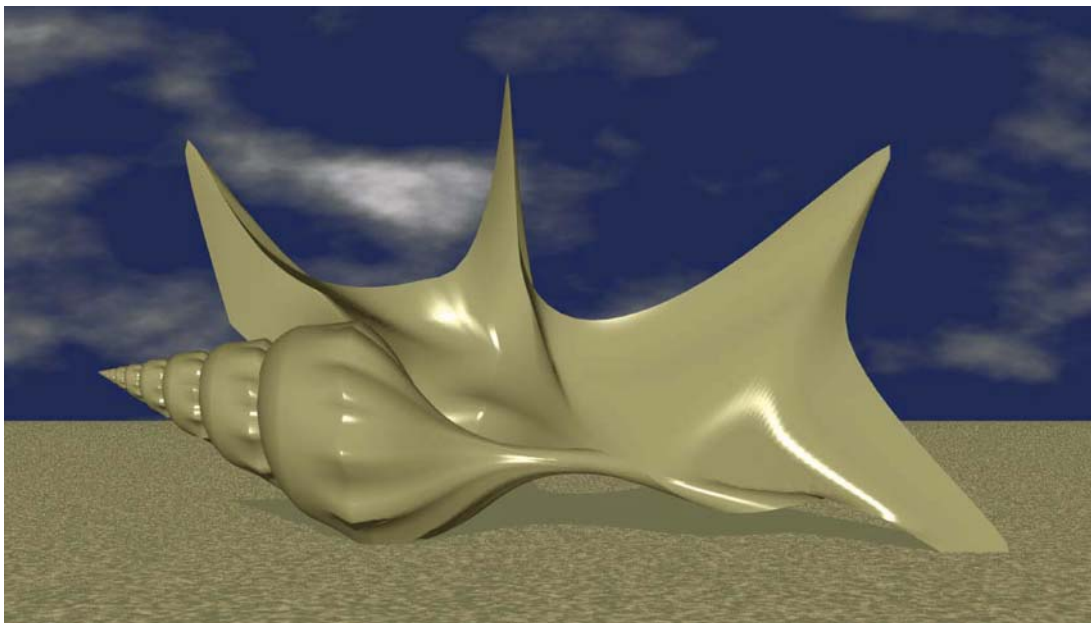


Figure 10.12. A pelican shell

10.7 Shells with patterns

As discussed in the previous chapters, patterns in shells result from the deposition of pigmented material at the shell margin. In this section, we illustrate this process using synthetic images of selected shells.

The basic technique for incorporating patterns into three-dimensional shell models is depicted in Figure 10.13. Instead of developing a pattern along a horizontal line moving downwards (left), we solve differential equations representing pigment deposition along the edge of the shell (right). The pattern unfolds on the shell surface as the shell grows.¹

The particular patterns shown in Figure 10.13 were generated using the activator-substrate model introduced in Chapter 2 (Equation 2.4). The parameter values were chosen to produce a stable distribution of pigmentation along the growing edge, yielding stripes parallel to the direction of shell growth.

¹ Technical details of the mapping of patterns to polygon meshes are discussed in Fowler *et al.*, (1992)

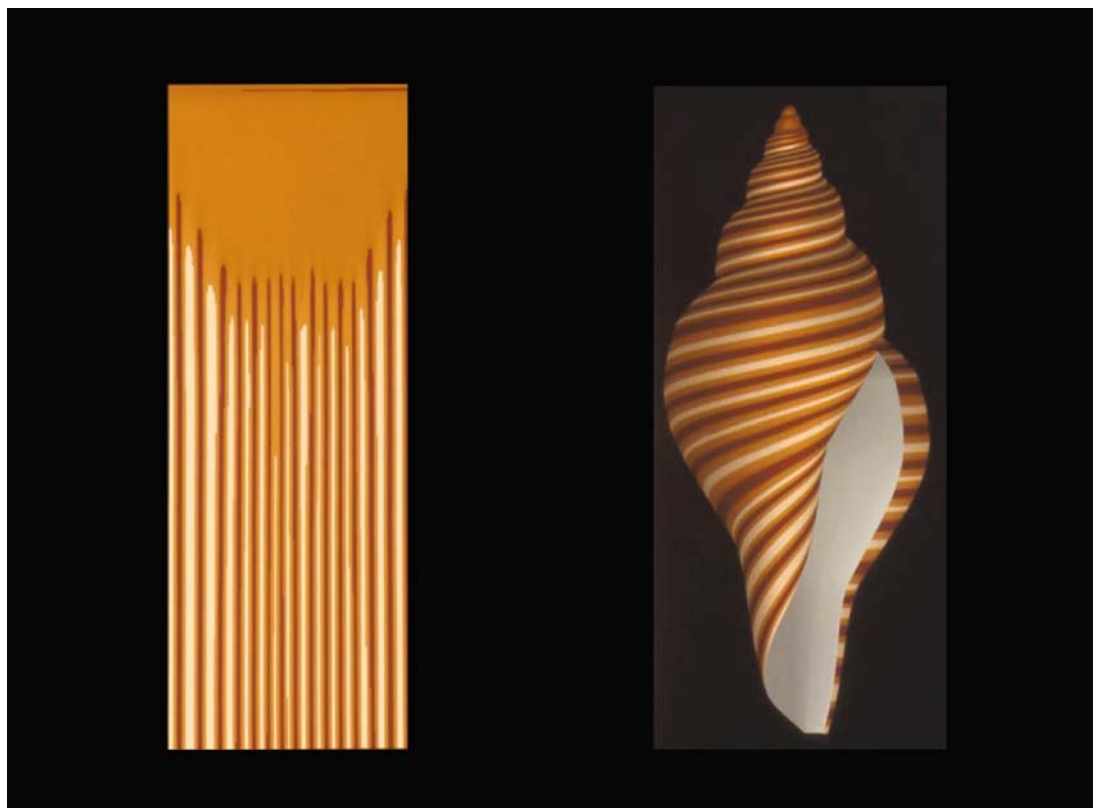


Figure 10.13. A stable pattern of stripes generated by the activator-substrate model (Equation 2.4)



Figure 10.14. A photograph and model of *Amoria ellioti*

Another pattern generated using the activator-substrate model, stripes perpendicular to the direction of growth, can be found in *Amoria ellioti* shown in Figure 10.14. As described in Chapter 3, the periodic character of this pattern is a manifestation of the oscillations of the activator concentration over time, which occur when the basic substrate production b_b is not sufficient to sustain activator removal at a constant rate r_a ($b_b < r_a$ in Equation 2.4).

Figure 10.15 shows a photograph and a model of *Amoria undulata*. Its pattern is a modification of that found in *Amoria ellioti*, with undulations superimposed on lines parallel to the growing edge. As explained in Sections 4.1 and 4.2, the activator-substrate process is regulated in this case by an additional pattern that modulates the substrate production b_b according to a periodic (sine) function of the cell position, $b_b = b_b(x)$. Undulations occur because oscillations are faster in regions with higher b_b values than in regions with lower values. The coherence of the lines is maintained by the diffusion of the activator.



Figure 10.15. A photograph (see Sabelli, 1979) and model of *Amoria undulata* (Waved Volute)

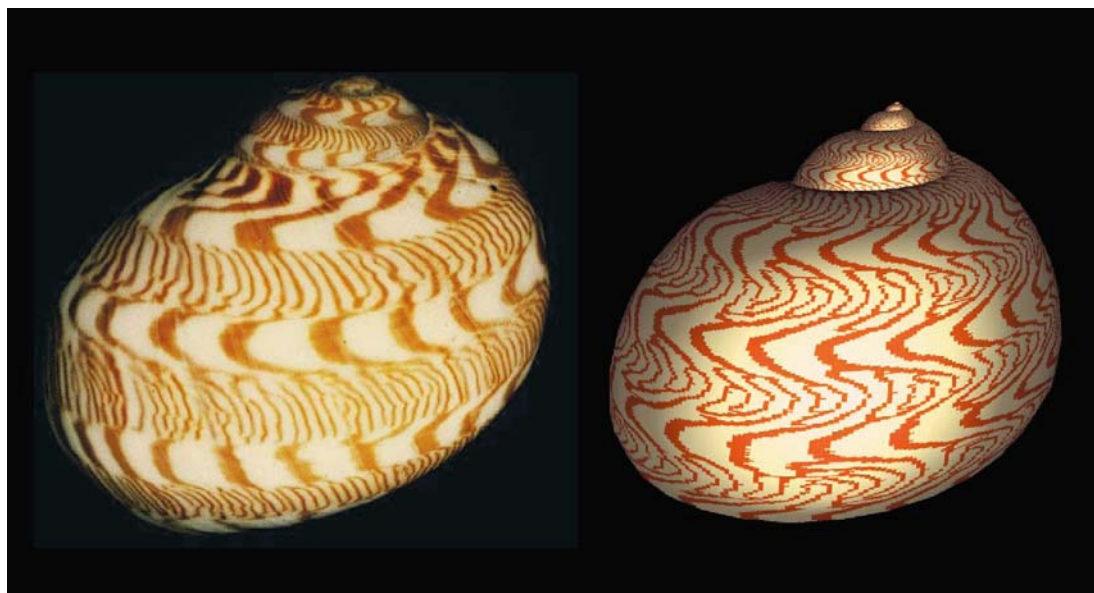


Figure 10.16. A photograph and model of *Natica euzona*



Figure 10.17. A photograph (see Sabelli, 1979) and model of *Volutoconus bednalli* (Bednall's Volute)

As the modulation of the substrate production increases, the undulations become even more pronounced, as observed in *Natica euzona* (Figure 10.16). Regions of high and low frequency of oscillations can be distinguished along the growing edge of the shell. Diffusion of the activator is insufficient to maintain the coherence of the lines, which merge and form blind endings as described in Section 4.1 (Figures 4.3 and 4.4).

Volutoconus bednalli (Figure 10.17) illustrates an extreme case of the same mechanism (see Section 4.7). The function $b_b(x)$, which describes the production of the substrate in Equation 2.4, exceeds the decay constant r_a for some locations x along the growing edge of the shell. This creates areas of permanently high activator concentration and yields a pattern of lines parallel to the direction of growth. Oscillations occur between these lines, producing arcs roughly parallel to the growing edge.

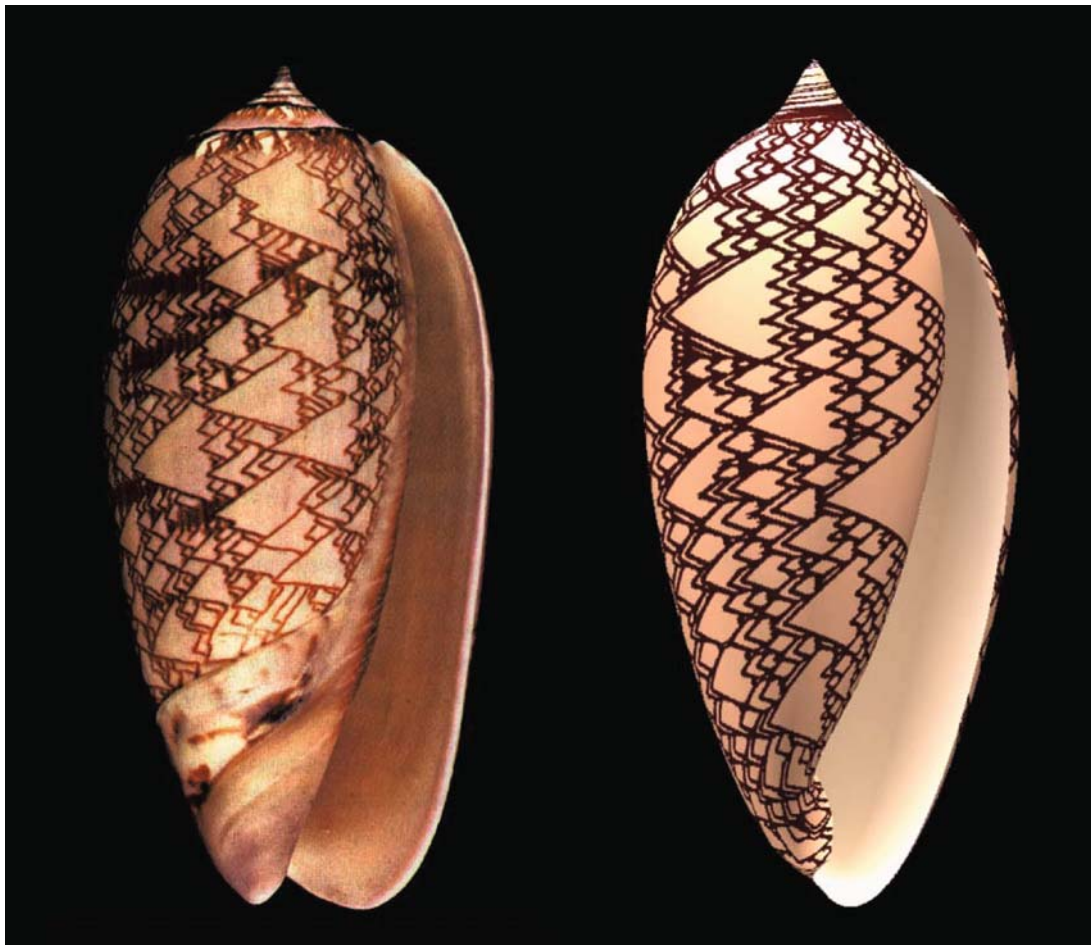


Figure 10.18. A photograph (see Sabelli, 1979) and model of *Oliva porphyria*

The formation of branches is an essential feature of the pigmentation pattern of *Oliva porphyria*, presented in Figure 10.18. Oblique lines represent waves of activator concentration, traveling along the growing edge. Colliding waves extinguish each other. New waves appear when the activated point of one wave spontaneously initiates another wave traveling in the opposite direction. Observations of the shell indicate that the number of traveling waves is approximately constant over time. This suggests a global control mechanism, or “hormone” that monitors the total amount of activator in the system, and initiates new waves when its concentration becomes too low. This mechanism has been modeled using a modified activator-inhibitor system (Equations 2.1 and 6.1), as described in detail in Section 6.2.

The model of *Conus marmoreus*, shown in Figure 10.19, is similar to that of *Oliva*. As described in Chapter 7, in this case the pigment producing process is controlled by another reaction-diffusion process, rather than a hormone.



Figure 10.19. A photograph (see Sabelli, 1979) and model of *Conus marmoreus* (Marble Cone)



Figure 10.20. A virtual museum of shells

The three-dimensional shell models collected in this chapter (Figure 10.20) present a small fraction of patterns described in this book. Other patterns can be incorporated into the models in a similar fashion.

This chapter contains edited parts of the paper *Modeling seashells* (Fowler, *et al.*, 1992), which is used with the permission of the Association for Computer Machinery. The reported research was sponsored by operating and equipment grants from the Natural Sciences and Engineering Research Council of Canada, and by a graduate scholarship from the University of Regina. We are indebted to Pat Hanrahan for providing Deborah with access to his research facilities at Princeton. Images 10.1, 10.8, 10.7 10.11 10.12 10.16 10.20 were rendered using the ray-tracer rayshade by Craig Kolb. Photographs of real shells included in Figures 10.9, 10.10, 10.15, 10.17, 10.18, and 10.19 are reproduced with the kind permission of Giuseppe Mazza.

For those in a hurry: a quick start for the computer programs

On the enclosed CD programs are supplied that run in a Windows or Unix environment. **sp** produces the normal space-time simulations, **xy** the simulations in two-dimensional fields. The programs can be started directly from the CD; no special installation is required. More convenient is to copy the directory [**simulation programs**] with all sub-directories onto the hard disk. After program start, a list of the most frequently used commands is given on the initial screen. Other commands and parameter changes can be selected from a menu by pressing F1. The character – > at the bottom right is the prompt, indicating that the program is waiting for a command.

Most figure captions in this book contain commands to reproduce the corresponding simulations. Such a command consists of the letter **S** (Simulation) followed by the figure number. For instance, **S61** will produce the simulation shown in Figure 6.1; **S** alone will start the simulation with the actual set of parameters, and **Rxx** reads a new set of parameters without starting the simulation and **I** sets the initial conditions according to the actual parameters. The case of the input letters does not matter.

Simulations that require more complex input from the keyboard have been simplified using “GUIDED TOURS.” In this case, the input is read from a file line by line; the tour only occasionally requires pressing of the <RETURN> key. For instance, the command **GT32** leads to the simulations shown in Figure 3.2. The command **GT** produces a list of all available GUIDED TOURS with the option to choose one. **GT1**, **GT2**, and **GT3** are introductory TOURS; **GT4** illustrates the use of different screen resolutions.

Additional information and information about the compilers and re-compilation of the programs can be found in the file COMPILER.TXT.

A word of precaution...

The software was written with care but the customer knows that software cannot be produced without errors. Springer-Company and the author disclaim any liability for software errors or their consequences.

All user rights to the software are held exclusively by the author. Springer-Company does not author data and programs but makes them available. Any commercial use or distribution independently of the book is not permitted.

Table 11.1. For those in a hurry: a quick start for the computer programs

The computer programs

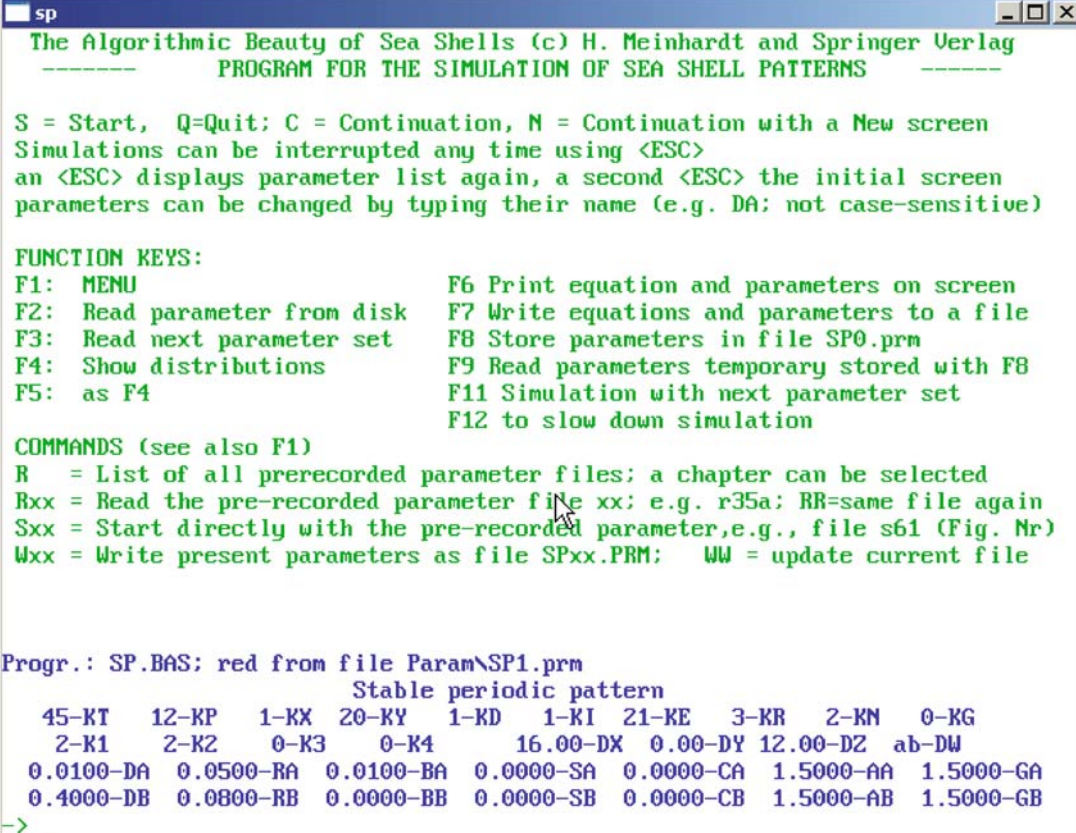
11.1 Introductory remarks

The programs supplied on the CD are modified versions of my own working programs. Originally written in FORTRAN, they have been translated into BASIC. The program **sp** is a Windows/Unix version, compiled with FreeBasic, a compiler that is freely available on the Web. Two-dimensional simulations can be performed with the program **xy**. DOS versions are mentioned further below. Do not expect the programs to be as perfect as a commercial product. Consider them as an extension of the book and as a tool to develop some intuition about the complex world of non-linear interactions. I am sure that the program is not free of errors and that it contains awkward parts left over from earlier versions. However, since the source code is provided, it should be possible to make corrections or improvements if desired. Conversion from the BASIC dialect to other programming languages should not be too difficult.

The program does not have a fancy interface. Instead of the mouse, it uses explicit short commands that may require getting used to. However, with some experience, changing parameters, inputting new commands, and starting the simulations require only very few key strokes, enabling a rapid and convenient operation. Certainly the best way to become familiar with the commands is to practice them. For those who do not want to delve too deeply into the program but would like to reproduce the simulations shown in this book, it may be encouraging to know that the very simple commands given in the figure captions are sufficient.

11.2 Using the program

As mentioned above, the programs can be started directly from the CD and do not require a special installation. However, more convenient is to make a copy on the hard disk including all subdirectories. The programs **sp** and **xy** should run in any standard WINDOWS or UNIX environment.



The screenshot shows a window titled "sp" with the following text:

The Algorithmic Beauty of Sea Shells (c) H. Meinhardt and Springer Verlag
PROGRAM FOR THE SIMULATION OF SEA SHELL PATTERNS

S = Start, Q=Quit; C = Continuation, N = Continuation with a New screen
Simulations can be interrupted any time using <ESC>
an <ESC> displays parameter list again, a second <ESC> the initial screen
parameters can be changed by typing their name (e.g. DA; not case-sensitive)

FUNCTION KEYS:

F1: MENU	F6 Print equation and parameters on screen
F2: Read parameter from disk	F7 Write equations and parameters to a file
F3: Read next parameter set	F8 Store parameters in file SP0.prm
F4: Show distributions	F9 Read parameters temporary stored with F8
F5: as F4	F11 Simulation with next parameter set
	F12 to slow down simulation

COMMANDS (see also F1)

R = List of all prerecorded parameter files; a chapter can be selected
Rxx = Read the pre-recorded parameter file xx; e.g. r35a; RR=same file again
Sxx = Start directly with the pre-recorded parameter, e.g., file s61 (Fig. Nr)
Wxx = Write present parameters as file SPxx.PRM; WW = update current file

Progr.: SP.BAS; red from file Param\SP1.prm

Stable periodic pattern

45-KT	12-KP	1-KX	20-KY	1-KD	1-KI	21-KE	3-KR	2-KN	0-KG
2-K1	2-K2	0-K3	0-K4	16.00-DX	0.00-DY	12.00-DZ	ab-DW		
0.0100-DA	0.0500-RB	0.0100-BA	0.0000-SA	0.0000-CA	1.5000-AA	1.5000-GA			
0.4000-DB	0.0800-RB	0.0000-BB	0.0000-SB	0.0000-CB	1.5000-AB	1.5000-GB			

-> -

Figure 11.1. The initial screen with basic commands and parameters read from the file sp1.prm

After the program starts, the first display is subdivided into two parts (Figure 11.1). The upper part contains the commands most frequently used as well as a list of the function keys. The lower part contains a list of parameters read from the prerecorded parameter file sp1.prm (in the directory param-sp). The arrow ($->$) at bottom left is the prompt, indicating that the program is waiting for an input. The input can be either a command or the name of a parameter. Either upper or lower case may be used. A simulation is started by entering S and can be continued by C or N (New screen). A simulation can be interrupted at any time by pressing the [ESC] key; q (quit) terminates the program and causes a return to the system. A more complete list of commands and parameter names can be accessed by pressing the function key F1. Using the arrow and page keys, commands may be selected and parameters can be changed using these menus.

Each parameter has a name, which is the same as that used in the equations. The value of a parameter may be changed by entering its name. For example, after typing da or DA, first the actual value of the diffusion constant of the activator (D_a in the equations) is shown. You can either type a new value or [ESC] to leave

the parameter unchanged. Pressing the [RETURN] key will set the parameter to zero. Table 11.2 provides a list of parameters.

The first 14 parameters are integer numbers and are used to control the program flow. They determine the number of iterations, the number of iterations between updating the display, left and right boundary of the field, type of display, initial condition and the type of equation (see Table 11.3). The rule that parameters starting with the letters H through N are integers has been maintained throughout the programs from the original FORTRAN program.

After a simulation, only the prompt line is redisplayed at the bottom of the screen, leaving the graphic output undisturbed. At this point, parameters can be changed or commands can be entered as described above. After pressing the [RETURN] or [ESC]-key the complete list of parameters is shown again. Pressing the [RETURN] or [ESC] key a second time redisplays the most essential commands, too.

Prerecorded parameter files can be read with the command **Rx**, where x is a number between 1 and 999 optionally followed by a letter. For example, **R1** reads the file **sp1.prm** that was used at the start of the program. The number usually corresponds to the figure number. For instance, the command **R23a** will read the parameters required for the simulation shown in Figure 2.3a. The first digit or the first two digits indicate the chapter number. With the full parameter list a message is displayed whenever the parameters have been modified. The original parameters can be re-read using the command **RR**. The command **Sx** may be used to directly start a simulation. The corresponding commands are given at the end of each figure legend. For instance, **S22** directly starts the simulation shown in Figure 2.2. Typing **R** without a number (or **F2**) will produce a list of the available prerecorded parameter files and the headlines of the corresponding simulations, with the option to select a particular file. It is possible to list only the files of a particular chapter. To save a modified set of parameters use the command **Wx** (**w** = write; again, x is the file number, x = 1...999, or chapter- and figure number); files for subpictures can be saved by a command **Wxa**. A warning is given when existing files are overwritten. **WW** saves a parameter set using the current file name.

The coding of the actual interaction can be inspected by the command **PE** (**PrintEquation**). Further below I have described how to read such a code. This also shows how a particular parameter is used. The parameters are not listed in the book. If a printout of a particular parameter set or the actual coding of an interaction is desired, the command **PEF** (**PrintEquationFile**) produces a **.txt** file that contains the code of the actual interaction and the list of parameters as they appear on the screen. As a standard, the file will be stored in the subdirectory **tmp**. This command also helps to deduce the interaction if a corresponding equation is not explicitly given in the book. The interactions used in the simulation 7.5ab represent an example for this. With the command **r75a** one can read the parameters. The command **PE** displays the corresponding program code.

11.3 GUIDED TOURS

Simulations that require more complex inputs from the keyboard have been simplified using “GUIDED TOURS.” The command **GT** produces a list of the available tours from which to choose. For example, the command **GT32** will produce the simulations shown in Figure 3.2; **GT3** provides an example for each of the implemented graphic display modes. With a GUIDED TOUR, the inputs that are normally given from the keyboard are read line by line from a file (in this example from the file **sp32.gt** in the directory **param-sp**). Comments explain what is happening. If the message [OK] appears at the lower right corner of the screen, a [RETURN] continues with the next simulation or message. Pressing at this stage **q** or **Q<RETURN>** terminates the actual GUIDED TOUR; **S** or **C** allows a restart or a continuation of the actual simulation. An actual simulation within a TOUR can be terminated by pressing the **ESC**, as in a normal simulation. With - (minus sign, followed by a RETURN), a tour can be interrupted, e.g., to inspect or modify the actual parameters or interaction, choose another display etc. The tour will be continued with the command **GT**. If changes were introduced, they will be used in the continuation. Before another TOUR can be started, an interrupted TOUR has to be continued and correctly terminated.

11.4 Implementation of the interactions

After setting the initial conditions, the program calculates the concentration changes over a given time interval. These changes are added to the existing concentrations and the next iteration is started, and so on. After a number of iterations (as defined by the parameter **KP**), the program plots the new concentrations. This will repeat **KT** times such that **KT * KP** iterations are calculated in all.

The adaptation of the equations into a form convenient for computer simulations is illustrated using Equation 2.1a:

$$\frac{\partial a}{\partial t} = s \left(\frac{a^2}{b} + b_a \right) - r_a a + D_a \frac{\partial^2 a}{\partial x^2}$$

Rather than considering a homogeneous space in which concentrations vary continuously, the space is subdivided into individual cells i , $i = 1...n$. The concentrations of substances a, b, \dots are stored in the array **axt(il, i)** where $il = 1, 2, \dots$ is the number of the substance; $il = 1$ corresponds to substance a , $il = 2$ to substance b and so on; and i denotes the position of the cell. The corresponding array name in two-dimensional simulations is **axy(il, ix, iy)**. Before the actual computation is carried out for a particular cell and time step, the actual concentrations of the substances a, b, c, \dots are stored in the floating point numbers a, b, c, \dots .

As a rule, the constant term in the production rate, s (source density), is set to the decay rate of r_a in order to obtain absolute concentrations around unity. This value is modulated by random fluctuations (parameter KR = \pm fluctuations in percent). The local source density is stored in the array `axt(0, i)` or `axy(0, ix, iy)`, the local value in the variable `s`. Random fluctuations remain unchanged during a simulation.

The loss or gain by diffusion depends on the concentration differences; more precisely on the second derivative $D_a \partial^2 a / \partial x^2$. In other words, not the concentration change but rather the change in the concentration change is decisive. The reason is easy to understand. Imagine three cells with the concentration 3, 2, and 1, respectively. Since the net exchange by diffusion depends on the concentration difference, the central cell will gain from its left neighbor the same amount as it loses into the right cell. Thus, although both neighbors have different concentrations, the gain or loss by diffusion is zero if the concentration changes in space are constant.

The diffusion term for a continuous space, $D_a \partial^2 a / \partial x^2$, is substituted by a term using the concentration differences of adjacent cells:

$$DA * (a_{i-1,t} - a_{i,t}) + DA * (a_{i+1,t} - a_{i,t})$$

Thus, the total change in activator concentration in the cell i at time t resulting from production, decay, and exchange with neighboring cells is given by

$$da_{i,t} = s * (a_{i,t}^2 / b_{i,t} + ba) - ra * a_{i,t} + DA * ((a_{i-1,t} - a_{i,t}) + (a_{i+1,t} - a_{i,t}))$$

Adding this change to the existing concentration of a at the time t leads to a new concentration of a in the cell i at the time $t + 1$

$$a_{i,t+1} = a_{i,t} + da_{i,t}$$

Communication between cells using diffusion requires special conditions at boundaries where cells have only a single neighbor. In most calculations it is assumed that the boundaries are closed, i.e., no loss or gain takes place through the boundary. This is achieved by assuming that virtual leftmost and rightmost cells have the same concentration as the cells at the boundary proper. Since no net exchange takes place between cells with identical concentrations, the no-flux boundary condition is satisfied. Some display modes assume a circular arrangement of ‘cells’. In these cases, circular boundary conditions are automatically assumed.

The calculation of the concentration changes due to decay and diffusion alone are the same for all interactions considered. Since the program contains many types of interaction, these common calculations are coded separately and are calculated first in each iteration. In the program, the change due to decay and diffusion are

termed `olddecaydiffA` for substance *a*, `olddecaydiffB` for substance *b*, etc. with

$$\text{olddecaydiffA} = a * (1 - RA - 2 * DA) + DA * (a(i-1) + (a(i+1))$$

Thus, for the interaction given above as an example, the new concentration of *a* (in the cell *i*) appears in the code as follows

$$\text{axt}(1, i) = \text{olddecaydiffA} + s * (a * a/b + ba)$$

Due to its similarity with the original equation, even those who are not computer specialists should be able to understand this type of notation. With the command **PE** (PrintEquation) the code for the interaction used in the actual simulation can be displayed on the screen. The program searches for the corresponding lines in the source code according to the equation-selecting parameter **KE**; the current source program, e.g., `sp.bas`, must be in the current directory. The following example shows the code for the activator-depleted substrate model (**KE** = 24, equation 2.4) as printed by this command.

```
CASE 24 '- activator-depletion mechanism: ----
' a activator, b substrate,
' axt(8,i) may contain a stable pattern (normalized to 1)
aq = s * b * (a * a / (1 + sa * a * a) + ba)
axt(1, i) = olddecaydiffA + aq
axt(2, i) = olddecaydiffB - aq + bb * axt(8, i)
```

The directory [**demo**] contains three very short and self-consistent programs, demonstrating pattern formation in general, the pole-to-pole oscillation in *E.coli*, and the shell pattern on *Oliva porphyria*. The many comment lines in these minimal programs should facilitate the user's understanding. The executable versions were compiled with FreeBasic for Windows.

11.5 Numerical instabilities that may cause errors

Concentration changes are calculated for a finite time interval. After each interval the changes are added to existing concentrations to obtain the new values. In reality, however, the concentrations change continuously over time. Therefore, to obtain a close approximation of the real situation, short time steps should be used. This, however, could require a prohibitive number of calculations if the total time frame is fairly long. Therefore, a compromise between speed and precision must be made.

There are some instances in which step-by-step calculations may become numerically unstable. This may be caused if the diffusion constants used are numerically too high. For example, imagine a chain of cells in which only a single cell has a

high concentration. With a numerical diffusion constant of 1 this cell would obtain a negative concentration (of the same absolute value) in the next iteration while both neighboring cells will have the same concentration as the original cell. Thus, the concentration differences between adjacent cells would increase by a factor of two. This is, of course, senseless since concentration differences should only smooth out by diffusion, not increase. Therefore, to avoid these instabilities the numerical value of diffusion constants must be smaller than 0.4 (0.2 in two-dimensional simulations). The program will display a message and refuse to accept higher diffusion rates.

Another possible source of a numerical instability exists in simulations of the depletion mechanism. During the autocatalytic burst, the extrapolation of a given substrate removal rate may lead to negative substrate concentrations, which, again, is senseless. This causes numerical instabilities since the sign change means the substrate is no longer being removed but is increasing. In this case, smaller time steps may cure the problem, requiring smaller constants for production, decay, and diffusion. A simpler way is to introduce a small saturation term (s_a in Equation 2.4a) to limit the autocatalytic burst. This usually avoids the instability without requiring more computer time and does not significantly change the outcome pattern. In critical interactions possible negative concentrations are explicitly prevented by the program.

11.6 Compilers and versions

The compiler **FreeBasic** was chosen since it is freely available from the Web. In contrast to the DOS versions, these programs can use all the available memory, they allow higher screen resolution and the results of simulations can be easily documented by producing screen copies. The problem is that major changes have been introduced with new compiler versions. So, I can only hope that the programs can be recompiled without problems if new versions are released. On the CD the current version 0.2 is supplied, which works. For recompilation, the following command and compiler options are: [path] fbc sp.bas -lang qb -ex [see the file Compiler.txt.] .

Versions for DOS are also supplied, **dsp.bas** and **dxy.bas** respectively. They have been compiled with Power-BASIC 3.5. The program codes are identical except for some compiler-specific elements. Usually they run very stably. In addition, the files DSPMS.BAS and DXYMS.BAS that run under Microsoft BASIC QBX have also been included. Simulations in QBX run somewhat slower, and the available memory space is more restricted. However, QBX allows an easy debugging and changes of the program code without recompiling. The two DOS-versions use identical subroutines. The minimal programs in the directory **demo** run under QBX, PowerBasic, and Freebasic. As an example for a C-program, a minimum program for *Oliva porphyria* can be found in the subdirectory **demo** that runs under Borland C.

11.7 Parameters used in the program

The following tables describe the parameters used in the program in more detail. These tables are also part of the menu system that can be called in with F1. The parameters are divided into several categories:

- Commands
- Floating point variables (rates of diffusion, life times, etc.)
- Parameters for program control (number of iterations, type of interactions etc.)
- Initial conditions
- Display types for XT plots
- Parameters for the graphic display
- Display types for XY plots

List of Commands

- F1** Help (shows these tables in the form of a menu)
- F2** Shows parameter files for a chapter of your choice
- F3** Reads the next parameter set (use F2 first)
- F4** Show distributions in a simplified and normalized form
- F5** As F4 (requiring in the program XY a RETURN)
- F6** Displays the source code of the interaction on the screen
- F7** Writes code and parameters to a .txt file
- F8** Writes the actual parameter to a temporary file (sp0.prm)
- F9** Read parameters from the temporary file stored by F8
- F10**
- F11** Starts directly with the next parameter set (use F2 first)
- F12** Introduces a delay between the individual displays (try .1)

- Q** Terminates the program; **QQ** terminates without confirmation
- ESC** Terminates the actual simulation, waits for a command
- S** Start of the simulation
- Sxx** Start of the simulation with the prerecorded parameter file spxx.prm, xx=1-999; xx is usually the chapter and figure number as given in the legends.
- C** Continues simulation, same screen
- N** Continues after refreshing screen (makes a difference in some space-time plots)
- D** Last simulation result is displayed again (e.g., after changing colors)
- R** Shows the list of parameter files; a selection is offered
- Rxx** Reads a particular parameter file, xx=1-999 (the file name is SPxx.prm)
- Wxx** Writes the present set of parameters to the file SPxx.prm, xx=1-999 and can be recovered by Rxx.
- PE** PrintEquation, as F6, displays the code of the equation as selected by **KE**
- PEF** as **PE**, and writes code and parameters to a file (F7)
 - I** Only the initial conditions are set; simulation is not started
 - II** Initial conditions are set; random fluctuation remains unchanged
- M** Manipulations
 - MS** Stores the present concentrations
 - MR** Recovers the stored concentrations
 - MC** Changes field size, e.g., to simulate regeneration
 - MA** Changes concentrations in a particular array in a particular region (for instance, to simulate local perturbation)
 - MT** Transplanting several regions into a new order; input number of the first and last cell for each fragment; input of, e.g., 9 and 5 as first and last cell reverses the polarity of that fragment; zero to exit. Distributions must be stored beforehand by the command MS
 - M** A list of the available manipulations is displayed

Table 11.1. List of commands

Floating point variables

Parameter names consist of two letters. The first indicates the function (D=Diffusion, R=Removal...), the second the substance **a**, **b**, **c**... to which it applies.

DA, DB, DC, ...: Diffusion constants for **a**, **b**, **c**... Diffusion constants larger than 0.4 (0.2 in the XY programs) lead to numerical instabilities and are correspondingly corrected. A message is displayed.

RA, RB, RC, ...: Removal (decay) rates

BA, BB, BC, ...: Basic (activator-independent) production

SA, SB, SC, ...: Saturation and Michaelis-Menten constants (and other use)

CA, CB, CC, ...: Coupling between several systems

AA, AB, AC, ...: Initial concentrations at particular positions, see Table 11.6

GA, GB, GC, ...: General initial concentrations

The following parameters play a special role:

CA Usually the general production strength (source density s) is set to the decay rate r_a . If CA is set to a value > 0 , s is set to this value rather than to the decay rate. Thus, with CA=0, a change in the decay rate automatically leads to a corresponding change in the production rate.

DX Pixels per cell in the graphic display

DY Used for some initial conditions, see Table 11.6

DZ Used for some modifications during simulations, see Table 11.3

DW “DisplayWhat” is a string variable that determines the substances to be plotted; with DW = ab, **a** is plotted on top of **b**; with DW = ba, it is the other way around (see Figure 11.3 and Table 11.5).

Table 11.2. Floating point variables

List of integer parameters to control program flow

- KT** Total number of plots per simulation
- KP** Number of iterations (time steps) between two plots. The total number of iterations is KT * KP
- KX** Leftmost cell of a field, usually = 1 (or X-field size in two-dimensional simulations)
- KY** Rightmost cell of a field (or Y-field size in two-dimensional simulations)
- KD** Type of display, see Table 11.4 and Figure 11.4
- KI** Initial conditions, see Table 11.6
- KE** Equation to be used, usually the equation number in the text, e.g., 21 for equation 2.1
- KR** Extent of random fluctuation superimposed, in percent; stored in the array elements `axt(0, i)` or `axy(0, ix, iy)`, substance **s** (source density) in the display
- KN** Number of substances, e.g., 2 if substances **a** and **b** are involved
- KG** Growth, 0 if no growth takes place. Insertion takes place after KG plots are displayed, i.e., after KG * KP iterations. The location of new cells is determined by K1
- K1** Mode of growth if KG > 0 (for other uses of K1-K4 see Table 11.6)
- 0 Insertion at both terminal ends (at the left side only if space is available, i.e., if KX > 1)
 - 1 Two insertions at random positions, one in the right and one in the left half of the field (see Figure 2.6)
 - 2 Insertion in the center
 - 3 Insertion in the right third of the field
 - 4 Insertion at a random position
- K2** Used for some initial conditions, see Table 11.6
- K3** After K3 plots, manipulations or parameter changes may be evoked. The type of manipulation is determined by K4. No manipulation takes place if K3 = 0.
- K4** Type of manipulation
- 1 Basic *a* (activator) production (BA) is changed to DZ
 - 2 Decay rate of *b* (RB) is changed to DZ
 - 3 Basic inhibitor / substrate production (BB) is changed to DZ
 - 4 Decay rate of the activator (RA) is changed to DZ
 - 5 **a** (activator) concentration is changed in a fraction of the field
 - 6 **a** concentration is changed across the entire field by a factor DZ
 - 7 Production and decay rate of **c** (RC) is changed to DZ
 - 8 Saturation of the activator SA is changed to DZ
 - 9 Coupling constant CB is set to DZ
 - ... for other options see menu F1

Table 11.3. List of integer parameters to control program flow

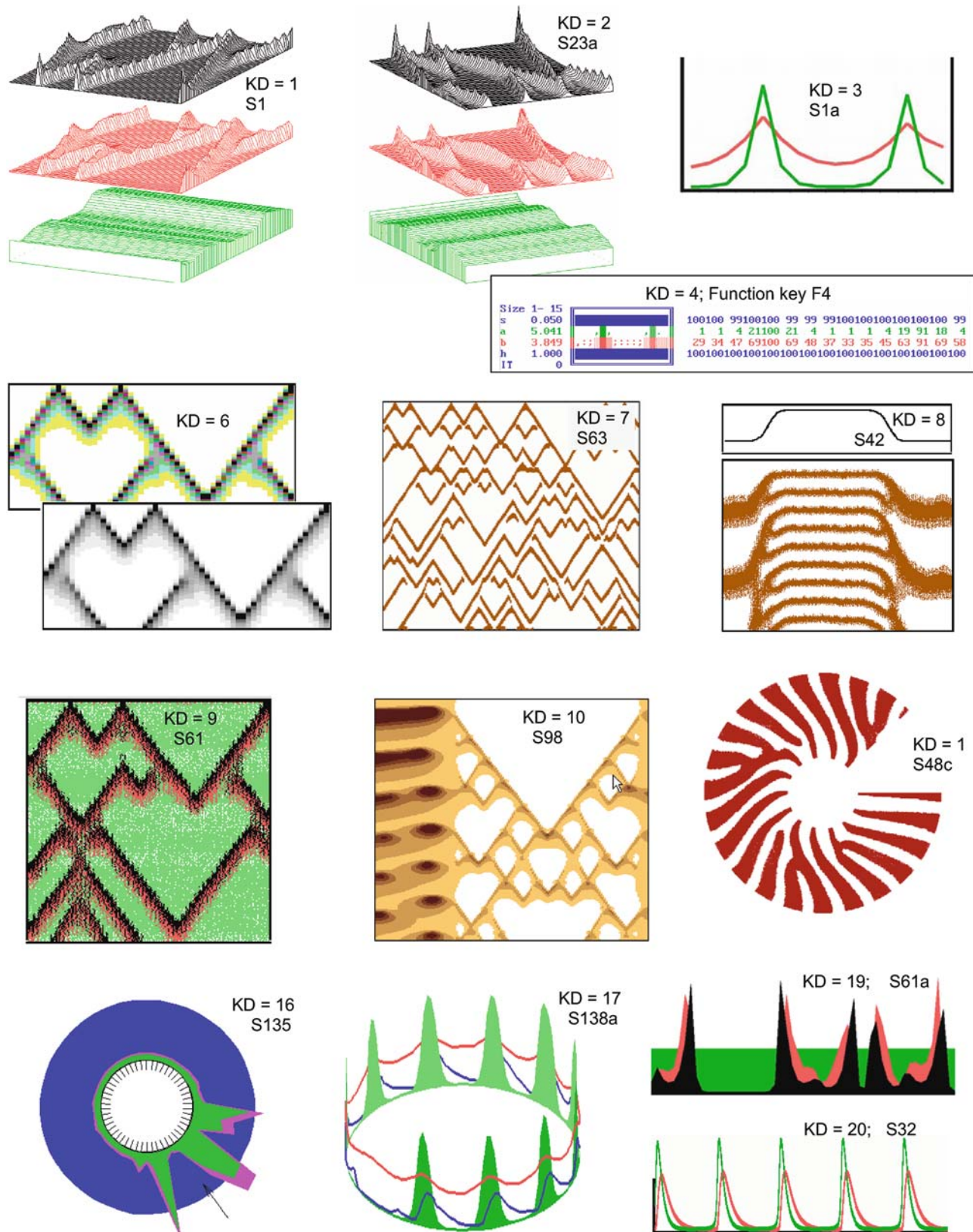


Figure 11.2. Display types used for space-time plots; for details see Table 11.4 (opposite page) and GT3; S** is the command to run a simulation using the corresponding display mode

Types of plots (parameter KD in program SP)

Examples are given in Figures 11.2 and Figure 11.3 (opposite and next page)

- 1 Three-dimensional XT plot, the past is in the background
- 2 Three-dimensional XT plot, the past is in the foreground
- 3 Single curves (width can be controlled by the command IWI)
- 4 Schematic plot with symbols and maximum concentrations (F4)
- 6 Concentration plotted in false color. This mode produces a fine gray scale in back-and-white screen prints. Use only when plotting a single array, e.g. DW = a, or side by side using different X-coordinates. A lower threshold level can be introduced by setting KROT > 1
- 7 Plot with a single threshold (local concentration * factor > 1)
- 8 As 9 with plot of stable prepattern [array a (8, i)]
- 9 Pixels proportional to concentration. Several arrays may be plotted on top of each other if they have the same X-position, or side by side if the X-positions are different
- 10 to 13 Give higher screen resolution in FreeBasic (see GT4 for demo)
- 10 Concentrations indicated by graded brownish colors
- 11 As 7
- 12 As 8
- 13 As 9
- 14 Plot bottom-up, for phyllotaxis
- 15 Circular plot, used for the Nautilus shell
- 16 Concentrations in a circular arrangement of cells, local concentr.= radial
- 17 Concentrations in a circular arrangement of cells, local concentr.= vertical
- 19 Similar to KD=3 but areas are filled
- 20 Plot of concentrations in a single cell (KX, KY = 1) or of the leftmost cell as a function of time (see Figures 3.2 and 3.3)
- 21 For display of gene activities in a single cell (see GT128)
- 23 Two plots of KD=3 type side by side, to display regeneration after bisection; to be used with KE= 211; calculation runs from 1 to K4-1 and from K4+1 to KY (see GT29)
- 25 Colored random dots in a band, IST= width, IH = downward shift (Figure 12.9b; simulation S129a)
- 27 Plot on shrinking circles if concentrations are above a threshold, for phyllotaxis
- 28 Plot on a transparent cylinder, for phyllotaxis

Table 11.4. Types of plots (parameter KD in program SP)

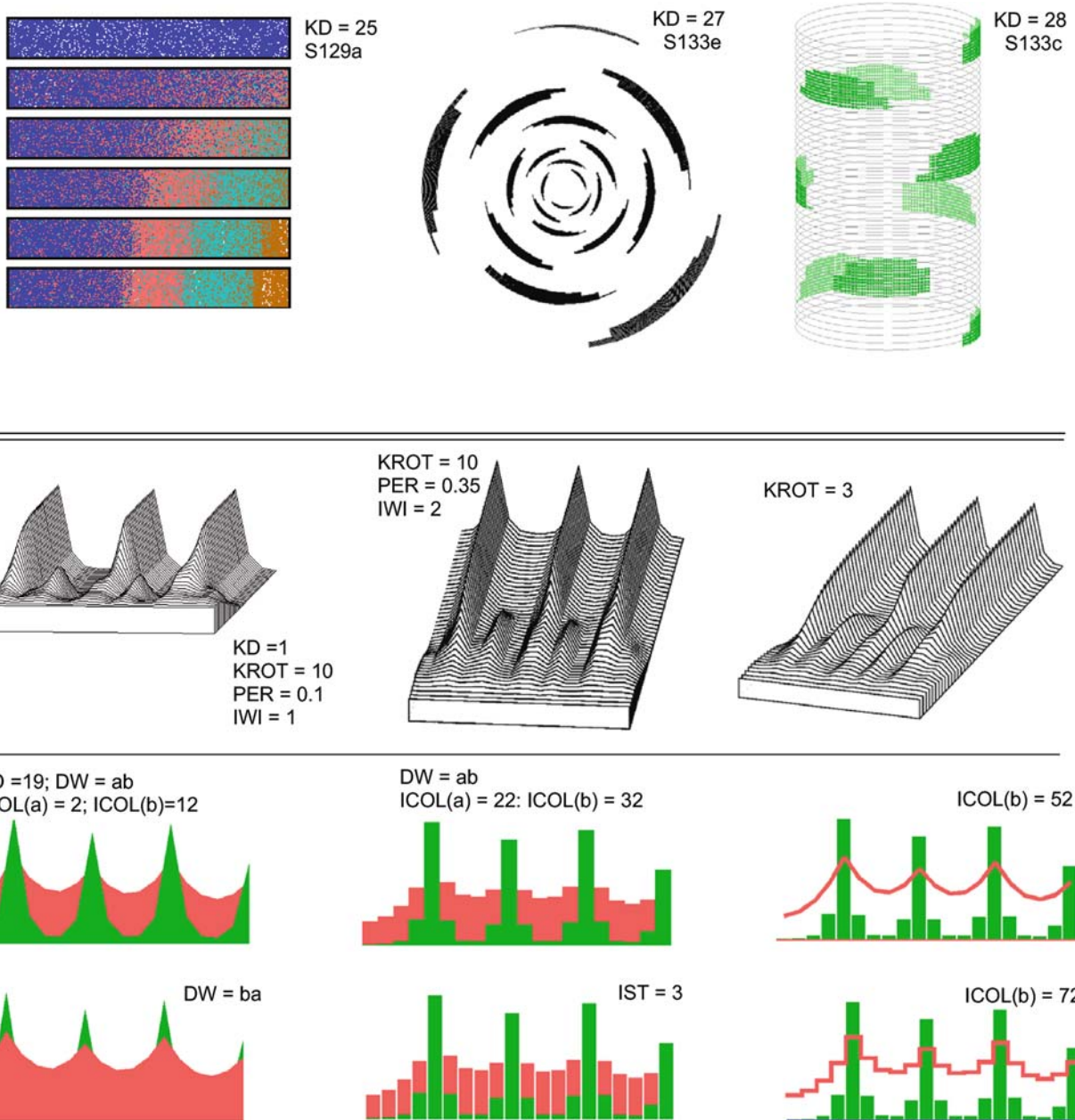


Figure 11.3. Top: Display types; continued from Figure 11.2 (see Table 11.4). Center and bottom: Examples of the influence of display parameters on the display for KD = 1 and 2 (center) and 19 (bottom); see also Table 11.5 (opposite page). In KD = 19: icol = 1...16, normal colors and filled areas, icol+20: filled step-like pattern, IST > 1 = gaps between blocks; icol + 40: nonfilled smooth curves; icol + 60: nonfilled step-like curves

Variables used for the graphic display

Examples are given in the lower part of Figure 11.3

- DX** Unit length of a cell in pixels, 2-6 is reasonable
- PER** Perspective in 3D-display mode; 0 is a front view, 1 is more from above, 0.15 - 0.5 is reasonable
- KROT** Side view in 3D-display mode, 1 is a more lateral view, higher numbers produce a more frontal view, but require more time and memory. If memory is exhausted, the plot will terminate. This may happen if several large arrays are plotted. For false-color plots (KD=6), KROT sets a lower threshold
- DW** “DisplayWhat” is a string and determines the substances to be plotted. For example, **ab** displays substances **a** and **b** [activator and inhibitor, array elements, e.g., **axt(1,i)** and **axt(2,i)**]. The sequence determines the plotting order. If DW is set to **ab**, the **a** distribution will be plotted on top of **b**; if DW is set to **ba**, they will be plotted in the reverse order (see Figure 11.3)

The following display parameters can be changed for each substance chosen with DW (DisplayWhat). The sequential input may be terminated by **q**, pressing <ESC> leaves a particular parameter unchanged and requests the next. Beginning a parameter value with the letter **g** (global) allows global definition, e.g., **X <RETURN> g50 <RETURN>** sets all X-coordinates to 50, causing all distributions to be plotted on the same X-coordinate.

- X** X-position of the plot (in pixel units, 640 * 480)
- Y** Y-position of the plot (in pixel units)
- F** Normalization factor, 1 is reasonable if concentrations are around 1
- ICOL** Color of the plot (0-15)
- IWI** Line width

In the Windows/Unix programs a screen resolution of 800 * 600 is used as standard; higher resolutions can be selected by the command **SCR** (Screen size):

SCR=1: VGA=640*480; **SCR=2:** 800*600 (default); **SCR=3:** 1024*768

SCR=4: 1280*1024; scaling of the screen remains 640*480, i.e., the relative size of the graphic remains constant

SCR 5 to 7: scaling as resolution, see **GT4** for use and effect

SCR =5: 800*600; **SCR=6:** 1024*768; **SCR=7:** 1280*1024

In the DOS versions, either the EGA or VGA screen may be used. The EGA screen has a lower resolution. However, since two screen pages are available, plots with frequent screen refreshes can be shown without much flicker; good for display modes KD=3 and KD=19 (see simulation S22); commands are **EGA** or **VGA**, respectively.

Table 11.5. Variables used for the graphic display

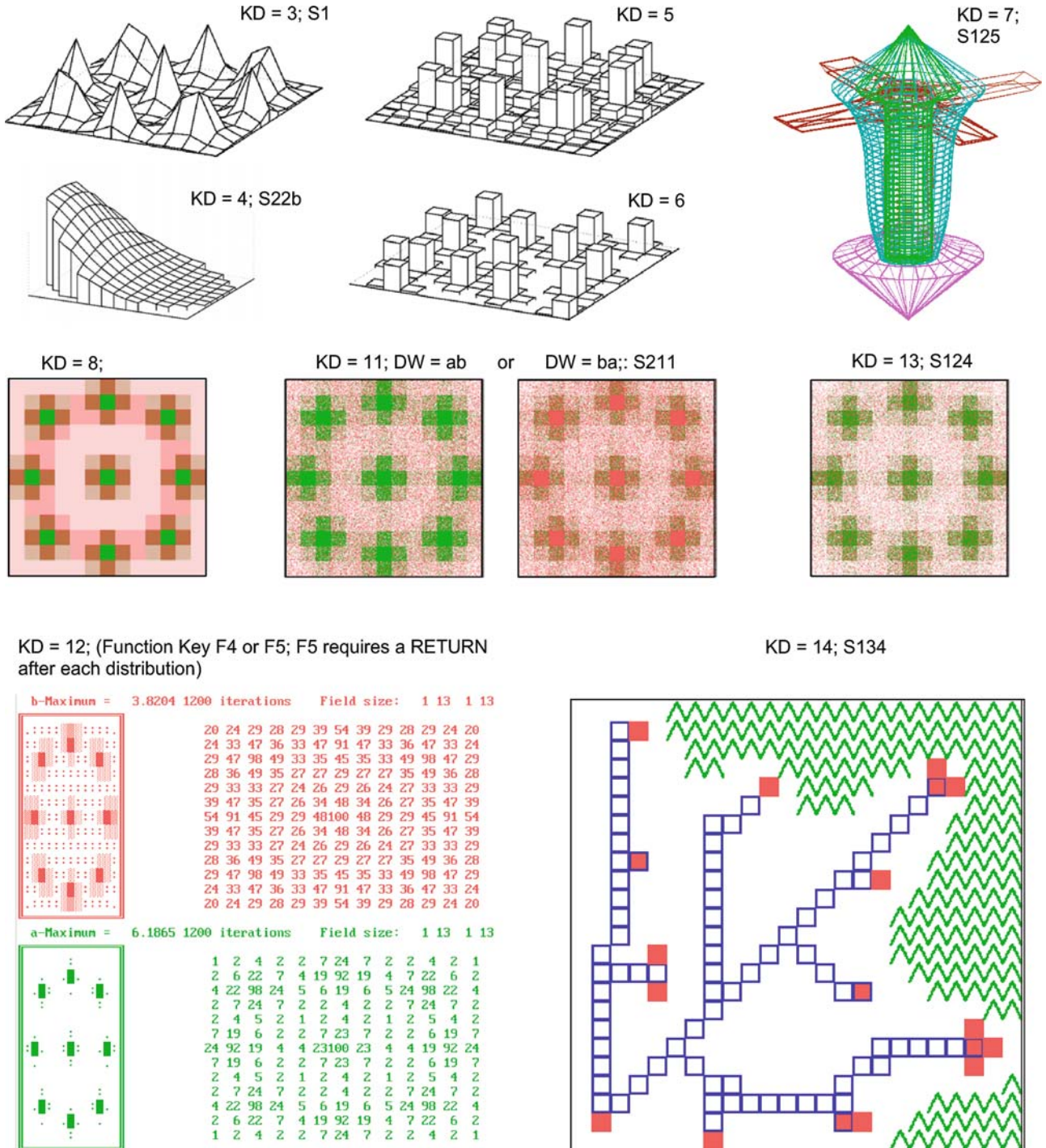


Figure 11.4. Display types for two-dimensional simulations; the parameter KD selects the display type indicated; Sxx is the command to run a simulation with the corresponding display type in the program XY. See also the GUIDED TOUR GT1 and the list by using F1

Initial conditions (parameter KI) for program SP

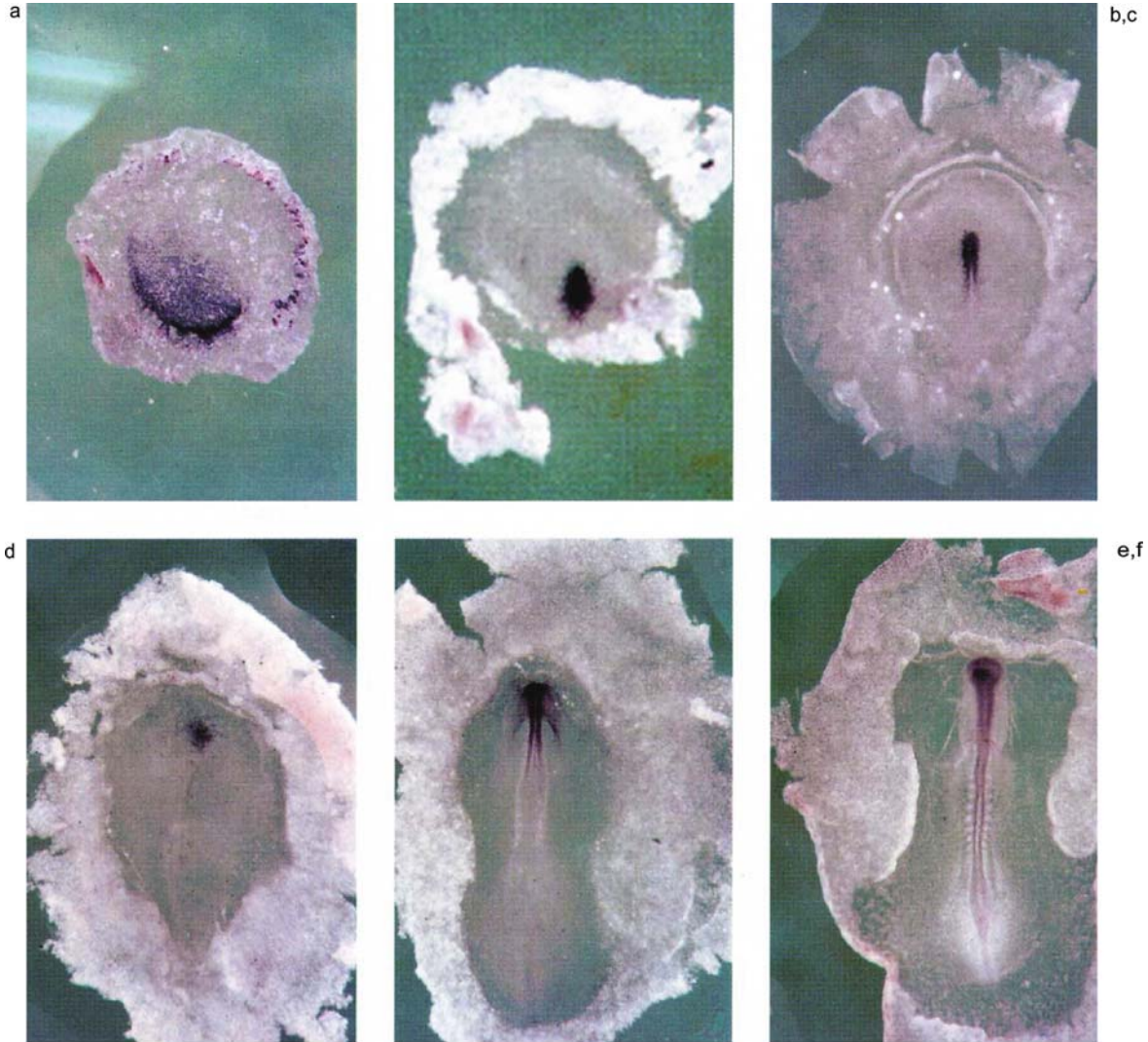
The first possibilities ($KI=1\dots6$) set the a , c , and e concentrations of specific cells to the concentrations given by parameters AA, AC, and AE, respectively.

- 1 Leftmost cell
- 2 Leftmost and rightmost cell
- 3 Central cell
- 4 Cell numbers are input from the keyboard (0=end of selection)
- 5 Specific cells (10, 22, 55, 75, 115, 180, 195, 240, 310, ...)
- 6 Cells at random positions within a distance of 10 - 40 cell

The following choices are available for the generation of stable prepatterns that act on substrate production. The patterns are stored in the array `axt(8, i)`. This mode is frequently used in the simulations for Chapter 4.

- 7 A sinusoidal prepatter is generated, maximum value = 1 (see Figure 4.9). Other variable settings required:
 - DY Degree of modulation, DY=1 causes a ratio of 1 to 0.5
 - K1 Repeat length of the pattern in cells
 - K2 Position of the maximum (phase)
- 8 Source density s has an exponential distribution, exponent given by AB.
- 9 A more step-like prepatter is generated (see Figure 4.2). Other variable settings required:
 - DY Degree of modulation, DY=1 causes a ratio of 1 to 0.5
 - K1 Repeat length of the pattern in cells
 - K2 Start of the HIGH cells
 - K4 End of the HIGH cells
 - DZ Degree of smoothing, 1-80 is reasonable
 - AB Slope of a superimposed linear gradient
- 10 Leftmost cell can have a different rate of substrate production. The factor is given in AB. This cell may act as a pacemaker region (see Figure 3.8)
- 11 Leftmost and rightmost cell may act as pacemaker regions (see Figure 3.9)
(see also list by using F1)

Table 11.6. Initial conditions (parameter KI) for program SP



Pattern formation in the development of higher organisms

The development of higher organisms out of a single cell is a most fascinating process. As an example, Figure 12.1 shows stages in the early development of a chick embryo. It was pointed out repeatedly that the mechanisms discussed for shell patterning are more general and of vital importance for pattern formation during embryonic development in higher organisms. In this chapter, some important steps in this development will be outlined and compared with corresponding models. In the subsequent chapter, some special biological phenomena will be discussed for which the lessons learned from the shell patterns were decisive for deriving the corresponding models.

The development of an organism is, of course, a highly complex process. It may appear hopeless to try and formulate an integral mathematically founded theory. Experiments revealed, however, that the individual steps are to some degree independent of each other. For the fruit fly *Drosophila* it has been shown that the pattern along the anteroposterior (head-to-tail) axis can be substantially modified without any effect on the dorsoventral (back-to-belly) patterning and vice versa. Different sets of genes are involved in establishing the two axes (Nüsslein-Volhard, 1996). Analogously, during the development of an arm, the anteroposterior (thumb to little finger) axis can be modified without much effect on the proximodistal axis (upper arm to digits, see Figure 12.10). Another example showing that closely



Figure 12.1. Stages in the development of a chick embryo. (a-f) The early chick embryo is a nearly flat disk located on the huge mass of yolk. Dark regions indicate a high activity of the gene *goosecoid*, a marker for the organizing region. First a crescent-like expression is seen (a) that sharpens to a small patch (b). Cells to the left and to the right of the organizing region move behind the organizer. Thus, part of the margin of the disk becomes deformed to a hair-pin-like structure, the primitive streak. The organizer, called Hensen's node, is initially still at the tip of the streak. The proper embryo emerges in a sequential process behind the organizer which moves towards the margin of the disk. Thus, new elements are added posteriorly until the tail is formed. This process goes on the expense of the primitive streak. (g-i) Schematic drawing showing the formation of the primitive streak by a hair-pin-like deformation of parts of the margin of the disk (g,h). The head lobe (yellow) is formed by an anterior movement of cells from the organizer (green). With the movement of the organizer, the primitive streak regresses in favor of the final organism (i) (for modeling, see Meinhardt, 2006 and material on the CD; photographs kindly supplied by Lydia Lemaire, see Lemaire et al., 1997)

related processes can be separated from each other comes from cell-to-cell communication. The *formation* of a signal can frequently be distinguished from the *response* of the cells. If the generation of the signal is abolished in the decisive patch of cells that produces the signal, this has long-ranging effects on the surroundings of the perturbed region; the effect is not cell-autonomous. In contrast, if a patch of cells can no longer receive the signal due to a mutation, only the defective cells are affected. Therefore, since one can separate the complex process into elementary entities, it makes sense to develop models for each of these elementary steps. To model more complex systems, several of these elementary processes must be linked to each other.

Basic principles have been deduced from meanwhile classical experiments in which normal development has been perturbed. Frequently, development returns to normal even after severe perturbations, revealing that development is a highly dynamic and robust process. The regeneration of removed parts is the most obvious example. Model organisms have been used that are especially accessible. The fresh water polyp hydra regenerates a new head after the head is removed. Similarly, an early sea urchin embryo can be divided in two or more fragments and each one will regenerate a complete embryo. In an early mammalian embryo, such a split can occur spontaneously. This is one of the mechanisms that can lead to identical twins. These observations demonstrate that the cells communicate with each other. Interrupting this communication can reprogram some of the remaining cells such that a fragment can give rise to a complete embryo.

Several generalizations and concepts have been extracted from these experiments. *Long-ranging inhibition* emphasizes the fact that a given structure frequently suppresses the formation of the same structure in its neighborhood (Browne, 1909; Schoute, 1913). The notation of the *organizing regions* has its origin from the observation that a particular group of cells can have the capability to direct the fate of the surrounding tissue (Spemann and Mangold, 1924; Browne, 1909; see Figure 12.3). The concept of *Positional Information* was derived from the fact that many experimental observations can be accounted for by the assumption that a local source region gives rise to a graded concentration profile of a signaling molecule. The exposed cells are assumed to measure the local concentration of this morphogen gradient and differentiate accordingly (Hörstadius, 1939; Wolpert, 1969).

We applied these classical results to determine what the minimum requirements would be for a molecular machinery to account for the observed patterns and pattern regulations. The mechanisms described in Chapter 2 resulted from an attempt to understand pattern formation from initially more or less homogeneous situations. In the following it will be shown that the proposed mechanism of *local self-enhancement and long-ranging inhibition* accounts for many observations in organizer formation and in generating periodic structures such as hairs or leaves. Some additional mechanisms will be discussed that are involved in generating more complex patterns. For instance, signaling between cells requires not only the generation of signals by specific groups of cells but also a response of the cells to such

signals. In this way particular genes are activated in a position-dependent manner, allowing cells to differentiate appropriately. An all-or-nothing response of cells can produce sharp borders. In turn, these new borders can become new signaling centers that provide positional information to further subdivide the adjacent regions. The initiation of legs and wings at precise positions depends on such a mechanism (see Figure 12.11). Many of these models were proposed at a time when the molecular basis of development was completely unknown. The models found strong support by more recent observations at the molecular-genetic level. A first example is given in Figure 12.2. This general correspondence shows that modeling is an appropriate tool to decode the logic behind the development of complex organisms.

In the search of the genes responsible for controlling development, the fruit fly *Drosophila* has turned out to be a convenient model organism. By introducing embryonic-lethal mutations, Nüsslein-Volhard and Wieschaus (1980) succeeded in establishing an almost complete list of genes involved in the early development of that organism. Their experiments have shown which structures can still be formed in the absence of a particular gene. When, a few years later, it became possible to clone particular genes and to sequence the corresponding DNA, a dramatic breakthrough was achieved. After cloning genes from the fly, it became possible to extract related genes from other organisms that are less accessible to molecular-genetic analysis, too. It turned out that most of these genes are remarkably well conserved during the evolution of the different species. For instance, closely related genes control the anteroposterior (head-to-tail) axis in *Drosophila* and in vertebrates. Also, the crucial genes required for patterning the dorsoventral (back-to-belly) axis and for initiating legs and wings are highly conserved. The latter is especially surprising since the common ancestor had presumably not yet evolved appendages. In this way, the *Drosophila* research opened a new era in the understanding of the molecular basis of development.

Drosophila was chosen as a model organism because of its short generation time. Starting with the fertilized egg, it takes only three hours to form the future embryo, which consists of a layer of about 5000 cells. At this stage essentially each of these cells is specifically programmed for its future fate by position-dependent gene activation (see Lawrence, 1992). This exceptional speed during early development is achieved by positional information systems that are already established within the developing egg under maternal influence. Thus, the formation of local signaling centers does not depend on a time-consuming communication and competition between the cells of the developing embryo as is the case in mice, frog, fish, or chick development. Therefore, the early development of *Drosophila* is not a prototype for early development in general. Even in other insects development proceeds in a different manner. In contrast, processes involved in later steps of *Drosophila* development seem to be more similar in all insects. The initiation of legs and wings is an example. Therefore, for the investigation of primary pattern formation, it is necessary to work with other model systems even though these are more difficult to handle.

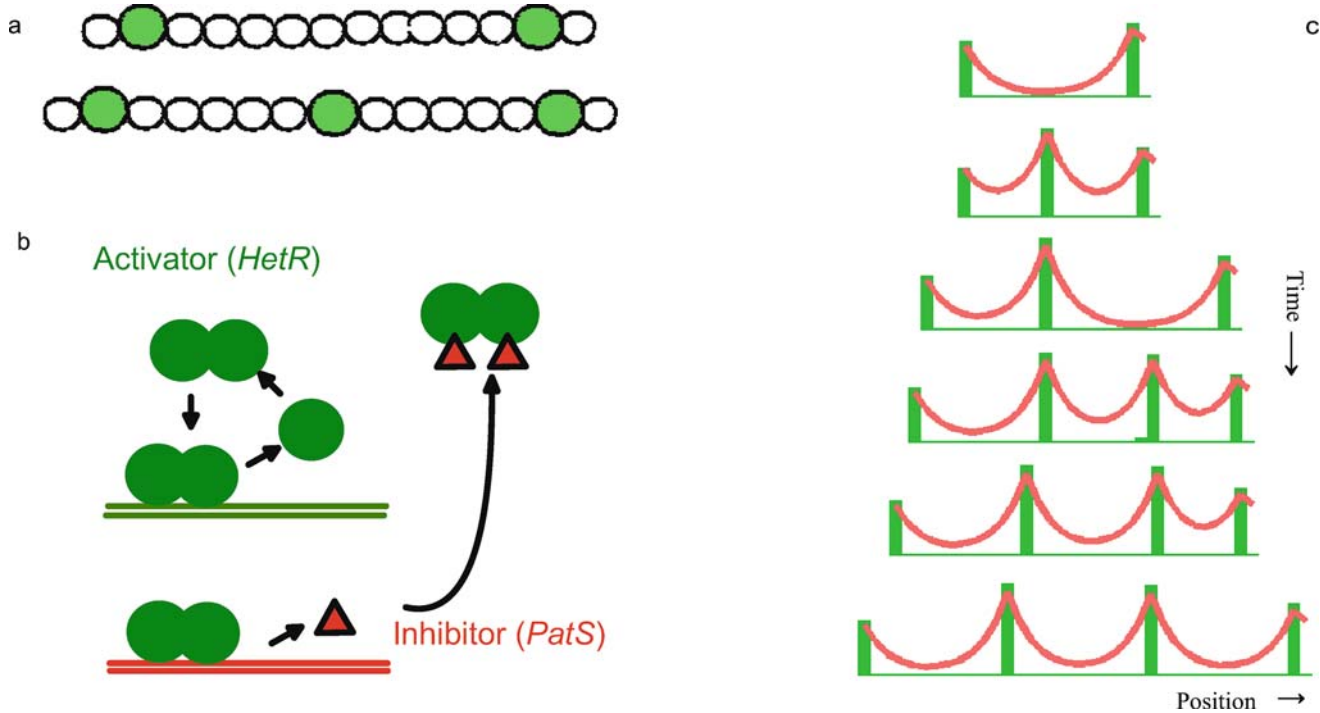


Figure 12.2. Pattern formation in *Anabaena* - an example for employing an activator-inhibitor system. The blue-green alga forms linear chains of cells. (a) Under low nitrogen conditions, nitrogen-fixating cells - so-called heterocysts - are formed. They are separated from each other by about 10 - 12 normal cells. Whenever the distance between two heterocysts (green circles) in the linear chain of cells becomes larger than ca. 12-14 cell, a normal cell differentiates into a larger, nondividing heterocyst. It is the cell that is farthest from the existing heterocysts. (b) Heterocyst formation is under control of the transcription factor *HetR*. *HetR* forms dimers that directly activate *HetR* transcription (Huang et al., 2004). Dimerization satisfies our prediction that the autocatalysis must be nonlinear (Eq. 2.1). *HetR* also activates the formation of a small peptide, *PatS* (triangles), that can spread through intercellular junctions (Yoon and Golden, 1998) and that can bind to *HetR*. If *PatS* is bound to *HetR*, DNA binding of *HetR* is no longer possible. Thus, *PatS* inhibits the activator autocatalysis, as predicted. (c) Simulation: only the inhibitor can diffuse across the cells. Therefore, activations occur in isolated cells. Whenever the inhibitor drops below a threshold level, the onset of autocatalysis of the activator is triggered from a baseline activation (b_a in Eq. 2.1a). Since the inhibitor distribution around a minimum is shallow, initially more than one cell can start this activation process. Due to competition only one isolated cell eventually becomes activated. In agreement with the expectation from our theory, if *HetR* is mutated, no heterocysts are formed. In contrast, if *PatS* is mutated, most cells form heterocysts (Buikema and Haselkorn, 2001). A closely related model for *Anabaena* was independently proposed by Wilcox et al. (1973) [S122]

12.1 Hydra, a versatile model system

The small freshwater polyp hydra is most famous for its almost unlimited capability for regeneration (Trembley, 1744; von Rosenhof, 1755; see also Gierer, 1977; Bode, 2003). Even more dramatic, hydra tissue can be dissociated into individual cells and, after re-aggregation, these clumps of cells again form viable organisms (Figure 12.3). Obviously, pattern formation does not require any initiating asymmetry and can proceed in a self-organized way.

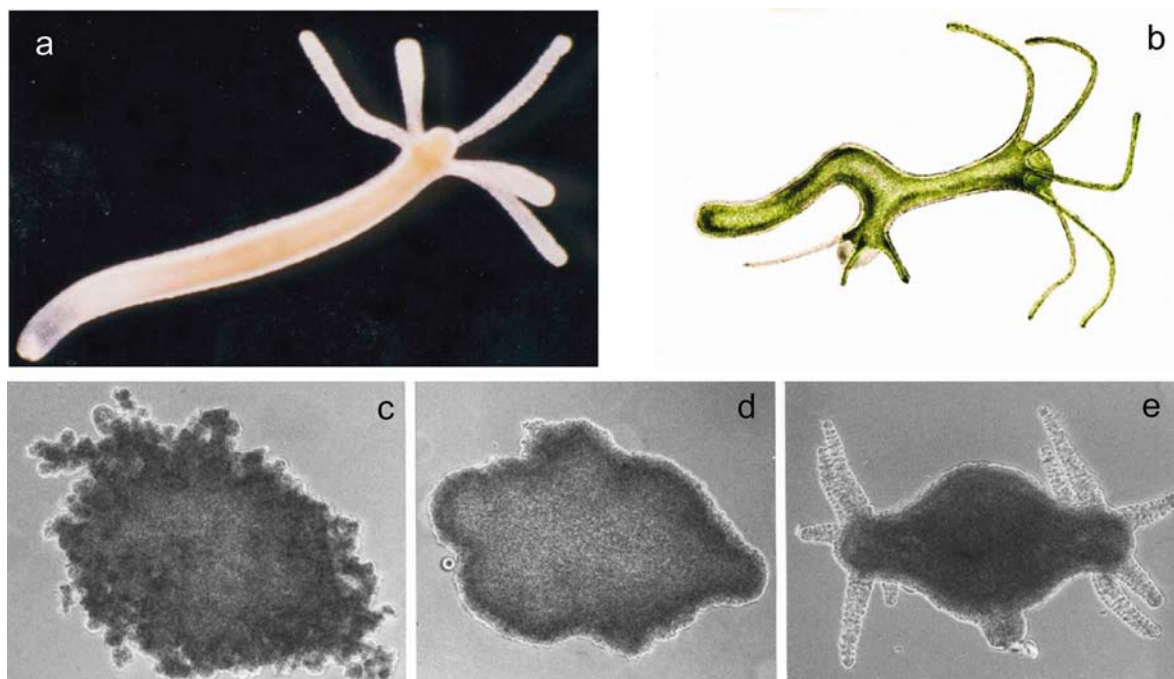


Figure 12.3. Pattern formation can start from an initially homogeneous situation. (a) The freshwater polyp hydra. (b) The tip of mouth opening, the so-called *hypostome*, can act as organizing region. Ethel Browne transplanted a small tissue fragment from the hypostome of a white hydra into the body column of a green hydra (adapted from Browne, 1909). The green staining of the newly formed tentacles indicates that they are formed from host tissue, demonstrating that the implanted hypostome tissue can instruct the surrounding cells. (c-e) Hydra tissue has an outstanding capability for self-organization. Even after complete dissociation into individual cells and re-aggregation, clumps of cells are able to reform complete animals (Gierer et al., 1972; figures kindly supplied by T. Holstein and U. Technau)

As discovered by Ethel Browne in 1909 by transplantation experiments, the small cone-shaped region around the gastric opening, the hypostome, has organizing capabilities (Figure 12.3b). A small tissue fragment from this region transplanted into the body column of another animal can induce the formation of a secondary body axis. Although Browne did not explicitly use the term ‘organizer’, she discovered a phenomenon that became of central interest 15 years later with the discovery of the amphibian organizer (Spemann and Mangold, 1924; see Lenhoff, 1991). Thus, hydra can be used as a guide to find the corresponding interactions that underlie de novo organizer formation and its regeneration. Moreover, hydra patterning displays several basic elements that are required for the patterning of higher organisms. Like many other systems, hydra is controlled by two organizing regions at antipodal positions, the head and the foot, raising the question how such a bipolar organization is achieved. With the formation of tentacles next to the organizing hypostome, hydra offers an inroad of how to initiate two structures at adjacent positions. Finally, hydra can maintain its overall polar pattern with a single organizer over a surprisingly large range of sizes, a precondition for small fragments to regen-

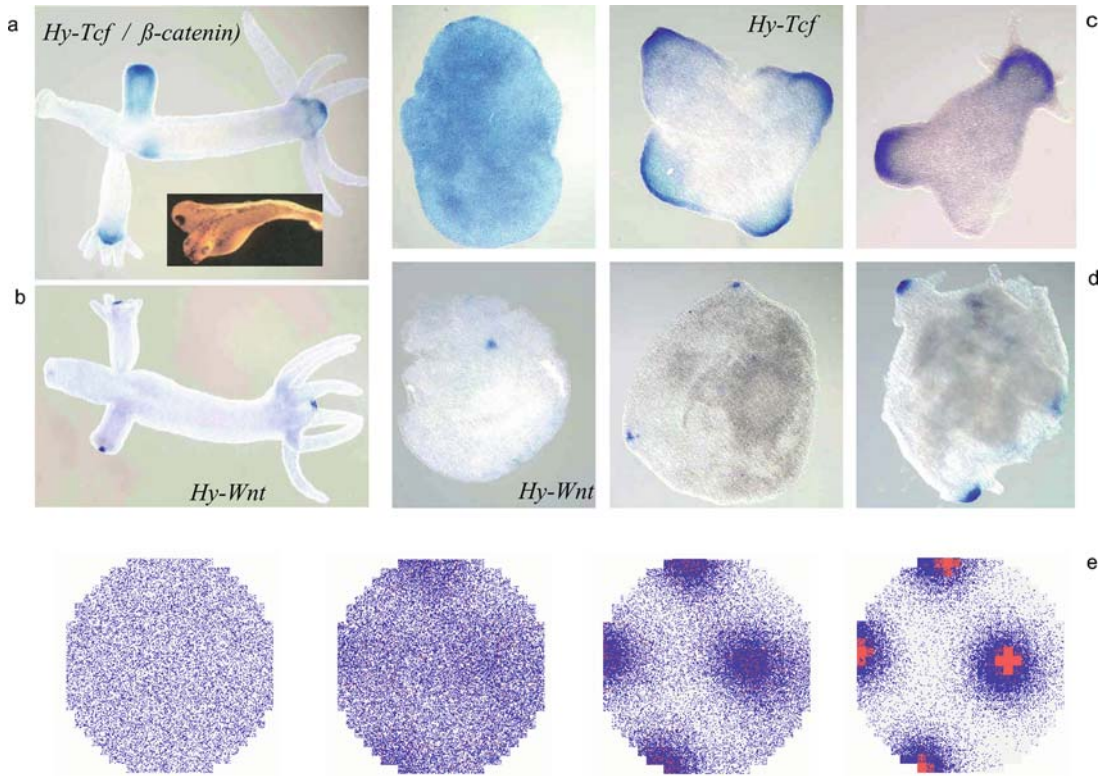


Figure 12.4. The *Wnt* pathway, involved in many developmental steps, is also involved in the formation of the hydra organizer. (a) *Tcf* (and β -catenin) expression occurs in a graded fashion at the hypostome and also precedes the formation of a new axis during bud formation. Insert: β -catenin isolated from hydra can trigger a second axis in *Xenopus* (Hobmayer et al., 2000). (b) *Hy-Wnt* expression is more sharply confined to the tip. (c) In re-aggregating cells, *Hy-Tcf* (and β -catenin) first appears uniformly distributed and becomes subsequently more restricted to regions that eventually form the new heads. This is the behavior as expected by the model. (d) In contrast, *Hy-Wnt-3a* appears directly in sharp spots that form the future oral opening. (e) This nested pattern formation can be accounted for by the assumption that both *Hy-β-catenin / Hy-Tcf* (blue) and *Hy-Wnt* (red) are pattern-forming systems and that a high *Hy-β-catenin* concentration is the precondition to trigger *Hy-Wnt*. Thus, *Wnt* peaks require a high *Hy-β-catenin / Hy-Tcf* level and appear as sharp spots at the highest level of the more graded *Hy-β-catenin / Hy-Tcf* distributions. Such a superimposed patterning allows to specify a large region for head formation and provides, nevertheless, a sharp signal, e.g., for the opening of the gastric column (Photographs by courtesy of B. Hobmayer, T. Holstein and colleagues; see Hobmayer et al., 2000). Other components required for the patterning of hydra such as the inhibitor are still unknown [program XY; S124]

erate. Possible molecular interactions found by modeling that account for these steps will be discussed in the next sections. Several molecules involved in hydra patterning are known (Figure 12.4) but essential components are still missing.

Coelenterates (to which hydra belongs) are presumably the evolutionary lowest phyla that have a clear axial polarity. In recent years it has turned out that the patterns of gene expression in hydra and its close relatives corresponds to that found in brain and heart formation in higher organisms, suggesting that the body of these evolutionary ancestral creatures evolved into the brain and the heart of higher

organisms (Meinhardt, 2002). Thus, hydra and its relatives provide a key to study the major evolutionary inventions that occurred on the way from ancestral organisms with a clear axial organization to the more complex body patterns of higher organisms. A milestone on this way was the invention of the trunk, supplementing the anterior body part that evolved towards the brain. Further, to be able to move efficiently, e.g., to swim, it was a great advantage that the extension of the head-to-tail axis became much greater than that of the back-to-belly axis. To organize a body with a tube-like geometry, a stripe-like organizing region is required to specify the structures around the cylinder. The local concentration of a corresponding signaling molecule can provide positional information for the dorsoventral axis. Usually the highest level determines the position of the central nervous system along the body axes. The formation of such a solitary stripe-like organizing region is a subtle patterning process for which nature found different solutions (Meinhardt, 2004). In the next paragraphs the elementary patterns mentioned above and the evolutionary aspects of axis formation will be discussed.

12.2 Tissue polarity and graded competence

Experiments have indicated that many tissues have a hidden asymmetry. Hydra is a well-investigated model system that illustrates this feature (Figure 12.5a). Isolated small pieces of the gastric column always regenerate the new head at the side that was closer to the original head. The same rule holds for the foot. Thus, after fragmentation, it depends on the *relative* position of the cells within a fragment as to whether they participate in head or in foot regeneration (Figure 12.5a). Cells closer to the original head have an advantage in the competition to produce the new head signal. In this way, each fragment has an internal asymmetry that *orients* the regenerating pattern, independent of its original position within the animal. This requires a long-ranging feedback either of the activator or the inhibitor on the ability of the cells to synthesize the components of the pattern-forming reaction. We termed this ability *source density* (s in Equation 2.1, page 23). A graded source density corresponds to the graded *competence* for organizer formation that is observed in many biological systems. Cells closer to the original head have thus a ‘head start’ in the competition to form a new head signal. After removal of the original head and the decay of the remaining inhibitor, it is clear which part will win. This type of feedback on the source density was already used in simulating some shell patterns (Figure 4.11). An organizing region thus exerts two seemingly conflicting effects. On the one hand, it inhibits the formation of other organizing regions. On the other hand, it promotes organizer formation by keeping the cells competent. Why do the two effects not cancel each other? Inhibiting and maintaining competence have different time constants. The inhibitor must have a rapid turnover such that a new organizer can reappear shortly after the original organizer is removed (as discussed in length in Chapter 3, a longer time constant of the antagonist leads to

oscillations rather than to stable distributions). In contrast, the competence has a long time constant; it remains almost unchanged within the period required for pattern regulation (Figure 12.5).

Since the complementary influence of organizing regions is crucial for explaining many biological observations, it is worth illustrating the situation with an anthropomorphic analogy. A king, president, or any other figure in power usually has a strong tendency to suppress others from taking over - a long-range inhibition. On the other hand, he promotes individuals among his courtiers to obtain a higher ranking, to become ministers, etc. In this way, the center of power generates a hierarchy. Inhibition and promotion are two closely interwoven processes. If the top position becomes vacant, due to this nonuniformity, a fight will commence only between the few who have high ranking in the hierarchy. Usually proximity to the former center is an advantage. In the short time interval until a new hero is selected, the ranking in the hierarchical pyramid remains essentially unchanged. This analogy also illustrates what can happen if the whole hierarchy is eliminated, for instance, in a revolutionary situation. Many rivaling centers and civil-war-like situations could emerge, with all their unpredictable consequences.

The described *stabilization* of an activator peak by a positive long-lasting feedback is in contrast to the *destabilization* of maxima shortly after their generation by a negative feedback, as used extensively to simulate particular shell patterns (Chapter 5: as shown in the next chapter, such destabilization also plays a role in many other systems).

12.3 How to avoid periodic structures during growth

Why does nature employ a graded competence although pattern formation also works without this feature? Modeling suggests that this is a means of maintaining a polar structure during growth. In a normal activator-inhibitor system, first a single activator maximum appears at one terminal end of a growing field (Figure 2.9). However, with further growth, more and more maxima would normally appear (see Figures 2.7 and 12.2). This is appropriate if certain periodic structures such as hairs, bristles, or leaves must be formed. For the generation of embryonic axes, however, a single organizer must be maintained despite substantial growth; otherwise, supernumerary and possibly partially fused embryos will be produced. Again, hydra is a good model system since a small hydra can grow by about a factor of ten without losing its polar character. According to the model this is achieved by the graded competence introduced above. With increasing distance to an existing maximum, not only the inhibitor concentration but also the source density, i.e., the ability to generate a new maximum, decreases (Figure 12.5). This dramatically enhances the dominance of the primary maximum. Cells distant to the organizer lose their competence to form an organizer. They can become unable to trigger a secondary organizer even when the inhibitor drops to very low levels due to growth. Such fad-

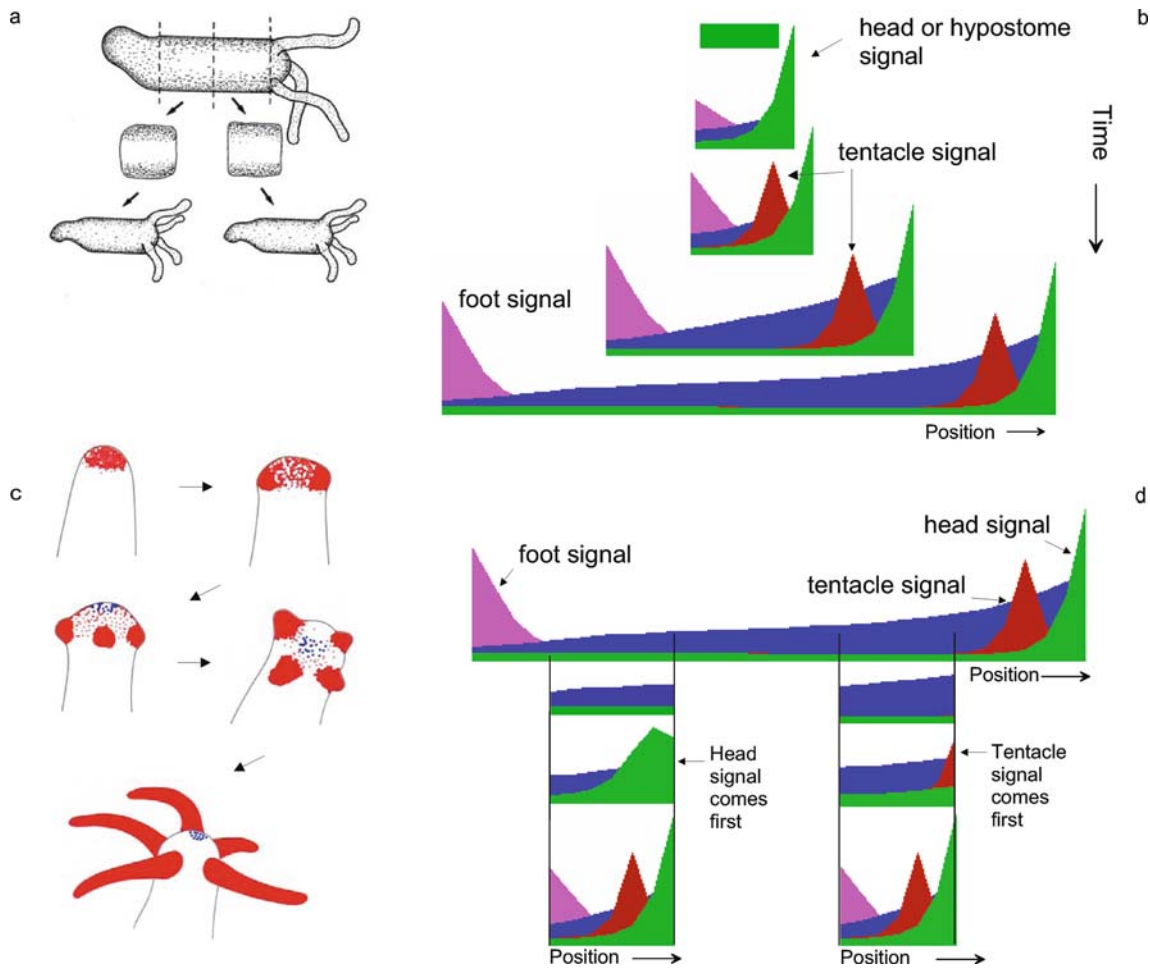


Figure 12.5. Model of pattern formation in hydra. (a) Small fragments of hydra always regenerate with the original polarity. Depending on their position within the fragment, cells that are originally adjacent may form either a head or a foot after separation. (b) Model: the signals for the formation of the head (green), tentacles (red), and foot (pink) are assumed to be generated by separate activator-inhibitor systems. Head and foot signals emerge spontaneously at opposite positions due to a feedback on the ability of the cells to perform the pattern-forming reaction, the source density (blue). (c) During regeneration, first the cells at the extreme tip become programmed towards tentacle formation (visualized by antibodies, shown here in red). The head signal (green) appears later. (d) In the simulation, small fragments regenerate all signals with the correct polarity. In a piece from near the head (right), the tentacle signal (red) is formed first at the very tip since there the source density is highest. Later it becomes displaced to its final position due to the repulsion of the later emerging head signal. In a fragment derived from a lower part of the body column (left), the source density is too low to trigger the tentacle system directly. Therefore, the head signal is formed first, and the tentacle signals appear subsequently after sufficient increase in source density at the correct positions, in agreement with the experiment (Bode et al., 1988; Technau and Holstein, 1995; simulations after Meinhardt, 1993) [hydra simulations are shown in GT125; for the role of the source density, see GT125a; for the formation of a sequence of structures by several coupled activator-inhibitor systems, see GT125b; for general properties and regeneration see GT29; for two-dimensional hydra simulations, use program XY: GT125].

ing of the competence is an essential process in making development reproducible; otherwise, new organizing regions would emerge in an uncontrolled way (see the computer simulations in the GUIDED TOUR GT12-6a on the enclosed CD).

12.4 How to generate structures at a distance: head and foot of hydra

Frequently, embryonic fields are organized by two organizing regions located at antipodal position. In early plant development, the shoot and the root are two such opposing organizers. In hydra, both the head and the foot act as organizing regions.

What interaction would force two organizers to emerge at the largest possible distance? One could envision two activator-inhibitor systems in which inhibitors have some cross-reaction. Then, the head inhibition would also inhibit the foot system and vice versa. The foot activation would appear at the largest possible distance since at this position the cross-inhibition would be least. For some systems such a simple cross-reaction could be sufficient. For hydra, however, a severe problem would emerge. In a small fragment containing the head, the regenerating foot must appear very close to the existing head. Cross-inhibition over such a short distance would be so strong that foot regeneration would be suppressed, in contrast to what is observed. (For the shell patterns, the possibility for suppressing spontaneous initiation of new activation peaks by low-level inhibition has been used repeatedly; see Figure 6.1).

The possibility that a head and a foot can appear close to each other suggests that their antipodal localization is not achieved by a direct inhibition. As explained, the head signal appears where the source density is highest. If the foot signal has the opposite behavior, it will appear where the source density is lowest, i.e., at maximum distance from the peak of the head activator. In this interaction, the head has no direct inhibitory influence on the foot, but is generated by means of the graded source distribution with a *preference* for the foot to appear at the opposite pole. Therefore, in a small animal, head and foot signals can coexist. Observations indicate that the foot also has an influence on the polarity. This feature can be integrated into this model by assuming that the foot reduces the source density. Therefore, in the model, both head and foot contribute to the generation and maintenance of the graded source density, and thus to the polarity of the tissue. The simulations in Figure 12.5 shows that the model accounts for the formation of the head and foot signal at the terminal ends, for the coexistence of the head and the foot in small regenerates, and for the maintenance of polarity during growth and regeneration.

12.5 Induction of adjacent structures

During development, many structures are formed close to each other in direct proximity. Again, hydra with the hypostome and the surrounding tentacles shows this feature (Figures 12.3 and 12.5). A controlled neighborhood can be achieved if a primary signaling system activates a second system with a range that exceeds the extension of primary structure. Locally, however, the two structures exclude each other, thus keeping them separate (Meinhardt and Gierer, 1980). This activating influence of one structure onto another can, but need not be mutual. The periodic nature of the tentacle pattern indicates that the tentacles are generated by a separate pattern-forming system, i.e., they are not just induced by a particular concentration of a signaling substance produced in the hypostome region.

The assumption of lateral inhibition accounts for the spacing of the tentacles but raises another question: why is tentacle formation restricted to this narrow ring. Considering their range of inhibition, why tentacles do not form all over the body column? Several lines of evidence indicate that tentacle formation depends on the source density, i.e., the competence, which is generated by the primary head organizer (Figure 12.5). In this way, the head organizer creates the precondition for tentacle formation. Due to the graded source density, the tentacles formed near the head are dominant over a long range and suppress other tentacles along the body column. If the source density is experimentally elevated everywhere, tentacles form all over the body column Figure 12.6.

The mechanism of long-range mutual activation and short-range exclusion is also widely used in other systems, e.g., in insect segmentation. Details and corresponding simulations are available on the enclosed CD and demonstrated in the GUIDED TOUR GT125b.

Taking these observations and their modeling together several conclusions can be made. (i) The primary organizer keeps nearby cells in a competent state. Cells further away become incompetent for organizer formation, making sure that only a single organizer exists in the system despite growth. (ii) This graded competence (source density), generated by the primary organizer, acts as a prerequisite to form adjacent structures. A local exclusion ensures that the secondary structures appear at a certain distance. (iii) Two organizers can be forced to appear at antipodal positions if each organizer creates local conditions that are nonfavorable for the other: what is good for head formation is bad for foot formation and vice versa. Since there is no direct inhibition between the two organizers, this antipodal positioning is attained within both large and small pieces of tissue.

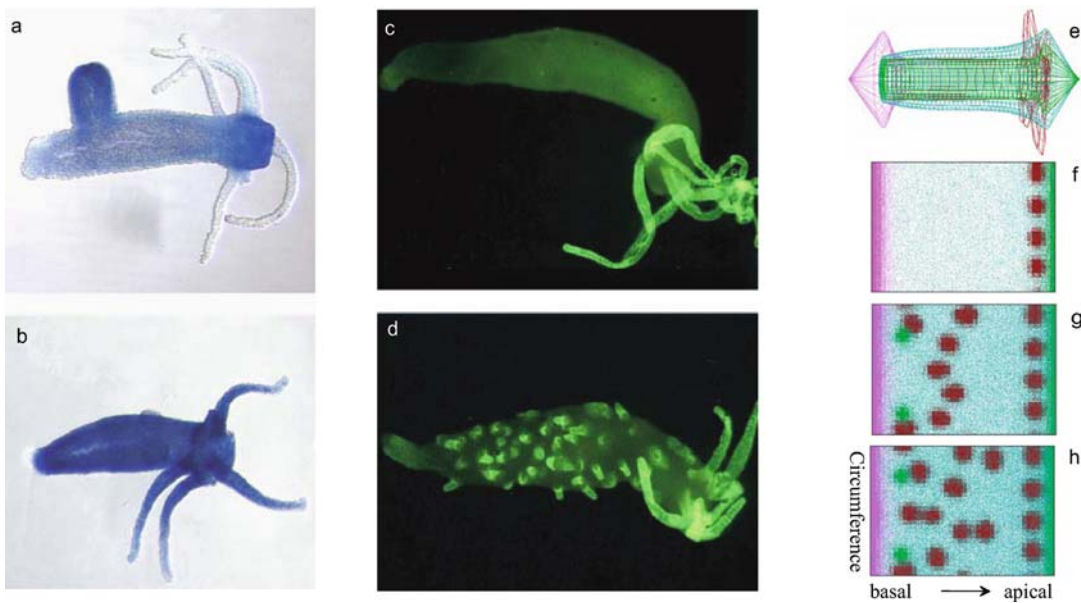


Figure 12.6. Drug-dependent formation of tentacles everywhere. (a) The expression of the gene *Tcf* (and β -catenin) is indicative for head formation (Hobmayer et al., 2000). (b) After treatment with the drug *Alsterpaullone* these genes are expressed everywhere in the hydra. (c) Normally tentacle formation is restricted to the head region; tentacle specification is visualized by a green staining with a specific antibody. (d) After treatment, tentacle formation occurs everywhere (Broun et al., 2005). (e-h) Model: normally the source density (competence, blue) is high enough for tentacle formation (dark red) only in the head region. In (e) the concentrations are plotted around a cylinder, in (f) the cylinder is cut open. (g,h) After an increase in the source density (competence, blue), tentacle formation is possible nearly everywhere. This process starts at a certain distance from the natural tentacles, in agreement with the observations (d). Also new head signals (green) may appear. Figures (a-d) kindly supplied by Hans Bode, see Broun et al., 2005. [program XY; GT126])

12.6 The evolution of the main body axes

Simple, more or less radial-symmetric animals, including hydra or the small sea anemone *Nematostella*, are descendants of evolutionary ancestral organisms that were close to the branch point at which bilaterality was invented. In recent years it has turned out that the molecular mechanisms on which development is based are surprisingly well conserved. As mentioned above (Figure 12.4) injection of a hydra-derived molecule (β -catenin) into an early frog embryo can cause axis duplication there. Therefore, it is reasonable to assume that hydra and its relatives can be regarded as living fossils and as a source for insights into the basic steps that lead from simple to more elaborate body plans. While the primitive organisms are more or less radially symmetric, higher organisms have an anteroposterior (head-to-tail), a dorsoventral (back-to-belly) and, especially vertebrates, a left-right axis. Parallel to this increased richness in the spatial organization was the formation of a wealth of organs, such as a clearly separated trunk, legs and wings, and the most intricate organ, the brain.

An exciting question was whether it is possible to relate the single axis of a hydra to one of the main body axes in higher organisms. Do the head-foot axis of hydra and the head-tail axis in higher organisms have anything in common? The answer was a surprise, at least for me. A comparisons of gene expression patterns revealed that the body pattern of a hydra corresponds, in terms of gene expressions, to the anteroposterior pattern of our brain. In addition, the orientations of the axes were a surprise. Although called ‘head’, the gastric opening of a hydra is the most posterior part, the anus. In contrast, the foot corresponds to the most anterior part, the forebrain and the heart (Meinhardt, 2002). The hydra foot has pumping activity for the gastric fluid; it is remarkable that foot formation depends on the *same* gene (*Nkx2.5*) that is crucial for heart formation in insects and vertebrates, suggesting that the hydra foot and the vertebrate heart have a common ancestry (Shimizu and Fujisawa, 2003). In most of the hydra body a gene is expressed that forms the fore- and midbrain in vertebrates (*Otx*). Hydra already has a diffuse nerve network. These observations suggest that the system that was once responsible for the body patterning of ancestral organisms evolved into the system that is now responsible for the initial patterning of the brain.

An important evolutionary novelty, essential for organized animal movement, was the trunk. Characteristic for the trunk in higher organisms are the so-called HOX genes. These genes are absent in hydra and its relatives, suggesting that the trunk was a later invention. Even the precise location at which the trunk became inserted into the ancestral body plan during evolution can be reconstructed. In hydra, two genes are expressed close to each other in the cone-shaped hypostome, *Goosecoid* and *Brachyury* (yellow and red ring in Figure 12.7a). Early in vertebrate development, these two genes were also expressed at adjacent positions but become separated during trunk formation. While *Goosecoid* expression remains restricted to the head, *Brachyury* is expressed at the posterior end and in the emerging midline (see below), suggesting that the border between the two regions of gene expression marks the zone where the trunk became inserted. The sequential formation of the trunk near the posterior pole is common in development of higher organisms.

In addition to the trunk, a second most important innovation was the organization of the axis perpendicular to the anteroposterior axis, i.e., the dorsoventral (DV) or back-to-belly axis. To allow a combinatorial positional specification of a long and extended tube-like organism and, for instance, a bundling of the nerves into a central nervous system, a stripe-like signaling center is required that stretches from the anterior to the posterior pole of the organism. The local concentration then provides information about the distance of a cell to the organizing midline. In modeling the formation of a solitary straight midline poses an intricate patterning problem. As shown above, stripe-like patterns can emerge if the self-enhancement in a patterning system saturates at high activation levels (Figure 2.12). However, these stripes not only bend and branch. The width of the stripe and the distance between the stripes is of the same order. These features are characteristic for many stripe-like patterns, such as the proverbial zebra stripes. These features, however,

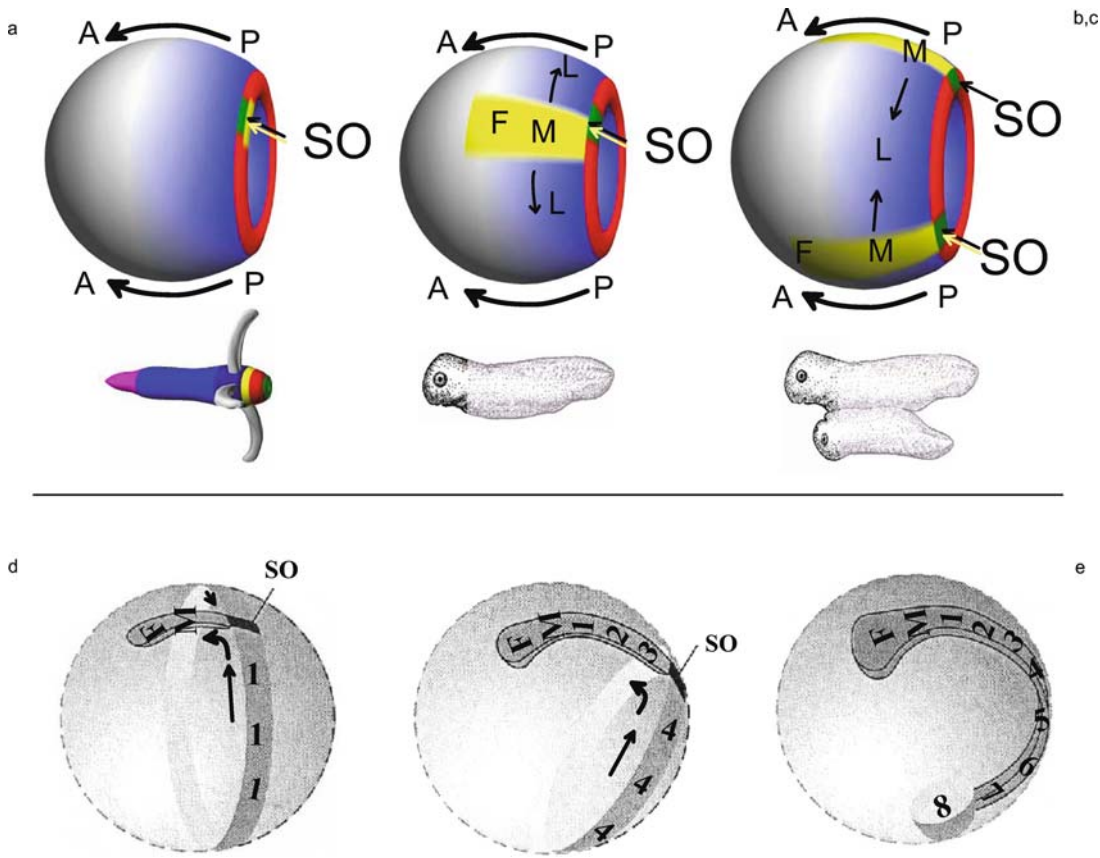


Figure 12.7. A model for the generation of a near-Cartesian coordinate system in two steps - taking the amphibian embryo as an example. (a) AP patterning of the early gastrula is assumed to be accomplished by a system that was already involved in the body patterning of ancestral organisms. The marginal zone (red) is assumed to be equivalent to the hydra organizer. These blastoporal rings, small in hydra and huge in amphibians, are the source region of a signaling substance, *Wnt*, that controls anteroposterior determination in a gradient-based manner (fading blue, see also Figure 12.9). The cells of the marginal zone form mesoderm. The Spemann organizer (SO, yellow), a small patch of cells with signaling properties, is located on this zone. (b) With the movement of the mesodermal cells between the inner endoderm and the outer ectoderm, the organizer-derived cells form in the future head region the prechordal plate (yellow), which acts as the midline organizer for the mediolateral (L-M-L) patterning and induces neuronal development in the overlying ectoderm. The distance from this midline determines the mediolateral specification, for instance, the distance and symmetrical arrangement of the two eyes. Both signaling sources have a stripe-like extension and provide together a near-Cartesian positional information system determining the pattern of the fore- (F) and midbrain (M). (c): Induction of a second organizer produces two embryos that are fused at the ventral side. (d-f) Patterning of the trunk: the cells at the blastopore obtain in a time-autonomous process more and more posterior determinations (1, 2, 3 . . .), as recently convincingly demonstrated by Wacker et al., 2004. Cells near the blastoporal ring move towards the organizer and the incipient midline (arrows). The organizer is required that cells leave the blastoporal region in which the stepwise posterior transformation takes place. In the course of time the blastoporal ring perpendicular to the AP axis shrinks while the axial rod, oriented parallel to the AP axis, elongates (compare with the chick development Figure 12.1; figures partially after Meinhardt, 2006 and 2008); for simulation of the formation of the Spemann organizer, see GT127

are inappropriate for an organizing region that should provide the line of reference for the patterning around the cylinder. Modeling has demonstrated that it is not possible to generate a single straight stripe directly. This would require a strong lateral inhibition over a large region. However, such strong lateral inhibition would also work *along* the midline, which would cause the stripe to disintegrate into a series of spots. Nature found different solutions for this problem. In vertebrates cells of a spot-like organizing region, e.g., the Spemann organizer in amphibians or Hensen's node in the chick, move relative to the other cells and *leave behind* the stripe-like midline structure (Figures 12.7 and 12.1; see also simulation S134d in the Program XY), the notochord, and the center of the central nervous system, the floor plate. The mechanism that leads to the formation of a single straight midline might be compared with a moving aircraft (organizer) that leaves a stripe-like vapor trail behind. Since the organizer is dorsally located, the central nervous system also appears on the dorsal side. In contrast, in insects, a dorsal organizer *repels* the midline. The midline appears, therefore, on the ventral side. This view provides an explanation for why the central nervous system is on the back side in vertebrates but on the 'belly' side in insects (Meinhardt, 2004).

12.7 Gene activation under the control of a morphogen gradient

With pattern-forming mechanisms that depend on diffusion, graded concentration profiles can be generated and maintained only in very small fields. This suggests that labile, graded distributions of signaling molecules can only be employed at early stages for space-dependent gene activation. Such position-dependent gene activation is faithfully transmitted to the daughter cells. The cells then remember what they have 'learned' and transmit this to their daughter cells even if, at later stages, the evoking signal is no longer present.

According to the classical view, graded distributions of signaling substances, so-called morphogens, cause a space-dependent cell determination due to a concentration-dependent response of the cells to this 'positional information' (Wolpert, 1969). There were two main objections against this type of model. The first was that it did not explain how a gradient is generated in the first place. As shown above, this problem can be regarded as having been solved. The second objection was related to the required precision with which cells can measure the local concentration. Imagine two adjacent cells. While the cell exposed to the lower concentration should activate, e.g., gene A, the neighboring cell, exposed to only a slightly higher signal concentration, should activate gene B. As it will be shown in this paragraph, molecular interactions to perform this task are feasible.

Gene activation and pattern formation in space share essential formal features, suggesting that related mechanisms are involved. In spatial pattern formation, activation becomes restricted to a small region, while the remaining cells are inhibited. Likewise, in cell differentiation, a particular path-controlling gene becomes

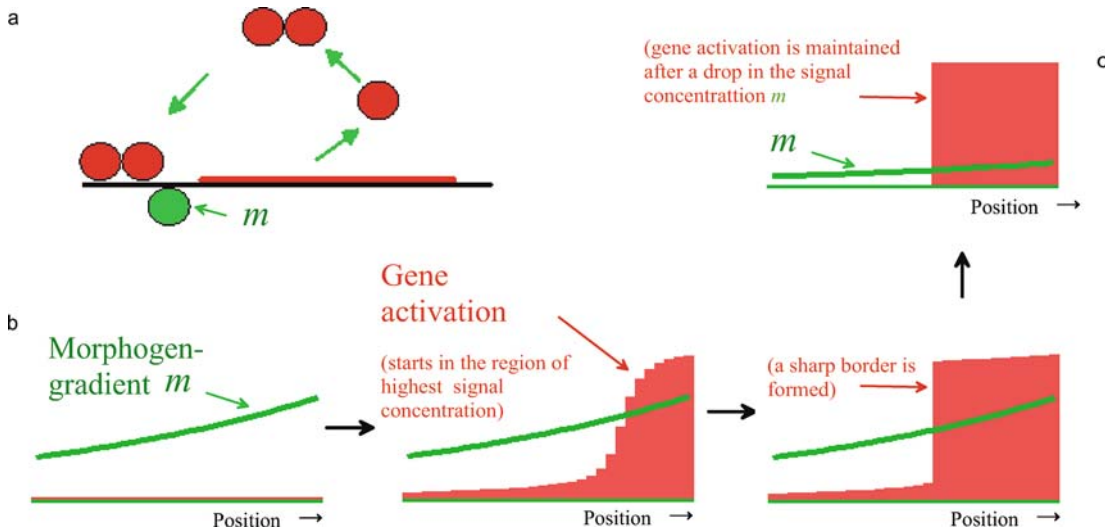


Figure 12.8. Model for a stable switch-like activation of a gene. (a) Assumed is a gene that codes for a gene product a that autocatalytically activates its own gene (Equation 12.1). Binding of a to the DNA requires a dimerization. A signal m elicits an additional production of a . (b) Stages in gene activation. Cells exposed to a certain signal concentration m (green) make the switch to high a levels; those exposed to higher m make this switch earlier. The region of high a concentration sharpens in the course of time. (c) After the signal is gone, the cells maintain this activation due to the positive autoregulation (Equation 12.1; Meinhardt, 1976) [S128; GT128]

activated while alternative genes that would evoke other cell fates become repressed. Thus, the selection of one out of several alternative genes can be regarded as a ‘pattern formation among alternative genes’. Based on this formal analogy I predicted that positive nonlinear autoregulation of particular genes combined with a mutual repression of alternative genes plays a crucial role in stable gene activation. Patterning of higher organisms can be regarded as a coupling of pattern formation in the real space with a ‘pattern formation among alternative genes’. The two together produce a stable pattern of space-dependent gene activation. A stable, switch-like activation of a single gene can result from a nonlinear autocatalytic feedback of a gene product on the activation of its own gene (Figure 12.8).

Meanwhile many genes with positive autoregulation are known. The gene *Deformed* is one of them. In *Drosophila* and in vertebrates it is responsible for specifying a particular region between head and thorax (Regulski et al., 1991). To demonstrate autoregulation, an additional copy of the gene was introduced into the fly embryo. It was different from the normal gene in that it was inducible by elevated temperatures, whereas an active copy of such a gene can be switched off by cooling of the embryo. A short warming up was sufficient to activate the artificially introduced gene. Due to the autoregulation, the normal gene became also active and remained active even after the introduced gene was turned off. As expected from the model, an artificial activation of the normal gene in the whole embryo causes a down-regulation of those genes required to specify the fate of the other regions.

Most remarkable was the observation that nearly normal flies developed even after such a severe perturbation. Development of an organism seems to be a tightly controlled and very robust process. Other examples for autoregulatory genes are *hunchback* (Simpson-Brose et al., 1994) and *twist* (Leptin, 1991); *deficiens* and *globosa* are examples from plants (Zachgo et al, 1995). As in pattern formation (Figure 2.8), the positive autoregulation can be implemented by an inhibition of an inhibition. Such a mechanism has been recently found to be at work in the specification of the border cells in *Drosophila* (Starz-Gaiano et al., 2008; see PowerPoint presentation on the enclosed CD).

To obtain the all-or-none switching behavior in gene activation, the positive feedback must be nonlinear. This occurs if the gene activation requires dimers, i.e., complexes of two molecules. Then, at low concentration, the chance that a molecule will find a partner for dimerization is low and the normal decay will be dominating. Only from a certain threshold onwards autoregulation overcomes the decay and a switch to high concentration occurs (Figure 12.8; equation 12.1)

12.8 Position-dependent activation of several genes

For a position-dependent activation of several genes under the influence of a graded morphogen distribution, a particular concentration range must activate a particular gene. An analysis of experiments with early development of certain insects suggested that measuring the concentration is not a single and instantaneous event, but instead proceeds step by step until a gene is activated that corresponds to the local morphogen concentration (Meinhardt, 1978). According to this model, the cells are ‘promoted’ in a stepwise fashion. Each of these steps is essentially irreversible (Figure 12.9). How far this proceeds depends on the morphogen concentration (Figure 12.9). Starting with a default activation of, e.g., the gene *A*, gene *B* becomes activated in those regions in which the morphogen concentration surpasses a particular threshold level. In this process, gene *A* may be switched off. In a still smaller region exposed to an even higher morphogen concentration, gene *C* will become active, and so on. Although only small concentration differences exist between adjacent cells, sharp borders are formed in which either one or another gene becomes active. According to the model, this is not because the cells themselves can detect concentration differences with high precision but rather because the internal dynamics of gene activation only allows an all-or-nothing transition. As will be shown further below, the resulting borders can play an important role in further subdividing the developing organism.

The biological significance of sensing the highest concentration is easy to understand. If a graded signal distribution is generated by a local source region and diffusion, any growth enlarges the distance between a given cell and the source. This leads necessarily to a decrease of the morphogen concentration to which a cell is exposed. If an already activated gene is insensitive to a lowering of the morphogen

Equations 12.1 and 12.2: Position-dependent activation of genes under the influence of a morphogen gradient

1. **Switch-like activation of a single gene:** The following equation describes the activation of a gene whose gene product a has a positive, nonlinear, and saturating feedback on its own activation. A switch from low to high a levels occurs whenever the concentration of the morphogen m is above a certain threshold. The gene activity is maintained after a decline of the signal (Figure 12.8) .

$$\frac{\partial a}{\partial t} = \frac{s_a a^2}{1 + s_a a^2} - r_a a + m \quad (12.1)$$

The self-enhancement has to be nonlinear ($s_a a^2$) to overcome the normal decay ($-r_a a$). The condition of nonlinearity is satisfied if the gene activation is accomplished by dimers. The signal m causes an additional activation of the gene that is independent of the autoregulation. If high enough, it initiates the switch. Due to the term $(1 + s_a a^2)$ in the denominator, the autoregulation saturates at high levels. In this way the activation of the gene reaches an upper bound.

2. **Activation of several genes:** Each of the alternative genes $A, B, C \dots$ leads to gene products $a, b, c \dots$ Each gene product has an autocatalytic feedback on its own gene. Due to the mutually repressive action, only one of these genes can be active in a particular cell. The morphogen m causes a stepwise transition from an activity of gene A to gene B , etc. until the local concentration of m is insufficient for a further ‘promotion’. The equations may have the same form for all the genes among which a decision is to be made. As an example, the equation for the gene product b is given:

$$\frac{\partial b}{\partial t} = \frac{s_b b^2 + b_a m a}{s_a a^2 + s_b b^2 + s_c c^2 + \dots} - r_b b \quad (12.2)$$

The terms describe the following components:

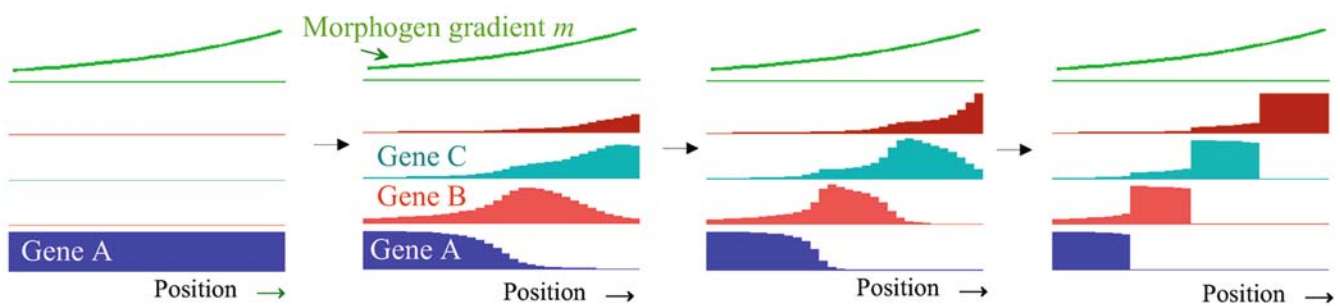
$s_b b^2$ The autoregulatory feedback of the gene product on the activation of its own gene, in the example the gene product b .

$b_a m a$ the morphogen m has an additional activating influence on the genes. In this example it is assumed the activation of the gene B requires the presence of the gene product of the A -gene, a ; b_a is a constant.

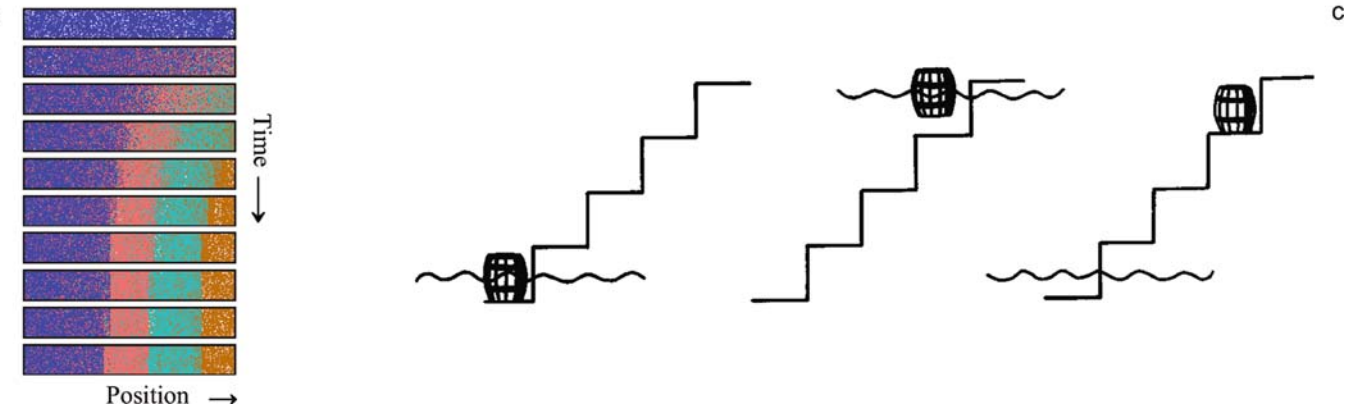
$1/(s_a a^2 + s_b b^2 + s_c c^2 + \dots)$ Each gene has an inhibitory effect on the activation of alternative genes. This has the consequence that within a particular cell only one of the alternative genes can remain active. The self-inhibition of a gene has the character of a saturation and leads to an upper limit of the activation that a gene can reach.

s_a, s_b, \dots The coupling constants for the self-amplification. For a position-dependent gene activation it is required that ‘higher’ genes are less sensitive to the morphogen but better in the mutual competition, i.e., the relation $s_c > s_b > s_a$ must be satisfied. Since these factors also appear in the denominator, a higher level of the signal m is required for each further step.

a



b



c

Figure 12.9. Space-dependent activation of several genes, A, B, \dots , under the influence of a morphogenetic gradient m . To generate stable cell states, genes are assumed whose products have a positive and nonlinear feedback on the activation of their own gene. They compete with each other for activity. (a) Starting with a default activation of the gene A (blue), the genes B, C , and D become activated step by step. Each step requires an even higher concentration of the morphogen m . Regions with sharp borders are formed. Due to the mutual competition, in a given cell only one of the alternative genes can be active. The sequential activation of genes proceeds faster in regions of high signal concentration, which leads to the apparent wave-like movement of gene activities. In such a system, activation can proceed only unidirectionally ('distal' or 'posterior transformation'). (b) A simulation as shown in (a). Gene activity is plotted as a density of pixels, analogously to what is frequently seen in visualizations of gene activities. The slowing down of the wave-like movement of particular gene activities and the sharpening of the borders is clearly visible. (c) The staircase analogy for detection of the highest level: although the height of a flood can vary continuously, the barrel can only come to rest at a particular level. A higher flood can lift the barrel to a higher step; a lowering or a second lower flood has no effect. (a,b) Calculated with Equation 12.2; Meinhardt, 1978, 1982; [S129; GT128])

concentration, existing subdivisions will be maintained even in the face of growth or stretching of the tissue domain. After the final determination is achieved, the signal is no longer necessary and can be turned off. This mode of response found support by transplantation experiments. If cells are transplanted from a region of low into a region of high concentration, the cells change their determination accordingly, whereas after transplantation from high to low levels the cells maintain their determination (Gould et al., 1998; Grapin-Botton, 1998; Udolf et al., 1995; Gurdon et al., 1995).

12.9 A problem that the mollusks don't have: the initiation of legs and wings

The structure of a higher organism is, of course, too complex to be generated by two gradients of signaling molecules that are orthogonal to each other. Classical experiments revealed that substructures such as arms, legs, and wings have their own coordinate systems, with an anteroposterior, a dorsoventral, and a proximodistal axis. The determination towards a particular structure precedes by far its actual formation. In axolotl, for instance, one can transplant the tissue that will form the arm to the head capsule and an arm will develop there. At the stage the operation was performed, there was no indication of the potential for arm formation in the transplanted tissue.

The systems that accomplish leg and wing formation have their own organizing regions. A well-known example is the ‘zone of polarizing activity’ (ZPA) at the posterior flank of the chick wing bud (Figure 12.10; Gasseling and Saunders, 1964). If cells of this region are transplanted to the anterior margin of another wing bud, additional digits are formed in a mirror-symmetric arrangement. These experiments are explained under the assumption that the ZPA produces a signaling substance (now known to be *Sonic hedgehog*) that provides positional information for the sequence of digits (Tickle et al., 1975). In this view, implantation of a second source into an anterior limb bud leads to a symmetric gradient and thus to a symmetric arrangement of the digits. The little finger is the structure that requires the highest gradient level.

However, important questions still remained unanswered by this simple model. How is the ZPA generated in the first place at a particular position within the body? Why are the digits formed along a line and not as a series of concentric rings, as expected if a local source generates a cone-shaped morphogen distribution? Arms, legs, and wings normally only appear at very specific positions of a developing embryo. They are always formed in pairs, one on the left and one on the right side of the organism, and have opposite handedness (nobody really has two left hands).

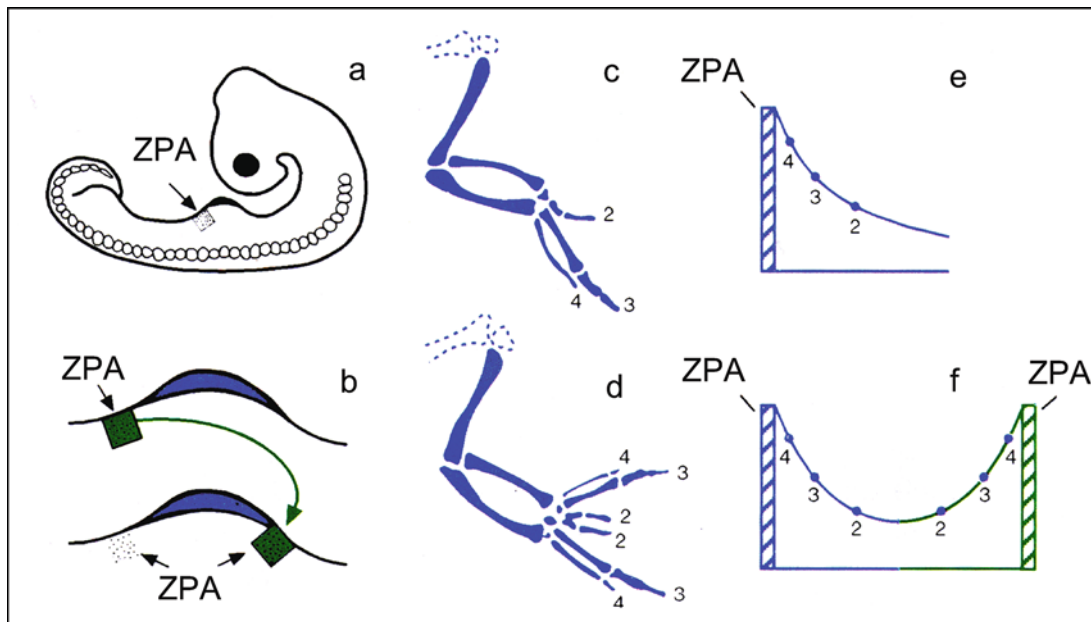


Figure 12.10. Evidence of an organizing region in chick wing development. (a) Position of the zone of polarizing activity (ZPA; arrows) at the posterior end of a chick wing bud. (b) Scheme of the transplantation of ZPA cells to an anterior position of the wing bud (arrows). (c) Normal pattern of the bones. (d) After the transplantation, a mirror-symmetric arrangement of the digits is formed. (e, f) Explanation based on the concept of positional information (Tickle et al., 1975): The ZPA is the source of a morphogenetic substance. A graded distribution is generated by diffusion and decay. The local concentration is decisive for which digits (2, 3, or 4) will be formed at which position. (f) After the transplantation, a symmetric distribution results, causing the symmetric arrangement of digits. Unexplained is how the gradient forms in the first place and why digits are formed in a plane (see Figure 12.11).

The classical view of how arms and legs are formed was much influenced by the American zoologist Ross G. Harrison (1918). He assumed that particular groups of cells receive first the signal to form, for instance, a limb. Only at later stages do such ‘limb fields’ obtain an internal structure, similar to the way it occurs in an early embryo. It is remarkable how long this model was dominant, even though it could not account for some of Harrison’s own experiments. In the following, a very different model is introduced that found strong support by recent molecular-genetic data. In essence, the boundaries between regions with different cell determinations become the new signaling centers for determining substructures. Thus, substructures including legs and wings emerge around boundaries that are formed in a preceding step (Figure 12.11; Meinhardt, 1982, 1983ab).

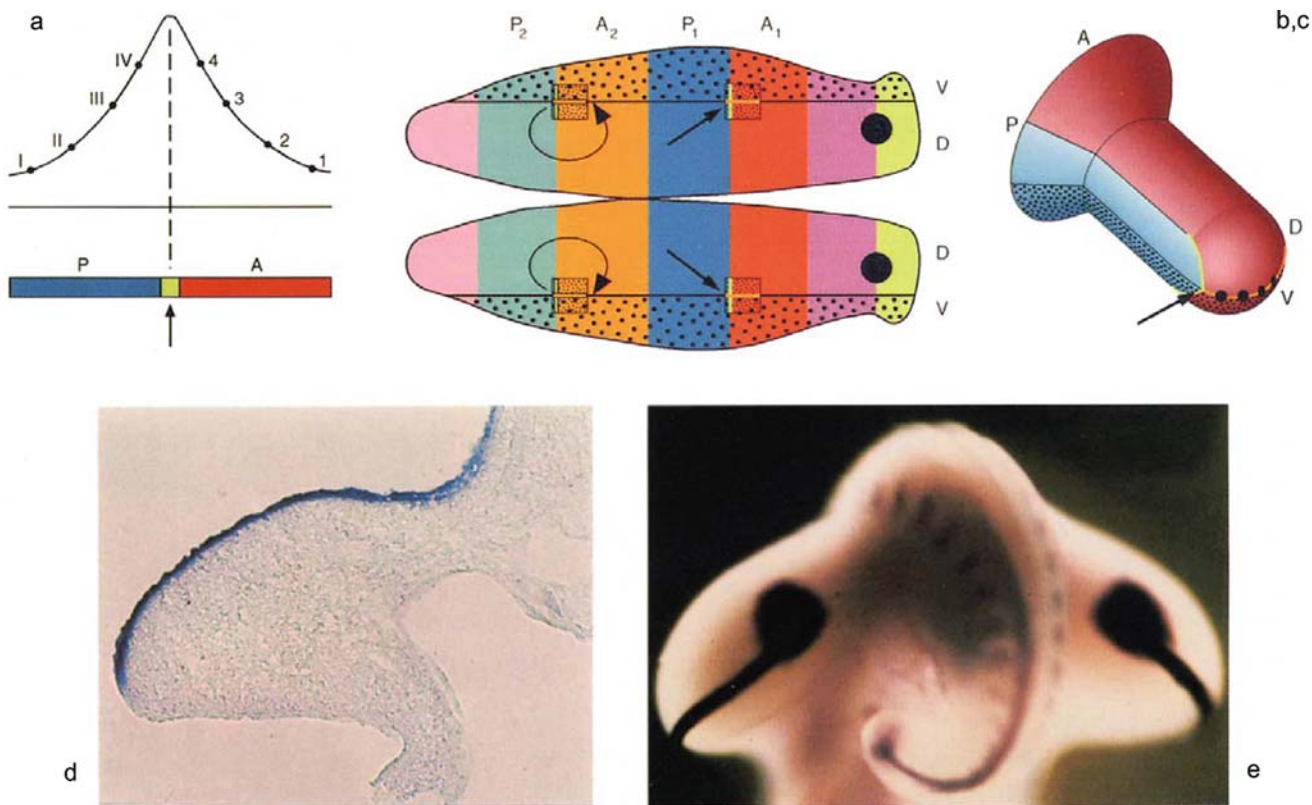


Figure 12.11. Initiation of arms or wings in vertebrates. (a) Boundary model: if two differently determined regions, A and P , have to collaborate to produce a new substance m , this production is restricted to the common border (arrow). The local concentration of m is a measure for the distance of a cell to the border. (b) If a cooperation of two pairs of different cell types is required (A/P and D/V), the organizing regions are formed at the intersection of the two borders (rectangles). In an embryo of roughly cylindrical shape, these are always formed in pairs, one at the right and the other at the left side. To illustrate the opposite handedness of these intersections (oval arrows) the left half of the body is flipped upwards to make it visible. (c) Scheme of a limb bud during outgrowth. The digits emerge along the D/V border (large dots); the type of the digits depends on the distance to the A/P border (see also Figure 12.10). (d) A wing bud of the chick. The protein $Wnt-7a$ (dark blue) is restricted to the dorsal region. (e) View from the tail. The thick black lines result from a staining of the protein ($FGF8$) that is produced at the D/V border (a $Wnt7-a/En-1$ border). The dark round spots mark high concentrations of *Sonic hedgehog* that is, according to the model, produced at an A/P and D/V border (thick arrows in b, c). *Sonic hedgehog* determines directly or indirectly the sequence of the digits (high concentration: little finger; low concentration: thumb) The gradient, if it exists, is not visible since the amount of molecules in the narrow cleft between the cells is below the detection level. Figures (d) and (e) kindly supplied by Dr. U. Grieshammer, see Grieshammer et al., 1996).

Let us assume that during primary pattern formation the embryo became subdivided into regions with distinct gene activities. Among these are two adjacent regions, which we call *P* (posterior) and *A* (anterior; Figure 12.11a). Corresponding mechanisms have already been discussed in Figure 12.9. If, for instance, a molecule *m* can be produced only when the *A* and the *P* cells collaborate, the production of *m* is confined to the *P/A* border. A possible scenario is that in one region precursor or cofactor molecules are produced and the adjacent region is able to synthesize the final signaling molecules. Only in a small region close to the border are both requirements satisfied: sufficient cofactor molecules are available and the ability to generate the final product is in place. If the molecule *m*, synthesized at the border, diffuses into the surroundings, the resulting *m* concentration at a particular position is a measure of the distance from the border. Although the distribution of *m* is symmetric, the resulting structure can be very asymmetric since the *A* and the *P* cells can respond very differently to the signal. This different responsiveness is especially pronounced in the formation of vertebrate limbs, where only the *A* cells are able to respond, a feature that underlies the polar pattern of the digits.

Such an *A/P* border encompasses the more or less cylindrically shaped embryo like a belt at the site of a future limb pair. To determine then the position of the limb at the correct back-to-belly position, a cooperation along a second border is required that separates more dorsally from more ventrally determined cells (*D/V* border). Cooperation between the *A/P* and the *D/V* pairs is possible only at the intersection of these two borders. Cells close to this intersection will form the distalmost structures. The intersections always occur in pairs, one on the left and one on the right side of the organism (Figure 12.11). The pairs necessarily have opposite handedness. A limb of the right type does not result from having a gene for ‘right’ active in this region, but rather because the four quadrants required for limb formation, *AD*, *AV*, *PV*, and *PD*, are arranged clockwise on the right side; on the left it is the reverse (oval arrows in Figure 12.11b). Thus, the model accounts for the initiation of the limbs in pairs at particular positions, and for their asymmetry. The *D/V* border determines the plane in which the digits can be formed. The distance from the *A/P* border determines the type of the digit. In contrast to the classical model, there is never a state in which a ‘limb-field’ exists without an internal structure. The model resolves the problems mentioned above with the simple gradient model for digit formation: The digits are formed in a plane since they are restricted to a region along the *D/V* border. The ZPA can emerge only at the appropriate intersections of *AP* and *DV* borders. The model also accounts for the fact that the inner face of our hand is different from the outer: The inner face is formed from the ventral, the outer from the dorsal territory.

The model has since found considerable support. In mice, genes have been found that have a common border at the expected *A/P* position (Oliver et al., 1989). At this position, the molecule *Sonic hedgehog* is produced. It acts as a signal, but, as expected, only the more anteriorly located cells respond. Genes involved in generating the *D/V* border have also been found; *WNT-7a* expression is restricted to

the dorsal half (Figure 12.11d) and *EN-1* to the ventral half of the limb bud. At this DV border, the so-called apical ectodermal ridge (AER) a new molecule, *FGF8*, is synthesized that is indispensable for limb outgrowth. The production of *FGF8* depends on *Sonic hedgehog* and vice versa (Parr and McMahon, 1995). Therefore, the expected cooperation between the two molecules is present. The mutant *limbless* has been known in mice for a long time. It turned out that in this mutant the *WNT-7a* gene is expressed in a much too large region. Therefore, the correct border does not from (Grieshammer et al., 1996; for more experimental details, see Martin, 1995, Cohn and Tickle, 1996; for analogous mechanisms in insect development, see Vincent and Lawrence, 1994; for models, Meinhardt 1983a,b).

The boundary model accounts for the fact that the new structures always have the correct spatial relation to the structures that have already been established. Variations or small errors in the positioning of the primary borders are compensated by a corresponding shift of the new structures. The use of borders as new signaling centers is not restricted to appendage formation. For instance, borders play a central role in the further patterning of the brain (reviewed in Kiecker and Lumsden, 2005).

12.10 Conclusion

The development of a higher organism is one of the most fascinating aspects of biology. Convinced that all biological processes are governed by molecular interaction, we developed molecularly realistic models that uncover what is required *at least* to describe basic steps in development. Our starting point was based on classical observations describing pattern regulation after perturbation of normal development. The criterion was that the hypothetical reactions must display in computer simulations the same dynamics as found in the experiments. Only a very restricted class of interactions turned out to be adequate. The basic reaction types can be summarized as follows:

- (i) Primary pattern formation and organizer formation require local self-enhancement and long-ranging inhibition.
- (ii) Permanent activation of a particular gene can be achieved by a positive non-linear feedback combined with a competition between genes responsible for alternative pathways.
- (iii) A dynamic stable neighborhood is enforced and stabilized if a structure activates its appropriate neighbors at a long range but excludes them locally.
- (iv) The borders between regions in which different genes are active, and especially the intersection of such borders, can become the new organizing regions to pattern legs, wings etc., allowing a finer and finer subdivision in an iterative way.

Reiteration of these rounds: signal generation, response to the signals and signaling again in a more restricted region allows a reliable finer and finer structuring of an organism in an iterative way. These models show that basically simple mechanisms can account for essential aspects of development. This, however, does not in any way reduce the fascination that the process evokes. Indeed, we stand humble in the face of the numerous problems that still remain to be solved.

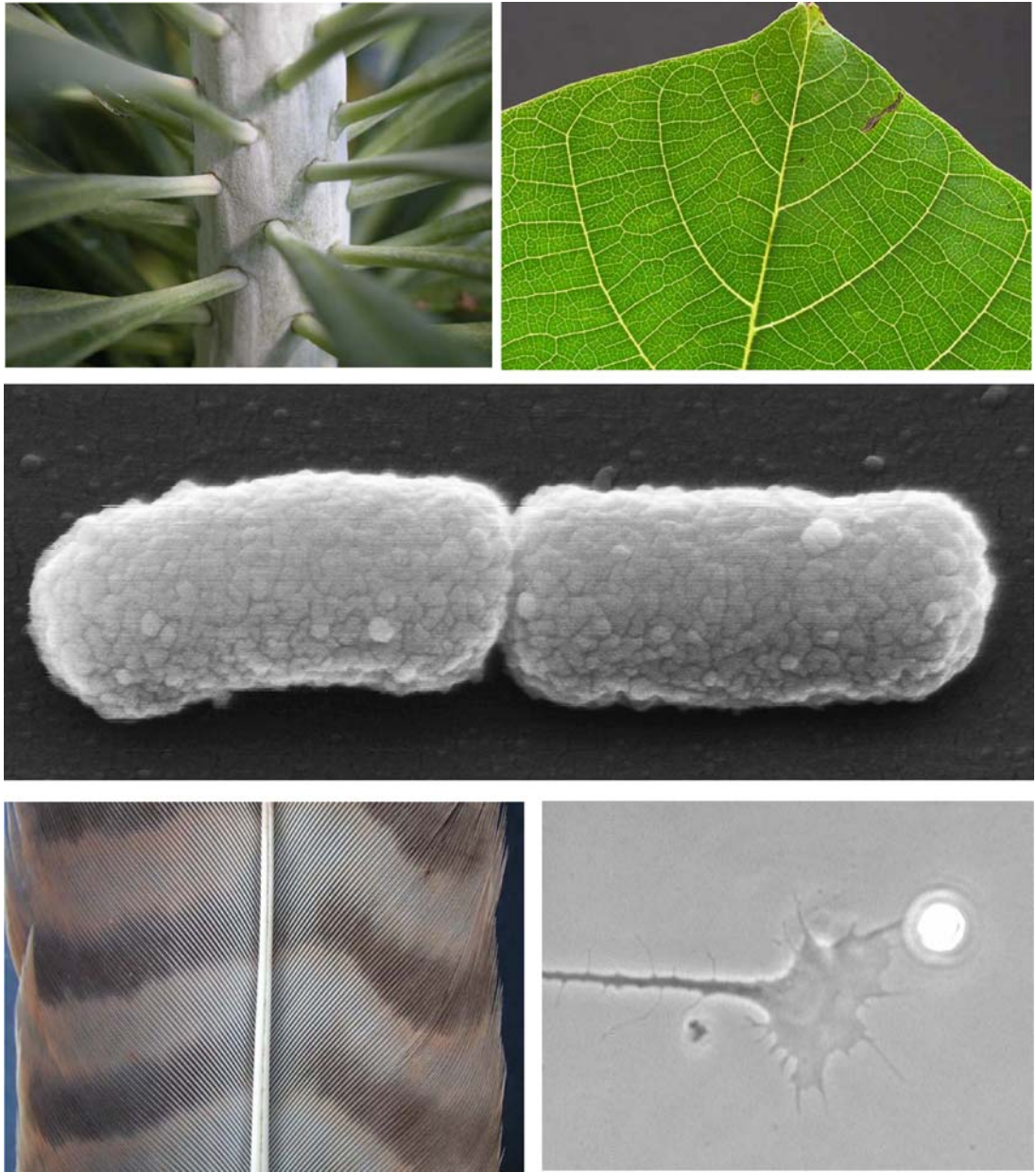


Figure 13.1. Helical arrangement of leaves, net-like structures, cell division in *E.coli*, barbs of feathers, and orientation of moving cells: quenching of signaling peaks shortly after their generation plays a crucial role in diverse biological systems

Pattern formation in development in which shell-related mechanisms are implicated

Many shell patterns can be explained by the assumption that peaks of signaling molecules are locally quenched shortly after they emerge. As shown in Chapter 5, this can lead either to traveling waves or to maxima, which disappear and reappear at more or less regularly displaced positions. In this chapter it will be shown that this mechanism is not restricted to shell patterning. Processes as diverse as the patterning of the barbs of avian feathers, determining the center of an *E.coli* bacterium to localize the initiation of cell division, orienting the movement of chemotactic cells or growth cones, and initiating of leaves in a helical arrangement are based on closely related mechanisms (Figure 13.1). To correlate the molecular mechanisms found for these systems with the hypothetical mechanisms deduced from the shell patterning it will be necessary to use the more or less arbitrary names of genes and other components. I hope that this ‘jargon’ will not be too frustrating for those not familiar with the field. To discuss the mechanisms, however, the components need names.

13.1 Arrangement of leaves and staggered dots on shells - two similar patterns

The regular arrangement of leaves, the so-called phyllotaxis, has fascinated people for centuries (for a recent review see Canales et al., 2005; Kuhlemeier, 2007). At first glance, leaf initiation seems to have nothing in common with the patterning on sea shells, but this impression is misleading. In both cases, the new elements appear only in a narrow stripe-shaped zone and the emerging patterns are time records of pattern-forming reactions that took place in these generative zones. The tip of a shoot, called the apical meristem, contains rapidly dividing cells. Cells just leaving this central zone become competent to form new leaves. The competence is present only for a short time; no further leaves are initiated in cells that left this zone. Thus, the zone in which leaf initiation can take place has the geometry of a narrow ring that surrounds the central meristem (Figure 13.2a).

Each plant has its own characteristic phyllotactic pattern. Leaves can appear at opposite positions in an alternating sequence (180° , distichous patterns), in pairs

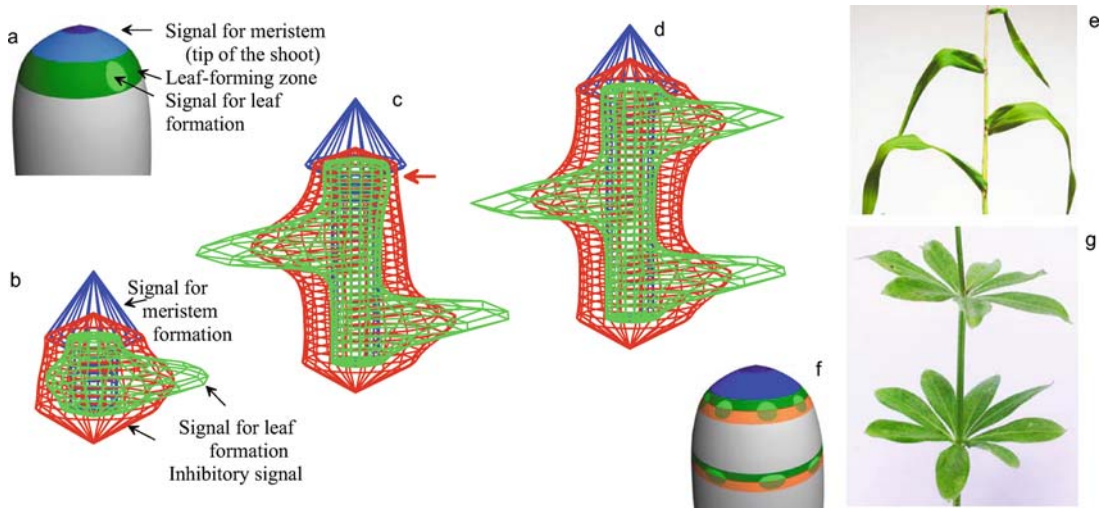


Figure 13.2. A simple model for leaf initiation at opposite positions. (a) Scheme of the leaf-forming zone surrounding the central meristem. (b-d) A growing shoot is simplified as a cylinder that grows by cell doubling at its upper margin. For the simulation an additional central element is assumed to which all of the upper cells of the cylinder have contact, shown as the tip of the cylinder. A primary pattern-forming system (blue) defines the meristem. This center inhibits the trigger of leaf-initiating signals locally but promotes them on longer range. Due to growth, the distance of the existing leaves to the leaf-forming zone increases. Whenever the inhibitory signal (red) drops in the leaf-forming zone below a threshold, a new signal is triggered. If the range of inhibition is long enough, only one new signal is formed opposite to the last leaf. Since in the leaf-forming zone the inhibitory influence of the penultimate leaf is negligible [red arrow in (c)], such a simple model cannot account for the helical arrangement of leaves. (e) Maize is an example for leaf patterning in a 180° arrangement. (f,g) Whorl-like patterns suggest that the spacing of leaves around the circumference and along the elongating axis is based on different mechanisms: the first is an inhibition in space, the second an inhibition in time. Leaves are proposed to appear at borders that separate ad- and abaxial (upper/lower, green/orange) leaf specification [Program XY; S132a, S132b, GT132]

with 90° displacement between successive pairs (decussate patterns), in a helical arrangement, or in whorls. Many models for phyllotaxis have been proposed. One such model postulates that leaves are formed at the “first available space” (Iterson, 1907, Adler, 1974). Another classical model is based on the assumption that each existing leaf exerts an inhibitory influence on the initiation of the subsequent leaves (Schoute, 1913). New leaves are assumed to be formed whenever this inhibitory influence drops below a threshold level. In this way, a certain distance is maintained between successive leaves. Curiously, in the classical inhibition model why a leaf does not inhibit itself has not been seen as a problem, although the leaf is in the center of the inhibition. Our model for pattern formation reconciles these apparently conflicting features: local self-enhancement is able to overcome the locally generated inhibition since the latter is diminished by diffusion. Figure 13.2 shows a simulation based on an activator-inhibitor model in which new signals for leaf initiation appear with an opposite (distichous) arrangement.

According to this concept of lateral inhibition the diameter of this leaf-forming zone is crucial for determining whether there is space for a single maximum or for two maxima. In accordance with this notion, a mutation was recently found in Maize that enlarges the meristem and thus increases the diameter of the leaf-forming zone, with the consequence that the normal alternating 180° pattern changes to pair-wise 90° (decussate) patterns (Giulini et al., 2004).

In many plants, leaves and seeds are initiated along spirals (Figure 13.1 and 13.3). Attempts to simulate helical leaf arrangements with a simple lateral inhibition model failed, at least in my hands. The reason is easily explained. To achieve a helical arrangement, not only the last but also the penultimate leaf must contribute to the inhibition of the subsequent leaf (otherwise leaves appear at opposite positions or in the pairwise 90° arrangement). Since the distance from one side of the ring-shaped, leaf-forming zone to an approximately opposite position is quite large, the inhibition must have a long range. Therefore, the distance at which a subsequent leaf can appear on the same side along the elongating cylinder would be large too (Figure 13.2). Consequently, the influence of the penultimate leaf would be too small to inhibit a robust helical arrangement.

A key to understanding helical patterning could come from a very different phyllotactic pattern, the whorls (Figure 13.2 f,g). In whorls, the mechanism that causes spacing around the circumference is obviously different from that responsible for the spacing of the whorls along the axis. The first depends on the spacing in *real space*, the second presumably on the spacing in *time* since a certain number of cells have to be inserted before the next whorl can be initiated. Leaves have a distinct upper and lower surface. This suggests that consecutive rings with the character ‘lower’ and ‘upper’ are generated during the outgrowth of a shoot. The new leaflets are initiated only on a lower/upper border (Figure 13.2 f). Each leaf consists then naturally of cells with a lower (abaxial) and upper (adaxial) specification in the correct spatial arrangement, a process that is analogous to the role of borders in limb formation (Figure 12.11). Each lower/upper ring would be separated by cells that are neither upper nor lower, causing the separation between the whorls. Since leaf growth is restricted to the ad/abaxial border, the cone-shaped leaf primordium can develop into a flat leaf; the leaf margin is a manifestation of the border (Koch and Meinhardt, 1994). For whorl formation, the restriction of leaf formation to this circular border would keep the leaflets on a perfect circle; the lateral inhibition between the leaflets cannot cause their displacement along the axis.

A central premise for this model is that the inhibition around the circumference - an inhibition in *space* - and the inhibition along the axis - an inhibition in *time* - are two separate processes. This corresponds to the model proposed for the oblique rows of dots on the shells (Figure 5.10) in which two antagonists are employed. Indeed, both patterns require a constant displacement of each new element. To describe the phyllotaxis, Bernasconi (1994) derived independently an equation nearly identical to Equation 5.1. For the simulation shown in Figure 13.3c, Equation 5.1 has been used. The long-range but fast reacting inhibition is accom-



Figure 13.3. Helical arrangements. (a) Arrangement of seeds on a fir cone. (b) Oblique rows of pigmented dots on a shell. In both cases successive pattern elements appear with a certain displacement. (c) Simulation: Two antagonistic reactions are assumed. The long-ranging inhibition results from a depletion of a substrate (red, e.g., auxin) from the surrounding. A new trigger is only possible after recovering of the auxin level. A long-lasting inhibitor (green) enforces the displacement of successive signals (black). Calculated with Equation 5.1 on a circle; time is plotted bottom-up [S133a - S133f; GT133]

plished by the depletion of a substrate (red, e.g. auxin, see below). In contrast, a more locally confined inhibition with a long time constant provides some sort of landmark indicating that this angular position was recently occupied (green in Figure 13.3c). Therefore, subsequent leaves keep a substantial distance from each other around the circumference but can appear relatively close to each other along the (time-) axis. Under this condition, the penultimate leaf can have a substantial influence and helical arrangements can emerge in a robust way. The actual mechanism is not yet completely understood, however, despite the fact that many molecular details that are known.

Meanwhile it is clear that in phyllotaxis the plant hormone auxin plays a crucial role (see Kuhlemeier, 2007). Auxin is transported in a polar way through the plant tissue. Blocking auxin transport abolishes local leaf initiation. Special molecules, the so-called *PIN*'s are localized in a polar fashion on one side of the cells and promote the auxin transport out of the cell. How these molecules become localized and to which direction this transport occurs is still unclear. For leaf venation (see below) an active *downhill* transport was assumed to occur, from regions of high auxin concentration in the leaf blade towards the veins that act as sink (Sachs, 1991). On the other hand, for leaf initiation it has been proposed that the same *PIN*-molecules are involved in an *uphill* transport: a small local increase in auxin polarizes the auxin transport in the surrounding cells such that more auxin is transported towards this incipient maximum, causing it to increase further (Smith et al., 2006).

In terms of our models, in an attempt to understand a complex patterning system it is a good strategy to ask whether a molecule is involved in the long-ranging communication or in the short-ranging generation of local signals. The fact that

auxin is actively transported suggests it is involved in the first category. Auxin could function in a similar way as the substrate in our activator-depleted substrate model. In this view, auxin molecules are collected, e.g., by complexing with auxin-binding molecules in a self-enhancing process. This would occur at the expense of the auxin concentration in the surroundings. In the activator-substrate model, the diffusion of the substrate proceeds towards the activator maximum since the substrate concentration is the lowest there (see Figure 2.5). In plants such net down-hill transport could be strongly enhanced by an active transport. In this view the position of a new leaf primordium would be a sink of *free* auxin although high local levels of auxin in a bound form could exist. In such a model auxin transport for leaf and for vein formation would go in the *same* downhill direction. As seen in the simulation Figure 13.3c, even if diffusion-controlled, the depletion of auxin must be a very rapidly-spreading process to suppress another signal at antipodal positions.

13.2 Veins and nerves: the formation of net-like structures

Net-like structures exist, of course, not only on the shells of mollusks (see Figures 5.8 and 5.9). The web of nerve cells, blood vessels, the veins of leaves, or the tracheae of insects are examples of these extended organs that supply tissues with water, nutrients, oxygen, or information. They consist of long filament-like structures that can branch.

A minimal model for such branched structures in two dimensions (Equation 13.1) has many similarities to those discussed for shells (Equation 5.1). Again, a local signal is required that migrates, leaving behind the structure in a trace-like manner. Instead of pigmentation, as in the case of mollusks, the signal here produces a local elongation of a filament, for instance, by incorporating further cells into the net-like structure. In comparison to the shell patterns, however, there is an important difference. Simple traveling waves are insufficient since in two dimensions these would have the shape of circles with increasing diameters, like the waves in a lake after throwing a stone (see Figure 13.8 for an example). The elongation of a filament requires not a moving front but a moving spot. Again, the signal must be localized by a long-range inhibition. Cells exposed to a certain threshold concentration are assumed to differentiate by activating a particular gene permanently (see Equation 13.1).

Essential in the mechanism envisaged here is that the signal causes its own shift. For instance, a local quenching of the signal can cause it to shift into an adjacent region, very similar to the mechanism proposed for the sea shell patterning. To generate an ordered network, this shift has to occur toward a region that contains cells not yet sufficiently supplied by veins. This can be accomplished by a trophic factor c (green in Figure 13.4) that is removed by the filament. The plant hormone *auxin* is a candidate for such a substance, as it is produced by the cells of a leaf, removed by vessels, and actively transported toward the roots. In the model, c will be depleted

Equation 13.1: Formation of net-like structures of differentiated cells

The signaling system is generated by an activator-inhibitor system (see Equation 2.1, page 23):

$$\frac{\partial a}{\partial t} = \frac{sca^2}{b} - r_a a + D_a \Delta a + b_{ad} \quad (13.1.a)$$

$$\frac{\partial b}{\partial t} = sca^2 - r_b b + D_b \Delta b + b_{bd} \quad (13.1.b)$$

The substance c (green in the simulation) acts as a **trophic factor**. It is required for the autocatalysis of a but preferentially removed by the differentiated cells (cell with high d levels; blue squares in the simulations in Figures 13.4 and 13.5).

$$\frac{\partial c}{\partial t} = b_c - r_c c - c_{cc} d + D_c \Delta c \quad (13.1.c)$$

To simulate the differentiation of the cells under the influence of the signal a , a bistable system d is used. The bistability results from a saturating autoregulation. Whenever the signal a is high enough, the cell switches irreversibly from a low to a high d level. This high level is maintained even if the signal is no longer available (see Figure 12.8, Equation 12.1 at page 222):

$$\frac{\partial d}{\partial t} = \frac{r_d d^2}{1 + s_d d^2} - r_d d + b_{da} \quad (13.1.d)$$

The terms have the following significance:

$D_a \Delta a$ Diffusion of a generalized for two-dimensional fields.

b_{da} The influence of the signal a on the bistable d system. It can cause an irreversible transition from low to high d concentrations (differentiation).

b_{ad} Only the differentiated cells ($d > 0$) have a baseline activator production. Therefore, new activations only occur along existing filaments. This initiates branching.

b_{bd} All differentiated cells have a low-level inhibitor production that is independent of the activator. This background level increases with increasing density of the filaments. If a certain density is achieved, a further elongation is suppressed.

$-c_{cc} d$ The differentiated cells remove the trophic substance c . Since the production of the signal a requires the factor c , an a peak moves away from the differentiated cells towards regions of higher c , i.e., towards regions in which still too few ‘veins’ are present.

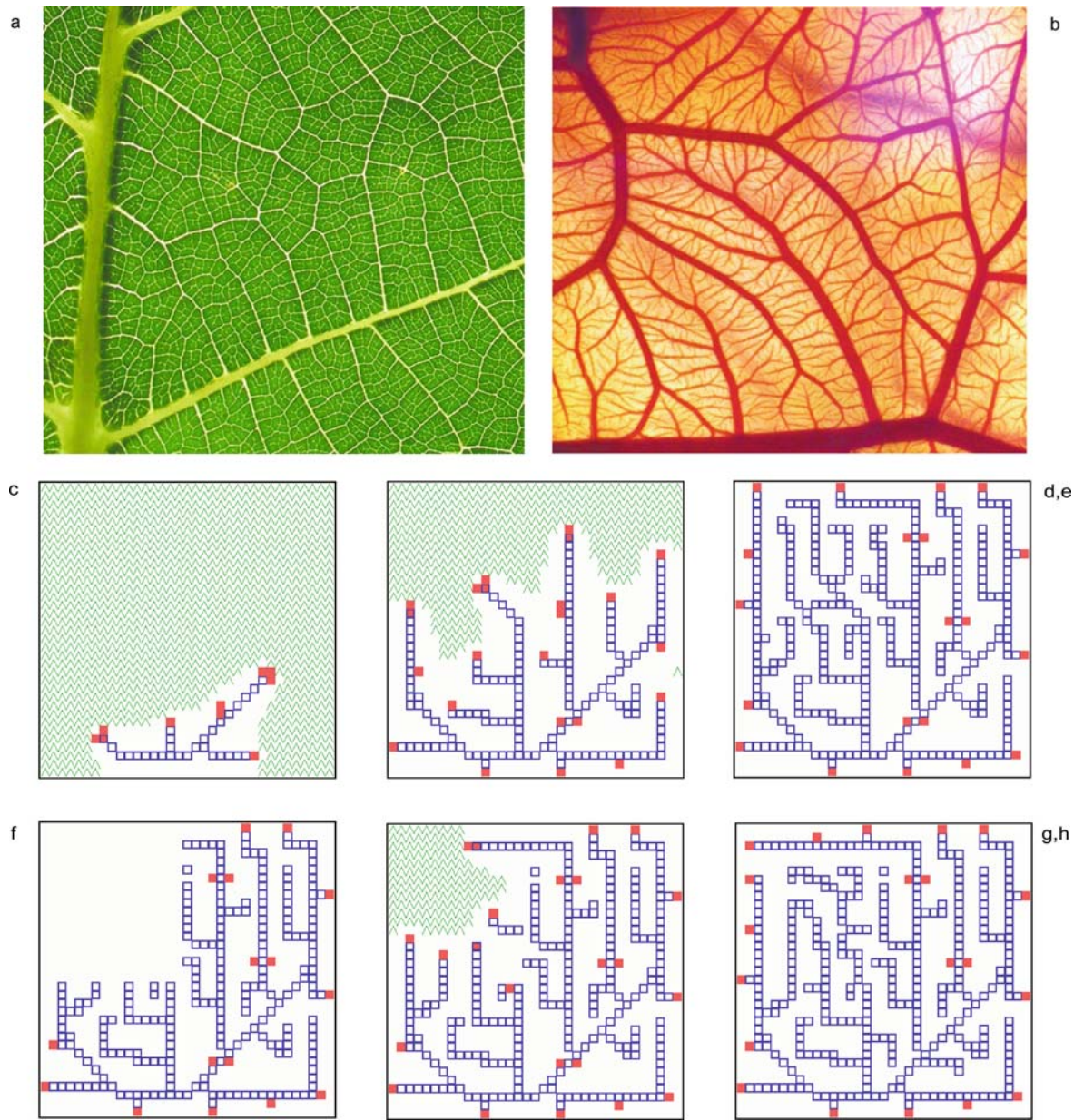


Figure 13.4. Net-like structures. (a) Veins of a leaf. (b) Blood vessels covering the yolk of a developing chick embryo. (c-e) Model: cells exposed to a high activator concentration (red) differentiate (blue squares). Differentiated cells remove a substrate with trophic functions (green, e.g., auxin or VEGF). Since the activator production depends on that substrate, substrate removal due to a new differentiation causes a local destabilization of a maximum and its shift towards a region with a higher substrate concentration. Long chains of differentiated cells are formed behind moving maxima. Branching results when new activator maxima are triggered along an existing filament. The process comes to rest if a certain density is obtained. (f-h) Regeneration: if some of the 'veins' are removed (f), substrate accumulates in the deprived region (g). New filaments grow in until the damage is repaired (h) [(Meinhardt 1976); Program XY: S134 and S134a; GT134]

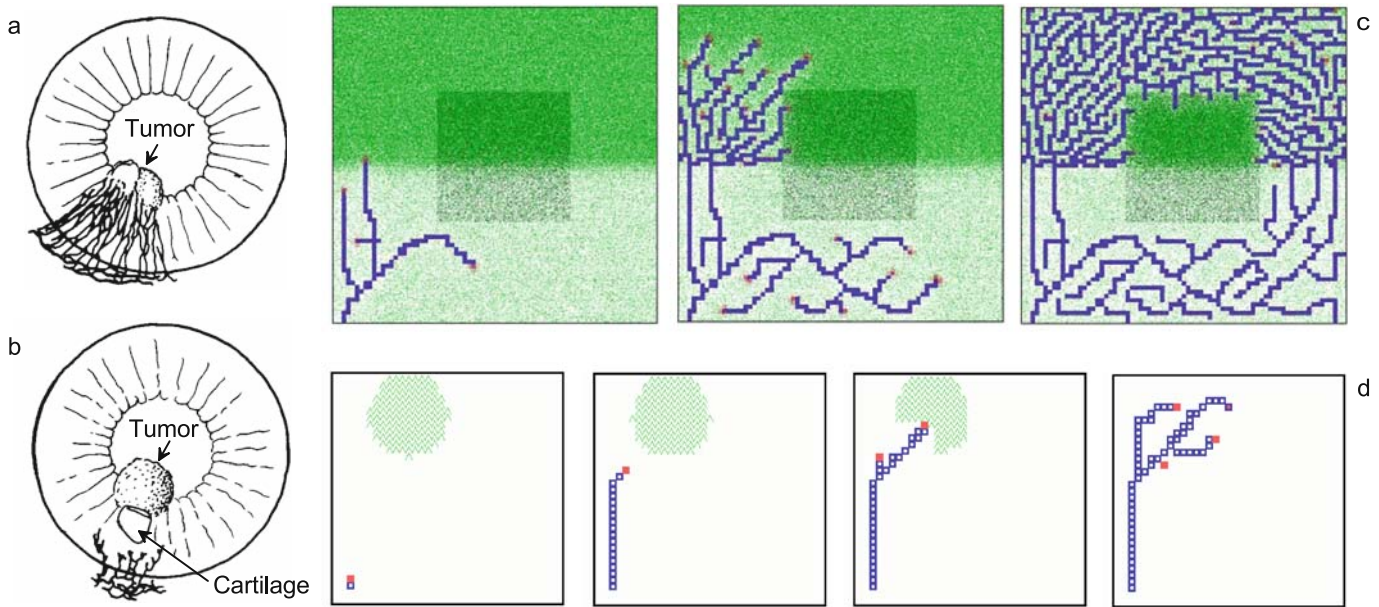


Figure 13.5. Regulating the density of a net. (a) A piece of tumor tissue grafted into the cornea of a rabbit causes a massive invasion of blood vessels (Folkman, 1976). (b) A piece of cartilage - a tissue that repels blood vessels - largely suppresses such invasion when grafted in front of the tumor. (c) Model: an increase in the level of the trophic factor (substrate c in Equation 13.1, VEGF in the case of blood vessels, green) by a factor of three in the upper part of the field leads to an increase in the number of branches. The influence of the cartilage is simulated by an increase in the baseline inhibitor production (b) in the center of the field (shaded). Veins preferentially circumvent this area. (d) Target finding: if a local source of the trophic substrate c is present, extension is directed towards that source; branching occurs preferentially in this target area; (a,b) redrawn after Folkman (1976); [Program XY; S135a, S135b, GT134]

around differentiated cells. If the activator production, i.e., the signal for filament elongation, depends on c , the activator maximum will be shifted to the neighboring region with the highest c concentration (for corresponding shifts of maxima in shell patterning, see Figure 5.7). In this way, the filaments are elongated into a region not yet sufficiently supplied by other filaments. Long chains of differentiated cells are formed as a trace behind wandering activator maxima. If the moving tips are sufficiently removed from each other, new activator maxima can be triggered along existing filaments when the inhibitor concentration drops below a critical threshold. In this way, branches are formed. If the trophic factor is produced everywhere, the resulting net-like structure spreads over the entire region. In contrast, if produced locally, the elongation will occur towards this target region (Figure 13.5d). Not yet explained by the model is the formation of closed loops in leaf venation. If an elongation always occurs away from existing veins, two veins should not be connected. Obviously nature has found a solution that has not yet been reproduced by the model.

Two leaves of a tree never have an absolutely identical vein pattern, although they are generated under the control of identical genetic information. Also, in identical twins with their otherwise striking similarities, the patterns of blood vessels visible in the background of their eyes are different. In the model, it is not necessary to

determine all the details of a ramifying network since these details are not important for the developing organism. It is sufficient to know that all cells are supplied by nearby vessels. In the simulations, random fluctuations are decisive for the precise positioning and orientation of a new branch. However, if one branch develops, for instance, to the left, the probability is higher that a subsequent branch leads to the right. Such regular alternation can be observed in many leaves. If random fluctuations have a strong influence on further decisions, and a decision has a strong feedback on the further fate, the resulting structures will never be identical. However, the genetically fixed interaction produces the typical and reproducible overall character of the particular pattern (see also Figure 6.5). If, on the other hand, the details of a structure are crucial, this is not an insurmountable problem for nature. For instance, the veins of the wing of each *Drosophila* fly are arranged in a reproducible way. This precision has a biological function, since it is crucial for the aerodynamic properties of the wing. In this case, using a multiplicity of genes, a precise coordinate system is generated that allows for unambiguous instruction of the cells (Diaz-Benjumea et al., 1989).

The trophic molecule in the formation of blood vessels is the *vascular endothelial growth factor*, VEGF. Oxygen-deprived cells produce high amounts of VEGF. The secreted form of VEGF is synthesized by organs that have to attract blood vessels such as the brain or the kidney. Local overexpression of VEGF causes hypervascularization. High amounts of this factor have been detected during embryonic and tumor angiogenesis. It orients the elongation of the vessels (reviewed in Risau and Flamme, 1995; Coultas et al., 2005), a feature that is reproduced in the model (Figure 13.5). The predicted lateral inhibition system that determines the position at which branching and active elongation can occur is realized by the *Delta-Notch* system (Hellström et al., 2007; Suchting et al., 2007).

In many net-like systems, the elongation of a filament is not achieved by the accretion of further cells but rather by the local elongation of individual cells. The formation of nerve nets is a prominent example. In this case a local signal has to be formed *within* a cell to determine the position at which the elongation needs to occur. Corresponding models will be discussed in the next section.

13.3 Chemotactic orientation of cell polarity

Many cells are able to migrate towards a source region that secretes attracting signalling molecules. Neutrophils, the most abundant type of white blood cells in humans that form an essential part of the immune system, move to a site of inflammation (reviewed in Kay et al., 2008). With the growth cone at the tip of an axon an outgrowing nerve can find its path (Figure 13.6a; reviewed in Farrar and Spencer 2008). Since the cells or growth cones are small, the concentration difference of the signalling substance between the front and rear end of the cells is small, too. The cells are able to detect concentration differences as low as 1-2% on their cell surface and orient their internal polarity accordingly (Zigmond, 1977; Baier and Bonhoeffer, 1992). A very sensitive detection system is required to generate local signals

within the cells that determine the position at which protrusions, the so-called pseudopods, are stretched out to accomplish a directed moving. Many molecules involved in this process are known (for review see Charest and Firtel, 2006).

Earlier attempts to find models that account for the extreme sensitivity of the cells with respect to external cues have revealed that the sensitivity as such is not the only challenging aspect. If a pattern-forming system is in the unstable uniform equilibrium, a minute asymmetry will orient the emerging pattern. However, without additional features of this system, the internal amplification is so dominant that, once the maximum is formed, its position will be insensitive for the small external signal. This creates a problem since a cell that has to find a particular target region must permanently check whether it is still on the correct path. There is abundant evidence that growing axons can correct their course en route. Thus, the problem is how a cell can maintain its sensitivity despite the fact that a strong internal amplification is required. In an early model we proposed that cells maintain their sensitivity over a long period by using an oscillating system. A cell would proceed in a cyclic manner through phases that are highly sensitive to external signals, followed by phases of internal amplification where the weak external signal is converted into a strong internal signal. Afterwards, the system collapses and again becomes susceptible to the external signal.

Subsequent observations, however, revealed that many chemotactic cells are not only sensitive during particular phases but remain permanently sensitive. Another argument against this early model was that stretching out of pseudopods at one part of the cell can occur simultaneously with a retraction of pseudopods at other parts of the same cell. An explanation for this behavior can be provided by the general scheme employing *two* antagonistic reactions (Chapter 5). One antagonist is distributed rapidly within the cell, which ensures that only a certain fraction of the cell cortex becomes activated. It creates a competition that is won by the side exposed to the highest signal concentration. Using a saturating system, the extension of the activated region obtains a certain fraction of the total cell cortex. Together with some unavoidable random fluctuation and little or no activator diffusion, this produces isolated maxima that point preferentially in the direction of the guiding cue (Fig. 13.6). These local activations on the cell surface are assumed to provide the signals for stretching out protrusions. A second and local-acting antagonistic reaction is responsible for a finite half-life of the protrusions. Local polymerization of actin that is required for the shape changes of the cells is a candidate for this quenching; it interferes with the formation of the local signal (see below). With the disappearance of an activated region, the global inhibition declines, too, and new spot-like activated centers emerge at the cell cortex. They appear preferentially at the side pointing towards the highest signal concentration even if the direction of the guiding signal has been changed. In this way, the highly dynamic three-component systems provide the flexibility to adapt to new situations. It also accounts for the fact that the formation and retraction of pseudopods continue in the absence of an external

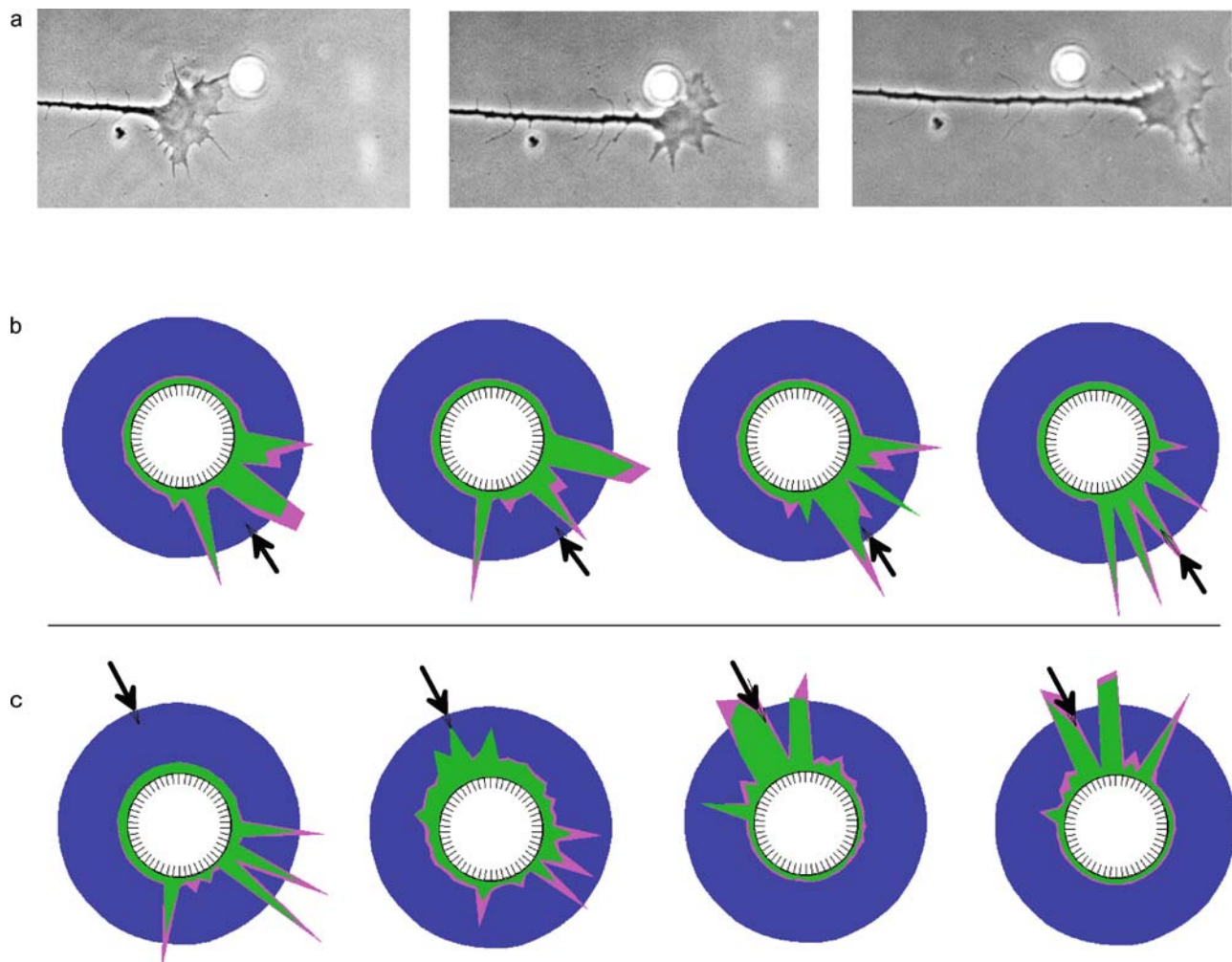


Figure 13.6. A cell or growth cone measures small concentration differences to orient its movement. (a) With growth cones, nerves cells have a special sensory ‘organ’ to detect orienting cues. The dynamic formation and retraction of pseudopods continues even in the absence of external signals in tissue culture. (b) Model: isolated signals for pseudopods (green) are generated by a saturating self-enhancing reaction together with an inhibition that covers the whole cell (not shown). They appear preferentially at the side where the guiding signal (blue, the highest levels are indicated by arrows) is slightly higher. A second antagonistic component (pink) quenches the signal locally after a certain time interval. Thus, signals for pseudopods appear and disappear permanently at the cell surface, preferentially at the side that has an advantage due to the asymmetry of the external signal. (c) After a change in the direction of the guiding signal, the internal signals emerge at the new high side, although the guiding asymmetry is minute; 2–4% concentration difference across the cell is sufficient even if this asymmetry is blurred by 1% random fluctuation between cell surface elements (Meinhardt, 1999); [S136; GT136]; see also animated simulations on a PowerPoint presentation on the CD)

signal. This dynamic behavior is most impressive to see in an actual simulation or in a movie (see enclosed CD).

The finite half-life of maxima is also important in other branches of biology. In a given population it may be important that leading individuals emerge. They obtain this position by improving their own status and by inhibiting competitors. It is also important, however, that these leading individuals lose their top position after a while so that the next generation obtains a chance to respond to new challenges in a different way.

13.4 Highly dynamic effects in preparing cell division in budding yeast

For cell division a preceding patterning is required that defines the future axis. The division proper occurs subsequently perpendicular to this axis. A much investigated example is the cell division in budding yeast. Crucial for determining the axis is a local accretion of *Cdc42* molecules at a particular position of the cell cortex. This local accumulation is a self-enhancing process (Butty et al., 2002). The long-ranging antagonistic effect as required for any patterning process results from a depletion of the freely diffusing monomers in the cytoplasm. Thus, this system is a perfect example of an intracellular activator-depleted substrate system (see Figure 13.7b). As mentioned above, minute cues are sufficient to orient an emerging pattern. In the case of budding yeast, remnants left over from the last cell division provide some ‘seed’ for the initiation of a new *Cdc42* maximum, making the orientation of the next cell division predictable. However, there are mutations in which these remnants no longer form. In this case, axis formation is determined by a de-novo pattern formation that produces corresponding signals at random positions (Chant, 1999). These maxima, however, do not remain at a stable position but start to move in a random way, sometimes around the whole circumference of the cell (Ozbudak et al., 2005). The reason for this is that in addition to the depletion of *Cdc42* in the cytoplasm, a second round of negative feedback takes place. The local polymerization of actin fibers, required to prepare the next cell division, quenches the accumulation *Cdc42* at the membrane, causing the *Cdc42* peak to move into adjacent positions. The repetition of this quenching and shift leads to large-scale movement of the peaks, in complete analogy to the mechanism for moving maxima derived for sea shell patterning. As expected from the mechanism formulated for the sea shell patterning (Chapter 5), this second antagonistic reaction is local and has a longer half-life than the *Cdc42* accumulation. If the local actin polymerization is blocked by a drug, the *Cdc42* maximum remains in a stable position. It is unclear whether this process plays a role in wild-type cells since there the bias caused by the remnants is so high that the movement does not occur.

In conclusion, the generation of axial polarity for the orientation of cell division is an important pattern-forming event. It is often oriented by cues from earlier patterning events. If these cues are missing, a spontaneous symmetry breaking will

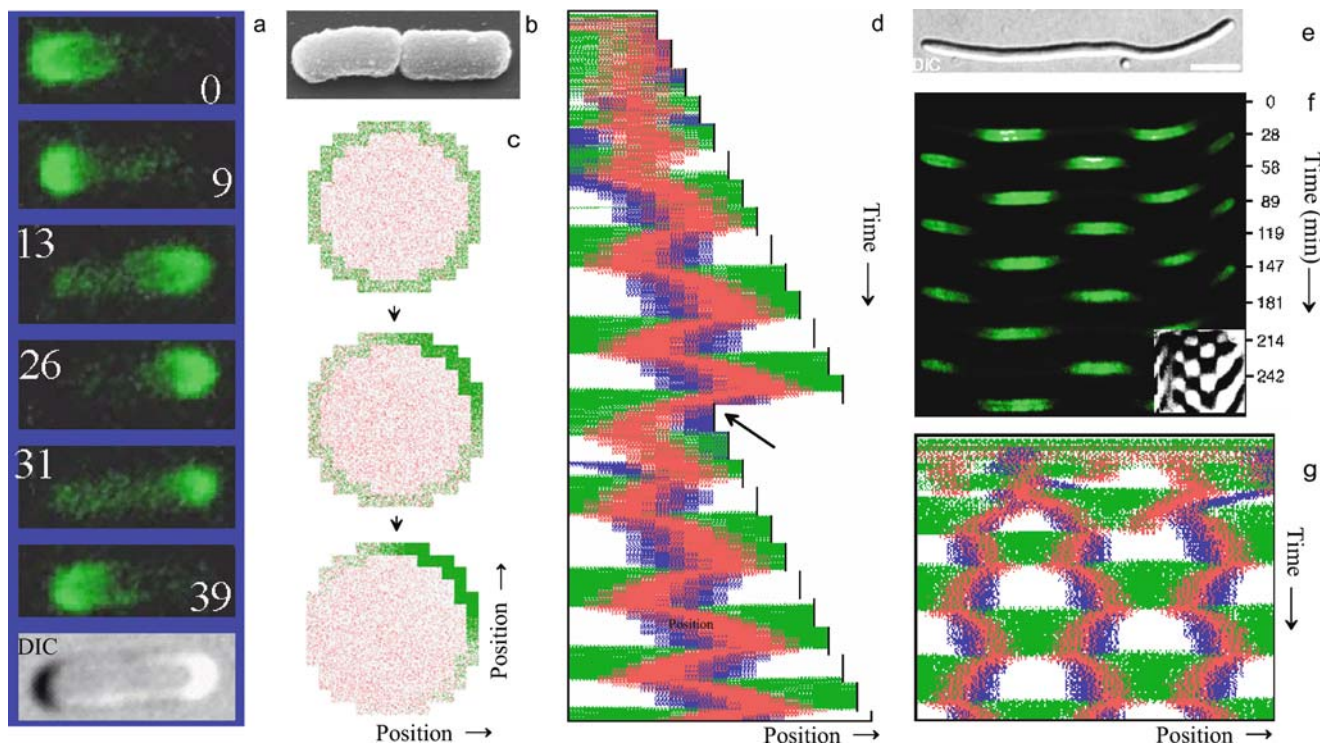


Figure 13.7. Out-of-phase oscillation in the *E. coli* bacterium to find the center of the cell to initiate cell division. (a) Binding of *MinD* protein to the membrane - visualized by GFP labeling - occurs at alternating poles (Raskin, and de Boer, 1999; Hu and Lutkenhaus, 1999). The numbers indicate lapsed time in seconds. DIC is a phase contrast photograph of the same bacterium. A full cycle occurs in ca. 45 seconds. *MinD* together with other components inhibit initiation of cell division. In this way, cell division becomes restricted to the center. (b) A just-dividing bacterium. (c) Formation of an intracellular polar pattern by an activator - depletion mechanism: cooperative aggregation at the membrane (green) occurs at the expense of precursors that diffuse freely in the cytoplasm; symmetry breaking is based on random fluctuations. A maximum appears on one side of the cell cortex. (d) Simulation: assumed is that *MinD* (green) binds everywhere to the membrane; *MinE* (red) needs *MinD* for binding to the membrane. After binding, the two molecules detach from the membrane together. In this way, a *MinE* maximum destabilizes itself and enforces therewith its own shift into a neighboring region where sufficient *MinD* is still present. Like the back and forth movement of a windshield wiper, the *MinE* wave keeps the center free of *MinD* and only allows the accumulation of molecules required to initiate division there (*FtsZ*, blue). This signal remains in the center although the distance to the poles increases. After cell division (arrow), the *FtsZ* signal appears rapidly at the new center. (e-f) If cell division is blocked, long cells are formed (e), in which *MinD* oscillates out-of-phase in several patches (f). This is reproduced in the simulations (g). For equations, parameters, movies, and animated simulations, see Meinhardt and de Boer, 2001 and the enclosed CD; photographs (a,e,f) kindly provided by Piet de Boer). This model was guided by the assumption that the out-of-phase oscillation found in the bacterium is based on a similar mechanism as postulated before for the out-of-phase oscillation that leads to the chessboard pattern on shells (insert in (f); see Figure 5.6) [S137 - 137d; GT137; program XY: S137b]

occur. At least in polarizing budding yeast and chemotactic cells, a mechanism is involved by which a second antagonistic reaction produces moving peaks due to a local quenching that allows a repositioning of established maxima.

13.5 Out-of-phase oscillations in *E.coli* bacteria for center-finding to determine the plane of cell division

An *E.coli* bacterium starts to divide by a constriction at the center whenever a certain size is exceeded. This zone is positioned with a great precision; the deviation from the real geometric center being not larger than 2%. It came as a big surprise that this more static-appearing center-finding process employs a highly dynamic process involving a rapid out-of-phase oscillation (Figure 13.7). High concentrations of a substance (*MinD*) appear at the cell membrane near the two poles in an alternating sequence and suppress the initiation of cell division there. The only remaining position at which cell division can be initiated is the region that is farthest from the two poles, i.e., the center of the cell.

Although all molecular ingredients were known, it was unclear how the system works. In a review Shapiro and Losick wrote in 2000: “we are left with two topological mysteries: how does a bacterial cell knows where its middle is and what is the medial mark that triggers polymerization”. The local destabilization mechanism that I learned from studying the sea shells was a guideline for deducing an appropriate mechanism (Meinhardt and de Boer, 2001).

The localization of the division plane is controlled by the family of *Min* proteins, *MinC*, *MinD*, and *MinE*. From the analysis of this system it became clear that none of the *Min* proteins act as an inhibitor. Thus, a direct utilization of the interactions developed for shell patterning was inappropriate. What else could act as long-ranging antagonist and what could cause the local destabilization, as required for out-of-phase oscillations? As mentioned, a very plausible mechanism to form a pattern within a cell is the activator-depletion mechanism (Equation 2.4). To satisfy our general conditions for pattern formation within a cell, the self-enhancing reaction has to be more localized, for instance, by causing a cooperative aggregation at the cell cortex. This operates at the expense of the molecules that can spread freely within the entire cytoplasm (Meinhardt, 2008). In such a system the condition for different ranges of the self-enhancing and of the antagonistic reactions is satisfied in a straightforward manner. In intracellular patterning ‘long range’ denotes a communication over the entire cell while ‘short range’ indicates a cooperative process that covers only a part of the cell cortex. Simulation in Figure 13.7c shows a polar localization at the membrane.

What could cause the destabilization? For the out-of-phase oscillations a third player is indispensable. We proposed that *MinE* has this function. Without *MinE*, no oscillation takes place and *MinD/C* binds everywhere to the membrane, abolishing any cell division. Initial visualization of the *MinE* protein has shown that it is

more centrally localized. The question was then: How can it be that a substance that accumulates in the center is responsible for an alternating activation at the poles?

To facilitate an understanding of this highly complex process, again an analogy should be provided (knowing that all analogies are a bit dangerous). Imagine a strip of very rapidly growing grass on which a cow is grazing. After eating up all grass in the immediate surrounding, the cow will move into a region in which more grass is available. The initial direction may be chosen at random but the cow will continue to move in this direction since less grass is left behind. After reaching the end of the strip, a very intelligent cow would now turn around to move rapidly to the other side of the strip where fresh grass is still available. After reaching the other end, the process will start anew, assuming that the grass recovered meanwhile. Since the cow passes the center twice as often as the poles, less grass will remain in the center.

This analogy also illustrates a point that came to me as a surprise. Oscillations are usually active processes, requiring activations and antagonists. In this case, however, the oscillation results from a more passive process. In the analogy given above: the grass grows continuously. The active process is the grass-removing cow that moves back and forth.

Back to the bacterium and to the model. *MinD* (the grass) would cover the membrane uniformly. A local signal (*MinE*, the cow) needs *MinD* to bind to the membrane. However, binding of *MinE* to *MinD* causes detachment of both molecules from the membrane. Therefore, a *MinE* maximum enforces its own local destabilization, causing its shift into a neighboring region that is still rich in *MinD*, and so on. The result is a ring-shaped zone of high *MinE* concentration that moves back and forth along the cylindrical cell cortex and ‘peels’ *MinD* off the membrane. These *MinE* waves have been directly visualized (Hale et al, 2001).

13.6 *Dictyostelium*: traveling waves at the border to multicellular organisms

The slime mold *Dictyostelium discoideum* can be found on the floor of North American forests. As long as the amoeboid cells find sufficient bacteria for nutrition, they live as single cells. When they run out of food, many thousands will aggregate into an assembly that has many of the properties of a multicellular organism (Figure 13.8a). The aggregate, the so-called slug, can move over much larger distances than a single starving cell could do on its own. New sources of food can be reached in this way. Within the slug, differently determined cells are formed. Among them are the spores that are able to survive a long period of starvation (Figure 13.8a).

To aggregate, the individual cells have to ‘know’ in which direction they need to move. For that, *Dictyostelium* forms traveling waves that have all the properties expected from theory. The signaling molecule is *cAMP* (cyclic adenosine monophosphate). The secretion of *cAMP* is obviously a self-enhancing process. If a sufficient number of molecules encounters a sensitive cell, an about hundredfold

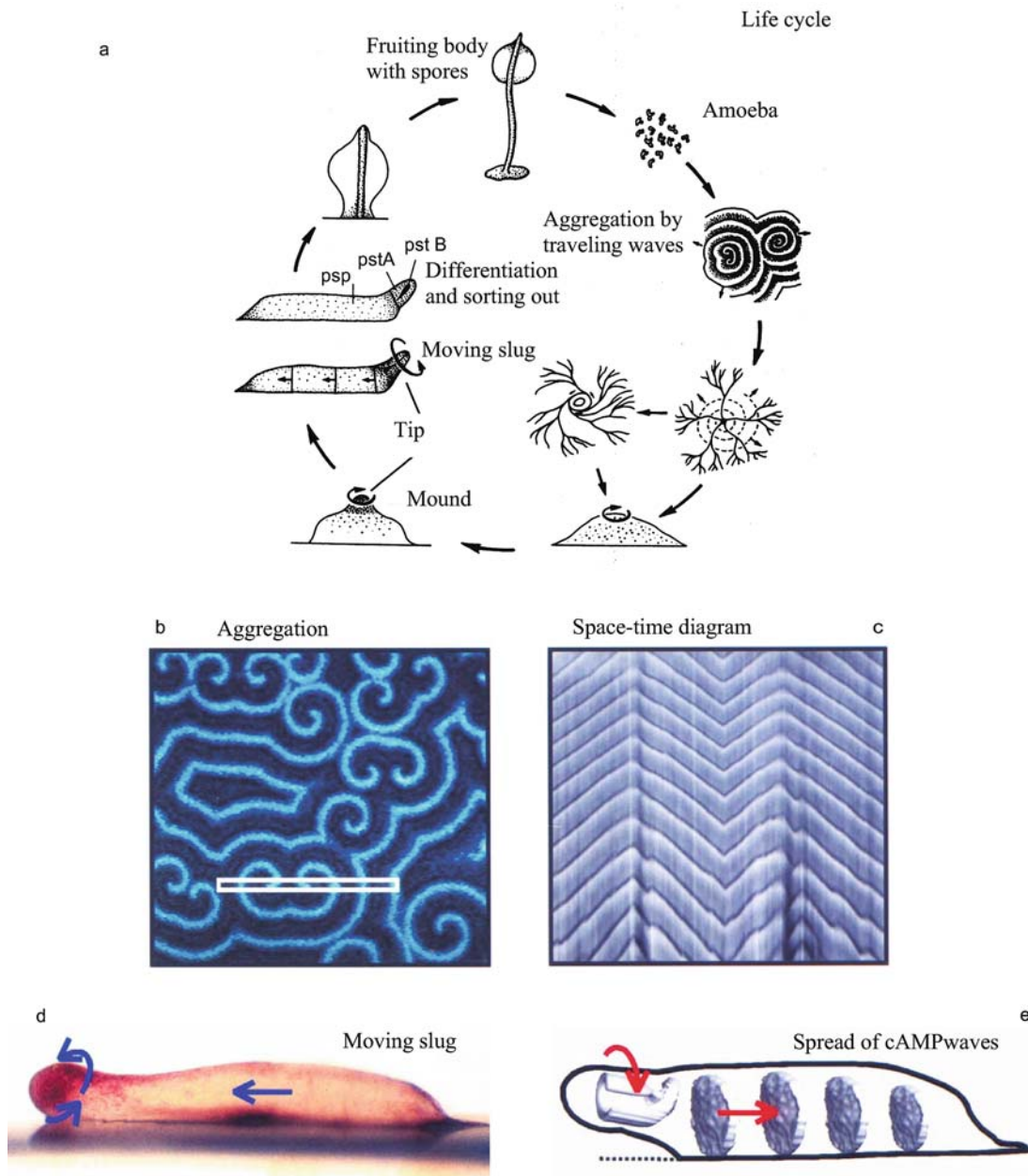


Figure 13.8. Traveling waves in the slime mold *Dictyostelium*. (a) Life cycle: After running out of food, cells aggregate to form a slug, and eventually, a stalk with spores at its tip. (b) By means of concentric or spiral-shaped traveling waves of a substance (cAMP), cells obtain information as to which direction they have to move. The bright regions result from the shape changes of the cells as they begin to move. The cells move only for a short period after encountering the wave. (c) Movement of cells marked in (b) in a space-time plot: as in the shell patterns, regions emerge in which wave initiations (\wedge) or annihilations (\vee) take place. (d) A moving slug: the arrows mark the direction in which individually marked cells move. (e) Simulations of cAMP waves in the slug. At the tip, spiral waves are formed that change further back into planar waves. The cells move toward these waves (arrows) (Siegert and Weijer, 1992; Bretschneider et al., 1995; figures kindly supplied by Florian Siegert and Cornelius Weijer).

amount of *cAMP* will be released by that cell within 30 seconds (Gerisch, 1968; Devreotes, 1989, Siegert and Weijer, 1992; Goldbeter, 1996). The antagonistic reaction results from an induced modification of the receptor molecules (by phosphorylation). After that modification, the receptor molecules can no longer bind other *cAMP* molecules. After a refractory period of about 5 minutes a further activation cycle starts. If the cell density is high enough, the activation will spread in a wave-like manner. Each activated cell emits a new signal and triggers neighboring cells. Cells that encounter a wave respond by moving in the direction from which the wave came, i.e., towards the aggregation center. In the course of time, cells become more competent for a free-running oscillation. Those cells that initiated the oscillation first have a good chance to become an aggregation center. Thus, using oscillations and traveling waves allows the signal to spread a long way, reaching many of the scattered cells. The large aggregates can move longer ways and have a better chance to survive the starvation period. Mechanisms that allow the polarization of a cell by minute external asymmetries has been discussed already (Figure 13.6). How faster oscillating cells become pace maker regions is described in Figure 3.7.

In contrast to the situation in shell patterning, the traveling waves are formed here in a two-dimensional domain, the plane to which the cells adhere. They annihilate each other like the elementary waves on some shells do (Figures 13.8b,c and 3.7). After aggregation of many cells, so-called slugs are formed that can move over larger distances. Traveling waves continue to exist within the slug, too (Figure 13.8e).

13.7 Feather patterns

Feather patterns of birds provide a rich ground for studying pattern formation. Feathers are initiated in very regular arrays. Each feather has a well-defined polarity with a fixed orientation relative to the main body axes. In the generation of the color patterns and in the formation of the barbs (the hair-like filaments) mechanisms are at work that share many features with those found for the sea shell patterning.

The initiation sites for feathers are determined at early stages of embryonic development. First, regions close to the dorsal midline become competent. Subsequently the competent region enlarges towards more lateral positions, allowing the initiation of more and more feathers (Figure 13.9a). The spacing of the feathers suggests that a mechanism of the activator-inhibitor type is involved. Indeed, molecular analysis revealed that *FGF4* acts as an activator and *BMP2,4* as inhibitor (Jung et al., 1998). Due to the sequential enlargement of the competent zone, the spacing becomes very regular since new feathers can only be initiated at a certain distance from existing feathers.

Feather formation begins by a cone- or cylinder-shaped outgrowth. This outgrowth is powered by a ring-shaped zone of proliferating cells at the base of the

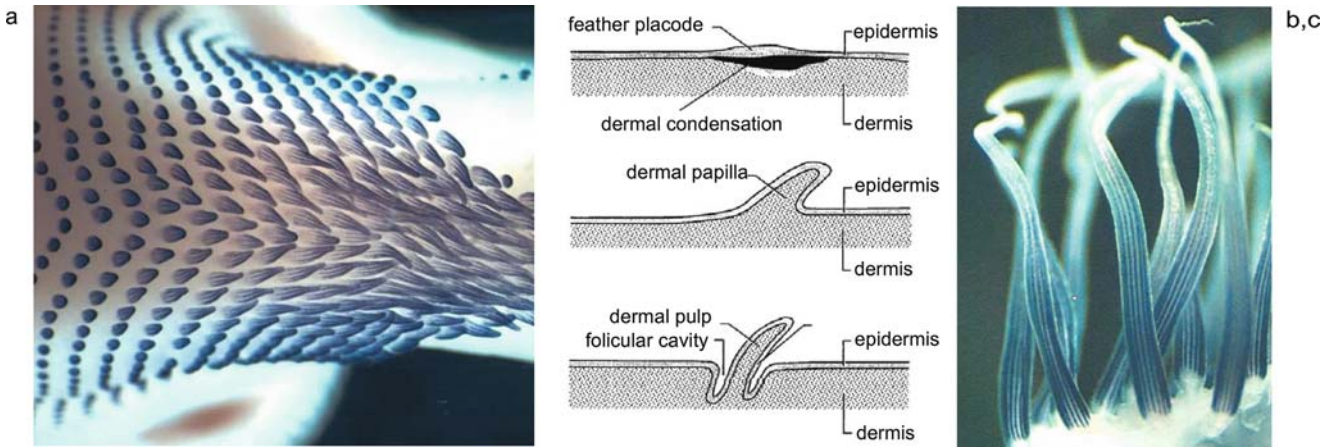


Figure 13.9. Initiation of feathers. (a) Feather buds form symmetrically on both sides of the dorsal midline on an embryonic chicken, visualized by the expression of the gene *Shh*. (b) Local signals such as shown in (a) trigger an interaction between ectoderm and the underlying mesoderm that leads to a cone-shaped outgrowth. (c) The first feathers are downy feathers, which consist of a bunch of individual barbs and which do not have a rachis. The separation into individual barbs is accomplished by an interaction of *Shh* (blue) and *BMP2*, which functions as an activator-inhibitor system. Stable signals are initiated in the ring of stem cells at the base of the cone. Due to the outgrowth, these local signals give rise to long extended stripes of high *Shh*. The regions between the signals form the proper hairs of the downy feathers. (Figure parts (a) and (c) courtesy of Matthew Harris, (b) of Richard Prum; see Harris et al. 2005 and Prum and Williamson, 2002)

outgrowing feather (Figure 13.9b). Thus, the tip of a feather is its oldest part, much in contrast to a growing plant. On flight feathers, one side of this outgrowing cylinder bears a special stabilizing structure, the rachis. The more-or-less flat feather results from an opening of the cylinder. Many adult feathers still have a remnant curvature. If the cut-open side is not precisely opposite to the rachis, the feather will be asymmetric.

13.8 Color patterns of feathers

Melanin, the dark pigment of the feathers, is produced in a gland next to the base of the feather. Melanin and other pigments are incorporated only in the newly formed cells at the base. Thus, like in shell patterns, the color pattern of feathers represents a time record of a one-dimensional pattern-forming reaction, accomplished by enabling or suppressing melanin incorporation in a ring at the base.

Some examples of feather patterns are shown in Fig. 13.10. Prum and Williamson (2002) used the interaction and basic parameter selection given in this book to simulate feather patterns. As in shells, synchronous oscillations produce stripes perpendicular to the axis of growth. Stable patterns in space produce stripes parallel to the rachis, and activations limited in space and time leads to isolated

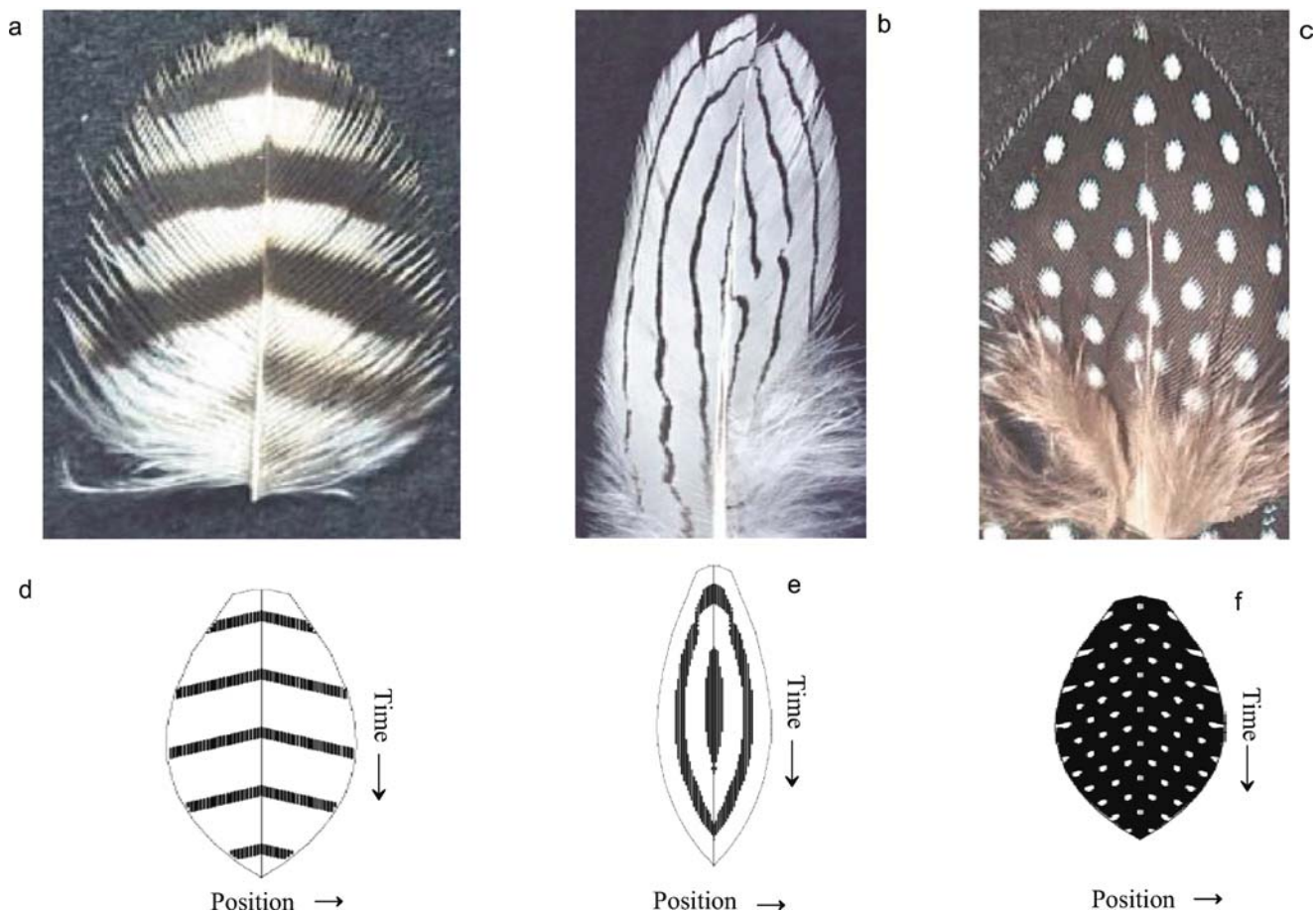


Figure 13.10. Color pattern of feathers. Like in shell patterning, feather patterns resemble a time record of a patterning that takes place in the ring-shaped stem cell zone at the base of a feather. Stripes perpendicular to the rachis result from synchronous oscillations (a,d), lines parallel to the rachis from a stable pattern (b,e), and isolated spots from a patterning that is restricted in space and time (c,f). Oblique lines would be records of traveling waves (Figures courtesy of Richard Prum; see Prum and Williamson, 2002)

spots. It is very remarkable that - as in shell patterning - almost perfect circles can appear (see Figures 13.10c and 9.7). This is surprising since the proximodistal and the lateral extension depend on different and independent mechanisms. The proximodistal extension of a white spot depends on how long the melanin incorporation was locally suspended, while its mediolateral extension depends on the spatial extension where melanin incorporation was downregulated. As in shell patterns, a spatially stable pattern is frequently superimposed whereby the rachis region acts as line of reference. During feather outgrowth, this organizing influence may first increase and later decline (Figure 13.10b), being in concert with the changing lateral (i.e., circumferential) extension of the feather. The size and the color pattern can be very different on the two sides of the rachis.

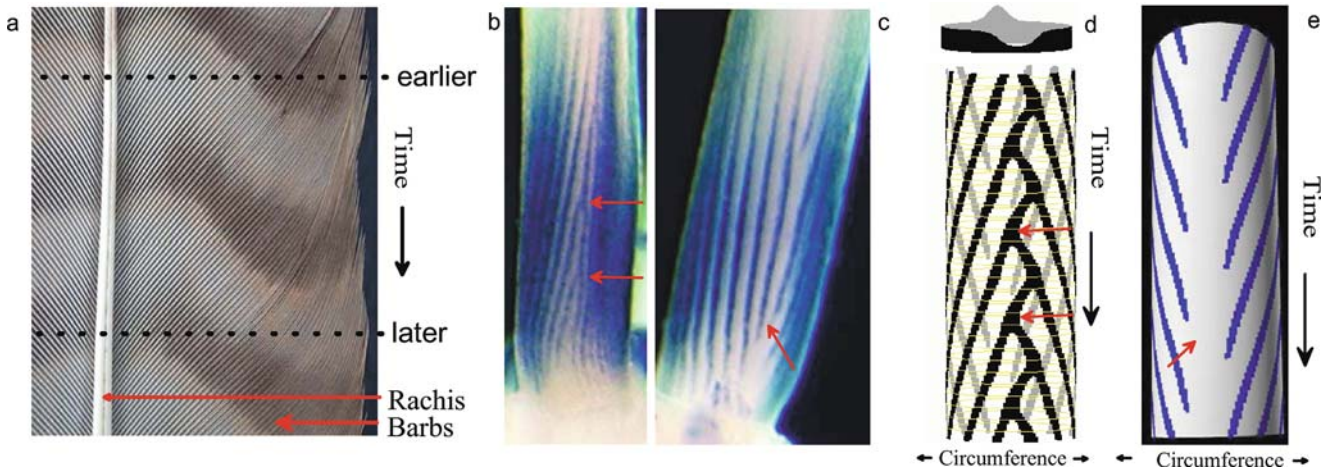


Figure 13.11. Formation of the oblique barbs by traveling waves. (a) Since the tip is the oldest part of a feather (in contrast, e.g., to the situation of a tree), the cells forming the tip of the oblique barbs are also born earlier than those formed close to the central shaft, the rachis. (b, c) Patterns of *Shh* expression on the outgrowing cylinder: (b) shows a view from cut-open, (c) from the rachis side (arrows). *Shh* together with *BMP2* acts as an activator-inhibitor system. (d) Model: *Shh* is assumed to accomplish a separation of barbs. A local, nearly stationary signal roughly opposite to the rachis [arrows in (b) and (d)] allows an opening of the cylindrical sheet into a plane. Like cutting with scissors, traveling waves of high *Shh* expression (oblique black lines) start from this cut-open position and separate the individual barbs (white oblique stripes). (e) This cutting comes to rest near the future rachis [wave-free regions, arrows in (e) and (c)]; Simulation (d) and (e) performed with an activator - two-inhibitor system (Equation 5.3). The molecular basis of the destabilizing reaction is unknown. Modulation in the inhibitor strength [top in (d)] determines the rachis and cut-open position. Figures (b) and (c) courtesy of Matthew Harris, see Harris et al. 2005 [GT139]

13.9 Barbs of flight feathers are separated by traveling waves of local signals

In flight feathers, the feather hairs, the barbs, have an oblique orientation. Since the feather represents a space-time record, it is obvious that the cells that form the tip of a particular barb are born earlier than the cells located next to the rachis. This is clearly visible in feathers showing horizontal stripes, which can be used as an internal timer (Fig. 13.11a). Obviously, the situation is very different from other branching structures such as a tree, where the branch is initiated first and the branch proper is the result of a subsequent outgrowth. How can a tip be formed earlier than the base of a branch? As mentioned, the feather is formed first as cone or cylinder that is cut open at one side. The oblique orientation of the hairs indicates that the feather hairs become separated from each other by waves that move from the cut-open side towards the rachis. The situation can be compared with cutting out a paper model of a feather from a sheet of paper. One would use a scissors to separate the hairs by cutting from the outer margin towards the center.

13.10 Nerve conduction as a traveling wave phenomenon

Neither vision, hearing, feeling, thinking, nor moving would be possible without an exchange of information by nerves, either from the sensory cells to the brain, between parts of the brain, or from the brain to the muscles. Sequences of electrical activity, the spikes that travel along the axons of neural fibers, play a key role. The underlying mechanism shares features of traveling waves in general. Here, however, the self-enhancing and antagonistic reaction is not achieved by production and degradation of substances, but rather by abrupt changes in ion concentrations within the cells. Therefore, the conduction of nerve pulses illustrates another example of how the general requirements for oscillations and traveling waves can be satisfied.

In resting nerve cells the concentration of potassium ions is higher than in the surrounding intercellular space. For the sodium ions the situation is the reverse. Special molecules in the membrane function as a pump transporting potassium ions into the cell and sodium ions out. In this way, the concentration differences are maintained and the nerve cell remains negatively charged. The membrane contains channels that are impermeable to sodium ions as long as the potential difference is negative. Excitation makes the potential difference less negative and the sodium channels become more permeable, allowing an influx of sodium ions. Their positive charge makes the inside of the nerve even less negative, causing the voltage-dependent channels to open further – a self-enhancing process. If a threshold is reached, the nerve ‘fires’. A voltage change results that is independent of the initial excitation (the overall excitation of a nerve is encoded by the frequency of the pulses, not by their amplitude). Since this voltage change also causes channels to open in neighboring membrane regions, the excitation can spread over the whole nerve in a wave-like manner.

In a strongly excited nerve, pulses follow each other in a rapid sequence. The self-enhancing reaction does not continue until the resources of the cell are depleted, however. As in the shell patterns in which short refractory periods are decisive for a rapid succession of pulses (Figures 6.1 and 6.7c), there is also a fast antagonistic process that switches the reaction off rapidly in nerves. This arises from the internal dynamics of the channel molecules. Opening initiates a cycle that rapidly also closes the channels. Later, by other processes, the negative potential within the cell is restored. The opening of potassium-specific channels and thus the removal of positive charges is one of these processes.

It is possible that such ion currents also play a role in shell patterning. The sensitivity of the pattern against changes in the ion concentration of the surrounding water (Figure 1.11) demonstrates that ion concentrations play at least some role. Ermentrout et al. (1986) proposed a model for the elementary shell patterns that is based on neuronal interactions.

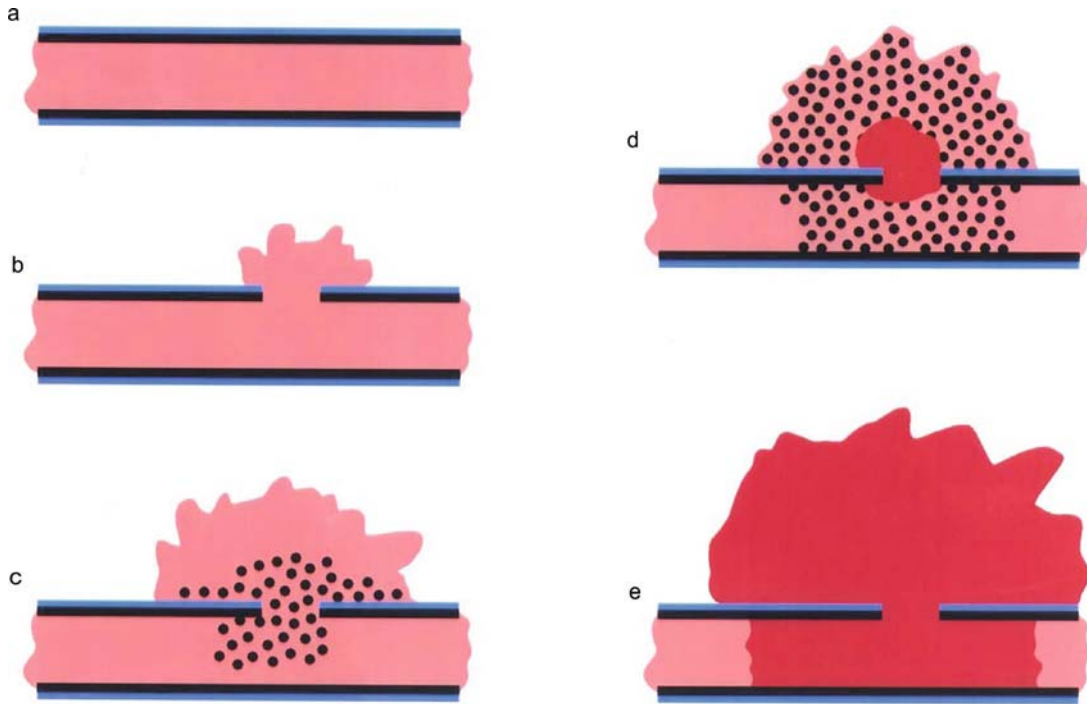


Figure 13.12. Blood coagulation: a race between an activating and an arresting wave. (a) Normally the blood (light red) is in contact only with the inner endothelial cell layer of a blood vessel (black). (b) Only after an injury does a contact with the collagen layer at the outer surface of the vessel (blue) occur. It triggers the release of *thrombin* molecules. (c) The release of *thrombin* is self-enhancing and spreads in a wave-like manner (dots). (d) A second, more rapid wave (dark red) is then triggered, which arrests the first. (e) In this way, the blood coagulation remains locally confined and the vessel is closed by a plug (model of Ataullakhanow and Guriya, 1994). In its logic, this reaction is closely related to that discussed for *Conus marmoreus* (Figure 7.2)

13.11 Activation and extinguishing waves in blood coagulation

Figures 7.2 and 7.3 provided an example for a slowly spreading wave, which after some delay triggers a much faster wave that catches up and extinguishes the first. This mechanism has a remarkable parallel in the process of blood coagulation.

After an injury, a wound starts bleeding. This goes on for only a short period before the blood starts to coagulate, forming a solid plug that seals the wound. The coagulation is not initiated, of course, by a contact of the blood with the air, since internal bleeding must be staunched as well. On their inner side the vessels consist of endothelial cells, and on their outer sides they are covered by a layer of collagen, an extracellular matrix molecule. Contact between blood and this outer layer (blue in Figure 13.12) functions as a trigger to start the coagulation. This can take place only after a vessel is damaged. Self-enhancing processes again play an essential role. *Thrombin* is released, and after passing a certain threshold concentration, more *thrombin* will be released. This release, therefore, spreads in a wave-like manner.

Under its influence, *fibrinogen* becomes converted into *fibrin*. The latter molecules form a densely packed network that functions as a plug (Figure 13.12).

Since the coagulation spreads in a wave-like manner, even large wounds can rapidly be sealed (as discussed above, a traveling wave is always much faster than diffusion, which depends on random walk). However, the wave mechanism on its own would lead to a catastrophe since coagulation would spread over the whole vascular system. Ataullakhanow and Guriya (1994) have proposed that with some delay a second, but significantly faster, wave is triggered that stops the self-enhancing action of *thrombin*. In this way, the wave-like spread of the coagulation comes to a halt (Figure 13.12). It is known that other components in the coagulation system exist that antagonize the action of *thrombin*; *protein C* is an essential component in this process. In its details, this antagonistic reaction is less well understood than the initiation of coagulation.

These examples demonstrate that the complex interactions proposed for shell patterning have close analogues in very common biological processes. This provides perhaps an additional motivation for learning the ‘ABCs’ of dynamical systems in general from the beautiful shell patterns.

References

- Adler, I. (1974). A model of contact pressure in phyllotaxis. *J. theor. Biol.* 45, 1–79.
- Ataullakhanov, F.I. and Guriya, G.T. (1994). Spatial aspects of the dynamics of blood clotting - I. Hypothesis. *Biophysics* 39, 91–97.
- Bär, M., Eiswirth, M., Rotermund, H.H. and Ertl, G. (1992). Solitary-wave phenomena in an excitable surface-reaction. *Phys. Rev. Lett.* 69, 945–948.
- Baier, H. and Bonhoeffer, F. (1992). Axon guidance by gradients of a target-derived component. *Science* 255, 472–475.
- Bellwinkel, H.W. (1992). Naturwissenschaftliche Themen im Werk von Thomas Mann. *Naturw. Rundsch.* 45, 174–183.
- Bernasconi, G.P. (1994). Reaction-diffusion model for phyllotaxis. *Physica D* 70, 90–99.
- Bode, H.R. (2003). Head regeneration in hydra. *Dev. Dyn.* 226, 225–236.
- Bode, P.M., Awad, T.A., Koizumi, O., Nakashima, Y., Grimmelikhuijen, C.J.P. and Bode, H.R. (1988). Development of the two-part pattern during regeneration of the head in hydra. *Development* 102, 223–235.
- Bretschneider, T., Siegert, F. and Weijer, C.J. (1995). 3-dimensional scroll waves of camp could direct cell-movement and gene-expression in *Dictyostelium* slugs. *Proc. Natl. Acad. Sci. USA* 92, 4387–4391.
- Bronsvort, W. and Klok, F. (1985). Ray tracing generalized cylinders. *ACM Transactions on Graphics* 4, 291–303 .
- Broun, M., Gee, L., Reinhardt, B. and Bode, H.R. (2005). Formation of the head organizer in hydra involves the canonical wnt pathway. *Development* 132, 2907–2916.
- Browne, E.N. (1909). The production of new hydrants in Hydra by insertion of small grafts. *J. Exp. Zool.* 7, 1–23.
- Buikema, W.J. and Haselkorn, R. (2001). Expression of the Anabaena hetR gene from a copper-regulated promoter leads to heterocyst differentiation under repressing conditions. *PNAS* 98, 2729–2734.
- Butty, A.C., Perrinjaquet, N., Petit, A., Jaquenoud, M., Segall, J.E., Hofmann, K., Zwahlen, C., Peter, M. (2002). A positive feedback loop stabilizes the guanine-

- nucleotide exchange factor Cdc24 at sites of polarization. *EMBO J.* 21, 1565–1576.
- Canales, C., Grigg, S. and Tsiantis, M. (2005). The formation and patterning of leaves: recent advances. *Planta* 221, 752–756.
- Chant, J. (1999). Cell polarity in yeast. *Annu. Rev. Cell Dev. Biol.* 15, 365–391.
- Charest, P.G. and Firtel, R.A. (2006). Feedback signaling controls leading-edge formation during chemotaxis. *Cur. Op. Gen. Dev* 16, 339–347.
- Cohn, M.J. and Tickle, C. (1996). Limbs - a model for pattern-formation within the vertebrate body plan. *Trends in Genetics* 12, 253–257.
- Comfort, A. (1951). The pigmentation of molluscan shells. *Biological Review* 26, 285–301
- Cook, T.A. (1914). Curves of Life. Constable and Company, London, reprinted 1979 by Dover Publications, New York.
- Cortie, M.B. (1989). Models for mollusc shell shape. *South African Journal of Science* 85, 454–460.
- Coultas, L., Chawengsaksophak, K. and Rossant, J. (2005). Endothelial cells and VEGF in vascular development. *Nature* 438, 937–945.
- Coxeter, H.S.M. (1961). Introduction to Geometry. J. Wiley and Sons, New York
- Crick, F. (1970). Diffusion in embryogenesis. *Nature* 225, 420–422.
- DeRobertis, E.M. (1995). Dismanteling the organizer. *Nature* 374, 407–408.
- Devreotes, P.N. (1989). *Dictyostelium discoideum*: A model system for cell-cell interactions in Development. *Science* 245, 1054–1058.
- Diaz-Benjumea, J., Gonzales Gaitan, M.A.F. and Garcia-Bellido, A. (1989). Developmental genetics of the wing vein pattern of *Drosophila*. *Genome* 31, 612–619.
- Diaz-Benjumea, J., Gonzales-Gaitan, M.A.F. and Garcia-Bellido, A. (1989). Developmental genetics of the wing vein pattern of *Drosophila*. *Genome* 31, 612–619.
- do Carmo, M. (1976). Differential Geometry of Curves and Surfaces. Prentice Hall, Englewood Cliffs
- Ermentrout, B., Campbell, J. and Oster, G. (1986). A model for shell patterns based on neural activity. *The Veliger* 28, 369–338.
- Farrar, N.R. and Spencer, G.E. (2008). Pursuing a 'turning point' in growth cone research. *Dev. Biol.*, 318, 102–111.
- Fassler, P.E. and Sander, K. (1996). Mangold, Hilde (1898–1924) and Spemanns organizer - achievement and tragedy. *Roux's Archives Dev. Biol.* 205, 323–332.
- Feininger, A. and Emerson, W.K. (1972). Shells. The Viking Press
- Foley, J.D., van Dam, A., Feiner, S. and Hughes, J. (1990). Computer graphics: Principles and practice. Addison-Wesley, Reading.
- Folkman, J. (1976). The vascularization of a tumor. *Sci. American* 234, May, 58–73.
- Fowler, D.R., Meinhardt, H. and Prusinkiewicz, P. (1992). Modeling seashells. Proceedings of SIGGRAPH '92. *Computer Graphics* 26, 379–387.
- Gasseling, MT and Saunders, JW Jr (1964). Effect of the "Posterior Necrotic Zone" on the early chick wing bud on the pattern and symmetry of limb outgrowth. *Amer. Zool.* 4, 303–304.

- Gerisch, G. (1968). Cell aggregation and differentiation in *Dictyostelium*. *Curr. Top. Dev. Biol.* 3, 157–232.
- Gierer, A. (1977). Biological features and physical concepts of pattern formation exemplified by hydra. *Curr. Top. Dev. Biol.* 11, 17–59.
- Gierer, A. (1981). Generation of biological patterns and form: Some physical, mathematical, and logical aspects. *Prog. Biophys. molec. Biol.* 37, 1–47.
- Gierer, A. and Meinhardt, H. (1972). A theory of biological pattern formation. *Kybernetik* 12, 30–39.
- Gierer, A., Berking, S., Bode, H., David, C.N., Flick, K., Hansmann, G., Schaller, H. and Trenkner, E. (1972). Regeneration of hydra from reaggregated cells. *Nature New Biology* 239, 98–101.
- Giulini, A., Wang, J. and Jackson, D. (2004). Control of phyllotaxy by the cytokinin-inducible response regulator homologue ABPHYL1 1031. *Nature* 430, 1031–1034.
- Glass, L. and Mackey, M.C. (1988). From clocks to chaos. Princeton University Press
- Goldbeter, A. (1996). Biochemical oscillations and the cellular rhythm: The molecular bases of periodic and chaotic behaviour. Cambridge University Press.
- Gordon, N.R. (1990). Seashells: A Photographic Celebration. Friedman group, New York
- Gould, A., Itasaki, N. and Krumlauf, R. (1998). Initiation of rhombomeric HoxB4 expression requires induction by somites and a retinoic acid pathway. *Neuron* 21, 39–51.
- Grüneberg, H. (1976). Population studies on a polymorphic prosobranch snail (*Clithon (Pictoneritina) oualaniensis* Lesson). *Phil. Transcctions Royal Soc. London B* 275, 385–437.
- Granero, M.I., Porati, A. and Zanacca, D. (1977). A bifurcation analysis of pattern formation in a diffusion governed morphogenetic field. *J. Math. Biology* 4, 21–27.
- Grapin-Botton, A., Bonnin, M.A., Sieweke, M. and Le Douarin, N.M. (1998). Defined concentrations of a posteriorizing signal are critical for MadB/Kreisler segmental expression in the hindbrain. *Development* 125, 1173–1181.
- Grieshammer, U., Minowada, G., Pisenti, J.M., Abbott, U.K. and Martin, G.R. (1996). The chick *limbless* mutation causes abnormalities in limb bud dorsal-ventral patterning: implication for apical ridge formation. *Development* 122, 3851–3861.
- Gurdon, J.B., Mitchell, A. and Mahony, D. (1995). Direct and continuous assessment by cells of their position in a morphogen gradient. *Nature* 376, 520–521.
- Hörstadius, S (1939). The mechanics of sea-urchin development studied by operative methods. *Biol. Rev.* 14, 132–179.
- Hale, C.A., Meinhardt, H. and de Boer, P.A.J. (2001). Dynamic localization cycle of the cell division regulator MinE in *Escherichia coli*. *Embo J.* 20, 1563–1572.
- Hammer, O. and Bucher, E (1999). Reaction-diffusion processes: application to the morphogenesis of ammonid ornamentation . *GeoBios*, 32, 841.852

- Harfe, B.D., Scherz, P.J., Nissim, S., Tian, F. and McMahon, A.P. (2004). Evidence for an expansion-based temporal Shh gradient in specifying vertebrate digit identities. *CELL* 4, 517–528.
- Harris, M.P., Williamson, S., Fallon, J.F., Meinhardt, H. and Prum, R.O. (2005). Molecular evidence for an activator-inhibitor mechanism in development of embryonic feather branching. *PNAS* 102, 11734–11739.
- Harrison, R.G. (1918). Experiments on the development of the fore-limb of *Amblystoma*, a self-differentiating equipotential system. *J. exp. Zool.* 25:413–46.
- Hellström, M., Phng, L.K., Hofmann, J.J., Wallgard, E., Coultas, L., Lindblom, P., Alva, J., Nilsson, A.K., Karlsson, L., Gaiano, N., Yoon, K., Rossant, J., Iruela-Arispe, M.L., Kalen, M., Gerhardt, H. and Betsholtz, C. (2007). Dll4 signalling through notch1 regulates formation of tip cells during angiogenesis. *Nature* 445, 776–780.
- Herman, G.T. and Liu, W.H. (1973). The dauther of Celia, the french flag and the firing quad: Progress report on a cellular linear iterative-array simulator. *Simulation* 21, 33–41.
- Hobmayer, B., Rentzsch, F., Kuhn, K., Happel, CM, Cramer von Laue, C., Snyder, P., Rothbacher, U. and Holstein, TW (2000). Wnt signalling molecules act in axis formation in the diploblastic metazoan hydra. *Nature* 407, 186–189.
- Hopfield, J.J. and Herz, A.V.M. (1995). Rapid local synchronization of action potentials: Toward computation with coupled integrate-and-fire neurons. *Proc. Natl. Acad. Sci. USA* 92, 6655–6622.
- Hu, Z., and Lutkenhaus, J. (1999). Topological regulation of cell division in *Escherichia coli* involves rapid pole to pole oscillation of the division inhibitor MinC under the control of MinD and MinE. *Mol Microbiol.* 34, 82–90.
- Huang, X., Dong, Y. and Zhao, J. (2004). HetR homodimer is a DNA-binding protein required for heterocyst differentiation, and the DNA-binding activity is inhibited by PatS. *PNAS* 2004 101, 4848–4853.
- Illert, C. (1989). Formulation and solution of the classical seashell problem. *Il Nuovo Cimento* 11 D, 761–780 .
- Izpisua-Belmonte, J.C., De Robertis, E.M., Storey, K.G., Stern, C., (1993). The homeobox gene *goosecoid* and the origin of organizer cells in the early chick blastoderm. *Cell*, 74, 645–659.
- Jones, C.M., Arnes, N. and Smith, J.C. (1996). Short-range signalling by Xnr-2 and BMP-4 contrasts with the long-range effects of activin *Current Biology* 6, 1468–1475.
- Jung, H.S., Francis-West, P.H., Widelitz, R.B., Jiang, T.X., Ting-Berreth, S., Tickle, C., Wolpert, L. and Chuong, C.M. (1998). Local inhibitory action of BMPs and their relationships with activators in feather formation: implications for periodic patterning. *Dev. Biol.* 196, 11–23.
- Kaandorp, J. (1994). Fractal modelling: Growth and form in biology. Springer-Verlag, Heidelberg

- Kawaguchi, Y. (1982). A morphological study of the form of nature. *Computer Graphics* 16, 223–232.
- Kay, R.R., Langridge, P., Traynor, D. and Hoeller, O. (2008). Changing directions in the study of chemotaxis. *Nat. Rev. Mol. Cell Biol.*, 9455–4, 3.
- Khaner, O. and Eyal-Giladi, H. (1989). The chick's marginal zone and primitive streak formation. I. Coordinative effect of induction and inhibition. *Dev. Biol.* 134, 206–214.
- Kiecker, C. and Lumsden, A. (2005). Compartments and their boundaries in vertebrate brain development. *Nature Rev. Neurosci.* 6, 553–564.
- Koch, A.J. and Meinhardt, H. (1994). Biological pattern-formation - from basic mechanisms to complex structures. *Rev. Modern Physics* 66, 1481–1507.
- Kuhlemeier, C. (2007). Phyllotaxis. *Trends Plant Sci* 12, 143–150.
- Kusch, I. and Markus, M. (1996). Mollusc shell pigmentation: Cellular automaton simulations and evidence for undecidability. *J. theor. Biol.* 178, 333–340.
- Ladher, R., Mohun, T.J., Smith, J.C. and Snape, A.M. (1996). Xom - a *Xenopus* homeobox gene that mediates the early effects of BMP-4. *Development* 122, 2385–2394.
- Lawrence, P.A., (1992). The making of a fly: The genetics of animal design Blackwell Scientific Publications, Oxford
- Lemaire,L., Roeser,T., Izpisua-Belmonte, J.C. and Kessel, M. (1997). Segregating expression domains of two *goosecoid* genes during the transition from gastrulation to neurulation in chick embryos. (*Development*, in press)
- Lenhoff, H. (1991). Ethel Browne, Hans Spemann, and the discovery of the organizer phenomenon. *Biol. Bull.* 181, 72–80.
- Leptin, M (1991). *twist* and *snail* as positive and negative regulators during *Drosophila* mesoderm development. *Genes Dev.* 5, 1568–1576.
- Lindsay, D.T. (1982). A new programmatic basis for shell pigment patterns in the bivalve mollusc *Lioconcha castrensis* L. *Differentiation* 21, 32–36.
- Lovtrup, S. and Lovtrup, M. (1988). The morphogenesis of molluscan shells: A mathematical account using biological parameters. *J. Morph.* 197, 53–62.
- Lutz, H. (1949). Sur la production experimentale de la polyembryonie et de la monstruosité double chez les oiseaux. *Arch. d'Anat. Micro. et de Morph.*, 38, 79–144.
- Martin, G.R. (1995). Why thumbs are up. *Nature* 374, 410–411.
- Meinhardt, H. (1976). Morphogenesis of lines and nets. *Differentiation* 6, 117–123.
- Meinhardt, H. (1978). Space-dependent cell determination under the control of a morphogen gradient. *J. theor. Biol.* 74, 307–321.
- Meinhardt, H. (1982). Models of Biological Pattern Formation. Academic Press, London (freely available from our website, <http://www.eb.tuebingen.mpg.de/meinhardt>)
- Meinhardt, H. (1983a). A boundary model for pattern formation in vertebrate limbs. *J. Embryol exp. Morphol.* 76, 115–137.

- Meinhardt, H. (1983b). Cell determination boundaries as organizing regions for secondary embryonic fields. *Devl. Biol.* 96, 375–385.
- Meinhardt, H. (1984). Models for positional signalling, the threefold subdivision of segments and the pigmentation pattern of molluscs. *J. Embryol. exp. Morph.* 83, (Supplement) 289–311.
- Meinhardt, H. (1993). A model for pattern-formation of hypostome, tentacles, and foot in hydra: how to form structures close to each other, how to form them at a distance. *Dev. Biol.* 157, 321–333.
- Meinhardt, H. (1999). Orientation of chemotactic cells and growth cones: Models and mechanisms. *J. Cell Sci.* 112, 2867–2874.
- Meinhardt, H. (2002). The radial-symmetric hydra and the evolution of the bilateral body plan: an old body became a young brain. *Bioessays* 24, 185–191.
- Meinhardt, H. (2004). Different strategies for midline formation in bilaterians. *Nat Rev Neurosci* 5, 502–510.
- Meinhardt, H. (2006). Primary body axes of vertebrates: generation of a near-Cartesian coordinate system and the role of Spemann-type organizer. *Dev Dyn.* 235, 2907–2919.
- Meinhardt, H. (2008). Models of biological pattern formation: from elementary steps to the organization of embryonic axes. *Curr. Top. Dev. Biol.* 81, 1–63.
- Meinhardt, H. and de Boer, P.A.J. (2001). Pattern formation in *E.coli*: a model for the pole-to-pole oscillations of Min proteins and the localization of the division site. *PNAS* 98, 14202–14207.
- Meinhardt, H. and Gierer, A. (1980). Generation and regeneration of sequences of structures during morphogenesis. *J. theor. Biol.* 85, 429–450.
- Meinhardt, H. and Klingler, M. (1987). A model for pattern formation on the shells of molluscs. *J. theor. Biol.* 126, 63–69.
- Mirollo, R.E. and Strogatz, S.H. (1990). Synchronization of pulse-coupled biological oscillators. *SIAM J. On Applied Mathematics* 50, 1645–1662.
- Moos, M., Wang, S.W. and Krinks, M. (1995). Anti-dorsalizing morphogenetic protein is a novel TGF- β homolog expressed in the spemann organizer. *Development* 121, 4293–4301.
- Murray, J.D. (1989). Mathematical biology. Springer, Heidelberg, New York
- Nüsslein-Volhard, C. (1991). Determination of embryonic body axes in the *Drosophila* embryo. *Development Supplement* 1, 1–10.
- Nüsslein-Volhard, C. (1996). Gradienten als Organisatoren der Embryonalentwicklung. *Spektrum der Wissenschaften Oktober* 10/1996, pp 38–46.
- Nüsslein-Volhard, C. and Wieschaus, E. (1980). Mutations affecting segment number and polarity in *Drosophila*. *Nature* 287, 795–801.
- Nellen, D., Burke, R., Struhl, G. and Basler, K. (1996). Direct and long-range action of a dpp morphogen gradient. *Cell* 85, 357–368.
- Neumann, D. (1959). Experimentelle Untersuchungen des Farbmusters auf der Schale von *Theodoxus fluviatilis* L. In: Verh. Deutsch. Zoolog. Gesellsch. Münster/ Westph. pp.152–156 (Akademische Verlagsgesellschaft Leipzig)

- Neumann, D. (1959). Morphologische und experimentelle Untersuchungen über die Variabilität der Farbmuster auf der Schale von *Theodoxus fluviatilis* L. Z. *Morph. Ökol. Tiere* 48, 349–411.
- Neumann, D. (1959). Musterumschlag auf der Molluskenschale. *Experientia* 15, 178.
- Niehrs, C., Steinbeisser, H. and DeRobertis, E.M. (1994). Mesodermal patterning by a gradient of the vertebrate homeobox gene *goosecoid*. *Science* 263, 817–820.
- Oliver, G., Sidell, N., Fiske, W., Heinzmann, C., Mohandas, T., Sparkes, RS and De Robertis, ED (1989). Complementary homeo protein gradients in developing limb buds. *Genes Dev.* 3, 641–650.
- Oppenheimer, P. (1986). Real time design and animation of fractal plants and trees. *Computer Graphics* 20, 55–64.
- Ozbudak, E.M., Becskei, A. and van Oudenaarden, A. (2005). A System of Counteracting Feedback Loops Regulates Cdc42p Activity during Spontaneous Cell Polarization. *Dev. Cell* 9, 565–571.
- Parr, B.A. and McMahon, A.P. (1995). Dorsalizing signal *Wnt-7a* required for normal polarity of D-V and A-P axes of the mouse limb. *Nature* 374, 350–353.
- Pickover, C.A. (1989). A short recipe for seashell synthesis. *IEEE Computer Graphics and Applications* 9, 8–11 .
- Pickover, C.A. (1991). Computers and the Imagination. St. Martin's Press
- Plath, P.J., Schwietering, J. (1992). Improbable event in deterministically growing patterns. In: Fractal Geometry and Computer. Graphics (J. L. Encarnucao, H. O. Peitgen, Skas, G. Englert, Eds.) Springer Verlag.
- Prigogine, I. and Lefever, R. (1968). Symmetry breaking instabilities in dissipative systems. II. *J. chem. Phys.* 48, 1695–1700.
- Prum, R.O. and Williamson, S. (2002). Reaction-diffusion models of within-feather pigmentation patterning. *Proc. R. Soc. London B* 269, 781–792.
- Prusinkiewicz, P. (1994). Visual models of morphogenesis. *Artificial Life* 1, 61–74.
- Prusinkiewicz, P. and Streibel, D. (1986). Constraint-based modeling of three-dimensional shapes. In *Proceedings of Graphics Interface '86 - Vision Interface '86*, pp. 158–163.
- Psychoyos, D. and Stern, C.D. (1996). Restoration of the organizer after radical ablation of Hensen's node and the anterior primitive streak an the chick embryo. *Development* 122, 3263–3273.
- Ptashne, M., Jeffrey, A., Johnson, A.D., Maurer, R., Meyer, B.J., Pabo, C.O., Roberts, T.M. and Sauer, R.T. (1980). How the lambda repressor and Cro work. *Cell* 19, 1–11.
- Raskin, D.M. and de Boer, P.A.J. (1999). Rapid pole-to-pole oscillation of a protein required for directing division to the middle of *Escherichia coli*. *PNAS* 96, 4971–4976.
- Raup, D.M. (1962). Computer as aid in describing form in gastropod shells. *Science* 138, 150–152 .
- Raup, D.M. (1969). Modeling and simulation of morphology by computer. Proceedings of the North American Paleontology Convention

- Raup, D.M. and Michelson, A. (1965). Theoretical morphology of the coiled shell. *Science* 147, 1294–1295.
- Regulski, M., Dessain, S., McGinnis, N. and McGinnis, W. (1991). High-affinity binding-sites for the deformed protein are required for the function of an autoregulatory enhancer of the deformed gene. *Genes & Development* 5, 278–286.
- Risau, W. and Flamme, I. (1995). Vasculogenesis. *Annu. Rev. Cell Dev. Biol.*, 11, 73–91.
- Sabelli, B. (1979). Guide to Shells. Simon and Schuster
- Sachs, T. (1991). Cell polarity and tissue patterning in plants. *Development Supplement* 1, 83–93.
- Saunders, B.W. (1984). *Nautilus* growth and longevity: Evidence from marked and recaptured animals. *Science* 224, 990–992.
- Schoute, J.C. (1913). Beiträge zur Blattstellung. *Rec. trav. bot. Neerl.* 10, 153–325.
- Segel, L.A. (1984). Modelling dynamic phenomena in molecular and cellular biology. Cambridge University Press, Cambridge
- Segel, L.A. and Jackson, J.L. (1972). Dissipative structure: an explanation and an ecological example. *J. theor. Biol.* 37, 545–549.
- Seilacher, A. (1972). Divaricate patterns in pelecypod shells. *Lethaia* 5, 325–343.
- Seilacher, A. (1973). Fabricational noise in adaptive morphology. *Systematic Zool.* 22, 451–465.
- Shapiro, L. and Losick, R. (2000). Dynamic spatial regulation in the bacterial cell. *Cell* 100, 89–98.
- Shimizu, H. and Fujisawa, T. (2003). Peduncle of Hydra and the heart of higher organisms share a common ancestral origin. *Genesis* 36, 182–186.
- Siegert, F. and Weijer, C.J. (1992). 3-dimensional scroll waves organize *Dictyostelium* slugs. *Proc. Natl. Acad. Sci. USA* 89, 6433–6437.
- Simpson-Brose, M, Treisman, J and Desplan, C (1994). Synergy between the *hunchback* and *bicoid* morphogens is required for anterior patterning in *Drosophila*. *Cell* 78, 855–865.
- Smith, R.S., Guyomarc'h, S., Mandel, T., Reinhardt, D., Kuhlemeier, C. and Prusinkiewicz, P. (2006). A plausible model of phyllotaxis. *PNAS* 103, 1301–1306.
- Spemann, H. and Mangold, H. (1924). Über Induktion von Embryonalanlagen durch Implantation artfremder Organisatoren. *Wilhelm Roux' Arch. Entw. mech. Org.* 100, 599–638.
- Starz-Gaiano, M., Melani, M., Wang, X., Meinhardt, H. and Montell, D.J. (2008). Feedback Inhibition of JAK/STAT signaling by apontic is required to limit an invasive cell population. *Dev. Cell* 14, 726–738.
- Stewart, I. (1991). All together now. *Nature* 350, 557–557.
- Suchting, S., Freitas, C., le Noble, F., Benedito, R., Breant, C., Duarte, A. and Eichmann, A. (2007). The notch ligand delta-like 4 negatively regulates endothelial tip cell formation and vessel branching. *PNAS* 104, 3225–3230.

- Technau, U. and Holstein, T.W. (1995). Head formation in hydra is different at apical and basal levels. *Development* 121, 1273–1282.
- Thompson, d'Arcy, W. (1952). On Growth and Form. Cambridge
- Thompson, d'Arcy, W. (1961). On Growth and Form (Abridged Edition). Cambridge University Press, Cambridge
- Tickle, C., Summerbell, D. and Wolpert, L. (1975). Positional signalling and specification of digits in chick limb morphogenesis. *Nature* 254, 199–202.
- Trembley, A. (1744). Memoires pour servir a l'histoire d'un genre de polypes d'eau douce. *J. u. H. Verbeek, Leiden*. , .
- Turing, A. (1952). The chemical basis of morphogenesis. *Phil. Trans. B.* 237, 37–72.
- Udolf, G., Lüer, K., Bossing, T. and Technau, G.M. (1995). Commitment of the CNS progenitors along the dorsoventral axis of *Drosophila* neuroectoderm. *Science* 269, 1278–1281.
- van Iterson, G. (1907). Mathematische und mikroskopisch-anatomische Studien über Blattstellungen. *Fischer, Jena*. , .
- Vincent, J.P. and Lawrence, P.A. (1994). It takes three to distalize. *Nature* 372, 132–133.
- von Rosenhof, R. (1755). Historie der Polypen und anderer kleiner Wasserinsecten. Insektenbelustigung. Vol. III. Nürnberg
- Wacker, S.A., Jansen, H.J., McNulty, C.L., Houtzager, E. and Durston, A.J. (2004a). Timed interactions between the Hox expressing non-organiser mesoderm and the Spemann organiser generate positional information during vertebrate gastrulation. *Dev. Biol.* 268.207–21, .
- Waddington, C. and Cowe, R. (1969). Computer simulation of a molluscan pigmentation pattern. *J. Theor. Biol.* 25, 219–225.
- Wanscher, J.H. (1971). Considerations on phase-change and decorations in snail shells. *Hereditas* 71, 75–94.
- Ward, P.D. and Chamberlain, J. (1983). Radiographic observation of chamber formation in *Nautilus pompilius*. *Nature* 304, 57–59.
- Wilcox, M., Mitchison, G.J. and Smith, R.J. (1973). Pattern formation in the blue-green alga, *Anabaena*. I. Basic mechanisms. *J. Cell Sci.* 12, 707–723.
- Willmann, R. (1983). Die Schnecken von Koos. *Spektrum der Wissenschaft* (Februar) pp. 64–76.
- Winfree, A.T. (1980). The geometry of biological time. Springer Verlag, New York, Heidelberg, Berlin.
- Wolfram, S. (1984). Cellular automata as models of complexity. *Nature* 341, 419–424.
- Wolpert, L. (1969). Positional information and the spatial pattern of cellular differentiation. *J. theor. Biol.* 25, 1–47.
- Yoon, H.S. and Golden, J.W. (1998). Heterocyst pattern-formation controlled by a diffusible peptide. *Science* 282, 935–938.
- Zigmond, S.H. (1977). Ability of polymorphonuclear leukocytes to orient in gradients of chemotactic factors. *J Cell Biol.* 75, 606–617.

Index

Names of mollusks

Ammonites 61

Amoria

dampieria 45

elliotti 40, 180

macandrewi 55, 56

turneri 69

undulata 56, 181

Austrocochlea adelaidea 66

Babylonia japonica 87

Babylonia papillaris 12, 70

Bankivia fasciata 76–78

Bednalli (*Volutococonus*) 118

Bursa rubeta 52

Cepea nemoralis 26

Clithon 105, 120, 147, 151, 155, 156,
159, 161, 162

oualaniensis 148, 154, 155

Clithon type 159

Conus

abbas 83

ammiralis 123, 125, 126

ammiralis archithalassus 125, 126

auratus 105, 121, 125

ebraeus 112

episcopus 112, 120, 122, 161

loroisi 18

marchionatus 105, 108–110, 116

marmoreus 105, 106, 108–111, 162,
183, 184, 252

marmoreus nigrescens 162

nicobaricus 162

pennaceus 105, 112, 115, 118, 119,
121

textile 15, 16, 105, 147–149, 151,
159, 161, 162

thalassiarchus 101, 102

vicweei 162

zeylanicus 12, 13

Cymbiola

innexa 132, 134

nobilis 48, 142, 144

pulchra wisemani 126, 127

vespertilio 105, 143, 144

Cypraea

diluculum 6, 59

scurra 37

tigris 37

ziczac 63, 64

Epitonium scalare 173

Ficus gracilis 52

Harpa major 164

Lioconcha 135, 136, 142

castrensis 105, 133, 135, 136

hieroglyphica 7, 136, 139, 141–143

lorenziana 48, 136, 138, 141

ornata 136

Lyria planicostata taiwanica 22

Marginella limbata 127

Natica

euzona 54, 55, 181, 182

-
- stercusmuscarum* 87
undulata 60
Nautilus 61–63, 67
Neptunea lyrata 18
Neritina
 communis 164
 natalensis 12
 oualaniensis 147
 oualaniensis, see *Clithon* 105
 penata 88
 virginea 156
Neritodryas dubia 76
Oliva bulbosa 88
Oliva porphyria 7, 91, 93, 95, 98, 164,
 183
Persicula persicula 87
Phalium strigatum 46
Pompilius belanensis 62
Puperita pupa 159
Rapa rapa 176
Scaphella junonia 66, 67
Strigilla 49, 51
Sunetta meroe 136
Tapes literatus 70, 81, 136, 142
Thatcheria mirabilis 172
Theodoxus
 doricus 75
 fluviatilis 15, 44
 oualaniensis, see *Clithon* 147
Turritella nivea 177
Voluta
 musica 62, 63
Volutoconus bednalli 118, 182
- Other objects**
- Activation
 of genes 221
 spontaneous 51, 132, 139, 140
 Activator - inhibitor reaction 19, 20
 equation 23
 oscillations 43
 plus a second inhibitor 85
- simple calculation 24
 Activator - substrate reaction 29
 equation 28, 30
 oscillations 43
Anabaena 21, 208
 Annihilation 51
 Antagonistic reactions 1
 combined action of two 71, 233
 Arms
 initiation of 225
 Autocatalysis
 by inhibition of inhibition 33
 by ion currents 251
 role of saturation 25, 43
 Autoregulation
 in gene activation 220
- Background 148, 164
 Blood coagulation 252
 Blood vessels 235
 Borders
 role as organizing regions 227
 Brachyury 217
 Breakdown of pigmentation
 large scale 108, 144, 145
- Cdc42*, 242
 Central oscillator 66
 in triangle formation 131
 Chaotic behavior 98
 Chemotaxis 240
 Chick development 205
 Competence 211
 Computer program
 quick guide 186
- Depletion mechanism 29
 intracellular 242, 244
 Descartes 167
 Development
 body axes 216
 chick 205
 tunk 218

- Dictyostelium 246
Diffusion
stabilization of oscillations by 62
Dots, rows of 47, 64
Drosophila 4, 205, 207
Dynamic systems 1

E.coli
Min-system 244
out-of-phase oscillations 244
Enhancing reaction 119
Extinguishing reaction 110, 111, 150

Feathers
barbs 250
color patterns 248, 249

Gene activation 37, 219, 221
equation 222
Global changes 91
Goosecoid 205, 217
Gradients 35
and gene activation 224
Growth 30, 32
insertion of peaks 31, 67, 208

Hensen's node 205, 219
Heterocyst formation 208
Hydra 5, 65, 208
Alsterpaullone 216
 β -catenin 210
foot formation 214
foot-vertebrate heart relation 217
models 213
tentacles 215, 216

Inhibition
by activator destruction 32
long range 19

Leg initiation 224
Lines
narrow unpigmented 66

oblique 6, 8
parallel with gaps 148
wavy 54
Logarithmic spiral 167

Michaelis-Menten kinetics 42
Midline problem 217

Net-like structures 235
equation 236

Oblique lines 47
spontaneous initiation 48, 101
Organizer formation 211
Oscillation frequency
growth rate-dependent 62, 67
position-dependent 53, 62
Oscillations 41, 43
and chemotaxis 240
entrainment 11
global 14
synchronization by diffusion 44
synchronous 7, 45
temporary interruption 148
Overshoot 115, 157, 159

Pace-maker 49, 50, 54, 71
Pattern
bird feathers 247
early fixation 27
gradients 35, 36
periodic in space 21
stable in time 19, 20
superposition of stable and periodic
52, 63
variability 73
Pattern formation 4, 19
two-dimensional 37–39
Pattern regulation 10, 37, 51
Periostracum 5
Perturbations 10
Phyllotaxis 231
auxin 234

- inhibition in time 234
- Polarity of the tissue 211
- Polarization in budding yeast 242
- Polarization of cells 239
- Positional information 35, 219
- Primitive streak 205
- Refractory period 41
- Sand dune paradox 3
- Saturation 25, 38
 - influence on stripe width 46, 47
 - survival of waves by 58
- Self-enhancement 1, 19
- Shell patterns
 - arches 60
 - background 12, 13, 147, 164
 - branches 91, 116, 118
 - breaches 80
 - chains of white drops 105, 120, 122, 162
 - chessbord 78
 - complex 15, 105
 - crescents 88
 - crossings 80–82, 132
 - diversity 75, 98, 136, 157
 - experimental interference 15
 - fishbone-like 63, 64
 - function 5
 - functional significance 5
 - global rearrangements 74, 76
 - juvenile 6
 - meshwork 75
 - modification by ionic strength 14
 - not realized 114
 - oblique lines 47, 50, 75
 - relief-like 9, 174
 - rows of dots 10, 47, 64
 - selective pressure on 5, 9
 - similarities 7, 105
 - staggered dots 84, 86–88
 - staggered wine glasses 82, 121
 - stalks 111
- theories 17
- triangles 88, 99, 100, 131
- two-dimensional process 6, 37
- waste disposal 5
- white drops 105, 109
- Shell shape 174
 - elements 168
 - generating curve 171
 - surface modelling 169
- Sierpinsky triangles 134
- Slime mold 246
- Spemann organizer 218, 219
- Stripes 38
 - formation in two dimension 39
 - parallel to the edge 6, 8
 - perpendicular to the edge 6, 8, 19, 45
 - splitting 32
 - width 25, 26, 46, 47
- Symmetry 11
- Synchronization 44
 - abolishment by a second antagonist 71
- Thrombin 252
- Tongues 147, 148
- Traveling tongues 156
- Traveling waves 41, 47, 48
 - annihilation 51, 77
 - feather patterns 250
 - hidden waves 60
 - in nerve fibers 251
 - splitting 91
 - termination 54, 55, 68
 - two-dimensional 247
 - with extinguishing function 111
- VEGF 239
- Veins 235
- Wave splitting 91
- Waves
 - annihilation during collision 48, 51

- Wings
 - initiation of 224, 225
- Wnt
 - as AP signal 218
 - in hydra 210
 - Zone of polarizing activity 224